CHARACTERISATION OF *Melicope ptelefolia* BIOACTIVITIES: ANTIOXIDANT, ANTICANCER, ANTI-CADMIUM-INDUCED CYTOTOXICITY AND MICROARRAY TRANSCRIPTOME PROFILING

MOHAMMAD FAUJUL KABIR

FACULTY OF MEDICINE
UNIVERSITY OF MALAYA
KUALA LUMPUR

2019

CHARACTERISATION OF *Melicope ptelefolia* BIOACTIVITIES: ANTIOXIDANT, ANTICANCER, ANTI-CADMIUM-INDUCED CYTOTOXICTY AND MICROARRAY TRANSCRIPTOME PROFILING

MOHAMMAD FAUJUL KABIR

THESIS SUBMITTED IN FULFILMENT OF THE REQUIREMENTS FOR THE DEGREE OF DOCTOR OF PHILOSOPHY

FACULTY OF MEDICINE
UNIVERSITY OF MALAYA
KUALA LUMPUR

2019

UNIVERSITY OF MALAYA
ORIGINAL LITERARY WORK DECLARATION

Name of Candidate: **Mohammad Faujul Kabir** [redacted]

Matric No: **MHA150022**

Name of Degree: **Doctor of Philosophy**

Title of Thesis ("this Work"):

Characterisation of *Melicope ptelefolia* bioactivities: antioxidant, anticancer, anti- cadmium-induced cytotoxicity and microarray transcriptome profiling

Field of Study: **Molecular Medicine**

I do solemnly and sincerely declare that:

(1) I am the sole author/writer of this Work;
(2) This Work is original;
(3) Any use of any work in which copyright exists was done by way of fair dealing and for permitted purposes and any excerpt or extract from, or reference to or reproduction of any copyright work has been disclosed expressly and sufficiently and the title of the Work and its authorship have been acknowledged in this Work;
(4) I do not have any actual knowledge nor do I ought reasonably to know that the making of this work constitutes an infringement of any copyright work;
(5) I hereby assign all and every rights in the copyright to this Work to the University of Malaya ("UM"), who henceforth shall be owner of the copyright in this Work and that any reproduction or use in any form or by any means whatsoever is prohibited without the written consent of UM having been first had and obtained;
(6) I am fully aware that if in the course of making this Work I have infringed any copyright whether intentionally or otherwise, I may be subject to legal action or any other action as may be determined by UM.

Candidate's Signature [redacted] Date: 12/03/2019

Subscribed and solemnly declared before,

Wi[redacted]

DR. JOHARI MOHD ALI
Lecturer
Dept. of Molecular Medicine
Faculty of Medicine
University Of Malaya
50603 Kuala Lumpur
Tel: 79675741 / 4906
johari@um.edu.my

Date: 14 MAR 2019

Name: Dr. Johari Bin Mohd Ali

Designation: Senior Lecturer

CHARACTERISATION OF *Melicope ptelefolia* BIOACTIVITIES: ANTIOXIDANT, ANTICANCER, ANTI-CADMIUM-INDUCED CYTOTOXICITY AND MICROARRAY TRANSCRIPTOME PROFILING

ABSTRACT

Melicope ptelefolia (MP), a well-known herb in a number of Asian countries, has been used as a traditional medicine. However, not many studies have been currently done to evaluate its medicinal benefits. The present study reports antioxidant, anticancer, anti-cadmium-induced cytotoxicity and gene expression modulating activities of MP leaf extracts. MP leaves were dried, powdered and extracted sequentially using hexane (HX), ethyl acetate (EA), methanol (MeOH) and water (W). Antioxidant activity was evaluated through chemical and cellular antioxidant activity (CAA) assays. Antiproliferative activity against HCT116, HepG2, HCC1937 and MDA-MB-231 cancer cell lines was evaluated through cell viability, apoptosis and cell cycle assays. The cytoprotective effect of MP extracts on Hs27 cells exposed to $CdCl_2$ was evaluated using cell viability assay. Microarray gene expression profiling was done using GeneChip™ Human Gene 2.0 ST Array. The transcriptome data was analysed using Expression Console, Transcriptome Analysis Console and Ingenuity Pathway Analysis (IPA) softwares, along with GATHER, PANTHER and STRING bioinformatics web tools. Microarray data was validated by profiling the expression of selected genes through quantitative reverse transcription PCR (RT-qPCR). Based on the chemical antioxidant assays, MP-HX exhibited the highest antioxidant potential. The CAA assay revealed that MP-HX had a lower EC_{50} value of 11.30 ± 0.68 µg/mL, compared to MP-EA, which was 37.32 ± 0.68 µg/mL. MP-HX and MP-EA demonstrated cytotoxic effect on all four cancer cell lines tested. MP-HX showed the most notable antiproliferative

activity against MDA-MB-231 (IC_{50} = 57.81 ± 3.49 μg/mL) and HCT116 (IC_{50} = 58.04 ± 0.96 μg/mL). MP-EA showed the strongest antiproliferative activity against HCT116 (IC_{50} = 64.69 ± 0.72 μg/mL). MP-HX and MP-EA were able to induce caspase-dependent apoptotic cell death in the four cancer cell lines tested and they altered the cell cycle distribution in most of the cancer cell lines. Gene expression study in HCT116 and HepG2 cells indicated that MP-HX induced differential expression of 1290 and 1325 genes, respectively (microarray fold change ≥ ±2.0). In both cell lines, MP-HX modulated the expression of many genes in directions that support antiproliferative activity. MP-HX upregulated the expression of pro-apoptotic, cell cycle arresting and metastasis suppression genes, while it also downregulated the expression of anti-apoptotic, cell cycle and tumor promoting genes. MP-HX and MP-EA treatments in Hs27 cells resulted to the upregulation of numerous antioxidant and cell cycle promoting genes, including genes that play vital roles in wound healing and aging processes. Bioinformatics data analysis revealed that MP-HX and MP-EA modulated canonical pathways and activated several upstream regulators associated with wound healing process in Hs27 cells. In Hs27 exposed to $CdCl_2$, the percentage of cell viability was increased in the presence of MP-HX or MP-EA pretreatments, suggesting cytoprotective effect of MP extracts. Microarray profiling of Hs27 cells exposed to $CdCl_2$ demonstrated modulation of apoptosis and heat shock protein genes expression when the cells were pretreated with MP extracts. This observation provided insights on the extracts cytoprotective mechanisms. The findings of the present study project the potential value of MP in nutraceutical and pharmaceutical industries.

Keywords: *Melicope ptelefolia*, antioxidant, anticancer, microarray, bioinformatics

PENCIRIAN BIOAKTIVITI *Melicope ptelefolia*: ANTIOKSIDAN, ANTIKANSER, ANTI-SITOTOKSIKSITI KADMIUM DAN PEMPROFILAN TRANSKRIPTOM *MICROARRAY*

ABSTRAK

Melicope ptelefolia (MP) adalah herba yang terkenal di beberapa negara Asia, yang telah digunakan sebagai ubat tradisional. Walau bagaimanapun, tidak banyak kajian dilakukan untuk menilai manfaat perubatannya. Kajian ini melaporkan aktiviti antioksidan, antikanser, anti- sitotoksiksiti aruhan kadmium dan pengubahan aktiviti pengungkapan gen oleh ekstrak daun MP. Daun MP dikeringkan, dikisar dan diekstrak secara urutan menggunakan pelarut heksana (HX), etil asetat (EA), metanol (MeOH) dan air (W). Aktiviti antioksidan dinilai melalui ujian kimia dan aktiviti antioksidan sel (CAA). Aktiviti anti-proliferatif terhadap sel-sel kanser HCT116, HepG2, HCC1937 dan MDA-MB-231 dinilai melalui kajian daya tahan sel, apoptosis dan kitaran sel. Kesan perlindungan ekstrak MP-HX dan MP-EA terhadap sitotoksisiti $CdCl_2$ pada sel fibroblas (Hs27) dinilai menggunakan ujian daya tahan sel. Pemprofilan aktiviti pengungkapan gen dijalankan menggunakan GeneChip ™ Human Gene 2.0 ST Array. Data transkriptom dikaji menggunakan perisian *Expression Console* dan *Transcription Analysis Console* dan *Ingenuity Pathway Analysis* (IPA), bersama dengan perisian bioinformatik dalam talian GATHER, PANTHER dan STRING. Data *microarray* telah ditentusahkan dengan mengukur ekspresi gen terpilih melalui kaedah transkripsi terbalik - kuantitatif PCR (RT-qPCR). Berdasarkan ujian antioksidan kimia, MP-HX mempamerkan potensi antioksidan tertinggi. MP-HX juga menunjukkan nilai CAA tertinggi dalam sel Hs27, dengan nilai EC_{50} 11.30 ± 0.68 μg/mL, manakala nilai EC_{50} MP-EA ialah 37.32 ± 0.68 μg / mL. MP-HX dan MP-EA menunjukkan kesan sitotoksik

kepada keempat-empat sel sel kanser yang diuji. MP-HX menunjukkan aktiviti antiproliferatif yang paling ketara terhadap MDA-MB-231 (IC_{50} = 57.81 ± 3.49 μg/mL) dan HCT116 (IC_{50} = 58.04 ± 0.96 μg/mL). MP-EA menunjukkan aktiviti antiproliferatif yang paling ketara terhadap sel HCT116 (IC_{50} = 64.69 ± 0.72 μg/mL). MP-HX dan MP-EA menyebabkan kematian sel kanser secara apoptosis yang bergantung enzim *caspase* dalam kesemua sel kanser yang diuji, dan mereka juga mampu mengolah aktiviti kitaran sel dalam hampir semua sel kanser yang diuji. Kajian ekspresi menggunakan sel HCT116 dan HepG2 menunjukkan MP-HX menyebabkan pengubahan ekspresi sebanyak 1290 dan 1325 gen masing-masing (gandaan perubahan> ±2.0). MP-HX mengolah eksprasi berbagai gen menurut arah perubahan yang menyokong aktiviti antiproliferatif dalam sel HCT116 dan HepG2. MP-HX mengaruh ekspresi gen pro-apoptosis, gen penyekat kitaran sel dan gen penindasan metastasis. MP-HX juga menindas ekspresi anti-apoptosis, gen pendorong kitaran sel, dan gen penggalak perkembangan tumor. Dalam sel Hs27, MP-HX dan MP-EA mengaruh ungkapan pelbagai gen antioksidan dan penggalak kitaran sel, dan gen yang memainkan peranan penting proses penyembuhan luka dan penuaan. Analisis data bioinformatik menunjukkan bahawa MP-HX dan MP-EA berupaya mengolah laluan kanonik dan mengaktifkan beberapa pengawal selia hulu bagi proses penyembuhan luka dalam sel Hs27. Dalam sel Hs27 yang ditindak dengan $CdCl_2$, kadar peratusan sel hidup didapati meningkat apabila sel dipratindak dengan MP-HX atau MP-EA, yang memberi gambaran kesan perlindungan kepada sel oleh ekstrak MP. Pemprofilan *microarray* sel Hs27 yang ditindak dengan $CdCl_2$ menunjukkan pengolahan ekspresi gen bagi protin *apotosis* dan protin renjat haba, jika sel tersebut dipratindak dengan ekstrak MP. Penemuan dalam kajian ini menunjukkan MP boleh menjadi herba yang bernilai untuk industri nutraseutikal dan farmaseutikal.

Kata kunci: *Melicope ptelefolia*, antioksidaan, antikanser, *microarray*, bioinformatik

ACKNOWLEDGEMENTS

At first, I would like to thank and express my gratefulness to the almighty Allah, without whom I would be nothing. He was always very near to me whenever I needed his help. Without his blessings and kindness, I would never be able to complete my PhD study on time.

I would like to express my sincere gratitude to my supervisor Dr. Johari Bin Mohd Ali. I am indebted for his inspiration, enthusiasm, invaluable advice, constant support and judgment throughout my PhD study. My study would never have been finished without the motivation and the good mentorship he provided. My gratitude also extends to my supervisor Prof. Onn Bin Haji Hashim for his kind assistance and encouragement during my study. I am grateful to him for sharing his honest thoughts and instructions.

I am very lucky to have the support and care of my family. I would like to express my deepest gratitude to my late mother, who continuously encouraged me during her lifetime to become a researcher. I want to give special thanks to my father for pushing me to do my best. I cannot express the debt I owe to my wife for her irreplaceable sacrifice, love, care, and encouragement throughout my PhD study. I am grateful for the invaluable support she provided, which made it possible to complete my study.

I am thankful to all the academic and support staff of the Department of Molecular Medicine, University of Malaya for their assistance and inspiration. I am also grateful to University of Malaya for providing sufficient training and research facilities.

At the end, I would like to express my thankfulness to others, those who are not mentioned here but assisted me during the study.

TABLE OF CONTENTS

LIST OF FIGURES

Page

LIST OF TABLES

Page

LIST OF SYMBOLS AND ABBREVIATIONS

ng	:	Nanogram (s)
µg	:	Microgram (s)
mg	:	Milligram (s)
g	:	Gram (s)
µL	:	Microliter (s)
mL	:	Milliliter (s)
nM	:	Nanomole
µM	:	Micromole
mM	:	Millimole
M	:	Mole
s	:	Second (s)
min	:	Minute (s)
h	:	Hour (s)
rpm	:	Rotation per minute
$^{\bullet}NO$	:	Nitric oxide
$^{\bullet}OOH$	:	Hydroperoxyl radical
$^{1}O_2$	:	Singlet oxygen
5-FU	:	5-fluorouracil
7-AAD	:	7-aminoactinomycin D
AA	:	Ascorbic acid
ABAP	:	2,2′-azobis (2-amidinopropane) dihydrochloride
ABC	:	ATP binding cassette
$ABTS^{\bullet+}$	:	2,2′-azinobis-(3-ethylbenzothiazoline-6-sulfonic acid)
AGE	:	Aged garlic extract

Al_2O_3	:	Aluminum oxide
$AlCl_3$	:	Aluminum trichloride
ANOVA	:	Analysis of variance
AP-1	:	Activator protein 1
APCs	:	Antigen presenting cells
AP-WP	:	Apoptosis Wikipathway
ATCC	:	American type culture collection
AURKA	:	Aurora kinase A
BIM	:	BCL-2 interacting mediator of cell death
BKB	:	Blackberry
BLB	:	Blueberry
BORA	:	Aurora kinase A activator
BR	:	Biological replicates
CAA	:	Cellular antioxidant activity
Cd	:	Cadmium
CASP8	:	Caspase-8
CAT	:	Catalase
CCNA2	:	Cyclin A2
CC-WP	:	Cell Cycle WikiPathway
CDKIs	:	Cyclin dependent kinase inhibitors
CDKN1A	:	Cyclin dependent kinase inhibitor 1A
CDKN2B	:	Cyclin Dependent Kinase Inhibitor 2B
CDKs	:	Cyclin dependent kinases
CEACAM1	:	Carcinoembryonic antigen family member
COPD	:	Chronic obstructive pulmonary disease
CPs	:	Canonical pathways

CT	:	Threshold cycle
DBP	:	Vitamin D-binding protein
DCFH	:	2',7'-dichlorodihydrofluorescein
DCFH-DA	:	2′,7′-dichlorofluorescin diacetate
DDK	:	Dbf4-dependent protein kinase
DDR-WP	:	DNA damage response" WikiPathway
DE	:	Dried extract
DEGs	:	Differentially expressed genes
DMEM	:	Dulbecco's Modified Eagle's Medium
DMSA	:	Meso 2, 3-dimercaptosuccinic acid
DMSO	:	Dimethyl sulfoxide
$DPPH^{\bullet}$	:	1,1-Diphenyl-2-picryl-hydrazyl
DSB	:	DNA double strand break
DX	:	Dexpanthenol
EC	:	Expression Console
EC_{50}	:	Median effective concentration
EGCG	:	Epigallocatechin-3-gallate
EIF2	:	Eukaryotic translation initiation factor 2
EMT	:	Epithelial to mesenchymal transition
ER	:	Endoplasmic reticulum
ERK	:	Extracellular-signal-regulated kinase
FC	:	Fold change
FC	:	Folin-Ciocalteu
$FeCl_3.6H_2O$	:	Ferric chloride
$FeSO_4$	:	Ferrous sulphate
FGF	:	Fibroblast growth factor

FGFR	:	Fibroblast growth factor receptor
FL	:	Fetal liver
FM	:	Focus molecules
FOS	:	Fos proto-oncogene, ap-1 transcription factor subunit
FRAP	:	Ferric reducing antioxidant power
G_1SCC-WP	:	G_1 to S cell cycle control Wikipathway
GA	:	Gallic acid
GABARAP	:	GABA type A receptor associated protein
GADD	:	Growth arrest and DNA damage
GAE	:	Gallic acid equivalent
GATA1	:	GATA binding protein 1
GATHER	:	Gene Annotation Tool to Help Explain Relationships
GCL	:	Glutamate-cysteine ligase
GCN2	:	General control non-derepressible-2
GINS2	:	GINS complex subunit 2
GPX	:	Glutathione peroxidase
GPX4	:	Glutathione peroxidase 4
GR	:	Glutathione reductase
GSH	:	Glutathione
GSR	:	Glutathione-disulfide reductase
GST	:	Glutathione S-transferases
H_2O_2	:	Hydrogen peroxide
HBSS	:	Hank's balanced salt solution
HELLS	:	Helicase, lymphoid specific
HMOX1	:	Hemeoxygenase-1
HRI	:	Heme-regulated inhibitor

HSP	:	Heat shock protein
HuGene	:	Human Gene
IAP	:	Inhibitor of apoptosis
IC_{50}	:	Half-maximal inhibitory concentration
IERGs	:	Immediate early response genes
IL-17	:	Interleukin-17
IntPA	:	Intrinsic pathway for apoptosis
IPA	:	Ingenuity Pathway Analysis
JNK	:	c-JUN N-terminal kinase
MA_FC	:	Fold change based on microarray data
MAPK	:	Mitogen-activated protein kinase
MCM	:	Minichromosome maintenance
MDD	:	Major depressive disorder
MDR	:	Multidrug resistance
MG_1-G_1SP	:	Mitotic G_1-G_1/S phases
MG_2-G_2MP	:	Mitotic G_2-G_2/M phases
MP	:	*Melicope ptelefolia*
MP-EA	:	MP ethyl acetate extract
MP-HX	:	MP hexane extract
MP-MeOH	:	MP methanol extract
MP-W	:	MP water extract
MRPs	:	Multidrug associated resistance proteins
MT	:	Metallothionine
MTS	:	[3-(4,5-dimethylthiazol-2-yl)-5-(3-carboxymethoxyphenyl)-2-(4-sulfophenyl)-2H-tetrazolium]
MTs	:	Metallothionines

MXR	:	Mitoxantrone resistance protein
Na_2CO_3	:	Sodium carbonate
NDRG1	:	N-myc Downstream Regulated 1
NF-κB	:	Nuclear factor kappa-light-chain-enhancer of activated B cells
NGS	:	Next generation sequencing
NI	:	Network ID
NO	:	Nitric oxide
NUPR1	:	Nuclear protein 1
$O_2^{\bullet-}$	:	Superoxide radical
$OH^{\bullet}$	:	Hydroxyl radical
$ONOO^-$	:	Peroxynitrite
PANTHER	:	Protein Analysis Through Evolutionary Relationships
PAP	:	Prostatic acid phosphatase
PBS	:	Phosphate buffered saline
PCD	:	Programmed cell death
PD1	:	Programmed cell death protein 1
PDGF	:	Platelet-derived growth factor
PDL1	:	Programmed cell death ligand 1
PDL2	:	Programmed cell death ligand 2
PERK	:	PKR-like ER kinase
P-gp	:	P-glycoprotein
PKR	:	Protein kinase double-stranded RNA-dependent
PLK1	:	Polo-like kinase 1
PP	:	Polyphenon-60
PRDX2	:	Peroxiredoxin 2
pre-RC	:	Pre-replication complex

QE	:	Quercetin equivalent
QN	:	Quercetin
RABL6	:	RAB, member RAS oncogene family like 6
RB	:	Raspberry
RG	:	Representative gene
RIC-WP	:	Retinoblastoma (RB) in cancer Wikipathway
RMI1	:	RecQ mediierated genome instability 1
RNAseq	:	RNA sequencing
RNR	:	Ribonucleotide reductase
RNS	:	Reactive nitrogen species
ROS	:	Reactive oxygen species
RPMI	:	Roswell Park Memorial Institute
RRM2	:	Ribonucleotide reductase regulatory subunit-M2
RT	:	Radiotherapy
RTKs	:	Receptor tyrosine kinases
RT-qPCR	:	Real-time quantitative polymerase chain reaction
RT-qPCR_FC	:	Fold change based on real-time qPCR data
SCF	:	Skp1–Cullin1–F-box
-SH	:	Sulfhydryl groups
SKP2	:	S-phase kinase-associated protein 2
SOD	:	Superoxide dismutase
SP	:	S-phase
SP1	:	Specificity protein 1
STRING	:	Search Tool for the Retrieval of Interacting Genes
TAC	:	Transcriptome Analysis Console

TFC	:	Total flavonoid content
TGF-β	:	Transforming growth factor-β
tHGA	:	2,4,6-trihydroxy-3-geranylacetophenone
TiO_2	:	Titanium dioxide
TP53	:	Tumor protein 53
TPC	:	Total phenolic content
TPTZ	:	2,4,6-tripyridyl-s-triazine
TR	:	Transcriptional regulator
TRCs	:	Tumor repopulating cells
TX	:	Trolox
TXNRD	:	Thioredoxin reductase
UPS	:	Ubiquitin–proteasome system
UR	:	Upstream regulator
URA	:	Upstream regulator analysis
URs	:	Upstream regulators
VC	:	Vehicle control
VEGF	:	Vascular endothelial growth factor
WHO	:	World Health Organization
WPs	:	Wikipathways
WT	:	Whole transcript
z-VAD-fmk	:	N-Benzyloxycarbonyl-Val-Ala-Asp(O-Me) fluoromethyl ketone

CHAPTER 1: INTRODUCTION

1.1 Overall introduction of the study

The plant kingdom is an essential source of novel phytochemicals for drug discovery. About 25% of the drugs prescribed worldwide originated from plants (Rates, 2001). Despite such fact, only a small percentage of plant species have been scientifically studied to date, for the isolation of phytochemicals of medical importance (Rates, 2001). Plant species demonstrating antioxidant and anticancer activities are important in nutraceutical and pharmaceutical industries, because they are considered as valuable sources of dietary phytochemicals with medicinal and health-promoting properties. Dietary intake of herbs that are rich with antioxidants may help the body to counteract oxidative stress, and such benefit could potentially reduce the risk of acquiring chronic diseases such as cancer (Halliwell, 2012).

Reactive oxygen species (ROS) and reactive nitrogen species (RNS) are important for various physiological functions such as cellular growth, apoptosis, energy production and biosynthetic reactions (Stepanic, Gasparovic, Troselj, Amic, & Zarkovic, 2015). However, an imbalance in ROS and/or RNS could introduce oxidative stress, which can cause oxidative damage and leading to the development of chronic disease such as cancer (Stepanic et al., 2015). Thus, a well-balanced level of antioxidant and ROS/RNS species in the body is key to maintaining optimal health. Antioxidants are generally taken to be capable of neutralizing excessive RNS/ROS, thereby counteracting oxidative stress and protecting the cells from oxidative damage. The plant kingdom provides a rich source of biologically active phytochemicals, which are beneficial to human health. Many plant phytochemicals are known to possess antioxidant activity and they also exert numerous other bioactivities that are beneficial

for human health (Sindhi et al., 2013); (Hamid, Aiyelaagbe, Usman, Ameen, & Lawal, 2010).

Cancer is among one of the main causes of mortality worldwide. Cancerous cells are recognized by their abnormal proliferation behavior and their elusive ability to evade programmed cell death. Lung, breast, colorectal, prostate and liver cancers are among the common types of cancers (Torre et al., 2015). The events leading to the development of cancer include the dysregulation of growth factors, cell signaling pathways, cell cycle, apoptosis and metabolic enzymes (L. T. Jia, Zhang, Shen, & Yang, 2015). An effective anticancer drug should ideally overcome these dysregulations and achieve the desired therapeutic effect with minimal side effects (Pérez-Herrero & Fernández-Medarde, 2015). Radiotherapy, chemotherapy, hormonal therapy and immunotherapy are among the strategies widely adopted for cancer treatment (Pérez-Herrero & Fernández-Medarde, 2015). Although there has been notable advancement in cancer therapeutics, the current methods in cancer therapy often have unwanted side effects. For this reason, the search for effective cancer drugs with minimal side effects is still being pursued. Medicinal plants have gained growing interest for their potential use to cure various human diseases, including cancer. Medicinal plants are typically used by local folklore in various regions and their use do not typically bring any pronounced side effects. Many medicinal plants have been shown to contain bioactive phytochemicals such as polysaccharides, quinoline derivatives, phenolic acids and flavonoids, of which some of these have been shown to exert notable anticancer activity (Tariq, Mussarat, & Adnan, 2015); (Zong, Cao, & Wang, 2012); (Afzal et al., 2015); (Ls & Nja, 2016); (Chahar, Sharma, Dobhal, & Joshi, 2011).

Dietary phytochemicals are thought to exert their anticancer benefits by maintaining/altering the redox status, modulate protein-enzyme binding and/or through adjustment of kinases activity (Maru, Hudlikar, Kumar, Gandhi, & Mahimkar, 2016). Phytochemicals are known to exert various bioactivities, of which some have been reported to prevent several types of cancers through their action in modulating molecular pathways such as cell proliferation and apoptosis (Maru et al., 2016). Some examples of therapeutic modern drugs that were isolated from the plant kingdom include colchicine, podophyllotoxin, vincristine, vinblastine and taxol (S. Singh, Sharma, Kanwar, & Kumar, 2016).

Heavy metals toxicity is a serious international concern because of the wide distribution of these metals throughout the environment and their detrimental effects to human health. Arsenic, lead, chromium, cadmium, mercury, aluminum and iron are among the widely recognized biologically toxic heavy metals. They produce severe toxicity in our body by inducing oxidative stress and causing damage to the brain, liver, kidney, lung and blood (Jaishankar, Tseten, Anbalagan, Mathew, & Beeregowda, 2014). Heavy metals are generally able to denature proteins including enzymes and this could render many biological processes in living organism to be inactivated (Banfalvi, 2011). Chronic exposure of heavy metals may lead to accumulation of the toxic metals in the body, and eventually leading to the development of various diseases including cancer, neurological disorders, cardiovascular diseases, diabetes, anemia and others (Jaishankar et al., 2014). Phytochemicals such as carotenoids and flavonoids could prevent heavy metal toxicity by counteracting oxidative stress induced by heavy metals and supplementing intracellular antioxidants defense mechanism (H. S. Kim, Kim, & Seo, 2015). Phytochelations could also reduce heavy metal toxicity by metal chelation (H. S. Kim et al., 2015). Many plant extracts (e.g. garlic, ginger, onion, tomato) and

phytochemicals (e.g. catechin, curcumin) have been reported to prevent heavy metal toxicity (Zhai, Narbad, & Chen, 2015).

Melicope ptelefolia (MP) belongs to the family of Rutaceae and it is a widely known herb in Asian countries. It is known as '*tenggek burung*', '*ampang Uam*' and '*Uam, Sam Ngam*' in Malaysia, Indonesia and Thailand, respectively (Aman, 2006). Fresh MP leaves have a slight crunchy texture and a pleasant hint of refreshing lemon-lime aroma that is mildly pungent, hence it is popularly being used as a vegetable salad. Traditionally, MP has been used to address various ailments such as fever, rheumatism, stomach ache, wounds, and itches (Aman, 2006); (Perry & Metzger, 1980); (Ab. Karim, Nasouddin, Othman, Mohd Adzahan, & Hussin, 2011). However, the full potential of its medicinal benefits has not yet been investigated exhaustively. MP leaves and roots have been reported to show anti-nociceptive and anti-inflammatory activities (Sulaiman et al., 2010); (Mahadi et al., 2016). Seven compounds have been identified from the Malaysian species of MP leaves (Abas et al., 2010b), whereby 2,4,6-trihydroxy-3-geranylacetophenone (tHGA) was one of the compounds reported to show anti-inflammatory activity (Shaari, Suppaiah, et al., 2011). Melicolones A and B, isolated from MP leaves were reported to inhibit glucose induced oxidative damage in HUVEC cells (J.-F. Xu et al., 2015).

In the present study, young leaves of MP were dried and sequentially extracted using four solvents of varying polarities, namely hexane, ethyl acetate, methanol and water. The solvents system used in the extraction procedure could allow the recovery of a wider spectrum of phytochemicals from the plant material. Characterisation of antioxidant activity of the extracts was performed based on *in vitro*/chemical and cell-based antioxidant assays. The anticancer activity was investigated using human

HCT116 (colorectal), HCC1937 (breast), MDA-MB231 (breast) and HepG2 (hepatocellular) cancer cell lines. Microarray gene expression study was also performed using HCT116 and HepG2 cancer cell lines, to uncover the key genes, biological pathways and molecular events induced by MP that are responsible for its anticancer activity. Moreover, microarray gene expression profiling in Hs27 (human normal skin fibroblast) cells was carried out to analyse the gene expression changes induced by MP on non-cancerous cells. The protective effect of MP from cadmium-induced cytotoxicity in Hs27 cells were also investigated through microarray gene expression study. This study may eventually lead to the isolation of novel phytochemicals from MP that are of importance in nutraceutical industry and cancer therapeutics.

1.2 Objectives of the study

The main objectives of the study were:

I) To evaluate antioxidant and anticancer activities of MP.

II) To characterise anticancer activity of MP in hepatocellular and colorectal cancer cell lines based on microarray and quantitative reverse transcription PCR (RT-qPCR) assays.

III) To characterise antioxidant activity of MP in Hs27 cells based on microarray and RT-qPCR assays.

IV) To characterise cytoprotective activity of MP against cadmium-induced cytotoxicity in Hs27 cells based on cell viability, microarray and RT-qPCR assays.

V) To understand possible molecular mechanisms associated with MP bioactivities through the analysis of transcriptome profiles/data induced by the leaf extracts using bioinformatics tools and softwares.

CHAPTER 2: LITERATURE REVIEW

2.1 Medicinal plants and their traditional uses

Medicinal plants are defined as the plants that contain constituents with medicinal value which can be used for the treatment of diseases. They could also be a source of novel drugs (Sofowora, Ogunbodede, & Onayade, 2013). Medicinal plants are used widely throughout the world to cure various illness. According to world health organization (WHO), 80% of world population, especially those from developing countries rely on medicinal plants for their health benefits (Synge, Akerele, & Heywood, 1991); (Akerele, 1993); (Mamedov, 2012). Examples of popular medicinal plants in various geographical areas are *Acacia senegal* (Africa), *Echinacea purpurea* (America), *Duboisia hopwoodii* (Australia and Southeast Asia), *Centella asiatica* (India), *Ephedra sinica* (China) and *Carum carvi* (Middle east) (Gurib-Fakim, 2006).

During the period of 2001 to 2014, America had the highest share of import (10.9%) of medicinal plant materials, while China had highest share of export (32.0%) (Vasisht, Sharma, & Karan, 2016). Other top importer of plant materials includes Germany (8.9%), Hong Kong (8.3%), China (6.9%), Republic of Korea (5.6%), Japan (5%) and Malaysia (2.1%) (Vasisht et al., 2016). The leading exporting countries other than China were India (9.5%), Mexico (6.6%), Egypt (5.5%), Germany (3%), Hong Kong (2.7%) and Indonesia (1.5%) (Vasisht et al., 2016).

In Malaysia, herbs and herbal products account for 40.70 % and 35.90 % usage for health disorders and health maintenance respectively (Siti et al., 2009). Example of popular medicinal plants and their use by Malaysians are *Orthosiphon aristatus* ("*Misai kucing*") for hypertension; *Labisia pumila* ("*Kacip Fatimah*") for flatulence and venereal disease and *Eurycoma longifolia* Jack. ("*Tongkat Ali*") for male virility and increasing libido (Samuel et al., 2010).

In North America, *Asclepias syriaca* (Milkweed) has been used for dermatological disorders, while *Achillea millefolium* (Yarrow) has been used as an analgesic, anti-diarrheal and anti-rheumatic in traditional medicine (Frey & Meyers, 2010). In Europe, *Matricaria chamomilla* (Chamomile) and *Rosmarinus officinalis* (Rosemary) have been used in traditional medicine to treat irritable bowel syndrome and depression, respectively (Teiten, Gaascht, Dicato, & Diederich, 2013).

In Asia, *Phyllanthus emblica* (Amla) and *Curcuma longa L.* (Turmeric) have been used to treat inflammation (Jaiswal, Liang, & Zhao, 2016). *Carica papaya* L. (Papaya) have also been used as traditional medicine against hypertension, syphilis, cold and dengue respectively (Samuel et al., 2010); (Siew et al., 2014).

2.2 Drug discovery from natural sources

Nature is an important source of novel drug discovery. Forty percent of new drug entities approved by FDA form the period 1827 to 2013 were derived from natural sources (L. Katz & Baltz, 2016);(Kinch, Haynesworth, Kinch, & Hoyer, 2014). Examples of natural drug sources include plants (e.g. verapamil, morphine, codeine, vinblastine), marine organisms (e.g. ziconotide, ecteinascidin 743, halichondrin B), microorganisms (e.g. anthracycline, bleomycin, mitomycin), snake (e.g. captopril, enalapril) and frog (e.g. epibatidine) (Cragg & Newman, 2013).

Plants are considered as the main source of natural drugs. In the period of 1984-2014, natural drugs such as artemisinin (malaria), colchicine (gout), dronabinol, paclitaxel (cancer) and solamargine (cancer) have been approved as therapeutic agents (Atanasov et al., 2015). Curcumin, epigallocatechin-3-O-gallate, genistein, quercetin and resveratrol are some of the examples of phytochemicals from plants which are currently under clinical trials (Atanasov et al., 2015). The isolation of plant derived

drugs could have been due to random selection of plant extracts/phytochemicals, traditional use, phylogeny and chemotaxonomy, interaction with environment, computational prediction of bioactivities or through bioactivity directed isolation (Atanasov et al., 2015).

Numerous medicinal plants have been noted to demonstrate beneficial and therapeutic bioactivities. For example, an extract from the combination of *Rosa roxburghii* tratt and *Fagopyrum cymosum* was reported to reduce the viability of human esophageal squamous cancer (CaEs-17), human gastric cancer (SGC-7901) and lung cancer (A549) cells through apoptosis induction, mainly through the upregulation of BAX (pro-apoptotic) and downregulation of anti-apoptotic BCL-2 genes (Sultana et al., 2014). The ethanolic extract of *Santalum spicatum* was reported to inhibit α-amylase and α-glucosidase. This extract may potentially be useful for diabetic patients in reducing carbohydrate absorption (Shori, 2015). In addition, the aqueous extract of *Portulaca oleracea* L. was reported to show potent anti-inflammatory activity in RAW.264.7 (macrophage) cells by inhibiting IL-6, TNF-α, PGE2 and nitric oxide (NO) levels and reducing the expression of i-NOS (Azab, Nassar, & Azab, 2016).

2.3 Free radicals, oxidative stress and antioxidants role

2.3.1 Free radicals

Free radicals are atoms or molecules containing unpaired electrons in their atomic or molecular orbital and are considered as chemically unstable and highly reactive species (Halliwell, 2011). Excessive level of free radicals in the body can lead to oxidative stress and could lead to the development of various chronic diseases (Pham-Huy, He, & Pham-Huy, 2008). Free radicals are generally classified into two major groups. The first group include reactive oxygen species (ROS) such as hydrogen peroxide (H_2O_2),

superoxide radical ($O_2^{\bullet-}$), hydroperoxyl radical ($^{\bullet}OOH$), hydroxyl radical ($OH^{\bullet}$) and singlet oxygen ($^1O_2$). The second group include reactive nitrogen species (RNS) such as nitric oxide ($^{\bullet}NO$) and peroxynitrite ($ONOO^-$) (Stepanic et al., 2015).

Although excessive free radicals level can be harmful, regulated amounts are synthesized in the body, for the involvement in normal physiological functions. The free radicals that are synthesized in the body could originate from either enzymatic (e.g. respiratory chain formation, prostaglandin synthesis, phagocytosis, and the cytochrome P450 system) or non-enzymatic reactions (e.g. oxidative phosphorylation) (Pham-Huy et al., 2008). Free radicals can therefore appear from various physiological processes inside the body, which include response to inflammation, immune cell activation, infection, mental stress, excessive exercise, ischemia and cancer. Their synthesis can also be induced in response to several exogenous factors, including cigarette smoke, alcohol consumption, heavy metals, drugs and radiation (Pham-Huy et al., 2008).

Thus, free radicals can originate from either pathological and normal processes in the body. In terms of normal physiological roles, ROS is known to be important for processes such as cellular growth, energy production, cellular defense, cell proliferation and apoptotic programmed cell death (Stepanic et al., 2015). ROS could activate receptor tyrosine kinases (RTKs) to modulate processes such as cellular growth, differentiation and apoptosis, through MAPK signaling pathways (Valko et al., 2007). ROS also activates non-receptor tyrosine kinases, protein tyrosine phosphatases and regulates several nuclear factors including AP-1, NF-κB, p53, NFAT and HIF-1 (Valko et al., 2007). On the other hand, RNS is vital for cellular defense, regulation of blood flow, neural activity, suppression of tumors and cell signaling processes (Pham-Huy et al., 2008).

2.3.2 Antioxidant defense

An antioxidant is defined as any constituent that, at its low concentration, effectively delays, prevents or eliminates oxidative stress mediated damage to a target molecule (Halliwell, 2007). There are generally two types of antioxidants, endogenous and exogenous. The endogenous antioxidants are classified as enzymatic antioxidants (e.g. superoxide dismutase, glutathione peroxidase, glutathione reductase, catalase) and non-enzymatic antioxidants (e.g. glutathione, lipoid acid, L-arginine, melatonin, coenzyme Q10, uric acid, metal-chelating proteins, bilirubin, transferrin) (Pham-Huy et al., 2008). The exogenous antioxidants can be classified as either natural or synthetic. The natural antioxidant includes minerals (e.g. copper, iron, selenium, zinc), vitamins (e.g. vitamin A, B, C, E) and phytochemicals (e.g. catechin, β-carotene, lycopene). The synthetic antioxidant examples include butylated hydroxy anisole, butylated hydroxy toluene, propyl gallate and EDTA (Hamid et al., 2010).

The endogenous antioxidants include superoxide dismutase (SOD), which reduces superoxide anion to hydrogen peroxide, which is then converted to water and oxygen molecule by catalase (CAT) (J. Q. Wu, Kosten, & Zhang, 2013). Glutathione peroxidase (GPX) is another type of endogenous antioxidant, which neutralizes peroxide and hydroxyl radicals using glutathione as the antioxidant agent. The oxidized form of glutathione (GSSG) is regenerated back to its reduced form (GSH) by glutathione reductase (GR) (J. Q. Wu et al., 2013). Non-enzymatic antioxidants are also able to counteract oxidative stress. They are capable of inactivating reactive species and chelate metal ions to prevent the formation of free radicals (Mirończuk-Chodakowska, Witkowska, & Zujko, 2018). The blood contains albumin, which is also a non-enzymatic antioxidant that can prevent oxidation induced by $O_2^{\bullet -}$, H_2O_2, $ONOO^-$ and hypochlorous acid. Transferrin acts as antioxidant by its binding of ferrous ions, and this can prevent ferrous-induced $OH^\bullet$ formation in the body (Mirończuk-Chodakowska

et al., 2018). In addition, dietary antioxidants could also modulate antioxidant defense system of the body to maintain oxidative balance. Vitamin E protects the cell from lipid peroxidation. It is capable of inhibiting lipid peroxyl radicals that can induce the propagation of lipid oxidation in the cell membrane (Nimse & Pal, 2015). On the other hand, vitamin C can help the regeneration of glutathione in the body (Mirończuk-Chodakowska et al., 2018). Dietary flavonoids are natural antioxidants which can prevent oxidative DNA damage via metal chelating activity (Nimse & Pal, 2015).

In summary, a combination of endogenous and exogenous antioxidant can help the body to counteract oxidative stress and maintain cellular oxidative balance.

2.3.3 Oxidative stress, oxidative damage and disease

Oxidative stress is defined as a condition caused by overproduction of ROS and inadequate antioxidant defense in our body, which causes oxidative damage (Halliwell, 2011). Excessive ROS has damaging effects on biomolecules (DNA, proteins and lipids) and this could result mutation in DNA or genes (J. Q. Wu et al., 2013).

Oxidative damage is the damage to cells and tissues caused by excessive ROS (Halliwell, 2011). Oxidative damage is a contributing factor for the development of various illnesses including cancer, cardiovascular disease, neurological disease (Alzheimer's disease), pulmonary disease (e.g. asthma, chronic obstructive pulmonary disease), rheumatoid arthritis, nephropathy and ocular disease (e.g. cataracts) (Pham-Huy et al., 2008).

Cancer is perhaps an important example of chronic disease affecting many populations, and this disease could have been caused by DNA damage or mutations that are induced by oxidative stress. The mutations could inactivate tumor suppressor genes

or contribute towards oncogene activation (Pham-Huy et al., 2008). Oxidative stress in the body could be measured by monitoring certain metabolites in the body that can be linked to free radicals' levels in the body. The plasma levels of malondialdehyde, GSH-GSSG ratio, 3-nitro-tyrosine and 8-hydroxy-20-deoxyguanosine are among important oxidative stress biomarkers which are thought to be linked to carcinogenesis (Valko et al., 2007). The plasma ratio of GSH-GSSG, 3-nitro-tyrosine, acrolein, 4-hydroxy-2-nonenal and F_2-isoprostanse are among the biomarkers that could indicate oxidative stress. The levels of these markers have been observed to be abnormal in patients affected with Alzheimer's and cardiovascular diseases (Valko et al., 2007). In Alzheimer's disease, continuous oxidative stress is thought to promote production of toxic peptide (β-amyloid) in the brain, leading to brain dysfunction (dementia) as observed in Alzheimer's disease (Pham-Huy et al., 2008). Chronic oxidative stress could also induce excessive inflammation, which is linked to chronic obstructive pulmonary disease (COPD), asthma and rheumatoid arthritis (Pham-Huy et al., 2008).

2.3.4 Sources of dietary antioxidants

Dietary antioxidants are widely distributed in many foods. The common plant-based foods with their antioxidants component(s) include *Allium cepa* (quercetin), *Camellia sinensis* (EGCG), *Curcuma longa* (curcuminoids) and *Zingiber officinale* (gingerol) (Sindhi et al., 2013); (Alok et al., 2014). Examples of other foods rich in dietary antioxidants include carrots (β-carotene); kale (lutein); tomatoes (lycopene); green tea (catechin); wheat (selenium); egg yolks (vitamin A); vegetables (vitamin C) and apple (quercetin) (Hamid et al., 2010).

2.3.5 Nutraceutical supplementation of antioxidants

Aging, environmental insults and dietary habit could modulate the antioxidant defense system and alter the body's antioxidant status (Sindhi et al., 2013). Supplementation with foods containing natural antioxidants such as lycopene, α-tocopherol, lutein, vitamin C and isoflavones are thought to provide beneficial effects that may help counteract oxidative stress and potentially prevent chronic diseases linked to redox imbalances (Sindhi et al., 2013). Dietary supplementation with antioxidants such as flavonoids, lycopene, vitamin C, vitamin E and selenium have been suggested for the prevention of prostate, colon and rectal cancers (Sindhi et al., 2013); (Hamid et al., 2010). Dietary supplementation with lipoic acid has also been suggested to reduce the risk of stroke, heart attack and cataract (Hamid et al., 2010).

2.3.6 Quercetin

Quercetin (QN) is one of the widely studied phytochemical with antioxidant activity. It is also widely sold as food supplement. QN [$C_{15}H_{10}O_7$; 3,3',4',5,7-pentahydroxyflavone] is a type of flavonoid that is widely distributed in the plant kingdom (G. S. Kelly, 2011); (D'Andrea, 2015). It is among the most renowned plant phytochemical for its antioxidant activity, being capable of scavenging free radicals such as superoxide and peroxynitrite (D'Andrea, 2015). QN has been reported to prevent liver and kidney damage by inhibiting oxidative stress (D'Andrea, 2015). QN is also suggested for the management of various illnesses which include inflammation, cardiovascular, neurodegenerative diseases and cancer (Anand David, Arulmoli, & Parasuraman, 2016); (G. S. Kelly, 2011).

2.4 Cancer and the treatment of cancer

2.4.1 Cancer

Cancer is one of the leading causes of death worldwide. It is characterised by uncontrolled growth of abnormal cells in the body. In 2012, approximately 14.1 million new cases and 8.2 million cancer deaths were recorded globally (Ferlay et al., 2015). The 2012 statistics also showed that cancer was most frequent in Asia (incidence: 48%, death: 54.9%), followed by Europe (incidence: 24.4%, death: 21.5%) and America (incidence: 20.5%, death: 15.8%) (Ferlay et al., 2015). The type and number of cancer cases reported worldwide include lung (1,824,700), breast (1,676,600), colorectal (1,360,600), prostate (1,111,700), stomach (951,600) and liver (782,500) cancers (Torre et al., 2015). Lung cancer recorded the highest number of fatality in 2012 with 1.6 million deaths reported worldwide. The number of deaths recorded globally for other cancers in 2012 is as follows: liver cancer (745,500), colorectal cancer (693,900) and breast cancer (521,900) (Torre et al., 2015).

2.4.2 Etiology of cancer

2.4.2.1 Environment induced cancer

About 90 to 95% cancers are due to environmental factors (Anand et al., 2008). Diet (30-35%) is the main cause of environment induced cancers followed by tobacco (25-30%), infection (15-20%), obesity (10-20%), alcohol (4-6%) and others (10-15%) (Anand et al., 2008). Environmental carcinogens could enter our body through foods, drinks, infection and occupational contact. Environmental carcinogens responsible for the progression of cancer include viruses, radiation, asbestos, polycyclic aromatic hydrocarbons, tobacco smoke, pesticides, dioxins and organochlorines (Belpomme et al., 2007).

2.4.2.2 Inheritance of defective genes

Cancer can also be caused by inheritance of defective genes. Inheritance of the following mutated genes are associated with cancers: APC, BMPR1, PTEN (colorectal cancer); BRCA1, BRCA2 (breast cancer); CDKN2A (familial malignant melanoma); ABL, BCR (chronic myeloid leukemia); MYC (Burkitt's lymphoma); SCLC1 (lung cancer); MEN1, RET (multiple endocrine neoplasia); RB1 (retinoblastoma); TLR1, 4, 6 and 9 (prostate cancer (Anand et al., 2008).

2.4.3 Mechanism of carcinogenesis

Carcinogenesis is a multistep process involving initiation, progression and metastasis of tumor cells. Initiation of cancer involves genetic alterations of healthy cells, leading to abnormal proliferation. Additional mutations of such abnormal cells promote rapid and uncontrolled cellular growth, leading to cancer progression. Subsequent mutations of the rapidly growing mutant cells promote malignancy through invasion and metastasis (Cooper & Hausman, 2007). Several characteristics for the hallmark of cancer have been identified: sustained proliferative signaling, evasion of growth suppressors, invasion and metastasis activation, replicative immortality, angiogenesis induction and resistance against programmed cell death (Hanahan & Weinberg, 2011). Cancer cells acquire such abnormal features through dysregulation of gene expression and cell signaling pathways. The aberrant expression of genes and abnormal cell signaling pathways which play critical roles in carcinogenesis are discussed in the following sections.

2.4.4 Abnormal expression of genes in cancer

Aberrant expression of many genes is observed in human cancers. Among them, oncogenes and tumor suppressor genes are of utmost importance. Sequence alteration of oncogenes and inactivation of tumor suppressor genes could promote carcinogenesis (Macheret & Halazonetis, 2015). Oncogenes alterations could induce their overexpression, which can promote cell proliferation while inhibiting programmed cell death (PCD), eventually causing abnormal growth and leading to the development of cancer (Cooper & Hausman, 2007). Oncogenic proteins are capable of inducing several growth pathways, such as ERK signaling, Wnt signaling, and PI3K/AKT signaling, while at the same time, suppress PCD to promote abnormal cells proliferation (Cooper & Hausman, 2007). In contrast, tumor suppressor genes are able to repress cell proliferation, repair damaged DNA and activate PCD (Szychot, Brodkiewicz, & Peregud-Pogorzelski, 2013). Tumor suppressor genes are able to prevent cancer development or progression by inhibiting oncogenes, inducing PCD and suppressing the activity of proteins that induce cell cycle progression (Sun & Yang, 2010). Genomic deletion and point mutations in cancer cells typically result in tumor suppressor genes inactivation, allowing the cancer cells to avoid cell cycle checkpoints and PCD mechanisms, leading to abnormal proliferation activity (Macheret & Halazonetis, 2015). The following are top oncogenes which are typically overexpressed in cancers: CCND1, EGFR, MYC, TERC, ERBB2, CCNE1, MCL1, MDM2 and WHSC1L1. Tumor suppressor genes that are frequently deleted or mutated in cancers include CDKN2A, STK11, ARID1A, PTEN, p53 and RB1 (Macheret & Halazonetis, 2015); (Cooper & Hausman, 2007).

2.4.5 Cell signaling and cancer development

2.4.5.1 Cell signaling and growth

The cell signaling pathways require participation of various proteins and biomolecules which interact dynamically together, to exert their cellular functions (Valdespino-Gómez, Valdespino-Castillo, & Valdespino-Castillo, 2015). The signaling pathways that play important role in cell proliferation are MAPK/RAS/RAF/ERK, PI3K/AKT, E2F/DP1/RB1/cyclin D-CDK4/6, TGF-β, Hedgehog and Hippo (Valdespino-Gómez et al., 2015); (Perrimon, Pitsouli, & Shilo, 2012). Growth factor mediated activation of MAPK/RAS/RAF/ERK signaling induces cyclin D expression. Cyclin D-CDK4/6 complexes facilitate G_1-S cell cycle progression by inhibiting RB1 through phosphorylation. This allows E2F transcription factor proteins recruitment to their target promoter sites to induce expression of genes that can promote cell cycle progression (Valdespino-Gómez et al., 2015).

2.4.5.2 Alterations of cell signaling, growth pathways and carcinogenesis

Oncogenic mutations often lead to overexpression of growth stimulatory protein(s) such as EGFR, RAS, RAF, AKT, PI3K, ER, Wnt, Hh, Hippo and Notch. The overproduction of such proteins associated with cell signaling and growth can induce uncontrolled proliferation (Sever & Brugge, 2015). On the other hand, mutation or deletion of tumor suppressors including p53, RB1 and cyclin dependent kinase inhibitors (CDKIs) deprive the cells from regulatory mechanism of growth suppression, and this can lead to cancer development (Sever & Brugge, 2015). Some of the growth signaling pathways are summarized below:

(a) ***Fibroblast growth factor (FGF) signaling***

The FGF family consists of 23 FGFs and five fibroblast growth factor receptors (FGFRs). They have pivotal functions in organogenesis, tissue injury and repair (Ornitz & Itoh, 2015). In FGF pathway, the association of FGF, EGFR and heparan sulfate facilitates the activation of PI3K-AKT, RAS-MAPK and STAT signaling pathways (Brooks, Kilgour, & Smith, 2012), leading to the induction of proliferation, angiogenesis, self-renewal, survival, differentiation and epithelial to mesenchymal transition (EMT) (Katoh, 2016). Mutation of FGFs and FGFRs trigger progression of numerous cancers including prostate (FGF2), breast (FGF3), hepatocellular (FGF8), colorectal (FGF9), small cell lung (FGFR1) and gastric cancers (FGFR2) (Ornitz & Itoh, 2015).

(b) ***Transforming growth factor-β (TGF-β) signaling***

The TGF-β regulates cell proliferation, apoptosis, EMT, invasion, metastasis and immune evasion (Meulmeester & Ten Dijke, 2011). The components of TGF-β signaling pathway are TGF-β (TGF-β1, TGF-β2 and TGF-β3 in mammals) and serine threonine kinase receptors TβRI and TβRII (L. H. Katz et al., 2013). The TGF-β/TβRI complex interaction with Smad, MAPK/TRAF6/TAK1-JNK/p38, PI3K-AKT and RHo-Rock signaling pathways could modulate cell proliferation and apoptosis (L. H. Katz et al., 2013); (Meulmeester & Ten Dijke, 2011). Although TGF-β is capable of suppressing tumor initiation in normal cells, it could also promote cancer development by inducing the evasion of cancer cells from immune surveillance, activating EMT and induction of metastasis and angiogenesis in mutated cells (L. H. Katz et al., 2013). Mutation in TGF-β receptors (TβRI and TβRII) is associated with colorectal, gastric, pancreas, ovarian and breast cancers (Meulmeester & Ten Dijke, 2011).

(c) ***Vascular endothelial growth factor (VEGF) signaling***

The VEGF proteins belong to the family of platelet-derived growth factor (PDGF) which are capable of modulating angiogenesis and embryonic development (Sia, Alsinet, Newell, & Villanueva, 2014). In VEGF signaling, the VEGF proteins (VEGFA, PIGF, VEGFB, VEGFC, FIGF in mammals) bind to their receptors (VEGFRs) and interact with PI3K and MAPK signaling pathways to regulate proliferation and survival (Sia et al., 2014). Abnormal VEGF signaling is associated with diverse cancers, including hepatocellular carcinoma (VEGFR2); breast, lung and colon cancers (VEGF, VEGFR1, VEGFR2); prostate cancer (VEGF, VEGFR1) and ovarian cancer (VEGF) (Goel & Mercurio, 2013).

(d) ***Phosphatidylinositol 3-kinase- protein kinase B (PI3K-AKT) signaling***

The PI3K is a family of lipid kinases, which are known to regulate cell growth and proliferation, while AKT is the downstream signaling molecule (Faes & Dormond, 2015). Upon activation by PDK1 and mTORC2, AKT then inhibit TSC2, FOXO, p21, p27, BAD and GSK3 functions, leading to cell proliferation (Faes & Dormond, 2015). PI3K is also able to facilitate cell proliferation without the involvement of AKT (Faes & Dormond, 2015); (Thorpe, Yuzugullu, & Zhao, 2015). Dysregulation of PI3K signaling has been reported to be associated with several cancers including breast and colorectal cancers (PIK3CA, PIK3R1); lung cancer (PIK3CA, PIK3CB) and prostate cancer (PIK3CA) (Thorpe et al., 2015).

(e) ***RAS signaling***

The RAS family of proteins has members that belong to a class of protein known as small GTPase. RAS is the downstream signaling molecule of the receptor tyrosine kinases (RTKs) (e.g. epidermal growth factor receptor) and upstream of the signaling pathways such as RAF-MEK-ERK and PI3K-PTEN-AKT. These RAS-associated pathways are known to be linked to cancer progression (Stites & Ravichandran, 2009). The RTKs are a family of tyrosine kinases that have domains for extracellular ligands (e.g. EGF, PDGF) and tyrosine kinase activity (Paul & Mukhopadhyay, 2004). The RTKs are activator of many signaling pathways (e.g. MAPK, PI3K) and enzymes (e.g. RAS) (Segaliny, Tellez-Gabriel, Heymann, & Heymann, 2015). Dysregulation of RTKs through genomic alterations, autocrine-paracrine stimulation, mutation and overexpression activates cell cycle and promotes carcinogenesis (Paul & Mukhopadhyay, 2004); (McDonell, Kernohan, Boycott, & Sawyer, 2015). RTKs such as EGFR, PDGFR, FGFR, HGFR are involved in the development of cancer (Segaliny et al., 2015). The most clinically notable RAS members include HRAS, NRAS and KRAS (Stites & Ravichandran, 2009). Abnormal RAS signaling due to RAS gene mutations have been linked to the development of several cancers including lung, pancreatic, and ovarian cancers (KRAS); colon cancer (KRAS, NRAS); thyroid and endometrial cancers (NRAS); cervical cancer (HRAS) and urothelial cancer (NRAS, HRAS) (H. Singh, Longo, & Chabner, 2015).

(f) ***Mitogen-activated protein kinase (MAPK) signaling***

The MAPK signaling plays vital role in cell proliferation, survival and migration (Rovida & Stecca, 2015). The mammalian MAPK family includes extracellular signal-regulated kinases1/2 (ERK1/2), c-JUN NH2-terminal kinases (JNKs) and p38 (p38α/β/

γ/δ) signaling (Huang, Han, & Hui, 2010). Among these, ERK1/2 signaling is most frequently dysregulated in cancer (Rovida & Stecca, 2015). The ERK1/2 is activated by hormones and growth factors through RAS-RAF-MEK signaling (Huang et al., 2010). Mutations in BRAF and RAS genes lead to increased activation of MAPK/ERK pathway, and this has been reported to cause melanoma and thyroid cancer progression (Burotto, Chiou, Lee, & Kohn, 2014). The BRAF V600E is very commonly reported mutation and resulted in the constitutive activation of BRAF and ERK signaling pathway (Wan et al., 2004). RAS mutations can also promote colorectal cancer through the stimulation of MAPK/ERK signaling pathway (Burotto et al., 2014).

(g) ***Cell cycle***

The RB1 protein, cyclins, cyclin dependent kinases (CDKs), CDKIs and E2Fs are the principle components of the cell cycle (H. Z. Chen, Tsai, & Leone, 2009). The RB1 protein is able to inhibit E2F transcription factors functions to control the cell cycle progression, and thus exert tumor suppressive role (Chinnam & Goodrich, 2011). On the other hand, CDKs through their association with cyclins are able to inactivate RB1, permitting E2F transcription factors to promote cell cycle progression. The CDKIs are capable of inhibiting CDKs to suppress cell cycle progression (H. Z. Chen et al., 2009). RB1 and CDKIs are commonly mutated or deleted genes in human cancers (Macheret & Halazonetis, 2015); (Cooper & Hausman, 2007). In many types of cancers, overexpression of CDKs and E2Fs have been reported and this can arise from their mutations or amplification (H. Z. Chen et al., 2009).

(h) ***p53 signaling***

The p53 protein is a classical tumor suppressor protein that has been long regarded as the guardian of genome. It regulates diverse biological functions, including apoptosis, cell proliferation, inflammation, autophagy, DNA damage response, stress response, EMT and invasion (Kastenhuber & Lowe, 2017). The p53 protein does not normally interfere with cell cycle progression. However, in response to DNA damage and oncogenic stress, p53 induces p21 and pro-apoptotic PUMA, NOXA and BAX to arrest the cell cycle and induce apoptosis (Mandinova & Lee, 2011). p53 is frequently mutated or deleted in diverse types of cancers (Cooper & Hausman, 2007). p53 mutations are associated with invasion, migration, proliferation, cell cycle activation, drug resistance, angiogenesis, cell survival and genomic instability (Muller & Vousden, 2014).

2.4.6 Cancer treatment modalities

2.4.6.1 Chemotherapy

Chemotherapy is a form of cytotoxic therapy that targets cancerous cells, specifically biological processes such as cell proliferation, apoptosis and angiogenesis (Kris, Hellmann, & Chaft, 2014). It is broadly divided into three categories: DNA damaging agents, antimetabolites and antimitotics. These are further sub-divided into following classifications (Thirumaran, Prendergast, & Gilman, 2007):

I) DNA damaging agents

- A. Alkylating agents: e.g. melphalan, cyclophosphamide, ifosfamide
- B. DNA topoisomerase inhibitors
  - a. Plant alkaloids: e.g. etoposide, irinotecan, topotecan
  - b. Antitumor antibiotics: e.g. doxorubicin, daunorubicin
- C. Platinum compounds: e.g. cisplatin, carboplatin, oxaloplatin

II) Antimetabolites

A. Folate antagonists: e.g. methotrexate

B. Purine antagonists: e.g. 6-mercaptopurine, 5-flurouracil

III) Antimitotics

A. Vinca compounds: e.g. vinblastine, vincristine, vinorelbine

B. Taxanes: e.g. paclitaxel, docetaxel

Diverse chemotherapeutic agents have been widely used for the treatment of various types of cancers such as melanoma (temozolomide), breast cancer (etoposide, doxorubicin, methotrexate), lung cancer (ifosfamide, irinotecan, doxorubicin), colorectal cancer (irinotecan, oxaloplatin), liver cancer (doxorubicin, 5-fluorouracil), prostate cancer (mitoxantrone, paclitaxel) and cervical cancer (Ifosfamide) (Thirumaran et al., 2007).

2.4.6.2 Immunotherapy

Immunotherapy is a form of therapy that targets the immune system components (antibodies, dendritic cells, cytokines) to treat/manage cancer disease (Arruebo et al., 2011). Some examples of cancer immunotherapy include the use of monoclonal antibodies, vaccines and adoptive cell therapy (ACT) (Snook & Waldman, 2013).

Sipuleucel-T is a vaccine indicated in the treatment of prostate cancer (Arruebo et al., 2011). Sipuleucel-T uses antigen presenting cells (APCs) of the patients to stimulate $CD4^+$ and $CD8^+$ T cell immune response against prostate cancer antigen, prostatic acid phosphatase (PAP) to inhibit prostate cancer progression (Mulders, De Santis, Powles, & Fizazi, 2015).

Monoclonal antibodies that have been used in cancer treatment include trastuzumab (breast cancer), cetuximab (colorectal cancer), pembrolizumab (melanoma, non-small cell lung carcinoma) (Snook & Waldman, 2013); (Kwok, Yau, Chiu, Tse, & Kwong, 2016). Pembrolizumab is an IgG4 monoclonal antibody, which targets programmed cell death protein 1 (PD1) (Jazirehi, Lim, & Dinh, 2016). PD1 is a surface membrane protein that is expressed on several immune cells including T-cells (Kwok et al., 2016). PD1 normally acts as a type of "off switch", preventing the T-cells from attacking normal cells in the body. Activated T-cells is capable of mounting immune response by mediating apoptosis in cancer cells (Jazirehi et al., 2016). However, cancer cells often overexpress PDL1 (programmed cell death ligand 1) and PDL2 (programmed cell death ligand 2). The binding of PD1 with PDL1 could halt or limit T-cells immune function, allowing cancer cells to evade from T-cells detection and destruction (Kwok et al., 2016). The binding of pembrolizumab onto PD1 on the T-cells prevents its interaction with PDL1 and PDL2 (Jazirehi et al., 2016), and this allows T-cells to detect and destroy cancer cells.

2.4.6.3 Radiotherapy

Radiotherapy (RT) is the use of ionizing radiation to kill cancer cells through activation of several cell death mechanisms including mitotic catastrophe, apoptosis, autophagy and necrosis (R. Baskar, Lee, Yeo, & Yeoh, 2012). In comparison to other treatment options, RT could be a better choice because of targeted regional therapy and lower toxicity profile, which could lead to better survival rate (Delaney, Jacob, Featherstone, & Barton, 2005). A survey for the treatment employed in patients affected with various types of cancers indicated that 52.3% of the cases received RT as a recommended strategy of treatment (Delaney et al., 2005). Early stages of cancers (e.g.

skin, prostate, lung) may be successfully treated with RT alone, while cancers at advanced stages (e.g. lymphomas, head and neck, cervical) require the use of RT and other therapeutic approaches (R. Baskar et al., 2012).

2.4.7 Limitations of current cancer therapeutics

The most notable issue in cancer therapy is drug resistance. Several cancer drug resistance mechanisms have been proposed, including alteration of drug efflux, mutation of drug targets, inhibition of apoptosis and autophagy, EMT, alteration of DNA repair and cell cycle and increased drug metabolism (Xia & Hui, 2014).

Elevated drug efflux could reduce chemotherapeutic drug delivery in cancer cells (Xia & Hui, 2014). The elevated efflux may occur by inducing elevated expression of ATP binding cassette (ABC) transporters namely P-glycoprotein (P-gp), multidrug associated resistance proteins (MRPs) and mitoxantrone resistance protein (MXR) (Xia & Hui, 2014).

Multidrug resistance (MDR) is a process of drug resistance which is regulated by ABC transporters and solute carrier transporters (F. S. Liu, 2009). Of note, resistance to chemotherapeutic agents such as doxorubicin, 5-FU, paclitaxel, etoposide, cisplatin, and many others arise from the activity of ABC transporters (Sodani, Patel, Kathawala, & Chen, 2012); (Saraswathy & Gong, 2013). It is therefore significant to mention that inhibition of ABC transporters could potentially be beneficial in cancer treatment. The inhibitors that are known to inhibit ABC transporters include polyphenols (e.g. quercetin, resveratrol), flavonoids (e.g. curcumin, epigallocatechin, epigallocatechin-3-galate), plant derived compounds (e.g. rosmarinic acid, polyacetylenes), plant secondary metabolites (e.g. terpenoids, alkaloids, digitonin) and Chinese herbal medicines (e.g.

emodin, artemisinin, tanshinone) (Karthikeyan & Hoti, 2015). These agents could potentially increase the efficacy of chemotherapeutic agents against cancer.

Drug resistance may also develop through target site mutations. Mutations of the target proteins may cause overactivity of biomolecules (e.g. genes, receptors), minimizing or blunting the effect of the therapeutic drugs (Housman et al., 2014). Activation of DNA repair processes upon treatment with DNA damaging agents may also facilitate drug resistance (Housman et al., 2014), leading to cancer cells survival. Inhibition of drug induced apoptosis is also another mechanism of resistance. This may involve overexpression of anti-apoptotic proteins (e.g. BCL-2, IAPs) and/or downregulation of pro-apoptotic proteins expression (e.g. BAX, BAD, BIM, NOXA) by cancer cells (Pan, Li, He, Qiu, & Zhou, 2016).

Severe toxicity is another main limitation of current cancer therapeutics, encouraging researchers to find alternative drugs that are more selective on cancer cells with lower side effects. Although radiotherapy and chemotherapy approaches are often used in cancer therapy, they may also cause damage to non-cancerous tissues, causing undesired toxicities (Cleeland et al., 2012). Common radiotherapy toxicities include fatigue, cognitive dysfunction, pneumonitis, gastroenteritis and mood disorders. Adverse reactions associated with chemotoxicities include fatigue, cognitive dysfunction, depression, peripheral neuropathy, cardiomyocyte damage, vascular complications and gastroenteritis (Cleeland et al., 2012). Immunotherapy toxicities include vitiligo, hypotension, fever, fatigue, depression and psychosis (Weber, Yang, Atkins, & Disis, 2015).

2.4.8 Use of plants in the treatment of cancer

The plant kingdom provides diverse source of phytochemicals and these can be evaluated for their potential use in cancer therapeutics. Many plant extracts and phytochemicals have been reported to show notable therapeutic activity against various cancers, which include breast cancer (e.g. *Annona squamosa* L., *Bauhinia variegata* L., curcumin), colorectal cancer (e.g *Taxus wallichiana* Zucc., quercetin, resveratrol), and hepatocellular carcinoma (e.g. quercetin, curcumin, epigallocatechin-3-gallate) (Tariq et al., 2015).; (L. Ouyang et al., 2014).

In the last three decades, plant derived drugs namely arglabin, masoprocol, paclitaxel and solamargine have been approved for cancer therapy (Atanasov et al., 2015). Numerous plant phytochemicals (e.g. resveratrol, lycopene, genistein, polyphenon E, curcumin, and epigallocatechin-3-O-gallate) are currently under clinical trials for their potential use in cancer treatment (Russo, Spagnuolo, Tedesco, & Russo, 2010); (Atanasov et al., 2015).

Lycopene is an example of a well-known plant phytochemical demonstrating anticancer activity. It is found in many foods including tomato, watermelon, papaya, guava and grapefruit. Lycopene is reported to inhibit cell proliferation, modulate cell cycle and induce apoptosis in prostate cancer cells (Holzapfel et al., 2013). Lycopene also upregulated cell cycle inhibitors p21, p27 and tumor suppressor p53, while it downregulated cell cycle promoter cyclin D1 to suppress proliferation of prostate cancer cell line LNCaP (Holzapfel et al., 2013). Lycopene suppressed PI3K/AKT proliferative signaling pathway by inhibiting IGF-1, IGF-1R and PI3K, and BCL-2 anti-apoptotic protein (J. Chen et al., 2014).

Numerous animal studies have demonstrated resveratrol as a potential therapeutic agent against colorectal, breast, prostate, liver and pancreatic cancers (Carter, D'Orazio,

& Pearson, 2014). Resveratrol induced apoptosis and cell cycle arrest while suppressed PI3K/AKT and hedgehog signaling in pancreatic cancer cell lines (BxPC-3 and Panc-1) (Q. Xu et al., 2015). Resveratrol also upregulated cell cycle inhibitors (p21 and p27) and downregulated cell cycle promoter cyclin D1 and anti-apoptotic BCL-2 protein expression in human pancreatic cancer cell line Panc-1 (Q. Xu et al., 2015). Moreover, resveratrol has been found to show potent antiproliferative, pro-apoptotic and cell cycle inhibitory activities in numerous gastric carcinoma cell lines (Zulueta, Caretti, Signorelli, & Ghidoni, 2015).

2.5 Application of plant extracts, phytochemicals and topical drugs in dermatology and cosmeceuticals

2.5.1 Skin diseases and topical agents used for their treatment

The skin is the largest organ in the human body. It acts as a protective barrier to the internal organs against environmental insult (e.g. UV-radiation and pathogenic microorganisms). Disorders associated with the skin include acne, actinic damage, dermatitis, benign and malignant skin cancer, pruritis, psoriasis, rosacea, seborrheic dermatitis, and vitiligo (H. W. Lim et al., 2017).

Some of the topical agents used for the treatment of common skin diseases are shown in **Table 2.1**.

Table 2.1: Topical agents for the treatment of skin diseases

Skin disease	Topical agent	Reference
Scabies	Ivermectin	(Panahi, Poursaleh, & Goldust, 2015)
Acne	Nicotinamide	(Rolfe, 2014)
Atopic dermatitis	Doxepin, menthol, cannabinoids, Betamethasone dipropionate	(Ghazvini, Pagan, Rutledge, & Goodman, 2010); (Yarbrough, Neuhaus, & Simpson, 2013)
Melasma	Tretinoin, nicotinamide	(Beckenbach, Baron, Merk, Loffler, & Amann, 2015); (Rolfe, 2014)
Rosacea	Nicotinamide	(Rolfe, 2014)
Psoriasis	Tacrolimus, pimecrolimus,	(C. Wang & Lin, 2014)
Actinic keratosis	5-fluorouracil	(Haque, Rahman, Thurston, Hadgraft, & Lane, 2015)
Kaposi's sarcoma	Alitretinoin	
Wound healing	Dexpanthenol	(Proksch, de Bony, Trapp, & Boudon, 2017)

2.5.2 Plants as medicinal agent for wound healing and skin disorders

Wound is a disturbance of the cellular and anatomic continuance of a tissue (Karapanagioti & Assimopoulou, 2016). A wound is formed when skin is injured by external stimuli. The process of wound healing is comprised of three main phases namely inflammatory, proliferation and remodeling (Maver, Maver, Stana Kleinschek, Smrke, & Kreft, 2015).

Plants can be used as a medicinal agent for wound healing. In clinical application, the use of plant extracts/phytochemicals as wound healing agent has been proven and some widely known plant species with wound healing activity include *Aloe vera* L. (Aloe), *Calendula officinalis* L. (common Marigold) and *Centella asiatica* L (Gotu kola) (Karapanagioti & Assimopoulou, 2016).

Plant phytochemicals (e.g. curcumin, gallic acid, resveratrol, quercetin, kaempferol) have also been documented to show wound healing activity (Ghosh & Gaba, 2013). Curcumin wound healing activity is achieved through enhancement of fibroblast migration, granular tissue formation, collagen deposition and re-epithelization during proliferative phase. It also facilitates wound contraction by increasing the production of TGF-β during remodeling (Akbik, Ghadiri, Chrzanowski, & Rohanizadeh, 2014). Aloe have also been used for wound healing. The wound healing activity of Aloe on burn tissues were suggested to be associated with enhancement of collagen synthesis, increased epithelialization and anti-inflammatory, antimicrobial and moisturizing effects (Maenthaisong, Chaiyakunapruk, Niruntraporn, & Kongkaew, 2007).

Medicinal plants such as *Azadirachta indica* (Neem), *Curcuma longa* (Turmeric), Aloe, tea tree oil and green tea have been used in the treatment of acne (Nasri et al., 2015); (Pazyar, Yaghoobi, Bagherani, & Kazerouni, 2013); (Zink & Traidl-Hoffmann, 2015).

Psoriasis is associated with abnormal epidermal keratinocyte hyperproliferation and altered differentiation. Psoriasis has been treated using medicinal plants such as *Centella asiatica*, *Echinacea angustifolia* and *Echinacea purpurea* (Bylka, Znajdek-Awizen, Studzinska-Sroka, Danczak-Pazdrowska, & Brzezinska, 2014); (Tabassum & Hamdani, 2014). *Centella asiatica* extract has been shown to reduce keratinocyte cell line proliferation and this observation is supportive to its therapeutic use in psoriasis (Sampson, Raman, Karlsen, Navsaria, & Leigh, 2001).

Contact dermatitis is associated with the release of inflammatory cytokines from human mast cells. Quercetin has been shown to inhibit the release of the inflammatory cytokines from mast cells that were exposed to substance P, and this provided a basis for the use of quercetin in the management of contact dermatitis (Weng et al., 2012).

2.5.3 Plants and phytochemicals applications in skin cosmetics

Plants are widely used for the preparation of cosmetics. The majority of herbal cosmetics patent application are for skin care products (skin whitening, skin tanning, cellulite prevention, anti-aging and washing or bathing) (César, Carnevale Neto, Porto, & Campos, 2017). According to the statistics, China is the leading country in herbal cosmetics patent applications (7,130) and this is followed by Korea (3,100), Japan (2,594), World Intellectual Property Organization (1,614), France (742), USA (585), Germany (345) and European Patent Office (249) (César et al., 2017).

The following common plant origin materials are used in cosmetics for skin moisturizing effect: castor oil, mango, sunflower oil, cocoa butter, coconut oil and olive oil (Aburjai & Natsheh, 2003). Omega-3 fatty acids, sterols and silymarin are also used as ingredients in cosmetics for skin hydration and moisturizing effect (Antignac, Nohynek, Re, Clouzeau, & Toutain, 2011).

Ginseng, lycopene, vitamin C and vitamin E have been used in anti-aging cosmetic products (Aburjai & Natsheh, 2003); (Antignac et al., 2011). Ginseng have been shown to inhibit free radicals and lipid peroxidation-induced oxidation, and thus confer antioxidant benefit to the skin cells. Ginseng is also suggested to impart anti-aging benefits by improving blood circulation to the skin and increasing the rate of skin cells proliferation (Aburjai & Natsheh, 2003).

Kojic acid, aloesin, vitamin C, soy proteins and arbutin have been used as skin whitening agents (Antignac et al., 2011). The skin whitening effect of arbutin and kojic acid is due to their inhibition of tyrosinase enzyme activity (Couteau & Coiffard, 2016).

2.5.4 Dexpanthenol as a topical skin agent

Dexpanthenol (DX) is the alcoholic analogue of pantothenic acid (vitamin B5). It is capable of acting as a moisturizing agent that can improve the rate of skin epidermal layer regeneration and thus, improve wound healing and skin barrier function (Proksch et al., 2017). It is used for the management of atopic dermatitis, nappy rash, diabetic feet care, cracked nipples, wound healing, prevention of scar, skin injury and irritated skin (Proksch et al., 2017); (Ebner, Heller, Rippke, & Tausch, 2002).

Gene expression study in human skin wound revealed that DX facilitated wound healing by modulating many genes, including CCL18, CCR1, CXCL1, CYP1B1, IL1B and IL-6 (Heise et al., 2012). DX was also reported to upregulate the expression of antioxidant gene HMOX1 in human skin fibroblasts. The HMOX1 gene encodes HO-1, which is a key protein that can inhibit free radical formation. This could improve skin antioxidant status and induce skin anti-inflammatory defense mechanisms (Wiederholt et al., 2009).

2.6 Cadmium toxicity and the prevention of cadmium toxicity

2.6.1 Heavy metals and their toxicity

Heavy metals are used in many industrial applications including smelting, welding, painting, ceramics, production of batteries and fertilizers (Jan et al., 2015); (Tchounwou, Yedjou, Patlolla, & Sutton, 2012); (H. S. Kim et al., 2015). Cadmium, mercury, arsenic, chromium, lead and nickel are considered as biologically toxic heavy metals. Inhalation and ingestion of these metals from natural and industrial sources cause potential health hazards. Mercury is highly toxic in its elemental form while some heavy metals are toxic in their cationic forms (Pb^{2+} or Pb^{4+}; Cd^{2+}; As^{3+}), as they are more soluble in water and easily transported throughout the body. Heavy metal cations

have a strong affinity for sulfhydryl groups (-SH) which is found in various proteins (e.g. enzymes) of living organism (Banfalvi, 2011). Heavy metals toxicity to living organisms is mainly contributed by their deleterious effects on enzyme functions. The binding of heavy metals to the -SH groups could inactivate enzymes, denaturing its native structure and causing enzyme catalytic function failure (Banfalvi, 2011). Inhibition may also occur when a heavy metal displaces an essential metal cofactor of the enzyme. For example, lead may displace zinc in the zinc-dependent enzyme δ-aminolevulinic acid dehydratase. This can inhibit the synthesis of heme, an important component of hemoglobin and heme-containing enzymes. Toxic metals may also disrupt enzymes and its function in certain subcellular organelles. Such disruption may lead to endoplasmic reticulum dysfunction, accumulation of metals in lysosomes, dysfunction of respiratory enzymes in the mitochondria and formation of metal inclusion bodies in the nucleus (Cope, Leidy, & Hodgson, 2004). The harmful effects brought about by heavy metals include cancer, infertility, brain damage, birth defects, osteoporosis, anemia, gastrointestinal damage and toxicities to kidney, liver and lung (Jan et al., 2015); (Tchounwou et al., 2012); (H. S. Kim et al., 2015).

2.6.2 Environmental sources of cadmium

The highest content of cadmium (Cd) is found in sedimentary rocks and marine phosphates (15 mg cadmium/kg) (Tchounwou et al., 2012). Cd is widely used in various industrial processes including electroplating, manufacturing of batteries, alloys, pigments and fertilizers (Tchounwou et al., 2012); (H. S. Kim et al., 2015). Human exposure to Cd is mainly from ingestion of contaminated food and water, tobacco smoking, inhalation of polluted air and dust particles polluted with Cd (Nawrot et al., 2010). Cd distributed in atmosphere, fertilizers and sewage sludge may accumulate and contaminate the soil, which could potentially contaminate food crops and expose human to Cd (Jarup & Akesson, 2009). It has been reported that several foods including crabs,

molluscs, oysters, cephalopods, kidney, liver, oil seeds, wild mushrooms, cocoa beans, rice wheat, carrot, potato, green leafy vegetables etc. contain high content of Cd (Jarup & Akesson, 2009).

2.6.3 Cadmium toxicity

Cd is detrimental to health as it can inhibit antioxidant defense and induce DNA strand breakage, chromosomal abnormalities, ROS production and apoptotic cell death. This can lead to several toxicities including Itai-itai disease, renal toxicity, reproductive toxicity, cardiovascular toxicity, neurotoxicity, skin toxicity and cancer development (Rahimzadeh, Rahimzadeh, Kazemi, & Moghadamnia, 2017).

Cd poisoning promotes oxidative stress by inducing the deficiency of glutathione (GSH) and antioxidant enzymes function (Rahimzadeh et al., 2017). GSH is a thiol containing antioxidant agent, which is important for the maintenance of many cellular functions including redox homeostasis, detoxification, proliferation, apoptosis and DNA repair (Kalinina, Chernov, & Novichkova, 2014). Depletion of GSH and inhibition of glutathione regulated enzymes such as glutamate cysteine ligase, glutathione reductases, glutaredoxins, glutathione peroxidases can alter cellular antioxidant status and leading to oxidative stress (Rubino, 2015). Cd-induced GSH depletion results in the formation of increased superoxide and hydrogen peroxide radicals, which are normally neutralised by antioxidant enzymes such as SOD and CAT, respectively (J. Liu, Qu, & Kadiiska, 2009). However, Cd can inhibit SOD and CAT, leading to free radicals accumulation and causing oxidative stress.

In humans, Cd is eliminated through urine as metallothionine (MT) bound complex (CdMT). MT is a low–molecular weight, cysteine-rich stress response protein with a high affinity for divalent heavy metals (Lynes & Yin, 2006). MT proteins have many

thiolate (-SH) groups that form covalent bonds with cadmium (Cd-S), to protect various tissues and organs in the body from Cd toxicity. However, rapid renal absorption of CdMT might induce renal toxicity through the breakdown of CdMT complex inside lysosome, which releases Cd from the complex and causing renal toxicity (Hodgson & Levi, 2004). As Cd has half-life of 10-12 years in humans, low level chronic exposure of Cd can ultimately lead to accumulation of Cd in the body at toxic concentrations (Hodgson & Levi, 2004).

Cd toxicity may also cause interference with DNA repair mechanisms, such as nucleotide excision repair, base excision repair, mismatch repair and DNA double-strand break repair. Cd may also cause the failure of cell cycle arrest and apoptosis execution in abnormal cells with damaged DNA by inhibiting p21, p53, CASP3 and BAX. This could contribute towards genomic instability and leading to cancer development (Filipic, 2012). In higher eukaryotes, DNA double-strand break repair require the use of DNA-dependent protein kinase (DNA-PK) (Filipic, 2012). This enzyme can be inhibited by Cd. Cd may also promote cancer by activating protooncogenes and disrupting cell adhesion, to encourage cancer metastasis (Rahimzadeh et al., 2017). Cd cytotoxicity may also occur through apoptosis induction, arising from Cd-induced oxidative stress. This cytotoxic effect is linked to c-JUN N-terminal kinase (JNK), p38 kinase and extracellular-signal-regulated kinase (ERK) signaling pathways (Filipic, 2012). Human renal mesangial cells treated with $CdCl_2$ exhibited apoptosis induction with inhibition of cellular proliferation and these were associated with activation of JNK signaling (Xiaocui Chen et al., 2016).

2.6.4 Alteration of gene expression by cadmium

The proto-oncogenes FOS (also known as c-FOS), MYC (also known as c-MYC) and JUN (also known as c-JUN) are among the immediate early response genes (IERGs) that can be induced by Cd (Waisberg, Joseph, Hale, & Beyersmann, 2003). Heat shock protein (HSP) genes, including HSP32, HSP60, HSP70 and MT genes are also upregulated from Cd exposure, to protect the cells from Cd toxicity (Sandbichler & Hockner, 2016); (Waisberg et al., 2003). Numerous apoptotic genes such as BAX, CASP8, CASP9 and TNFRSF1B were also upregulated by Cd (Luparello, Sirchia, & Longo, 2011).

In rat renal cells WKPT-0293 Cl.2, Cd exposure was reported to induce upregulation of antioxidant genes SOD1, GCLC and GCLM (Nair et al., 2015). However, Cd also upregulated pro-apoptotic BAX gene expression in WKPT-0293 Cl.2 cells and this resulted in Cd-induced cytotoxic effect (Nair et al., 2015).

Cd exposure was also reported to increase the expression of DNA damage response genes GADD45B, GADD45G and DDIT3 in BEAS-2B cells (human bronchial epithelial cells) (J. Kim et al., 2017).

2.6.5 Treatment and management of cadmium toxicity

The human body may protect itself from Cd toxicity through mechanisms such as induction of antioxidant defense, metal chelation, and excretion of Cd (Sandbichler & Hockner, 2016). The antioxidant molecule GSH inhibits cadmium toxicity by its metal chelation activity. The formation of a complex between Cd and thiol residues of GSH prevents Cd toxicity and promotes Cd excretion. The MT proteins also play vital roles for Cd detoxification thorough its metal chelation activity (Sandbichler & Hockner,

2016). Furthermore, the expression of many antioxidant enzymes is induced during Cd exposure, including catalase (CAT), superoxide dismutase (SOD), peroxiredoxin 2 (PRDX2), glutathione peroxidase 4 (GPX4), thioredoxin reductase (TXNRD), hemeoxygenase-1 (HMOX1) and glutamate-cysteine ligase (GCL) (Sandbichler & Hockner, 2016).

Many antioxidant vitamins (vitamin A, C, E) and minerals (Zn, Mg) also prevent Cd toxicity through improvement of antioxidant status (Rahimzadeh et al., 2017).

For medical intervention, individuals affected with Cd toxicity may also be treated with specific chelating agents such as N- tetramethylene dithiocarbamate; 2, 3-dimercapto-1-propane sulfonic acid; meso 2, 3-dimercaptosuccinic acid (DMSA), monoisoamyl DMSA, monomethyl DMSA and monocyclohexyl DMSA. These are effective chelating agents for the treatment of Cd toxicity (Rahimzadeh et al., 2017). N-tetramethylene dithiocarbamate have been reported to increase the excretion of Cd and reduce side effects of Cd toxicity (Rahimzadeh et al., 2017). MiADMSA was reported to increase δ-aminolevulinic acid dehydratase activity and improve the levels of GSH and MT (Flora & Pachauri, 2010).

Soil that is contaminated with Cd can be treated with chemical agents that could decrease the solubility and reduce Cd concentration. The use of suitable crops that are capable of absorbing Cd from the soil for its removal is another option that could help reduce Cd exposure. Water sources contaminated with Cd may also be purified using medicinal plants seed (*Moringa oleifera*, *Arachis hypogaea*, *Vigna unguiculate*, *Vigna mungo* and *Zea mays*), aluminum oxide (Al_2O_3) and titanium dioxide (TiO_2) (Rahimzadeh et al., 2017).

2.6.6 Potential use of plant extracts and phytochemicals for the prevention and treatment of cadmium toxicity

Numerous plant extracts (e.g. ginger, grapefruit, garlic, rosemary, onion and green tea) and phytochemicals (e.g. catechin, curcumin, narigenin, resveratrol and sulforaphane) have been reported to prevent Cd-induced toxicity (Sandbichler & Hockner, 2016); (Zhai et al., 2015). Catechin was reported to protect human peripheral blood lymphocyte cells from cadmium chloride ($CdCl_2$) toxicity by promoting cell viability and inhibition of apoptosis (Alshatwi et al., 2014). Fresh and pickled garlic extracts were also reported to reduce $CdCl_2$ cytotoxicity in human embryonic kidney HEK293 cells (Boonpeng, Siripongvutikorn, Sae-Wong, & Sutthirak, 2014). Aged garlic extract (AGE) was also reported to exert cytoprotective effect on HEK293 and 1321NI (human astrocytoma) cells treated with $CdCl_2$. The AGE was noted to increase HEK239 and 131NI cells viability by increasing the levels of reduced glutathione and upregulating the expression of antioxidant gene NQO1 (Lawal & Ellis, 2011).

Hwanggunchungyitang (also known as HGCYT) is a herbal medicine containing nine herbs (Glycyrrhizae Radix, Zingiberis Rhizoma, Angelicae Gigantis Radix, Rehmanniae Radix, Mori Cortex, Aurantii Fructus, Citri Pericarpium, Gardeniae Fructus and Scutellariae Radix), has been reported to reduce Cd toxicity in HEI-OC1 auditory cells (S. J. Kim et al., 2009). HGCYT increased cell viability, inhibited oxidative stress, and downregulated the expression of caspase-9 and ERK in Cd treated HEI-OC1 cells (S. J. Kim et al., 2009).

2.7 *Melicope ptelefolia*

2.7.1 Nomenclature and taxonomy

Melicope ptelefolia (MP) is locally knows as '*tenggek burung*' in Malaysia (Aman, 2006). The local name for MP in Indonesia and Thailand are '*sampang Uam*' and '*Uam, Sam Ngam*', respectively (Aman, 2006).

2.7.2 Description

MP belongs to Rutaceae family and the genus of Melicope. Rutaceae is widely distributed in tropical and subtropical areas. In Malaysia, 23 genera with 75 species are known (Ab. Karim et al., 2011). The genus 'Melicope' is distributed in many tropical areas including south Asia, east Asia, Mascarene island and Polynesia. MP is found in many Asian countries including Malaysia, Indonesia, Thailand and Vietnam. Approximately 24 species of Melicope are found in Malaysia (Ab. Karim et al., 2011). The MP leaves are widely consumed as vegetable salad in Malaysia. The leaves have a crunchy texture and slightly pungent taste, with a pleasant lemon-lime aroma (**Figure 2.1**).

2.7.3 Traditional uses

MP has been used traditionally for the treatment of several diseases including wound infections, itches, inflammation, hypertension, abdominal pain, headache, erectile dysfunction, trauma, fever, eczema, hemorrhoids, dermatitis, diarrhea, bacterial infection, fungal infection, fatigue and others (Ab. Karim et al., 2011).

Figure 2.1: Malaysian species of *Melicope ptelefolia* (*tenggek burung*). *Image was retrieved from "http://karyaku-paridahishak.blogspot.com/2016/01/tenggek-burung-dan-serai-kayu.html".

2.7.4 Phytochemical compounds isolated from MP

Compounds isolated from MP leaves include β-sitosterol; lupeol; oleanolic acid; kokusaginine; genistein; melicoester; melicopeprenoate; p-O-geranyl-7′′-acetoxy coumaric acid (Shaari, Zareen, Akhtar, & Lajis, 2011); kokusagine; 5-methoxymaculine; 2,4,6-trihydroxy-3-prenylacetophenone; 2,4,6-trihydroxy-3-geranylacetophenone (tHGA); 2,4,6-trihydroxy-3-geranylgeranylacetophenone; p-O-geranylcoumaric acid; 2,4,6-trihydroxy-3-farnesylgeranylacetophenone (Abas et al., 2010a); (Shuib et al., 2011); bisquinolinone alkaloids N- methylflindersine; melicobisquinolinone A and melicobisquinolinone B (Kamperdick, Van, Sung, & Adam, 1999). Twenty benzopyran compounds have also been isolated from MP leaves (Kamperdick, Van, Van Sung, & Adam, 1997); (Van, Kamperdick, Sung, & Adam, 1998). Melicolone A (±) and melicolone B (±) are two stereoisomeric compounds that were isolated from MP leaves (J.-F. Xu et al., 2015). A recent study reported the

isolation of four novel chroman derivatives (pteleifolones A–D), and nine other compounds from MP stems, which include acronyculatin B, dictamnine, acronylin, marmesin, 5-methoxymarmesin, evolitrine, (+)-peucedanol, N-methylatanine and atanine (J. Xu et al., 2016).

2.7.5 Bioactivities

Phytochemical compounds with known anticancer activities have been identified in MP and they include β-sitosterol, lupeol, oleanolic acid, kokusaginine and genistein (A. A. Baskar, Ignacimuthu, Paulraj, & Al Numair, 2010); (Rauth et al., 2016); (Shaari, Zareen, et al., 2011); (Tiwari BK, Brunton N, & CS, 2013); (X. Li et al., 2016); (Molnar et al., 2013). The ethanol and methanol extracts of MP were reported to show antinociceptive activity (Sulaiman et al., 2010); (Mahadi et al., 2016). The methanol root extract was reported to show anti-inflammatory activity (Mahadi et al., 2016). The phytochemical compound tHGA has been extensively studied. It demonstrated potent anti-inflammatory activity in human leucocytes by inhibiting 5-lipoxygenase (5-LPO) and cyclooxygenase-2 (COX-2), with an IC_{50} concentration of 0.42 and 0.40 μM, respectively (Shaari, Suppaiah, et al., 2011). Intraperitoneal administration of tHGA in mice was observed to inhibit ovalbumin-induced pulmonary inflammation by counteracting cysteinyl leukotriene synthesis (Ismail et al., 2012). Oral administration of tHGA was also demonstrated to prevent ovalbumin-induced chronic asthma in BALB/c mice (Lee et al., 2017). tHGA showed prominent anti-allergic activity which was associated with significant inhibition of β-hexosaminidase and histamine release (inducers of mast cell degranulation) in rat basophilic leukaemia (RBL-2H3) cells. The anti-allergic activity of tHGA on rat basophilic leukaemia cells RBL-2H3 was due to inhibition of LAT-PLCɣ-MAPK and PI3K-p65 pathways (J. W. Tan et al., 2017). The

anti-allergic activity of tHGA was also demonstrated *in vivo* by its inhibition on the release of interleukin-4, tumour necrosis factor-α, prostaglandin D2 and leukotriene C4 (mediator of systemic anaphylaxis) in animal model (Ji Wei Tan et al., 2017). tHGA also protected human umbilical vein endothelial cells (HUVECs) from lipopolysaccharide-induced inflammation by inhibiting monocyte adhesion, endothelial migration and hyperpermeability, and prostaglandin secretion (Chong et al., 2016).

Kokusaginine, isolated from MP leaves has been shown to promote cell viability and inhibit nitric oxide production in murine macrophage cell line RAW 264.7, with an IC_{50} value of 13.42 ± 0.43 μg/mL (Abas et al., 2010a). MP leaves also contain melicolone A (±) and melicolone B (±) which demonstrated protective effect against high glucose-induced oxidative stress in HUVEC cells (J.-F. Xu et al., 2015).

2.8 Characterisation of bioactivity through gene expression study

Gene expression study is an essential tool that can be used to analyse how the genome (and genes) are used by the living organism to carry out various biological functions. Pattern of gene expression can change from one scenario to the other. A change in gene expression pattern in the body can be induced by various cues, which include behavioral, activity, diet, mental state, drug intake or disease. Gene expression study can therefore provide valuable insights regarding the function and regulation of genes and the genome in living organism.

2.8.1 Nutrigenomics

Nutrigenomics is a field of study that examines gene expression profile induced by nutrients and bioactive food compounds (Fenech et al., 2011). Nutrigenomics identifies the association of nutrients with the genome to improve human health (Dang, Walker, Ford, & Valentine, 2014). The aim of this field is associated with the prevention of

many diseases such as coeliac disease, obesity, diabetes, cardiovascular disease, neurological disorders and cancer (Lundstrom, 2013).

The United States is assumed to be the leading country in nutrigenomics research, followed by United Kingdom, Spain, Netherlands, Canada and many others (Neeha & Kinth, 2013). Major techniques that are used in nutrigenomics research include genomics (microarray, RT-PCR), proteomics (2D gel electrophoresis) and metabolomics (Neeha & Kinth, 2013).

2.8.2 Nutrigenomics and human health

A balanced diet is essential for the body to achieve optimum health. The health status of the human body is dependent on the intake of nutrients. An optimal health could be achieved from the consumption of nutrient rich foods and this may help prevent the development of chronic diseases such as obesity, cardiovascular disease, Alzheimer's disease, dementia and various cancers (Lundstrom, 2013). Nutrients may also potentially alter human life span by modulating various biological processes related to aging (Riscuta, 2016).

Foods rich in phytonutrients are thought to be helpful in preventing the development of chronic disease, such as cancer (Salminen, Kaarniranta, & Kauppinen, 2018). For example, the phytonutrient resveratrol which is found in grapes, wine, peanuts, and soy (Burns, Yokota, Ashihara, Lean, & Crozier, 2002) have been shown to inhibit proliferation of breast cancer cells MDA-MB-231 by upregulating antiproliferative proteins p21, p53 and BAD, while it downregulated PCNA, which is an inducer of cell cycle progression (Chin et al., 2014). Resveratrol also exert antiproliferative effect and induced apoptosis in HT1080 fibrosarcoma cells by inhibiting PI3K/AKT signaling. The components of PI3K/AKT signaling, namely IGFR1, IRS2, CBL, PI3KCB and

AKT3 were downregulated by resveratrol (Harati et al., 2015). Parkinson's disease is a neurodegenerative disorder associated with oxidative stress and damage of nerve cells due to inflammation-induced injury (Dzamko, Geczy, & Halliday, 2015).; (Dias, Junn, & Mouradian, 2013). Resveratrol is suggested to be beneficial for the prevention of Parkinson's disease, as it demonstrated neuroprotective effect in Parkinson's (PD) disease animal models, preventing behavioral, biochemical, and histopathological changes associated with PD (Bureau, Longpre, & Martinoli, 2008); (Khan et al., 2010). Nutrients can also influence development of cardiovascular disease. Excessive inflammation and alteration in lipid metabolism are associated with the development of cardiovascular disease (M. D. Shapiro & Fazio, 2016); (van Diepen, Berbée, Havekes, & Rensen, 2013). Docosahexaenoic acid is suggested to prevent cardiovascular disease through its various bioactivities, which include reducing levels of chemokines, cytokines and adhesion molecules in macrophages and endothelial cells. These can result in inhibition of inflammation and thus, protective against the development of cardiovascular disease (Merched & Chan, 2013).

Phytonutrients may also help lower the risk of developing diabetes. Epigallocatechin-3-gallate (EGCG) was reported to increase the viability of β-cells and insulin secretion in rat RIN-m5F cells by increasing the expression of IRS2, AKT, FOXO1 and PRDX1. EGCG was also reported to increase the secretion of insulin while preserving the structure of islet of Langerhans in diabetic mice by reducing the expression of L-CPT-1, DDIT3, PPP1R15A and CDKN1A (Berna et al., 2014). Quercetin has also been shown to enhance pancreatic cell proliferation and plasma insulin levels in diabetic mice by suppressing CDKN1A expression (Berna et al., 2014).

2.8.3 Methods of gene expression study

2.8.3.1 Microarray

Microarray is a tool that have been widely used to measure gene expression. The microarray platform uses probes (approximately 10000 to 40000) on solid surface such as glass slide to measure gene expression (Ness, 2007). The type of arrays used includes oligonucleotide arrays, cDNA arrays and protein arrays in microarray experiment (Govindarajan, Duraiyan, Kaliyappan, & Palanisamy, 2012).

The quantity of mRNA of a particular gene in a sample reflects the level of expression for that gene (Govindarajan et al., 2012). In microarray experiment, mRNA is converted to cDNA, which may then be fragmented with the use of restriction endonucleases, followed by their labelling with fluorescent dyes (e.g. Cy3 and Cy5). The labelled DNA fragments are then subjected to array hybridization. The arrays are washed to remove unbound materials and hybridization signals from the fluorophores are detected using laser beam with the corresponding excitation energy (Govindarajan et al., 2012). The hybridization signal strength is dependent on the number of mRNA copies that can bind to the target spot(s) on the array, which then specifies the expression level of genes (Naidu & Suneetha, 2012). The microarray data can be verified by performing additional assays such as statistical analysis, real-time quantitative polymerase chain reaction (RT-qPCR), southern blot or northern blot (Jaluria, Konstantopoulos, Betenbaugh, & Shiloach, 2007).

The microarray platform can be used in drug development study, disease characterisation and identifying gene mutations, oncogenes, tumor suppressors, precancerous lesions and the genes responsible for chemoresistance (Jaluria et al., 2007); (Govindarajan et al., 2012).

For example, microarray platform has been used to identify biomarkers for the diagnosis of lung carcinoids. This was done by comparing the gene expression profile in low-grade typical carcinoid and intermediate grade atypical carcinoid. The study revealed that vitamin D-binding protein (DBP) and carcinoembryonic antigen family member (CEACAM1) could be used as potential biomarkers, as they were significantly upregulated in atypical carcinoid (Toffalorio et al., 2014). By the same mode of analysis, GPC3, PEG10, MDK, SERPINI1, and QP-C was differentially modulated in hepatocellular carcinoma and could potentially be used as biomarkers for the disease (H. L. Jia et al., 2007).

Microarray platform could also reveal dysregulation of genes and could help us uncover potential mechanism underlying various types of cancers. For example, the oncogenic activity of "regenerating islet-derived protein 3 alpha" (REG3A) in SW1990 pancreatic cancer cells was investigated by microarray profiling and the result suggested that upregulation of JAK1, STAT3, IL10, FOXM1, KRAS, MYC, CyclinD1 and FOS, and activation of TGFβ, PDGF and RAS growth pathways were involved in REG3A-mediated cell proliferation of SW1990 cells (Q. Xu et al., 2016).

Microarray study could also potentially help uncover anticancer activity of phytochemicals. The anticancer activity of genistein against HCT116 colon cancer cells was characterised through microarray profiling, revealing upregulation of checkpoint kinase ATM, p53, cell cycle inhibitory p21, GADD45A, while downregulation of cell cycle activator CDK1 and CDC25A. The study concluded that that differential expression of these genes was associated with antiproliferative and apoptotic activity of genistein in HCT116 (Z. Zhang et al., 2013).

Microarray could also help reveal transcriptome profile or gene expression signature associated with major depressive disorder (MDD) and antidepressant therapy. It has

been reported that many genes such as MLC1, PROK2, CAPRIN1, FKBP5 and EDN1 were involved in the development of MDD while genes such as IRF7, CHL1, PPT1, TNF and IL1B were induced in antidepressant therapy (Lin & Tsai, 2016).

2.8.3.2 RNA sequencing

RNA sequencing (RNAseq, also known as whole-transcriptome shotgun sequencing) uses "next generation sequencing" (NGS) technology to measure gene expression level. Several approaches may be applied for RNAseq, including tag-based sequencing (3' end sequencing, 5' end sequencing, 5' and 3' end sequencing), shotgun sequencing, immunoprecipitation and ribosome profiling methods (de Klerk, den Dunnen, & 't Hoen, 2014).

In RNAseq, RNA is reverse transcribed into cDNA; then a library for the sequencing reaction is constructed; followed by the sequencing reaction. The sequencing reads generated are mapped to the reference genome and the number of mapping reads are counted to provide a basis of measuring gene expression (Wolf, 2013).

RNAseq has the advantages of low background noise, requiring lower amount of RNA and capable of detecting higher fold of gene expression changes (>8000 fold) (Z. Wang, Gerstein, & Snyder, 2009) with lower background signal. This method can also be applied using a single cell or formalin-fixed paraffin-embedded tissue (Whitley, Horne, & Kolls, 2016).

Another unique advantage provided by RNAseq is its ability to detect/quantify alternative splicing variants (Z. Wang et al., 2009). RNAseq can also be applied to identifying gene mutations, micro-RNAs and microbial RNAs (Whitley et al., 2016).

2.8.3.3 Real-time quantitative polymerase chain reaction (RT-qPCR)

RT-qPCR is a method of gene expression measurement, that is now routinely used in molecular biology labs worldwide. This method requires the presence of the template nucleic acid, oligonucleotide primers, dNTPs, thermostable DNA polymerase and magnesium ions in the PCR buffer (Kubista et al., 2006). The PCR reaction consists of three steps: denaturation at 95^{o}C to separate the DNA strands; annealing at temperature slightly lower than the melting temperature of primers to enable binding of primers with target sequence; and extension at 72^{o}C to amplify the target gene (Kubista et al., 2006). The quantification of gene expression in RT-qPCR requires the use of a suitable DNA binding dye (e.g. ethidium, bromide, YO-PRO-1, SYBR® Green I, SYBR® and EvaGreen) or fluorophore-linked probes (e.g. Scorpions, Cyclicons, Angler®, TaqMan, TaqMan-MGB and FRET). These binding dyes could emit fluorescence signal when bound to the amplified DNA (Navarro, Serrano-Heras, Castano, & Solera, 2015), allowing the detection of target DNA amount present in the reaction mixture. A higher fluorescence signal implies higher quantity of target amplicon presence in the reaction mixture.

In RT-qPCR, the target gene can be quantified through absolute or relative quantification method. Absolute quantification is done by plotting standard curve using serial dilution of known standard DNA; and comparing the CT (threshold cycle at which fluorescence signal is detected) values of unknown samples, compared to the known standard (Kaltenboeck & Wang, 2005). Relative quantification is performed by measuring the expression rate of a particular gene relative to that of a reference gene. An ideal reference gene should have a profile that should not be affected by the experimental manipulation/treatment, i.e. it should demonstrate a relatively constant rate of expression across various samples (Kaltenboeck & Wang, 2005); (de Jonge et al., 2007). For the relative quantification method, there are several approaches that can be

adopted, which include “relative standard curve”, “comparative CT”, “linear regression PCR”, “data analysis for real-time PCR” and “Sigmoid curve-fitting” (Cikos, Bukovska, & Koppel, 2007). Among these, comparative CT is the most widely used method for relative quantification. Comparative CT method uses threshold cycle (CT) for the relative quantification of target genes with the help of a reference gene, which acts as normalizer. In comparative CT method, the relative quantification is deduced based on $2^{-\Delta\Delta CT}$ formula. For this method, ΔCT is calculated by subtracting the CT value of reference gene from the target gene. Then ΔΔCT is calculated by subtracting the ΔCT value of reference sample from the target sample. Finally, relative gene expression is quantified using $2^{-\Delta\Delta CT}$ formula (Livak & Schmittgen, 2001). The RT-qPCR technique has numerous applications, including detection, quantification and genotyping of microorganisms, detecting viral infection, human genetic testing, forensic science and cancer diagnosis (Kaltenboeck & Wang, 2005).

CHAPTER 3: METHODOLOGY

3.1 Reagents, solvents and chemicals

Solvents used for the extraction were purchased from Fisher Scientific and Merck. Sodium carbonate (Na_2CO_3), gallic acid, quercetin, polyphenon 60, ascorbic acid, catechin, ferrous sulfate ($FeSO_4$), 2,2-diphenyl-1-picryl hydrazyl **(**DPPH), 2,4,6-tripyridyl-s-triazine (TPTZ), 2,2′-azobis (2-amidinopropane) dihydrochloride (ABAP), and phosphate buffered saline (PBS) were purchased from Sigma-Aldrich. Folin-Ciocalteu reagent, aluminum trichloride ($AlCl_3$), potassium acetate, ferric chloride ($FeCl_3.6H_2O$), potassium persulfate, dimethyl sulfoxide (DMSO), 5-flurouracil, Muse™ MultiCaspase assay kit, Muse™ Annexin V and dead cell assay kit, Muse™ cell cycle assay kit were purchased from Merck. Trolox, 2,2′-azinobis-3-ethylbenzothiazoline-6-sulphonic acid (ABTS), 2′,7′-dichlorofluorescin diacetate (DCFH-DA) were purchased from Calbiochem. Dulbecco's Modified Eagle's Medium (DMEM), Roswell Park Memorial Institute (RPMI)-1640 medium, penicillin-streptomycin and potassium persulfate were purchased from Nacalai Tesque. Fetal bovine serum (FBS) and TrypLE were purchased from Gibco. Cell Titer 96 Aqueous One solution cell proliferation (MTS) assay kit and Apotox-Glo™ triplex assay kit were purchased from Promega. Caspase inhibitor (z-VAD-FMK) was purchased from Biovision. PureLink RNA mini kit was purchased from Invitrogen. GeneChip™ Whole Transcript plus kit, GeneChip™ Expression, Wash and Stain kit, and Human Gene (HuGene) 2.0 ST array were purchased from Applied Biosystem. Maxima First Strand cDNA synthesis kit, Luminaris color HiGreeen High ROX qPCR master mix were purchased from Thermo Scientific. SensiFast™ SYBR® Hi-ROX qPCR master mix was purchased from Bioline.

3.2 Sample and extracts preparation

Fresh, healthy and young MP leaves were purchased from the local wet market and processed on the same day. The sample identity was authenticated by a plant taxonomist at the University of Malaya herbarium, Dr. Sugumaran Manickam. A voucher specimen was also deposited at the herbarium, with a registration number KLU 49190. The leaves were washed with distilled water and air dried for 3 days at room temperature. Sample drying was completed by incubating the leaves in an oven at 40 ºC for 24 h. The dried leaves were then powdered using a table blender and stored at –20 °C until needed for extraction. Organic raspberry, blueberry and blackberry were also purchased from a local supermarket. The berries were washed with distilled water and dried in a 40 ºC oven until no weight reduction was observed. They were powdered using a table blender and stored at –20 °C until needed for the extraction.

Powdered dried MP leaves were extracted sequentially, using solvents of varying polarity in the following order: hexane>ethyl acetate>methanol>water. Fifty grams of the powdered leaves was mixed with 500 mL of hexane (1:10 ratio of sample weight to solvent volume). The mixture was constantly shaken (150 rpm) for 6 h at 37 ºC using Innova 4300 Incubator Shaker (New Brunswick Scientific). The mixture was centrifuged at 1500 rpm for 10 min, after which the supernatant was collected and filtered using a Whatman filter paper (No. 4). The residues were extracted again with the same solvent twice. The extraction was then continued using the remaining three solvents following the method as indicated above. The resulting hexane, ethyl acetate and methanol solvent collected (~1500 mL) for each extraction was evaporated at 40 °C using a rotary evaporator (Buchi Rotavapor R-215). The water extract was evaporated using a freeze dryer. The same extraction procedure was performed for the berries fruit. The dried extracts were dissolved in 10% DMSO at 2 mg/mL and stored at –20 ºC.

3.3 Cell lines and tissue culture protocol

The following American type culture collection (ATCC) human cancer or normal cell lines were used in the present study: HCT116, HCC1937, HepG2, MDA-MB-231, CCD841, Hs27. Among them, HCT116, HepG2, MDA-MB-231, CCD841 and Hs27 cells were cultured in DMEM (Catalogue No. 08458-45, Nacalai Tesque) while HCC1937 was cultured in RPMI-1640 media (Catalogue No. 30264-85, Nacalai Tesque). Growth media was supplemented with 10% FBS (Catalogue No. 10270, Gibco), 100 U/mL penicillin and 100 µg/mL streptomycin (Catalogue No. 09367-34, Nacalai Tesque). TrypLE^{TM} Express enzyme (Catalogue No. 12604-021, Gibco) was used for cells detachment. Incubation of culture was done at 37 ºC, in a humidified incubator containing 5% CO_2.

3.4 Antioxidant potential assays

3.4.1 Total phenolic content assay

Total polyphenol content (TPC) was determined using Folin-Ciocalteu (FC) reagent (Singleton & Rossi, 1965). Twenty µL of the plant extracts were each mixed with 100 µL of 10% FC reagent in a 96-well plate and incubated for 30 min. Seventy µL of Na_2CO_3 (1M) was added to the mixture and incubated for 2 h at room temperature. Absorbance was then measured at 735 nm using Tecan Infinite® M1000 Pro Multimode reader & HydroFlex microplate washer (Tecan Trading AG). A standard curve was constructed using gallic acid (0 - 0.250 mg/mL). The TPC value was expressed as mg gallic acid equivalents (GAE) per gram of dried extract.

3.4.2 Total flavonoid content assay

Total flavonoid content (TFC) was determined according to Chang et al. (C.-C. Chang, Yang, Wen, & Chern, 2002) with slight modifications. Five µL each of aluminium trichloride (10% w/v) and potassium acetate (1M) were mixed with 25 µL of the plant extract. Seventy-five µL of ethanol (95% v/v) and 140 µL of distilled water were added to the mixture. The mixture was incubated for 30 min at room temperature followed by absorbance reading at 415 nm using Tecan Infinite® M1000 Pro Multimode reader & HydroFlex microplate washer (Tecan Trading AG). Quercetin was used as a standard and TFC values were expressed as mg quercetin equivalent per gram of dried extract.

3.4.3 Ferric reducing antioxidant power (FRAP) assay

FRAP assay (Benzie & Strain, 1996) was carried out using freshly prepared FRAP reagent by mixing 10 mM TPTZ in 40 mM HCl, acetate buffer (300 mM, pH 3.6) and $FeCl_3.6H_2O$ (20 mM) in 1:10:1 ratio (v/v/v). Ten µL of the plant extract was mixed with 300 µL FRAP reagent and incubated for 4 h at room temperature. The absorbance of ferrous-TPTZ complex was measured at 593 nm using Tecan Infinite® M1000 Pro Multimode reader & HydroFlex microplate washer (Tecan Trading AG). A standard curve using $FeSO_4$ solution (0 to 3.5 mM) was plotted. Antioxidant power of the extracts was expressed as mM Fe^{2+} per gram of dried extract. Gallic acid, ascorbic acid and catechin were used as positive controls.

3.4.4 $ABTS^{\bullet+}$ radical-scavenging activity assay

The 2,2′-azinobis-3-ethylbenzothiazoline-6-sulphonic acid ($ABTS^{\bullet+}$) radical-scavenging activity was evaluated according to Re *et al*. (Re, Pellegrini, Proteggente,

Yang, & Rice-Evans, 1999). $ABTS^{\bullet+}$ cation was produced by mixing 7 mM ABTS solution with 2.45 mM potassium persulfate and allowing them to react in the dark for 16 h at room temperature. The absorbance of solution was measured at 734 nm and adjusted to ~0.7 using absolute ethanol. Ten µL of the plant extract at different concentrations (up to 2000 µg/mL) was mixed with 90 µL of $ABTS^{\bullet+}$ solution and the absorbance at 734 nm was taken after 30 min using Tecan Infinite® M1000 Pro Multimode reader & HydroFlex microplate washer (Tecan Trading AG). Trolox, ascorbic acid, catechin and quercetin were used as positive controls. $ABTS^{\bullet+}$ scavenging activity was calculated as follows: $ABTS^{\bullet+}$ radical-scavenging activity = $[(A_{control}-A_{sample})/A_{control}]$ X 100%, where $A_{control}$ and A_{sample} are the absorbances in the absence and presence of extracts, respectively. The IC_{50} value is the concentration at which 50% of the $ABTS^{\bullet+}$ is scavenged. IC_{50} concentration of the extracts was determined using GraphPad Prism version 5.0.

3.4.5 $DPPH^{\bullet}$ radical-scavenging activity assay

The 2,2-diphenyl-1-picryl hydrazyl ($DPPH^{\bullet}$) radical-scavenging activity was evaluated according to Sharma and Bhat (Sharma & Bhat, 2009) with slight modifications. One hundred µM $DPPH^{\bullet}$ solution was prepared in methanol and incubated at room temperature in the dark for 30 min. Twenty µL of plant extracts, at different concentrations up to 2000 µg/mL, was mixed with 150 µL of 100 µM $DPPH^{\bullet}$ solution. The absorbance of the reaction mixture was measured at 517 nm using Tecan Infinite® M1000 Pro Multimode reader & HydroFlex microplate washer (Tecan Trading AG) after 30 min of incubation at room temperature. Ascorbic acid, quercetin, catechin and trolox were used as positive controls. The scavenging activity of the extracts was calculated as follows: $DPPH^{\bullet}$ radical-scavenging activity = $[(A_{control}-$

$A_{sample})/A_{control}]$ X 100%, where $A_{control}$ and A_{sample} are the absorbances in the absence and presence of extracts, respectively. The IC_{50} value is the concentration of the extracts that inhibited 50% of DPPH•, and this value was determined using GraphPad Prism version 5.0.

3.4.6 Cellular antioxidant activity assay

The cellular antioxidant activity (CAA) assay was carried out according to Wolfe and Liu (Wolfe & Liu, 2007) with minor modifications. Briefly, Hs27 cells were seeded in 100 µL DMEM media at a density of 5 x 10^4 cells/well in a black 96-well plate. The cells were then incubated for 24 h, after which the growth medium was removed, and the wells were washed with cold PBS. The wells were applied with 100 µL medium containing MP extracts (up to 1000 µg/mL) and 25 µM DCFH-DA and incubated for 1 h. The cells were then washed with 100 µL of cold PBS. One hundred µL of 600 µM ABAP in HBSS was applied to the cells and the fluorescence reading was recorded using Tecan Infinite® M1000 Pro Multimode reader & HydroFlex microplate washer (Tecan Trading AG). Emission at 538 nm was measured with excitation at 485 nm every 5 min for 90 min. The assay included a triplicate control and blank. The control wells consisted of treated cells with DCFH-DA and ABAP while the blank contained cells treated with the dye and HBSS only. After blank subtraction from the fluorescence readings, the area under the curve of fluorescence versus time was integrated to calculate the CAA value according to the following formula: CAA unit = 100-(∫SA ⁄∫CA) X 100, where ∫SA is the integrated area under the sample fluorescence versus time curve and ∫CA is the integrated area under the control fluorescence versus time curve (Wolfe & Liu, 2007). The median effective dose (EC_{50}) for the pure phytochemical compounds (positive controls) and MP extracts were determined from the median effect

plot of log (f_a/f_u) versus log (dose), where f_a is the fraction affected and f_u is the fraction unaffected by the treatment, respectively (Wolfe & Liu, 2007). The EC_{50} value of extracts was obtained when the ratio of f_a/f_u equals to 1.

3.5 Anticancer activity assays

3.5.1 MTS cell viability assay

The antiproliferative activity of the extracts against cancer and normal cell lines was evaluated using CellTiter 96® AQueous One Solution Cell Proliferation Assay (MTS) kit (Catalogue No. G3581, Promega), according to the manufacturer's instructions. The cells were seeded at 37 °C at a density of (~1×10^4) cells/well/100 µL media in 96-well plate. In the preliminary screening, cells were treated with the extracts at 250 µg/mL. After 48 h, 20 µL of MTS reagent was added and the mixture was incubated for another 4 h, after which absorbance reading at 490 nm was taken using Tecan Infinite® M1000 Pro Multimode reader & HydroFlex microplate washer (Tecan Trading AG). Cell viability was determined as follows: Viability (%) = (absorbance of sample/absorbance of control) X 100 %. The plant extract that reduced cancer cells viability significantly (< 50%) were taken as positive for antiproliferative activity and was further investigated. The cancer cells were treated with the positive MP extracts for 48 h at various concentrations (25, 50, 100, 150, 200 and 250 µg/mL) to determine the IC_{50} value. The IC_{50} value is the concentration of extracts at which the cell viability was reduced to 50%. The IC_{50} value was calculated using GraphPad Prism version 5.0. 5-flurouracil (5-FU) was used as a positive control drug.

3.5.2 Caspase-3/7 activity assay

The assay was carried out using Apotox-Glo™ Triplex assay kit (Catalogue No. G6321, Promega), following manufacturer's protocol. Briefly, $7x10^3$ cells/well/100 µL culture media were seeded at 37 °C in a 96-well white plate for 24 h. The cells were then treated with MP-HX and MP-EA for 24 h and 48 h. The concentration of the extracts used in the assay were at ~IC_{50} values for HCT116, HCC1937, HepG2 and MDA-MB-231 cells, where MP-HX concentrations were 70 µg/mL, 90 µg/mL, 75 µg/mL, and 45 µg/mL, respectively, while MP-EA concentrations were 75 µg/mL, 90 µg/mL, 130 µg/mL and 90 µg/mL, respectively. After adding the Caspase-Glo® 3/7 reagent, the cells were incubated for 30 min at room temperature and the luminescence reading was measured using Tecan Infinite® M1000 Pro Multimode reader & HydroFlex microplate washer (Tecan Trading AG).

3.5.3 Multicaspase assay

The detection of multiple caspases (caspase-1, 3, 4, 5, 6, 7, 8 and 9) activation was done using Muse™ multicaspase assay kit (Catalogue No. MCH100109, Merck Millipore), following the manufacturer's instruction. Briefly, $1x10^5$ cells/well/1 mL culture media were seeded at 37 °C in a 12-well plate for 24 h. The cells were then treated with MP-HX and MP-EA extracts for 24 or 48 h. The concentration of the extracts used were at ~IC_{50} values for HCT116, HCC1937, HepG2 and MDA-MB-231 cells, where MP-HX concentrations were 70 µg/mL, 90 µg/mL, 75 µg/mL, and 45 µg/mL, respectively, while MP-EA concentrations were 75 µg/mL, 90 µg/mL, 130 µg/mL and 90 µg/mL, respectively. After treatment with the extracts, the cells were resuspended in 1X caspase buffer and 50 µL of the cells were transferred to 1.5 mL microcentrifuge tubes. Five µL of Muse™ multicaspase reagent working solution was added to the cells and incubated for 30 min in a 37 °C incubator. Then, 150 µL of

Muse™ caspase 7-aminoactinomycin D (7-AAD) working solution was added in each tube and mixed and incubated in the dark for 5 min at room temperature. The percentage of cells with multicaspase activity was then measured using Muse™ cell analyzer (Merck Millipore) flow cytometer.

3.5.4 Annexin-V and dead cell assay

The assay was determined using Muse™ Annexin-V & Dead Cell (7-AAD) kit (Catalogue No. MCH100105, Merck Millipore), according to manufacturer's instruction. Briefly, $1x10^5$ cells/well/1 mL culture media were seeded in a 12-well plate and incubated at 37 °C for 24 h. The cells were then treated with MP-HX and MP-EA extracts for 24 or 48 h. The concentration of the extracts used were at ~IC50 values for HCT116, HCC1937, HepG2 and MDA-MB-231, where MP-HX concentrations were 70 µg/mL, 90 µg/mL, 75 µg/mL, and 45 µg/mL, respectively, while MP-EA concentrations were 75 µg/mL, 90 µg/mL, 130 µg/mL and 90 µg/mL, respectively. After treatment with MP-HX and MP-EA extracts, the cells were resuspended in 1% FBS. One hundred microliter of the cells were transferred to 1.5 mL microcentrifuge tubes and 100 µL of Muse™ Annexin-V & Dead Cell reagent was added and mixed with the cells, followed by 20 min incubation at room temperature in the dark. The cells were then analyzed using Muse™ cell analyzer. The assay could identify four types of cells: i) non-apoptotic live cells: Annexin-V (-) and 7-AAD (-), ii) early apoptotic cells: Annexin-V (+) and 7-AAD (-), iii) late apoptotic cells: Annexin-V (+) and 7-AAD (+), and iv) non-apoptotic dead cells: Annexin-V (-) and 7-AAD (+).

3.5.5 Caspase inhibition assay

The pan caspase inhibitor z-VAD-fmk (Catalogue No. K220, Biovision) was used to inhibit caspases that are responsible for apoptosis induction. Briefly, 1×10^4 cells/well/100 µL culture media were seeded in 96-well plate and incubated at 37 °C for 24 h. The cells were then treated with MP-HX and MP-EA extracts for 48 h in the absence and presence of z-VAD-fmk (4 µM and 8 µM). The concentration of the extracts used were at ~IC_{50} values for HCT116, HCC1937, HepG2 and MDA-MB-231 cells, where MP-HX concentrations were 70 µg/mL, 90 µg/mL, 75 µg/mL, and 45 µg/mL, respectively, while MP-EA concentrations were 75 µg/mL, 90 µg/mL, 130 µg/mL and 90 µg/mL, respectively. After 48 h, the cell viability was determined using Promega's MTS cell viability kit (Catalogue No. G3581, Promega), following the manufacturer's instruction.

3.5.6 Cell cycle assay

This assay was performed using Muse™ cell cycle kit (Catalogue No. MCH100106, Merck Millipore), according to manufacturer's protocol. Briefly, $3x10^5$ cells/well/1 mL culture media were seeded in T25 culture flask and incubated at 37 °C for 24 h. The cells were then treated with MP-HX and MP-EA extracts for 24 h to measure DNA content at various stages of the cell cycle. The concentration of the extracts used were at ~IC_{50} values for HCT116, HCC1937, HepG2 and MDA-MB-231 cells, where MP-HX concentrations were 70 µg/mL, 90 µg/mL, 75 µg/mL, and 45 µg/mL, respectively, while MP-EA concentrations were 75 µg/mL, 90 µg/mL, 130 µg/mL and 90 µg/mL, respectively. The cells were fixed and washed with cold PBS and added with 200 µL of Muse™ cell cycle reagent. After 30 min of incubation at room temperature in the dark,

the percentage of cells in various stages (G_o/G_1, S and G_2/M) was analysed using Muse^{TM} cell analyzer flow cytometer.

3.6 MTT cell viability assay

The 3,(4,5-dimethythiazol-2-yl)-2,3-diphenyl tetrazolium bromide (MTT) cell viability assay was done according to Twentyman and Luscombe (Twentyman & Luscombe, 1987) with minor modifications. The details of MTT assay is described in the following sections.

3.6.1 Effect of MP-HX, MP-EA, quercetin and dexpanthenol on Hs27 cell viability

Hs27 cell lines were cultured and maintained according to the protocol specified by ATCC. The cells (~1×10^4) were incubated overnight in 100 µL culture media/well in a 96-well plate and thereafter treated with varying concentrations of MP-HX and MP-EA (60, 30, 15 µg/mL), QN (200, 100, 50, 25, 10, 5 µg/mL) and DX (60, 50, 40, 30, 20, 10 mg/mL). After 48 h of incubation, 10 µL of MTT (5 mg/mL) solution was added into each well and incubated for another 4 h. The culture solution was then discarded and 150 µL DMSO was added to solubilize the formazan crystals. The absorbance at 595 nm was then taken using Tecan Infinite® M1000 Pro Multimode reader & HydroFlex microplate washer (Tecan Trading AG).

3.6.2 Effect of $CdCl_2$ on Hs27 cell viability

Hs27 cell line was cultured and maintained according to the protocol specified by ATCC. The cells (~1×10^4) were incubated 24 h in 100 µL culture media/well in a 96-well plate and thereafter treated with varying concentrations of $CdCl_2$ (200, 100,

50,25,12.5, 6.25, 3.12, 1.56 µM). After 24 h of treatment, 10 µL of MTT (5 mg/mL) solution was added into each well and incubated for another 4 h. The culture solution was then discarded and 150 µL DMSO was added to solubilize the formazan crystals. The absorbance at 595 nm was then taken using Tecan Infinite® M1000 Pro Multimode reader & HydroFlex microplate washer (Tecan Trading AG). IC_{50} concentration of the $CdCl_2$ was determined using GraphPad Prism version 5.0 (GraphPad Software, Inc., USA). The IC_{50} value is the concentration of $CdCl_2$ at which the cell viability was reduced to 50%.

3.6.3 Protection from $CdCl_2$ cytotoxicity by MP-HX and MP-EA

Hs27 cells (~1×10^4) were incubated 24 h in 100µL culture media/well in a 96-well plate and thereafter pretreated with MP-HX (15 µg/mL) and MP-EA (15 µg/mL) or 0.075% DMSO (vehicle control) for another 24 h. Then 30 µM (~IC_{50} concentration) of $CdCl_2$ was added to MP-HX and MP-EA pretreated cells to induce toxicity. Cells treated with $CdCl_2$ (30 µM), MP-HX (15 µg/mL) and MP-EA (15 µg/mL) only were also included. After 24 h of treatment, 10 µL of MTT (5 mg/mL) solution was added into each well and incubated for another 4 h. The culture solution was then discarded and 150 µL DMSO was added to solubilize the formazan crystals. The absorbance at 595 nm was then taken using Tecan Infinite® M1000 Pro Multimode reader & HydroFlex microplate washer (Tecan Trading AG). An increase in cell viability by MP-HX+$CdCl_2$ and MP-EA+$CdCl_2$ compared to $CdCl_2$ treatment indicates protection from $CdCl_2$ toxicity.

3.7 Summary of workflow for gene expression study

For assessment of gene expression, total RNA was extracted from HCT116, HepG2 and Hs27 cells and subjected to microarray analysis. The summary for the scheme employed in the present study is depicted in **Figures 3.1, 3.2** and **3.3**.

The workflow for gene expression in HCT116 and HepG2 involves seeding of HCT116 and HepG2 cells, treatment of the cells with either MP-HX or 0.39 % v/v DMSO (vehicle control), extraction of total RNA, cDNA synthesis & labelling, microarray hybridization and scanning, bioinformatics analysis of the dataset and validation of microarray data through quantitative reverse transcription PCR (RT-qPCR) (**Figure 3.1**).

For gene expression in Hs27, the workflow involves seeding of Hs27 cells, treatment of the cells with MP-HX, MP-EA, QN, DX and 0.075 % v/v DMSO (vehicle control), extraction of total RNA, cDNA synthesis & labelling, microarray hybridization and scanning, bioinformatics analysis of the dataset and validation of microarray data through quantitative reverse transcription PCR (RT-qPCR) (**Figure 3.2**).

The workflow for gene expression in Hs27 upon cadmium-induced cytotoxicity involves seeding of Hs27 cells, pretreatment of the cells with MP-HX, MP-EA and 0.075 % v/v DMSO (vehicle control), induction of cadmium (Cd) toxicity in MP-HX and MP-EA pretreated cells using 30 μM $CdCl_2$, extraction of total RNA, cDNA synthesis & labelling, microarray hybridization and scanning, bioinformatics analysis of the dataset and validation of microarray data through quantitative reverse transcription PCR (RT-qPCR) (**Figure 3.3**). The experimental protocols are detailed in the next sections.

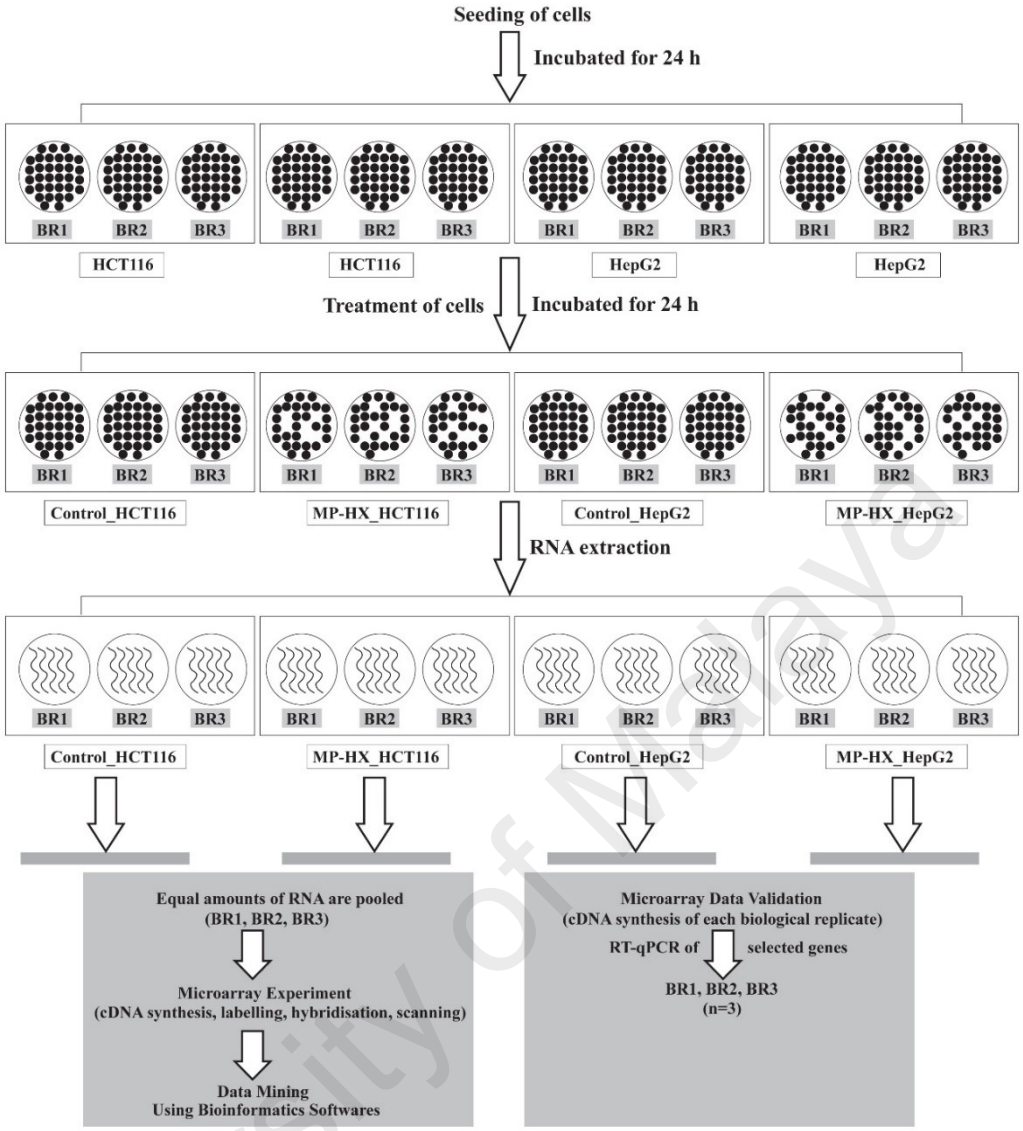

Figure 3.1: Workflow scheme for microarray profiling of HCT116 and HepG2 cells treated with MP-HX. The cells were seeded, treated with either MP-HX or 0.39% DMSO (vehicle control), followed by total RNA extraction, cDNA synthesis & labelling, microarray hybridization, scanning of array, bioinformatics analysis of the dataset and validation of microarray data through RT-qPCR. *BR, biological replicate.

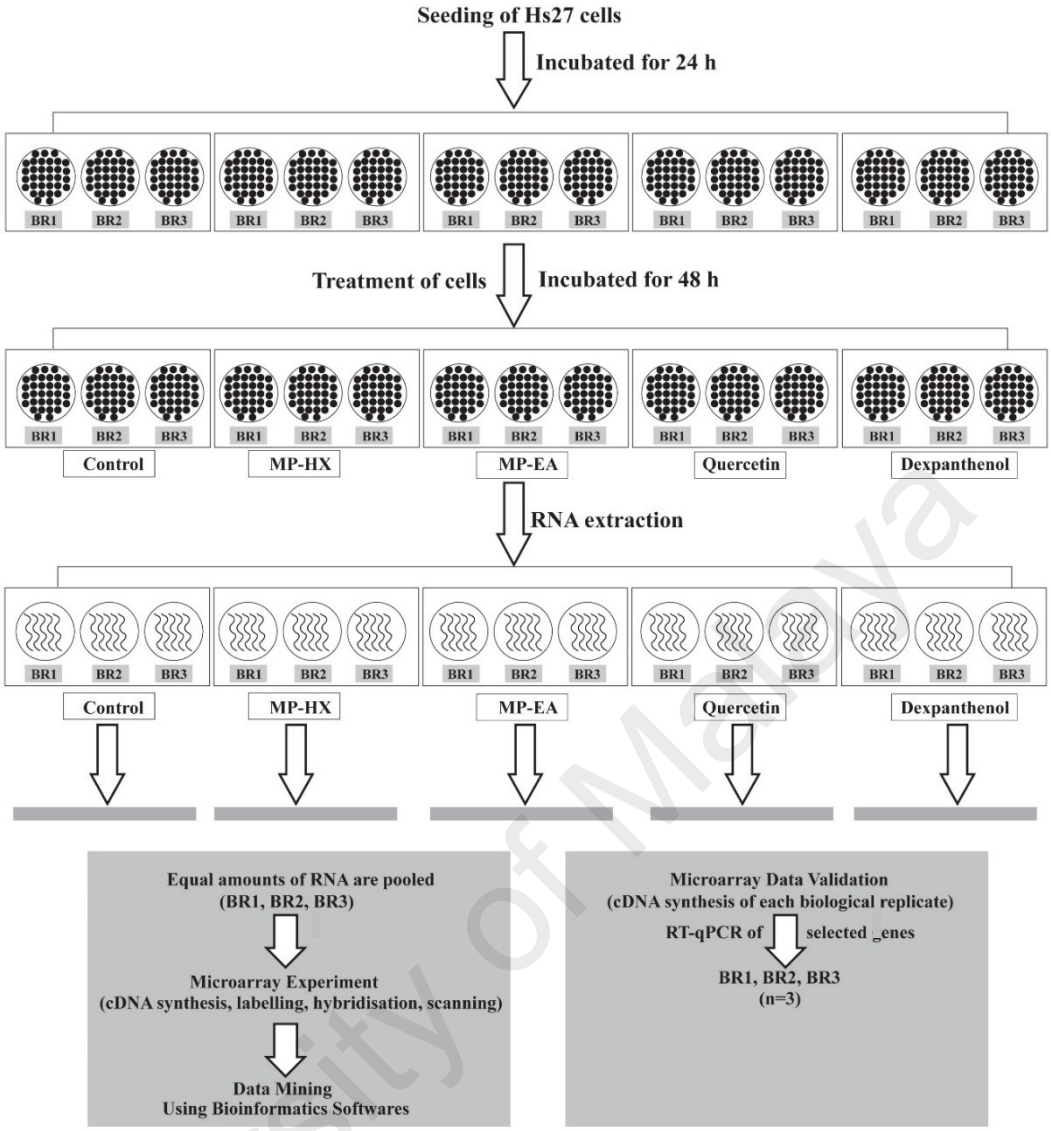

Figure 3.2: Workflow scheme for microarray profiling of Hs27 cells treated with MP-HX, MP-EA, quercetin and dexpanthenol. The cells were seeded, treated with either MP-HX, MP-EA, quercetin, dexpanthenol or 0.075% DMSO (vehicle control), followed by total RNA extraction, cDNA synthesis & labelling, microarray hybridization, scanning of array, bioinformatics analysis of the dataset and validation of microarray data through RT-qPCR. *BR, biological replicate.

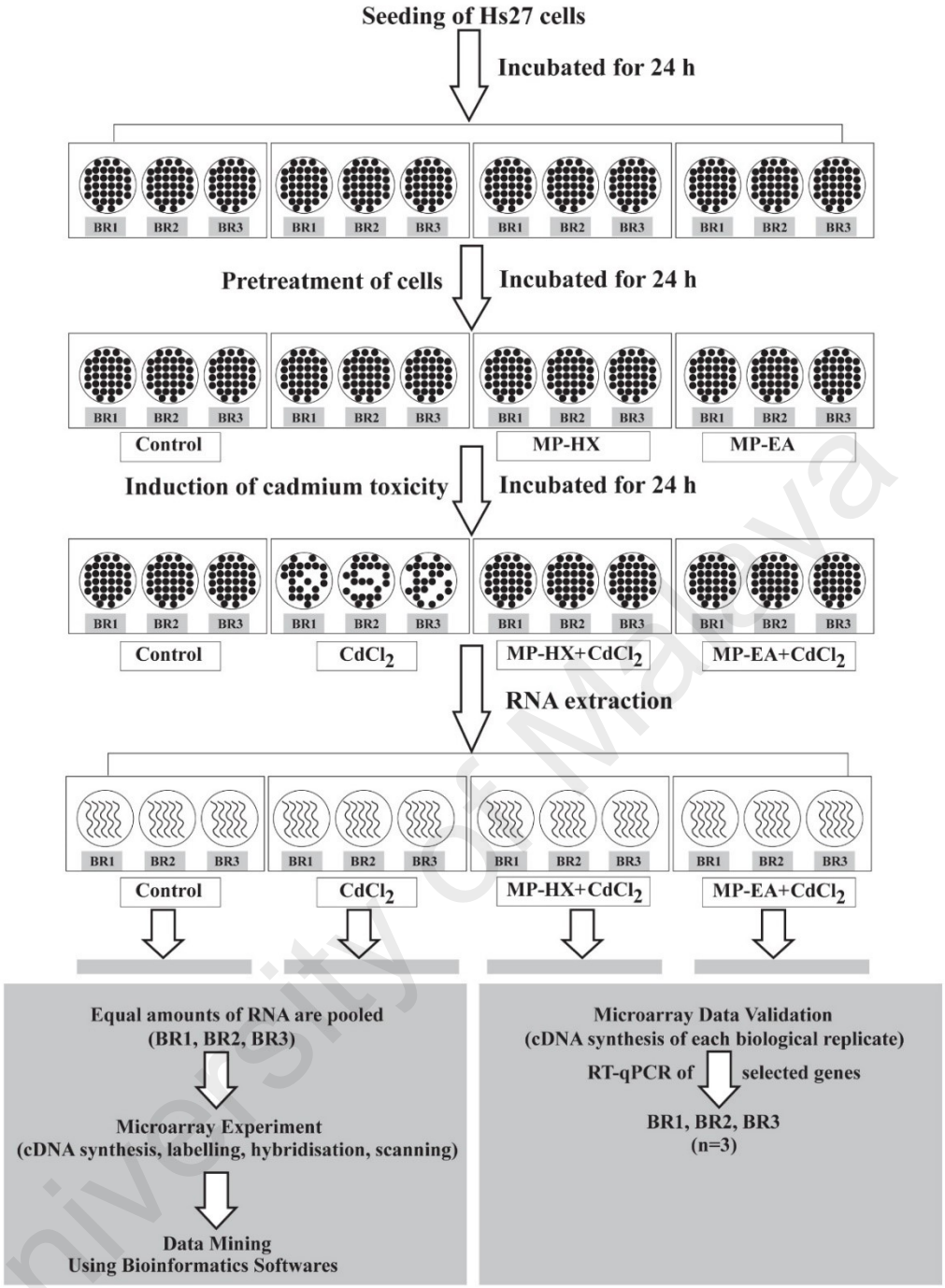

Figure 3.3: Workflow scheme for microarray profiling of Hs27 cells treated with $CdCl_2$, MP-HX+$CdCl_2$ and MP-EA+$CdCl_2$. The cells were seeded, pretreated with either MP-HX, MP-EA, or 0.075% DMSO (vehicle control), cadmium toxicity was induced in MP-HX and MP-EA pretreated cells using 30 µM $CdCl_2$, followed by total RNA extraction, cDNA synthesis & labelling, microarray hybridization, scanning of array, bioinformatics analysis of the dataset and validation of microarray data through RT-qPCR. *BR, biological replicate.

3.8 Microarray gene expression profiling

3.8.1 General methods for microarray gene expression profiling

3.8.1.1 Total RNA extraction

Total RNA was extracted and purified using PureLink RNA mini kit (Catalogue No. 12183018A, Invitrogen), according to manufacturer's instructions. RNA quantity and purity were verified using Nanodrop™ 2000 (Thermo Scientific), by measuring absorbance ratios at 260/280 and 260/230. The RNA quality and integrity were also assessed using agarose gel electrophoresis. Only RNA of good quality and integrity with an absorbance ratio of at least 2.0 was used for microarray and RT-qPCR assays.

3.8.1.2 Microarray experiment

Microarray gene expression profiling was performed using Human Gene (HuGene) 2.0 ST array (Catalogue no. 902499, Applied Biosystem). Briefly, equal amounts of RNA from three biological replicates of an assay point were pooled to get a minimum of 500 ng total RNA (Ruiz-Laguna, Velez, Pueyo, & Abril, 2016). The RNA was then reverse transcribed to synthesize complementary RNA (cRNA) using GeneChip™ Whole Transcript (WT) plus kit (Catalogue No. 902280, Applied Biosystem). The purified cRNA was quantified using Nanodrop™ 2000 (Thermo Scientific). Following this, cDNA was synthesized from 15 µg of cRNA. The purified cDNA (5.5 µg) was fragmented, labelled and hybridized onto GeneChip™ Human Gene 2.0 ST (Catalogue no. 902499, Applied Biosystem) array, according to manufacturer's guidelines. After 16 h of hybridisation in GeneChip™ Hybridization Oven 645, the arrays were washed and stained using GeneChip™ Expression, Wash and Stain kit (Catalogue No. 900720, Applied Biosystem) on GeneChip™ Fluidics Station 450. The stained arrays were scanned using GeneChip™ Scanner 3000 7G. Raw data (CEL files) was generated

using GeneChip Operating Software (GCOS). The CEL files were analyzed by Expression Console (EC) software (version 1.4) (Applied Biosystem), to ensure the quality control parameters and the data produced by the arrays were acceptable. Gene expression data was analyzed using Transcriptome Analysis Console (TAC) software (version 4.0) (Applied Biosystem). The dataset was also analyzed using bioinformatics softwares to identify the biological pathways, biological functions, gene networks and key processes that were enriched/modulated. Microarray data was validated using RT-qPCR assay.

The steps involved in microarray experiment are summarized below:

I) **Preparation of total RNA/Poly-A RNA control mixture:** 500 ng of total RNA (3 µL) and Poly-A RNA control (2 µL) were mixed.

II) **First strand cDNA synthesis:** First strand buffer (4 µL), first strand enzyme (1 µL) and total RNA/Poly-A RNA control mixture (5 µL) were mixed and incubated for 1 h at 25°C, then for 1 h at 42°C, then for at least 2 min at 4°C.

III) **Second strand cDNA synthesis:** Second strand buffer (18 µL), second strand enzyme (2 µL) and first strand cDNA (10 µL) were mixed and incubated for 1 h at 16 °C, then for 10 min at 65 °C, then for at least 2 min at 4 °C.

IV) **Synthesis of cRNA by in vitro transcription (IVT):** IVT buffer (24 µL), IVT enzyme (6 µL) and second strand cDNA (30 µL) were mixed and incubated for 16 h at 40 °C, then at 4 °C.

V) **Purify cRNA:** The cRNA was bound to purification beads, washed with 80% ethanol. The purified cRNA was eluted in nuclease free water.

VI) cRNA quantity and purity was assessed by Nanodrop™ 2000 spectrophotometer (Thermo Scientific).

VII) **Synthesis of second cycle single stranded cDNA (ss-cDNA):** Fifteen µg of purified cRNA (24 µL) and second cycle primers (4 µL) were mixed and incubated for 5 min at 70 °C, then 5 min at 25 °C, then 2 min at 4 °C. Then second cycle ss-cDNA buffer (8 µL), second cycle ss-cDNA enzyme (4 µL) and cRNA/second cycle primers mix (28 µL) were mixed and incubated for 10 min at 25 °C, then 90 min at 42 °C, then 10 min at 70 °C, then for at least 2 min at 4 °C.

VIII) **Hydrolyse RNA using RNase H:** RNase H (4 µL) and second cycle ss-cDNA (40 µL) were mixed and incubate for 45 min at 37 °C, then for 5 min at 95 °C, then for at least 2 min at 4 °C. Add 11 µL nuclease free water.

IX) **Purify second cycle ss-cDNA:** The ss-cDNA was bound to purification beads, washed with 80% ethanol and eluted in nuclease free water.

X) The quantity and purity of ss-cDNA was assessed by Nanodrop™ 2000 spectrophotometer (Thermo Scientific).

XI) **Fragmentation and labeling of ss-cDNA:** Nuclease free water (10 µL), 10X cDNA fragmentation buffer (4.8 µL), Uracil-DNA glycosylase (UDG) (1 µL), Apurinic/apyrimidinic endonuclease 1 (APE1) (1 µL) and 5.5 µg of purified ss-cDNA (31.2 µL) were mixed and incubated for 1 h at 37 °C, then for 2 min at 93 °C, then for at least 2 min at 4 °C. For labeling, 5X terminal deoxynucleotidyl transferase (TdT) buffer (12 µL), DNA labeling reagent (1 µL), TdT (2 µL) and fragmented ss-cDNA (45 µL) were mixed and incubated for 1 h at 37 °C, then for 10 min at 70 °C, then for at least 2 min at 4 °C.

XII) **Preparation of hybridisation cocktail:** Control oligo B2 (2.5 µL), 20X hybridization controls (bioB, bioC, bioD, cre) (7.5 µL), 2X hybridization mix (75 µL), DMSO (10.5 µL), nuclease free water (13.5 µL), and 3.5 µg of fragmented and labeled ss-cDNA (41 µL) were mixed and incubated for 5 min at 99 °C, then for 5 min at 45 °C.

XIII) **Inject and hybridise array:** Hybridisation cocktail (130 µL) was injected into the array and incubated with rotation at 60 rpm for 16 h at 45 °C.

XIV) Array was washed and stained using GeneChip^{TM} Fluidics Station 450.

XV) Array was scanned using GeneChip^{TM} Scanner 3000 7G.

XVI) The raw data (CEL) file was generated by GeneChip Operating Software.

XVII) The quality of data was checked using Expression Console software (version 1.4) (Applied Biosystem).

XVIII) The gene expression data was analysed using Transcriptome Analysis Console software (version 4.0) (Applied Biosystem).

XIX) Bioinformatic analysis of gene expression data was performed.

XX) Microarray data was validated using RT-qPCR assay.

3.8.2 Gene expression profiling in HCT116 and HepG2 cells treated with MP-HX

3.8.2.1 Total RNA extraction

The cells (~3×10^5) were seeded using 6 wells plate in DMEM media (**Section 3.3**) and incubated for 24 h. Following that, the cells were treated for 24 h with MP-HX at ~IC_{50} concentration (**Table 4.4**), which was 60 µg/mL for HCT116 and 78 µg/mL for HepG2 or vehicle control (0.39 % v/v DMSO). After 24-hour treatment, total RNA

from HCT116 and HepG2 cells were extracted and purified using PureLink RNA mini kit (Catalogue No. 12183018A, Invitrogen), according to manufacturer's instructions. RNA quantity, purity, quality and integrity were assessed according to the procedure described in the general method section (**Section 3.8.1.1**).

3.8.2.2 Microarray experiment

For each assay point indicated below, equal amounts of total RNA from three biological replicates were pooled, to get a minimum of 500 ng total RNA for the reverse transcription and labelling reactions using GeneChip™ Whole Transcript (WT) plus kit (**Section 3.8.1.2**) (**Figure 3.1**). In summary, the experiment in this section utilized a total of four (4) Human Gene 2.0 ST microarray chips:

- Control HCT116 cells (vehicle control, DMSO 0.39% v/v)

- HCT116 cells treated with MP-HX (60 µg/mL)

- Control HepG2 cells (vehicle control, DMSO 0.39% v/v)

- HepG2 cells treated with MP-HX (78 µg/mL)

Gene expression data was analyzed using Transcriptome Analysis Console (TAC) software (version 4.0) (Applied Biosystem). The dataset was also analyzed using Ingenuity Pathway Analysis (IPA) (http://www.ingenuity.com) software to identify the canonical pathways, biological functions, gene networks and key processes that were enriched/modulated.

3.8.2.3 Validation of microarray data through RT-qPCR assay

Each data point presented for the quantitative PCR assay was derived from three biological replicates (BR). Total RNA from each BR (**Figure 3.1**) was reversed transcribed and the cDNA from each BR was used as a template for the RT-qPCR. One microgram of RNA sample was converted to cDNA using Maxima First Strand cDNA synthesis kit (Thermo Scientific). The RT-qPCR was performed using Luminaris color HiGreeen High ROX qPCR master mix (Thermo Scientific) on StepOne Plus PCR thermocycler (Applied Biosystem). Seventeen genes were selected to validate the microarray data, comprising of nine upregulated genes (BBC3, CDKN1A, CDKN2B, DDIT3, GABARAPL1, GADD45A, JUN, NDRG1, TP53) and eight downregulated genes (CCNA2, GINS2, HELLS, MCM2, MCM10, PLK1, RRM2 and SKP2). The primers used in the assay are listed in **Table 3.1**. The thermocycling condition for the RT-qPCR was 50 °C for 2 min, 95 °C for 10 min, followed by 40 cycles of 95 °C for 15 s, 60 °C for 30 s (except for MCM2 and CDKN2B, 63 °C) and extension at 72 °C for 30 s. RPS29 was selected as the internal control gene to normalize the gene expression data (de Jonge et al., 2007). Relative quantification of the target genes was calculated by comparative $2^{-\Delta\Delta CT}$ method (Livak & Schmittgen, 2001).

Table 3.1: Primer sequences used for RT-qPCR validation of DEGs in HCT116 and HepG2 cells that were treated with MP-HX. *DEGs, differentially expressed genes.

Gene name	Forward (5´-3´)	Reverse (5´-3´)
BBC3	cccgtgaagagcaaatgag	acccccctgatgaaggtgag
CDKN1A	gaccatgtggacctgtcac	ggcttcctcttggagaagatc
CDKN2B	atcccaacggagtcaaccg	agtctcagacaggcttgcagg
DDIT3	tcaccacacctgaaagcag	gagccgttcattctcttcag
GABARAPL1	gaccatccctttgagtatcgg	gaagaataaggcgtcctcaggtc
GADD45A	gttttgctgcgagaacgac	gaacccattgatccatgtag
JUN	ttctatgacgatgccctcaacgcctc	gaagccctcctgctcatctgtcacgttc
NDRG1	gcagagtaacgtggaagtggtcc	acggcatccactgcaggc
TP53	tgactgtaccaccatccactacaac	ttgcggagattctcttcctctg
CCNA2	cagaaaaccattggtccctc	cactcactggcttttcatcttc
GINS2	gccgagaaggagctggttac	gtttcaggttaatcgccagc
HELLS	gcttgatgggtccatgtctt	gacatctatcctgggcctga
MCM2	aagtgcaatttcgtcctgggtc	gcaaccttgttgtccttcttgg
MCM10	gcaaaaatcccctgtagagaag	tccccacaatttgacctctag
PLK1	acttcgtgttcgtggtgttgg	gcttgaggtctcgatgaataac
RRM2	gcgatttagccaagaagttcag	cccagtctgccttcttcttg
SKP2	cgctgcccacgatcatttat	ggagattctttctgtagccgct
RPS29	gcactgctgagagcaagatg	ataggcagtgccaaggaaga

3.8.3 Gene expression profiling in Hs27 cells treated with MP-HX, MP-EA, quercetin and dexpanthenol

3.8.3.1 Total RNA extraction

Hs27 cells (~5×10^5) were seeded in T25 tissue culture flask in DMEM media (**Section 3.3**) and incubated for 24 h. Following that, the cells were treated for 48 h with MP-HX (15µg/mL), MP-EA (15µg/mL), QN (5µg/mL) and DX (10 mg/mL). The control cells were treated with the vehicle (DMSO) at a final concentration of 0.075 % v/v. After 48-hour treatment, total RNA from Hs27 cells were extracted and purified using PureLink RNA mini kit (Catalogue No. 12183018A, Invitrogen), according to manufacturer's instructions. RNA quantity, purity, quality and integrity were assessed according to the procedure described in the general method section (**Section 3.8.1.1**).

3.8.3.2 Microarray experiment

For each assay point, equal amounts of total RNA from three biological replicates were pooled, to get a minimum of 500 ng total RNA for the reverse transcription and labelling reactions using GeneChip™ Whole Transcript (WT) plus kit (**Section 3.8.1.2**) (**Figure 3.2**). In summary, the experiment in this section utilized a total of five (5) Human Gene 2.0 ST microarray chips:

-Control Hs27 cells (vehicle control, DMSO 0.075% v/v)

-Hs27 cells treated with MP-HX (15 µg/mL)

-Hs27 cells treated with MP-EA (15 µg/mL)

-Hs27 cells treated with quercetin (5 µg/mL)

-Hs27 cells treated with dexpanthenol (10 mg/mL)

Gene expression data was analyzed using Transcriptome Analysis Console (TAC) software (version 4.0) (Applied Biosystem). The data was also analyzed using "Gene Annotation Tool to Help Explain Relationships" (GATHER) (http://changlab.uth.tmc.edu/gather/gather.py) to categorize biological processes enriched in the dataset (J. T. Chang & Nevins, 2006). Moreover, the dataset was analyzed using Ingenuity Pathway Analysis (IPA) (http://www.ingenuity.com) software to identify the canonical pathways, biological functions, gene networks and key processes that were enriched/modulated.

3.8.3.3 Validation of microarray data through RT-qPCR assay

Each data point presented for the quantitative PCR assay was derived from three biological replicates (BR). Total RNA from each BR (**Figure 3.2**) was reversed transcribed and the cDNA from each BR was used as a template for the RT-qPCR. One microgram of RNA sample was converted to cDNA using Maxima First Strand cDNA synthesis kit (Thermo Scientific). The RT-qPCR was performed using SensiFast™ SYBR® Hi-ROX qPCR master mix (Bioline) on StepOne Plus PCR thermocycler (Applied Biosystem). The expression profile of 15 genes were validated, comprising of 8 upregulated genes (CAT, GSR, GSTP1, HELLS, PCNA, RRM2, RRM2B and HIRA) and 7 downregulated genes (CASP8, CDKN1C, FOS, GABARAPL1, GADD45A, HSPB2 and TNF). The oligonucleotide primers used in the assay are listed in **Table 3.2**. The thermocycling condition for the real-time PCR was 95 °C for 2 min, followed by 40 cycles of 95 °C for 5 s, 60 °C for 10 s and extension at 72 °C for 20 s. RPS29 was selected as the internal control gene to normalize the gene expression data (de Jonge et al., 2007). Relative quantification of the target genes was calculated by comparative $2^{-\Delta\Delta CT}$ method (Livak & Schmittgen, 2001).

Table 3.2: Primer sequences used for RT-qPCR validation of DEGs in Hs27 cells that were treated with MP-HX, MP-EA, QN and DX. *DEGs, differentially expressed genes.

Gene Name	Forward (5´-3´)	Reverse (5´-3´)
CAT	gaggttgaacagatagccttcg	cgttatcatcattggcagtgttg
GSR	aagcccacaatagaggtcagtg	gccgtatcatcagtgatgtcttag
GSTP1	gcaaatacatctccctcatctacac	tcatggatcagcagcaagtc
HELLS	gcttgatgggtccatgtctt	gacatctatcctgggcctga
PCNA	ctaacttttgcactgaggtacc	tggcatcttagaagcagttctc
RRM2	gcgatttagccaagaagttcag	cccagtctgccttcttcttg
RRM2B	gaggctcgctgtttctatgg	atctgctatccatcgcaagg
HIRA	aactgtgtgcggtggtcaaac	atgacgacagtgttatccacgc
CASP8	gagactgattcagaggagcaac	cttcatagttcacttcagtcagg
CDKN1C	aagagatcagcgcctgagaag	ggaccagtgtaccttctcgtg
FOS	ctaaccgccacgatgatgttc	tcctgtcatggtcttcacaacg
GABARAPL1	gaccatccctttgagtatcgg	gaagaataaggcgtcctcaggtc
GADD45A	gttttgctgcgagaacgac	gaacccattgatccatgtag
HSPB2	agtacgaatttgccaacccg	ggttatccacagtcctcacagtc
TNF	agcctcttctccttcctgatc	atgaggtacaggccctctgatg
RPS29	gcactgctgagagcaagatg	ataggcagtgccaaggaaga

3.8.4 Gene expression profiling in Hs27 cells treated with $CdCl_2$, MP-HX+$CdCl_2$ and MP-EA+$CdCl_2$

3.8.4.1 Total RNA extraction

Hs27 cells (~5×10^5) were seeded in T25 tissue culture flask using DMEM media (**Section 3.3**) and incubated for 24 h. Following that, the cells were pretreated for 24 h with either MP-HX (15 µg/mL), MP-EA (15 µg/mL) or 0.075% DMSO (vehicle control). Thereafter, 30 µM $CdCl_2$ was introduced into the media to induce cadmium (Cd) cytotoxicity in MP-HX and MP-EA pretreated cells. Cells treated with $CdCl_2$ (30 µM) only was also included. After 24 h, total RNA from Hs27 cells were extracted and purified using PureLink RNA mini kit (Catalogue No. 12183018A, Invitrogen), according to manufacturer's instructions. RNA quantity, purity, quality and integrity were assessed according to the procedure described in the general method section (**Section 3.8.1.1**).

3.8.4.2 Microarray experiment

For each assay point, equal amounts of total RNA from three biological replicates were pooled, to get a minimum of 500 ng total RNA for the reverse transcription and labelling reactions using GeneChip™ Whole Transcript (WT) plus kit (**Section 3.8.1.2**) (**Figure 3.3**). In summary, the experiment in this section utilized a total of four (4) Human Gene 2.0 ST microarray chips:

- Control Hs27 cells (vehicle control, DMSO 0.075% v/v)

-Hs27 cells pretreated with MP-HX (15 µg/mL) and then 30 µM $CdCl_2$

-Hs27 cells pretreated with MP-EA (15 µg/mL) and then 30 µM $CdCl_2$

-Hs27 cells treated with 30 µM $CdCl_2$ only

Gene expression data was analyzed using Transcriptome Analysis Console (TAC) software (version 4.0) (Applied Biosystem). The data was also analyzed using "Gene Annotation Tool to Help Explain Relationships" (GATHER) (http://changlab.uth.tmc.edu/gather/gather.py) to categorize biological processes enriched in the dataset (J. T. Chang & Nevins, 2006). DEGs were further analyzed using "Protein Analysis Through Evolutionary Relationships" (PANTHER) (http://www.pantherdb.org/) to categorize molecular functions and biological processes based on GO functional annotations (Mi & Thomas, 2009); (Mi, Muruganujan, Casagrande, & Thomas, 2013); (Mi et al., 2017). Moreover, an online protein-protein interaction analysis tool "Search Tool for the Retrieval of Interacting Genes" (STRING) (https://string-db.org) was used to uncover physical, as well as functional interactions of differentially expressed genes (Szklarczyk et al., 2015).

3.8.4.3 Validation of microarray data through RT-qPCR assay

Each data point presented for the quantitative PCR assay was derived from three biological replicates (BR). Total RNA from each BR (**Figure 3.3**) was reversed transcribed and the cDNA from each BR was used as a template for the RT-qPCR. One microgram of RNA sample was converted to cDNA using Maxima First Strand cDNA synthesis kit (Thermo Scientific). The RT-qPCR was performed using SensiFast™ SYBR® Hi-ROX qPCR master mix (Bioline) on StepOne Plus PCR thermocycler (Applied Biosystem). The expression profile of 16 genes were validated, comprising of 8 upregulated genes by $CdCl_2$ (DDIT3, GADD45A, JUN, FOS, PMAIP1, MYC, CDKN1C and HSPB2) and 8 downregulated genes by $CdCl_2$ (HIRA, MDM2, PCNA, RRM2B, NFKB1, PRKDC, RMI1 and ARAF). The oligonucleotide primers used in the assay are listed in **Table 3.3**. The thermocycling condition for the real-time PCR was 95 °C for 2 min, followed by 40 cycles of 95°C for 5 s, 60 °C for 10 s and extension at 72 °C for 20 s. RPS29 was selected as the internal control or reference gene to normalize the gene expression data (de Jonge et al., 2007). Relative quantification of the target genes was calculated by comparative $2^{-\Delta\Delta CT}$ method (Livak & Schmittgen, 2001).

Table 3.3: Primer sequences used for RT-qPCR validation of DEGs in Hs27 cells that were treated with $CdCl_2$, MP-HX+$CdCl_2$ and MP-EA+$CdCl_2$. *DEGs, differentially expressed genes.

Gene Name	Forward (5´-3´)	Reverse (5´-3´)
DDIT3	tcaccacacctgaaagcag	gagccgttcattctcttcag
GADD45A	gttttgctgcgagaacgac	gaacccattgatccatgtag
JUN	ttctatgacgatgccctcaacgcctc	gaagccctcctgctcatctgtcacgttc
FOS	ctaaccgccacgatgatgttc	tcctgtcatggtcttcacaacg
PMAIP1	tgcaggactgttcgtgttcag	atcagattcagaagtttctgccg
MYC	taccctctcaacgacagcagc	gactctgacctttgccaggag
CDKN1C	aagagatcagcgcctgagaag	ggaccagtgtaccttctcgtg
HSPB2	agtacgaatttgccaacccg	ggttatccacagtcctcacagtc
HIRA	aactgtgtgcggtggtcaaac	atgacgacagtgttatccacgc
MDM2	cttgatgctggtgtaagtgaac	cttcaggaagccaattctcac
PCNA	ctaacttttgcactgaggtacc	tggcatcttagaagcagttctc
RRM2B	gaggctcgctgtttctatgg	atctgctatccatcgcaagg
NFKB1	gaaaccacagagcaagatcagg	attctcatcctgcacagcagtg
PRKDC	ccagaagatcgcaccttactc	gctctcttactgctgatgtcatc
RMI1	ctgagcagtggaggtttcaag	ccagttaatacaagcttccagcc
ARAF	actcaggctattactgggaggtac	acatgcaggtgatggtagagg
RPS29	gcactgctgagagcaagatg	ataggcagtgccaaggaaga

3.9 Statistical analysis

Unless otherwise specified, each determination was done in triplicate and results were expressed as means ± standard deviation. Statistical analysis was perfomed using SPSS statistical software version 22.0. Independent t-test was performed to compare means between two groups. One-way analysis of variance (ANOVA) and Welch-ANOVA test were used to compare means among three or more than three groups. One-way ANOVA (when variances are equal) or Welch-ANOVA (when variances are not equal) was followed by Tukey's or Games-Howell's post hoc test, respectively. Values were considered to be statistically significant if the *p* value was less than 0.05. Pearson correlation were used to investigate the correlation between antioxidant components and the antioxidant activities. A correlation was considered statistically significant if the *p* value was less than 0.01 ($p < 0.01$).

CHAPTER 4: RESULTS

4.1 Extraction yield

The extraction yields of MP using various solvents are shown in **Table 4.1**. The extraction yields obtained appear to increase with increasing polarity of the solvents used in the study, whereby the water extract (MP-W) showed the highest yield of 12.00%, while the hexane extract (MP-HX) had the lowest yield of 2.65%. This suggests that the extractable constituents of MP leaves are mostly polar and water soluble.

Table 4.1: Extraction yields and antioxidant components of MP leaf extracts. Values are mean ± SD (n = 3). Mean values with different letters (a-d) are significantly different (p <0.05). *TPC, total phenolic content; TFC, total flavonoid content, GAE, gallic acid equivalent; QE, quercetin equivalent; DE, dried extract.

Extraction solvent	Extraction yield (%)	TPC (mg GAE/g DE)	TFC (mg QE/g DE)
Hexane	2.65	28.39 ± 0.63^{a}	36.13 ± 2.48^{a}
Ethyl acetate	3.84	31.41 ± 1.07^{b}	56.45 ± 1.73^{b}
Methanol	5.78	61.31 ± 1.39^{c}	97.85 ± 3.71^{c}
Water	12.00	$30.29 \pm 0.75^{a,b}$	5.42 ± 0.27^{d}

4.2 Antioxidant activity of *Melicope ptelefolia*

4.2.1 Total phenolic content

Total phenolic content (TPC) was determined from gallic acid standard curve (**Figure 4.1**). The TPC values of MP extracts are shown in **Table 4.1**. MP-MeOH showed the highest TPC value of 61.31 ± 1.39 mg GAE/g DE, followed by MP-EA, MP-W and MP-HX extracts. To gauge a comparative picture on the antioxidant potential of MP, berries fruit extracts were prepared employing the same sequential extraction protocol as of MP leaves. Interestingly, the TPC values of MP-HX, MP-EA

and MP-MeOH extracts were significantly higher than raspberry, blackberry and blueberry equivalent extracts (**Figure 4.2**).

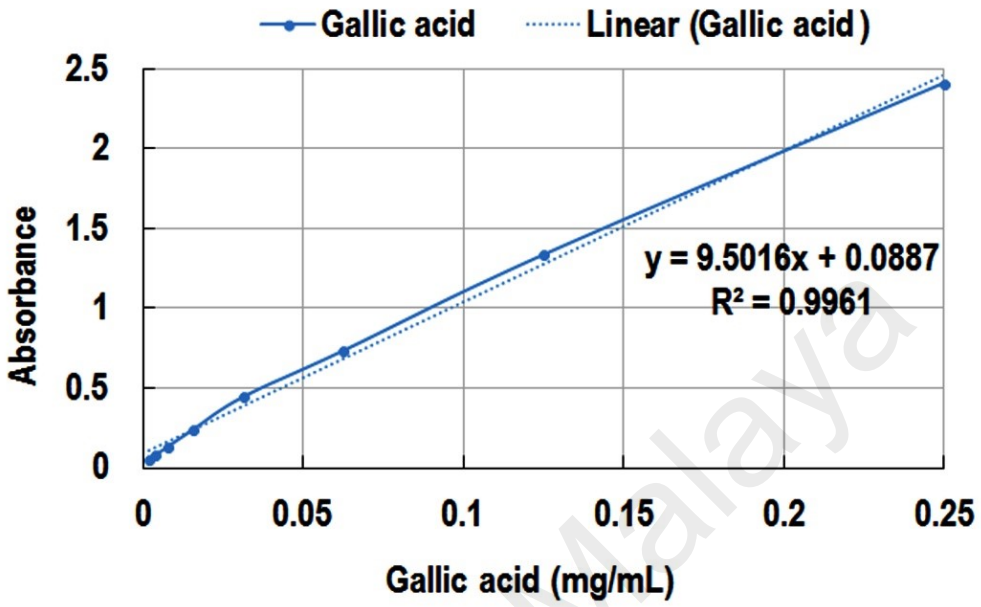

Figure 4.1: Gallic acid standard curve for the determination of total phenolic content.

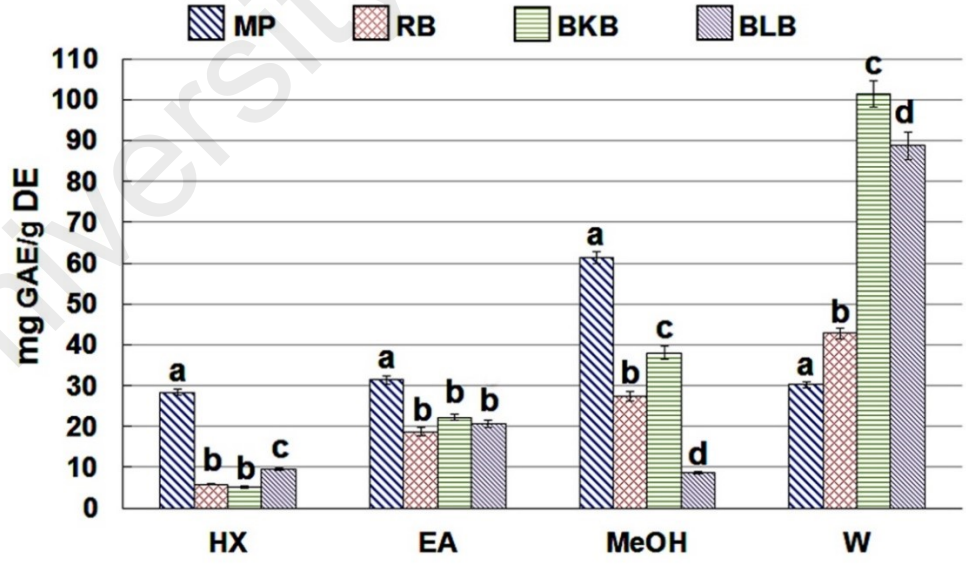

Figure 4.2: Determination of total phenolic content of MP leaf extracts. Values are mean ± SD (n = 3). Mean values with different letters (a-d) are significantly different (p <0.05). *GAE, gallic acid equivalent; DE, dried extract; RB, raspberry; BKB, blackberry; BLB, blueberry; HX, hexane; EA, ethyl acetate; MeOH, methanol; W, water.

4.2.2 Total flavonoid content

Total flavonoid content was determined from quercetin standard curve (**Figure 4.3**). The total flavonoid content (TFC) values of MP extracts are presented in **Table 4.1**. Among MP extracts, MP-MeOH exhibited the highest TFC, followed by (in descending order) MP-EA, MP-HX and MP-W. For berries fruit extracts (raspberry, RB; blackberry, BKB; blueberry, BLB), the TFC values obtained were in the following descending order: BLB-HX, BKB-EA, BKB-MeOH and BLB-W extracts (**Figure 4.4**). Interestingly, the TFC values of MP-HX, MP-EA and MP-MeOH were notably higher than the same extracts of berries fruit. The TFC value of MP-HX was 2.0 times higher than BLB-HX, while MP-EA TFC value was 4.3 times higher than BKB-EA. The TFC value of MP-MeOH was 20.9 times higher than BKB-MeOH. However, the TFC value of MP-W was 2.3 times lower than BLB-W.

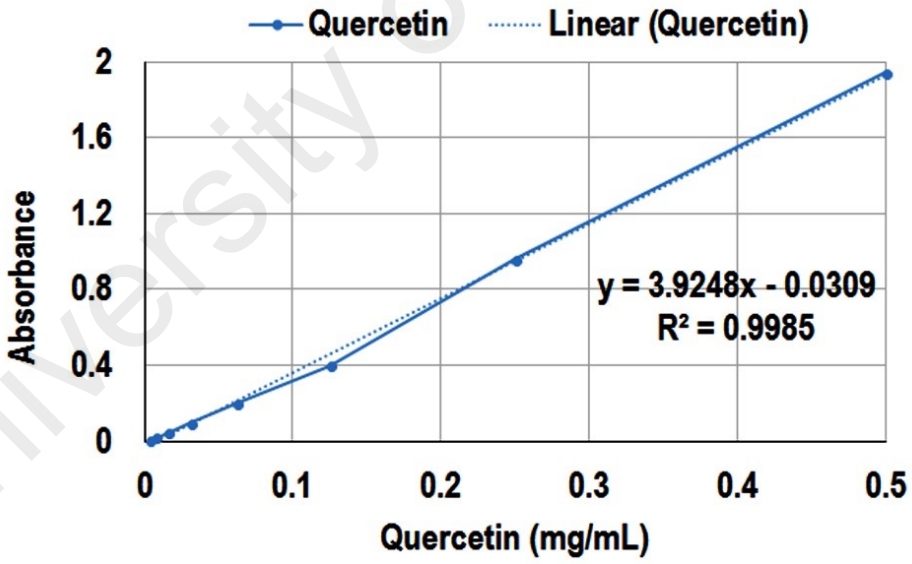

Figure 4.3: Quercetin standard curve for the determination of total flavonoid content.

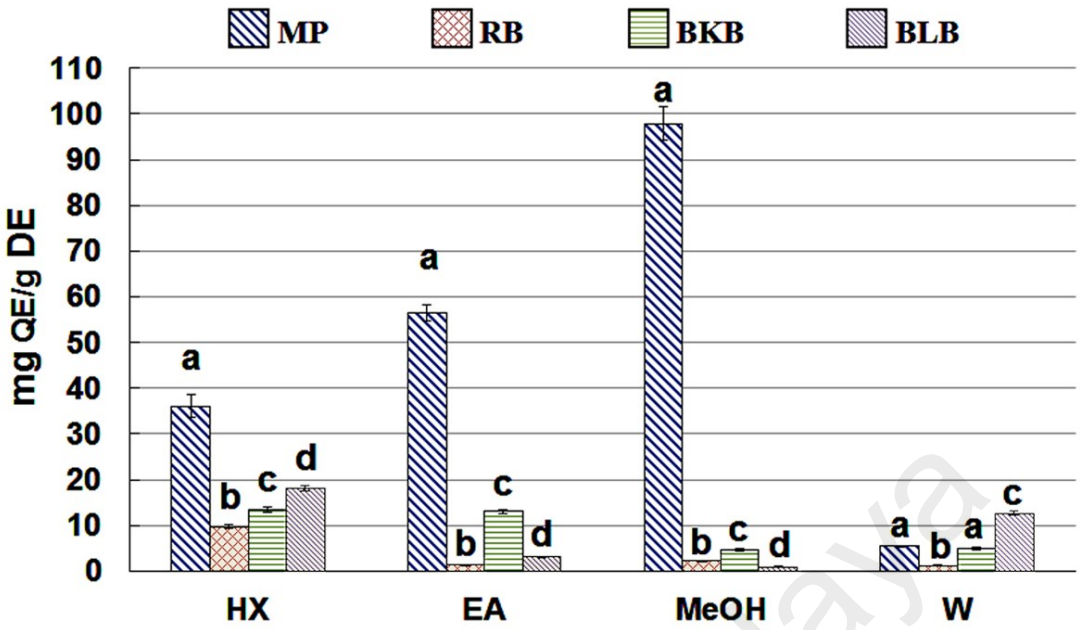

Figure 4.4: Determination of total flavonoid content of MP leaf extracts. Values are mean ± SD (n = 3). Mean values with different letters (a-d) are significantly different (p <0.05). *QE, quercetin equivalent; DE, dried extract; RB, raspberry; BKB, blackberry; BLB, blueberry; HX, hexane; EA, ethyl acetate; MeOH, methanol; W, water.

4.2.3 Ferric reducing antioxidant power (FRAP) activity

The FRAP value of the extracts were deduced based on $FeSO_4$ standard curve (**Figure 4.5**). All MP extracts demonstrated high FRAP values, ranging from 300.65 ± 3.54 to 1150.97 ± 2.93 mM Fe^{2+}/g DE (**Table 4.2**). The highest activity was exhibited by MP-W (1150.97 ± 2.93 mM Fe^{2+}/g DE) followed by (in descending order) MP-MeOH, MP-EA and MP-HX. MP-W demonstrated notable FRAP values as compared to the positive controls, although the values were approximately 48%, 45% and 40% of that shown by catechin, gallic acid and ascorbic acid, respectively.

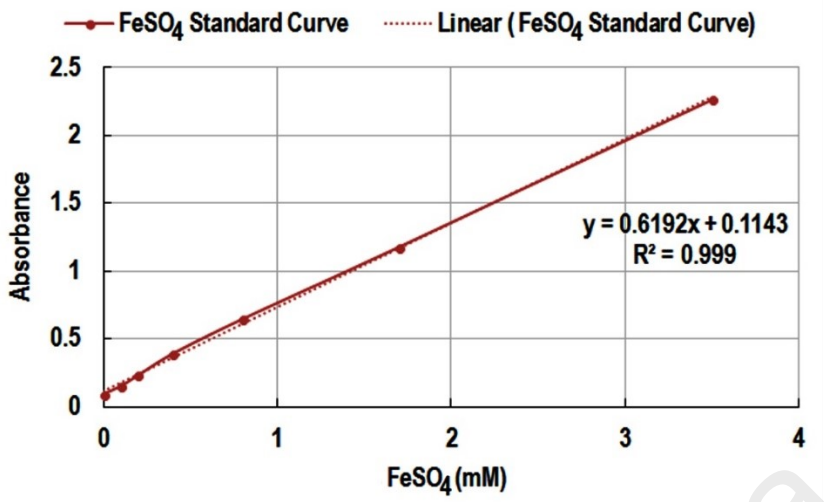

Figure 4.5: Ferrous sulphate ($FeSO_4$) standard curve for the determination of ferric reducing antioxidant power.

4.2.4 $ABTS^{\bullet+}$ radical-scavenging activity

The $ABTS^{\bullet+}$ scavenging activity of MP extracts are shown in **Figure 4.6**. At 1.0 mg/mL, MP-HX and MP-EA were able to scavenge more than 80% of $ABTS^{\bullet+}$ radicals, whereas MP-MeOH and MP-W scavenging activity were approximately 41 and 55%, respectively. The IC_{50} values of the extracts are presented in **Table 4.2**. MP-HX showed the most notable scavenging activity, with an IC_{50} value of 267.73 ± 5.58 µg/mL, followed by (in descending order) MP-EA, MP-W and MP-MeOH. MP-HX showed notable $ABTS^{\bullet+}$ radical-scavenging activity, although its IC_{50} values were ~3.0, 3.3, 5.7 times higher than trolox (TX), ascorbic acid (AA) and quercetin (QN), respectively. Similarly, MP-EA showed notable scavenging activity, although its IC_{50} values were 3.6, 4.0 and 6.8 times higher than TX, AA and QN, respectively.

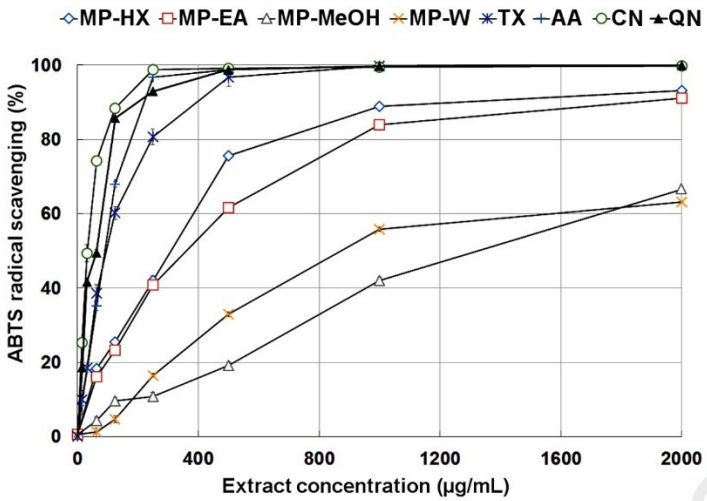

Figure 4.6: Determination of ABTS$^{\bullet+}$ radical-scavenging activity of MP leaf extracts. Values are mean ± SD (n=3). *TX, trolox; AA, ascorbic acid; CN, catechin; QN, quercetin.

4.2.5 DPPH$^{\bullet}$ radical-scavenging activity

The results are shown in **Table 4.2** and **Figure 4.7**. MP-HX exhibited the strongest DPPH$^{\bullet}$ scavenging activity, similar to that seen in ABTS$^{\bullet+}$ scavenging assay. Based on the IC_{50} values, the relative DPPH$^{\bullet}$ scavenging activity of the extracts (in descending order) were: MP-HX > MP-EA > MP-MeOH > MP-W.

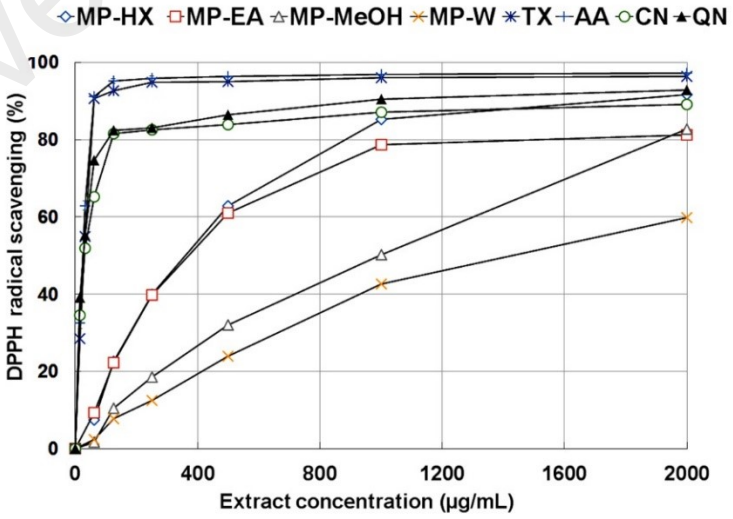

Figure 4.7: Determination of DPPH$^{\bullet}$ radical-scavenging activity of MP leaf extracts. Values are mean ± SD (n=3). *TX, trolox; AA, ascorbic acid; CN, catechin; QN, quercetin.

Table 4.2: Antioxidant activities of MP leaf extracts. Values are mean ± SD (n = 3). The mean values in each column with different letters (a-g) are significantly different ($p < 0.05$). *TX, trolox; AA, ascorbic acid; GA, gallic acid; CN, catechin; QN, quercetin; PP, polyphenon-60; DE, dried extract; ND, not done.

Extraction solvent	**FRAP (mM Fe^{2+}/g DE)**	**$ABTS^{\bullet+}$ (IC_{50} µg/mL)**	**$DPPH^{\bullet}$ (IC_{50} µg/mL)**	**CAA (Hs27) (EC_{50} µg/mL)**
Hexane	300.65 ± 3.54^{a}	267.73 ± 5.58^{a}	327.40 ± 3.80^{a}	11.30 ± 0.68^{a}
Ethyl acetate	482.23 ± 5.81^{b}	322.63 ± 4.67^{b}	363.60 ± 4.26^{b}	37.32 ± 0.68^{b}
Methanol	811.07 ± 11.02^{c}	1264.33 ± 28.38^{c}	838.93 ± 27.40^{c}	208.94 ± 2.67^{c}
Water	1150.97 ± 2.93^{d}	997.73 ± 14.21^{d}	1368.00 ± 28.93^{d}	339.62 ± 2.07^{d}
Positive controls				
TX	ND	88.84 ± 3.76^{e}	26.08 ± 0.42^{e}	4.02 ± 0.15^{e}
AA	2889.59 ± 13.56^{e}	79.64 ± 2.22^{e}	22.95 ± 0.50^{f}	ND
GA	2560.15 ± 28.86^{f}	ND	ND	ND
CN	2387.02 ± 46.65^{f}	31.29 ± 1.11^{f}	28.73 ± 0.34^{g}	ND
QN	ND	46.95 ± 0.58^{g}	22.43 ± 0.58^{f}	0.57 ± 0.01^{f}
PP	ND	ND	ND	1.12 ± 0.08^{g}

4.2.6 Cellular antioxidant activity

In the present study, the CAA assay was carried out using the non-cancerous ATCC human fibroblast cell line, Hs27. The results showed that the pure phytochemical compounds (positive controls) and MP extracts were able to inhibit the oxidation of DCFH by ABAP-generated peroxyl radicals in a dose-dependent manner **(Figure 4.8)**. The median effective dose (EC_{50}) was determined from the median effect plot (**Figure 4.9**). The EC_{50} value of quercetin in Hs27 cell line was 1.88 ± 0.03 μM, and this value is 2.7 times lower than that observed in HepG2 cells, which was 5.09 ± 0.19 μM (Wolfe & Liu, 2007). This difference may have been due to the fact that HepG2, being a type of cancer cell line, experienced higher oxidative stress environment compared to non-cancerous Hs27 cell line. As for MP extracts, all of them showed notable cellular antioxidant activity **(Figure 4.10)**. Based on the EC_{50} values **(Table 4.2)**, MP-HX showed the most notable CAA value, followed by MP-EA. However, MP-HX and MP-EA showed lower activities compared to trolox, with EC_{50} values that were 2.8 and 9.3 folds higher than trolox, respectively. MP-MeOH and MP-W exhibited lower antioxidant potential, since their EC_{50} values were significantly higher than MP-HX and MP-EA.

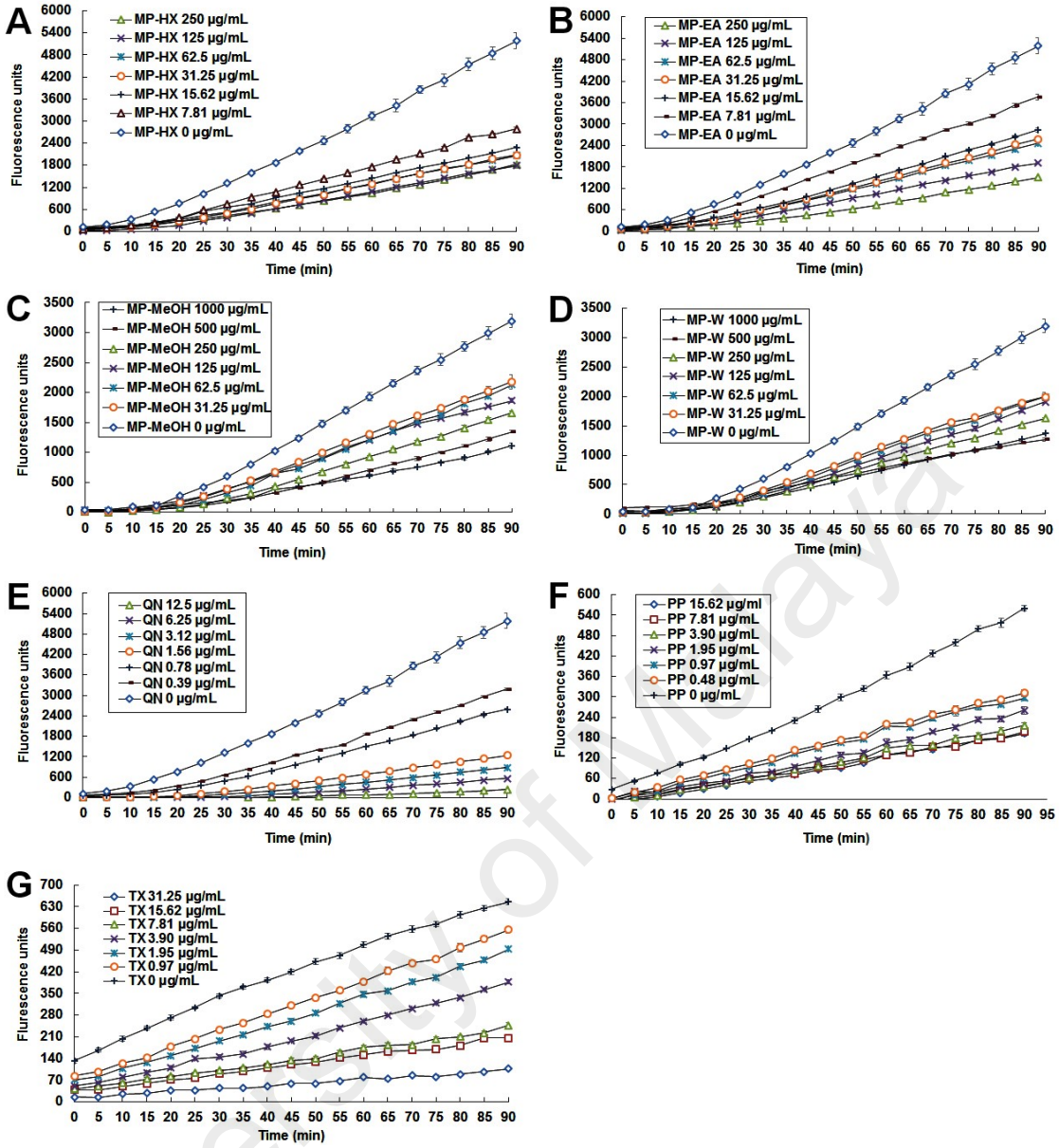

Figure 4.8: Cellular antioxidant activity of MP leaf extracts and positive controls. Inhibition of peroxyl radical-induced oxidation of DCFH in Hs27 cells by (A) MP-HX, (B) MP-EA, (C) MP-MeOH, (D) MP-W, (E) QN (F) PP and (G) TX. The curves shown in each graph are from a single experiment (mean ± SD, n =3). *QN, quercetin; PP, polyphenon-60; TX, trolox.

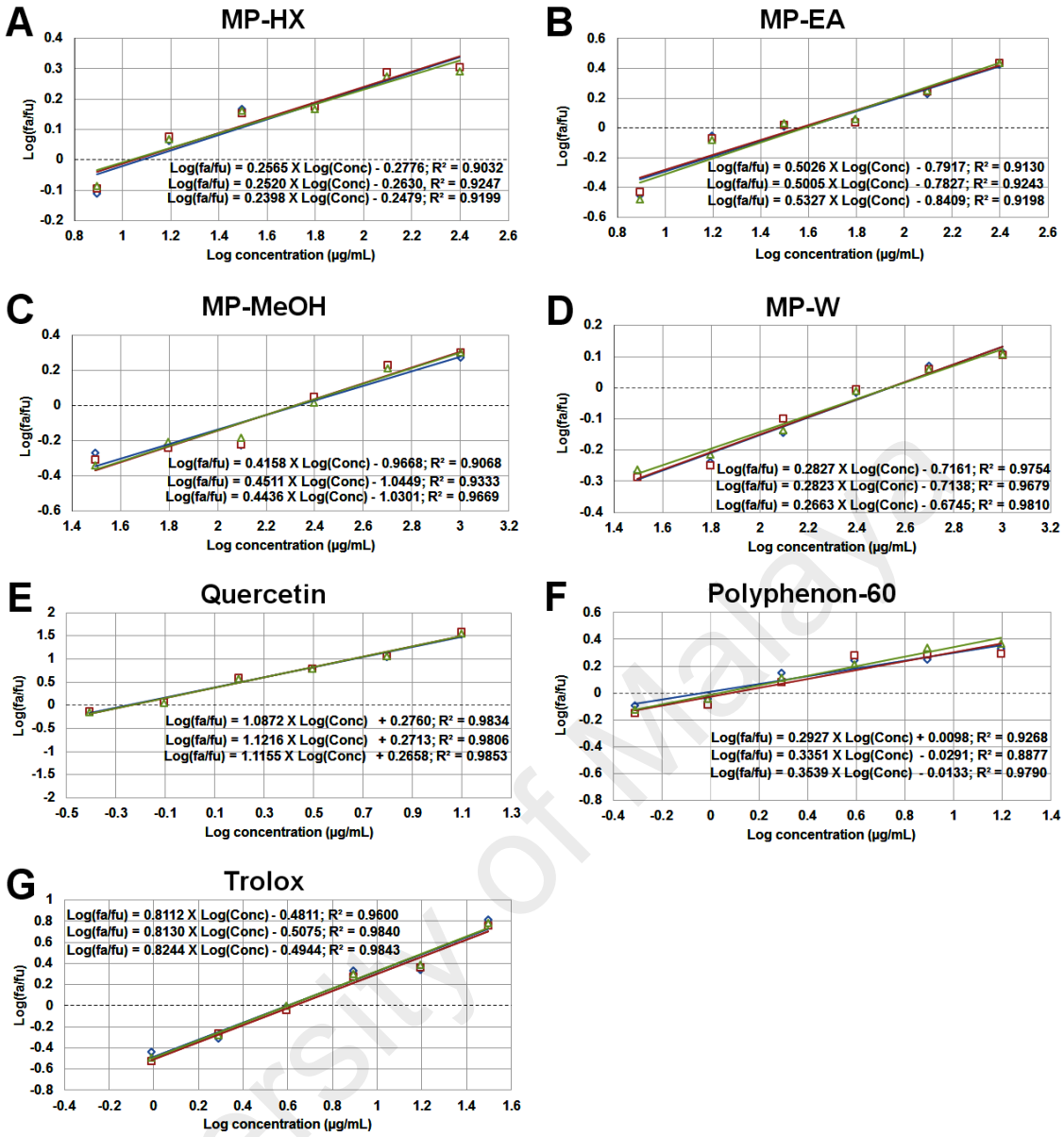

Figure 4.9: Median effect plots for the inhibition of peroxyl radical-induced DCFH oxidation in Hs27 cells by MP leaf extracts and positive controls. (A) MP-HX, (B) MP-EA, (C) MP-MeOH, (D) MP-W, (E) quercetin, (F) polyphenon-60 and (G) trolox. The curves shown in each graph are from a single experiment (mean ± SD, n =3).

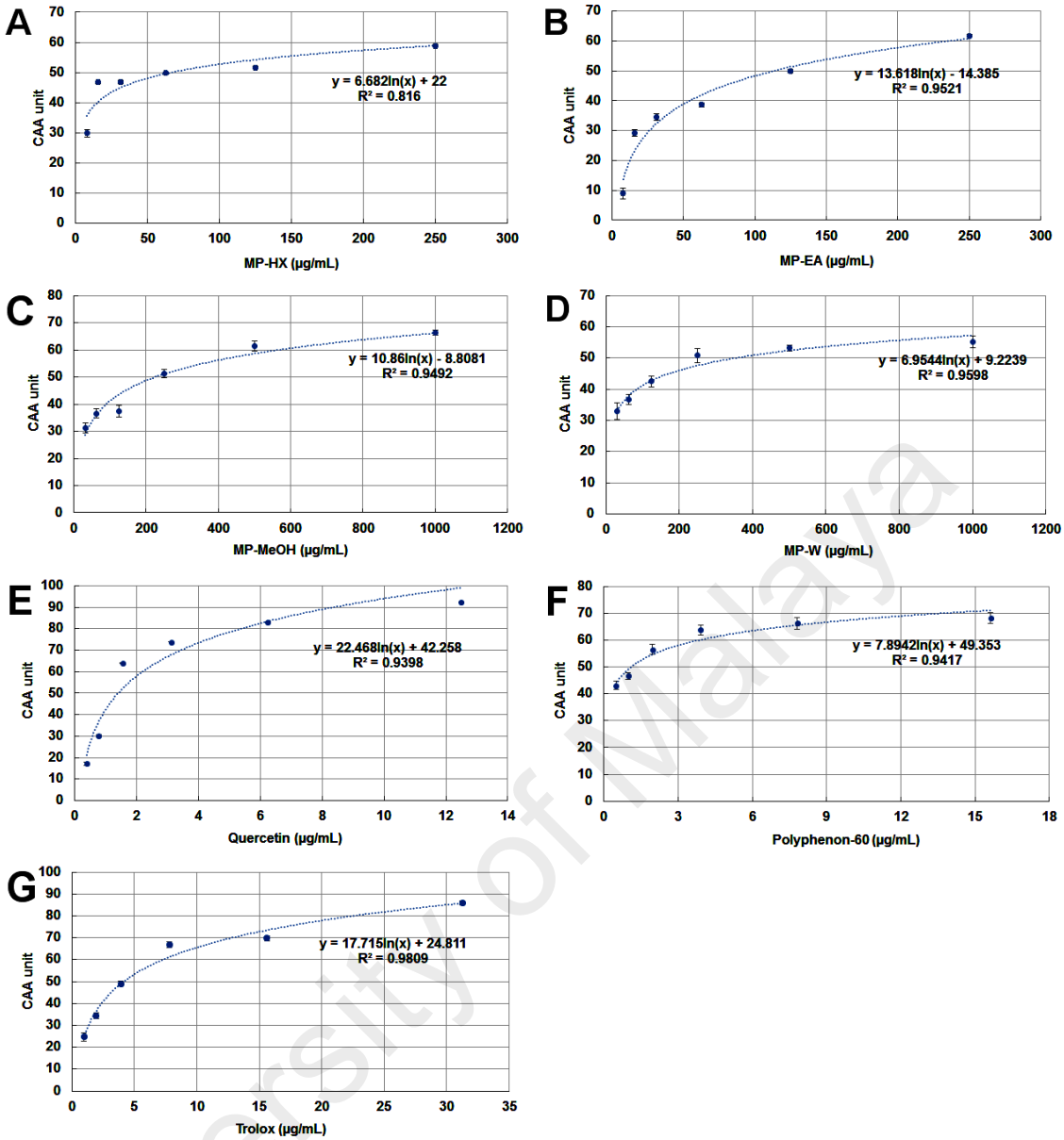

Figure 4.10: Dose-response curve for the inhibition of peroxyl radical-induced DCFH oxidation in Hs27 cells by MP leaf extracts and positive controls. (A) MP-HX, (B) MP-EA, (C) MP-MeOH, (D) MP-W, (E) quercetin, (F) polyphenon-60 and (G) trolox. The curves shown in each graph are from a single experiment (mean ± SD, n =3).

4.2.7 Correlation analysis

Correlation analysis between antioxidant components and antioxidant activities of MP extracts are shown in **Table 4.3**. Comparing the value of antioxidant activities of MP extracts as indicated by the different assays, there was a strong to very strong positive correlation between the assays, ranging from 0.777 to 0.993. This suggest that

$ABTS^{\bullet+}$, $DPPH^{\bullet}$, and CAA assays could provide a consistent picture on the antioxidant activity potential of MP extracts.

A correlation analysis between TPC and TFC with antioxidant activities was also performed, to evaluate their relationship. A strong positive correlation of 0.849 was observed between TFC and TPC, suggesting that flavonoids are the predominant phenolic compounds in MP. Although TPC demonstrated a positive correlation (0.750) with $ABTS^{\bullet+}$ assay, its correlation with $DPPH^{\bullet}$ and CAA assays was weak. In contrast, the correlation of TFC with $ABTS^{\bullet+}$ assay was weak, and negative correlation of TFC with $DPPH^{\bullet}$ and CAA assays were also observed.

Table 4.3: Pearson correlation analysis for antioxidant components and activities of MP leaf extracts. *Significant correlation at $p < 0.01$.

	TPC	**TFC**	**$ABTS^{\bullet+}$**	**$DPPH^{\bullet}$**	**CAA**
TPC	1	0.849*	0.750*	0.171	0.273
TFC	0.849*	1	0.302	–0.351	–0.247
$ABTS^{\bullet+}$	0.750*	0.302	1	0.777*	0.838*
$DPPH^{\bullet}$	0.171	–0.351	0.777*	1	0.993*
CAA	0.273	–0.247	0.838*	0.993*	1

4.3 Anticancer activity of *Melicope ptelefolia*

4.3.1 Antiproliferative activity

The antiproliferative activities of the extracts were initially evaluated against the cancer cell lines at 250 µg/mL, using Promega CellTiter 96® AQueous One Solution Cell Proliferation Assay (MTS assay). The result indicated that MP-HX and MP-EA

were able to reduce the viability of all cancer lines tested to about 30%, indicating notable antiproliferative activity (**Figure 4.11**). MP-MeOH and MP-W did not demonstrate notable antiproliferative activity. They exerted modest inhibition of HCT116 cells proliferation at 250 µg/mL, reducing viability to only 73.8% and 78.7%, respectively.

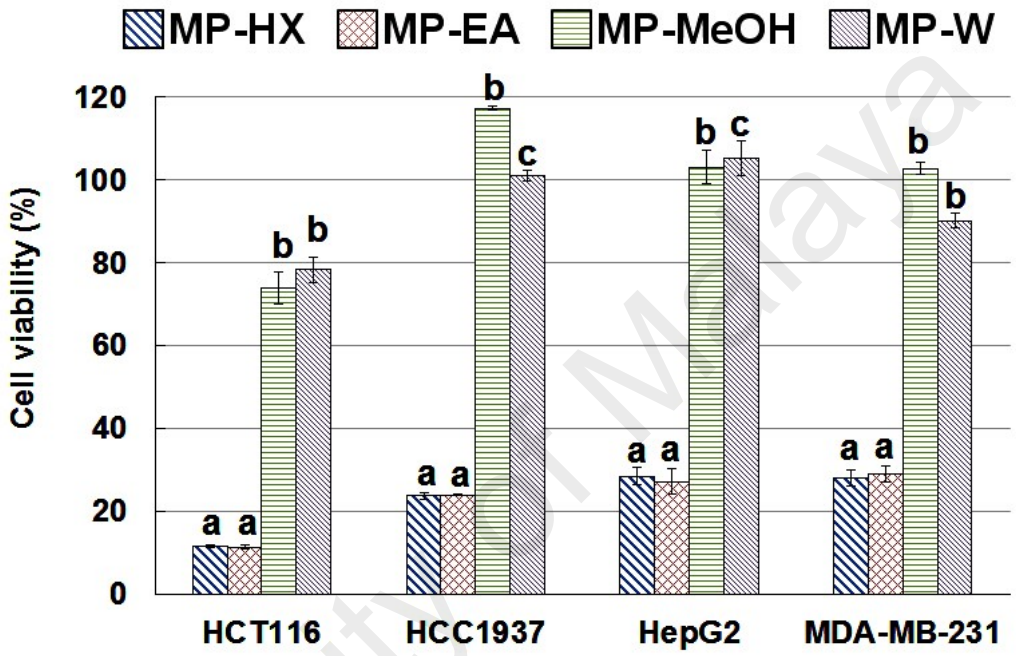

Figure 4.11: High dose MTS cell viability assay. Effect of MP leaf extracts (250 µg/mL, 48 h) on the cell viability of HCT116, HCC1937 and HepG2 and MDA-MB-231 cell lines. Values are mean ± SD (n=3). The mean values with different letters (a-c) are significantly different, p <0.05.

The IC_{50} values of MP-HX and MP-EA against the cancer cell lines were then investigated further. A dose-dependent antiproliferative activity was observed for MP-HX and MP-EA extracts on HCT116, HCC1937, HepG2 and MDA-MB-231 cell lines (**Figure 4.12**). MP-HX exhibited promising antiproliferative activity against the entire cancer cell lines tested, with IC_{50} concentrations ranging from 58.04 ± 0.96 to 94.80 ± 3.01 µg/mL (**Table 4.4**). MP-EA also exhibited potent antiproliferative activity against HCT116, HCC1937 and MDA-MB-231, with IC_{50} values ranging from 64.69 ± 0.72 to

97.09 ± 1.10 µg/mL (**Table 4.4**). Interestingly, IC_{50} value of MP-HX on HepG2 cells was lower than that shown by 5-FU.

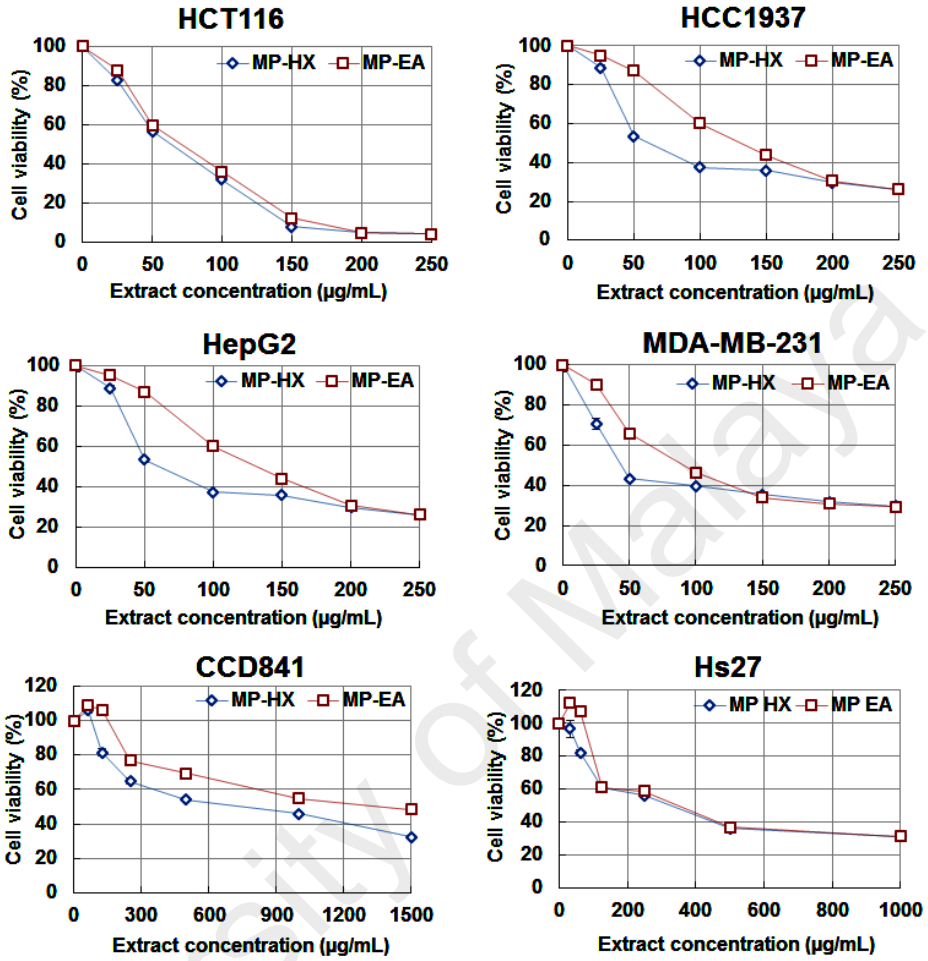

Figure 4.12: MTS cell viability assay. Dose response curves for the cytotoxic effect of MP-HX and MP-EA (48 h treatment) on cancerous (HCT116, HCC1937, HepG2, MDA-MB-231) and non-cancerous (CCD841, Hs27) cell lines.

To evaluate the selectivity and toxicity of MP-HX and MP-EA against non-cancerous cell lines, they were tested against CCD841 and Hs27 cell lines, which were normal colon and fibroblast cell lines, respectively. Both extracts showed relatively higher IC_{50} values on these cell lines (ranging from 311.30 ± 12.41 to 1218.33 ± 5.50 µg/mL) (**Table 4.4**), suggesting the extracts were selectively more toxic towards the cancer cell lines.

Table 4.4: MTS Cell viability assay. IC_{50} values of MP-HX and MP-EA on cancer and non-cancerous cell lines. Values are mean ± SD (n = 3). Mean values in each row with different letters (a, b and c) are significantly different ($p < 0.05$).

Cell line	**MP-HX** **IC_{50} (µg/mL)**	**MP-EA** **IC_{50} (µg/mL)**	**5-FU** **IC_{50} (µg/mL)**
HCT116	58.04 ± 0.96^a	64.69 ± 0.72^b	13.81 ± 0.58^c
HCC1937	94.80 ± 3.01^a	95.71 ± 0.36^a	79.02 ± 2.12^b
HepG2	79.41 ± 1.88^a	130.93 ± 3.17^b	95.02 ± 3.56^c
MDA-MB-231	57.81 ± 3.49^a	97.09 ± 1.10^b	24.45 ± 4.52^c
CCD841	680.93 ± 8.76^a	1218.33 ± 5.50^b	9.64 ± 0.02^c
Hs27	311.30 ± 12.41^a	357.13 ± 5.11^b	> 250

4.3.2 Caspase-3/7 induction activity

Caspase-3/7 assay was done using Promega Apotox-Glo™ assay kit which included a luminogenic caspase-3/7 substrate. An increase in luminescence value indicates caspase-3/7 activation. The results indicated that both MP-HX and MP-EA extracts were able to significantly ($p < 0.05$) activate caspase-3/7 activity in almost all of the cancer cell lines tested (**Figure 4.13**). The cancer cells treated with MP-HX showed caspase-3/7 activation in MDA-MB-231, HepG2 and HCT116 that was 2.38, 4.39 and 5.53 folds higher respectively, compared to the corresponding vehicle control. MP-HX apparently did not induce caspase-3/7 activation in HCC1937. MP-EA treatment induced caspase-3/7 activation in HCC1937, HCT116, MDA-MB-231 and HepG2, that was 1.60, 1.79, 2.29 and 5.10 folds higher respectively, compared to the corresponding vehicle control.

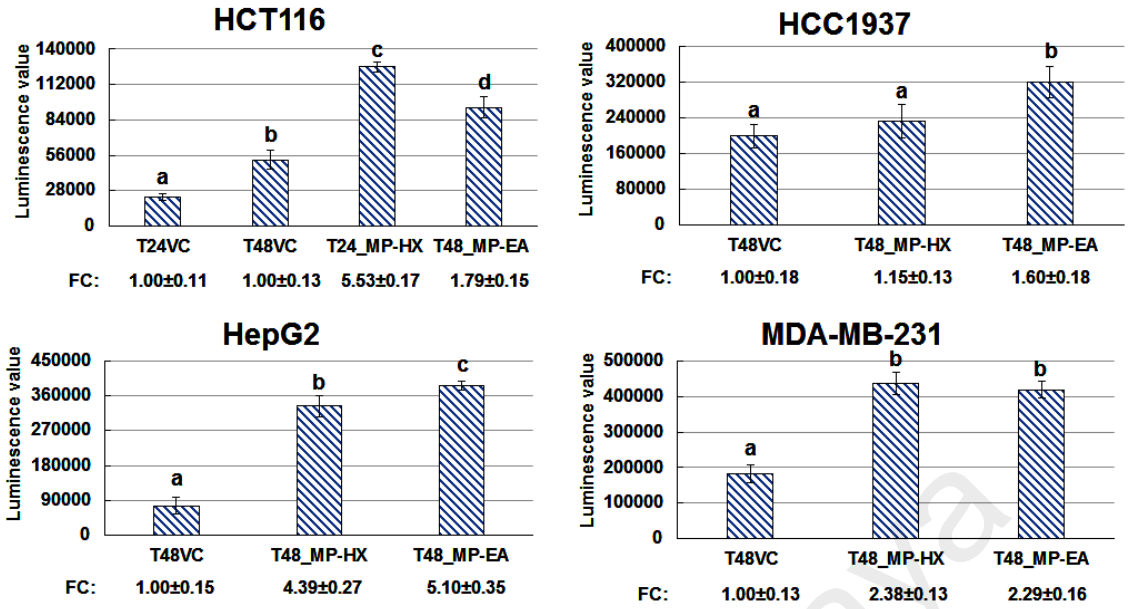

Figure 4.13: The effect of MP-HX and MP-EA on caspase 3/7 activity in cancer cell lines. The bar charts depict luminescence value for caspase 3/7 activity. The concentration of the extracts used in each treatment was at ~IC_{50} value for the corresponding cell lines indicated. Values are mean ± SD (n=3). The values with different letters (a-d) are significantly different, p <0.05. *T24/T48, 24 or 48 h treatment, respectively; VC, vehicle control; FC, fold change compared to VC.

4.3.3 Multicaspase induction activity

Muse™ multicaspase (Merck Millipore, USA) assay kit was used to detect initiator as well as executioner caspases activation (caspase-1, 3, 4, 5, 6, 7, 8, and 9). The results indicated that both MP-HX and MP-EA were able to significantly increase the percentage of cells with activated caspases in the entire cancer cell lines tested **(Figures 4.14** and **4.15)**. MP-HX and MP-EA treatments on HCT116 significantly increased the percentage of cells with caspases activation, whereby the percentage of cells were 8.2 and 17.4 folds higher than the corresponding vehicle control, respectively.

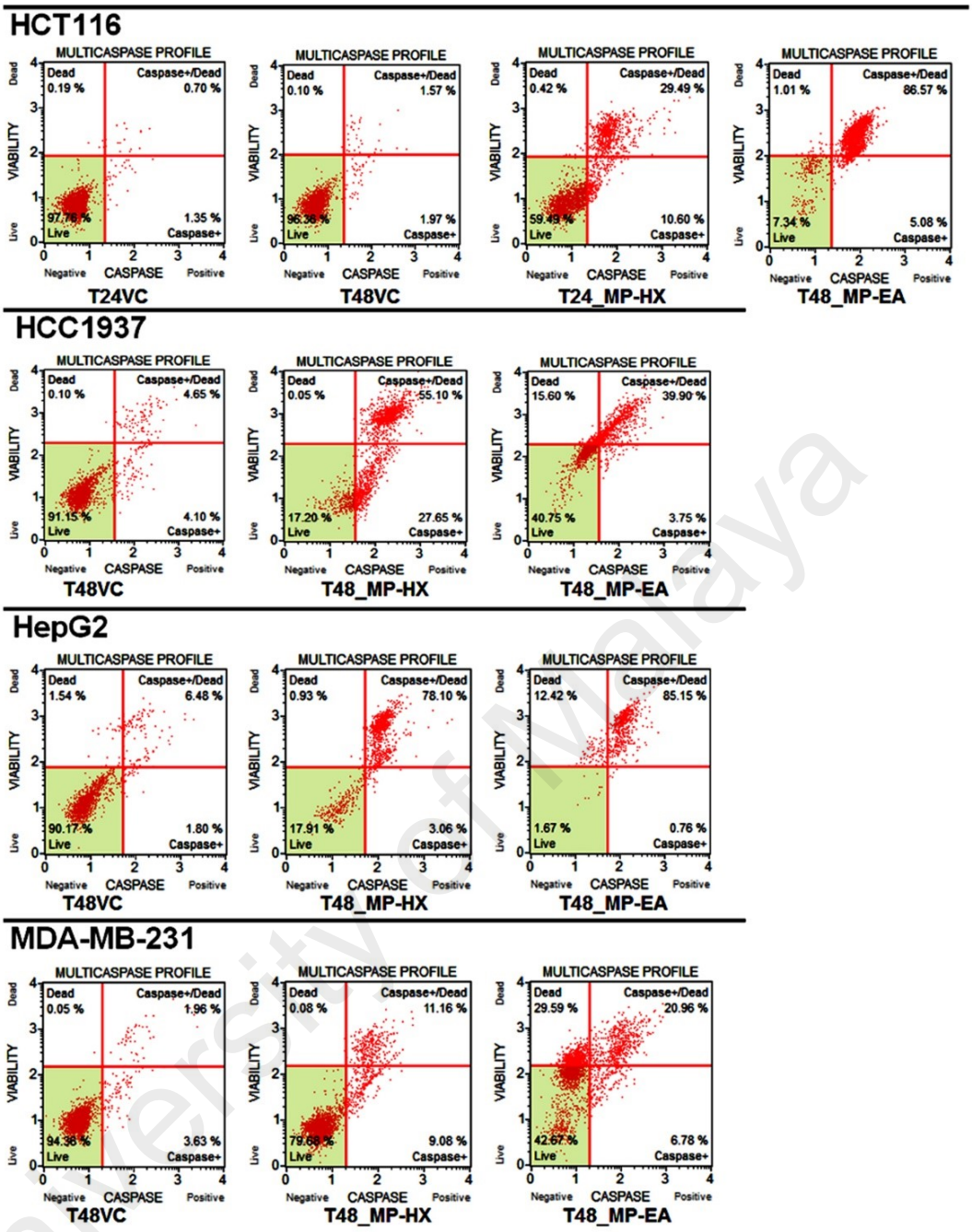

Figure 4.14: Flow cytometry plots of multicaspase enzyme activation assay. The plots depict the effect of MP-HX and MP-EA treatments in the cancer cell lines indicated. Each plot is a representative figure of the three replicates of each determination. The concentration of the extracts used in each treatment was at ~IC_{50} value for the corresponding cell lines indicated. *T24/T48, 24 or 48 h treatment, respectively; VC, vehicle control.

MP-HX and MP-EA treatments on HCC1937 significantly increased the percentage of cells with caspases activation, whereby the percentage of cells were 9.4 and 5.0 folds higher than the corresponding vehicle control, respectively. For HepG2 cell line, MP-

HX and MP-EA treatments significantly increased the percentage of cells with caspases activation, whereby the percentage of cells were 6.5 and 6.6 folds higher than the corresponding vehicle control, respectively. For MDA-MB-231 cell line, MP-HX and MP-EA treatment significantly increased the percentage of cells with caspases activation, whereby the percentage of cells with caspases activation were 3.5 and 4.7 folds higher than the corresponding vehicle control, respectively. Taken together, caspase-3/7 and multicaspase assays result suggest that MP-HX and MP-EA were able to induce caspase-dependent apoptotic cell death in the entire cancer cell lines tested.

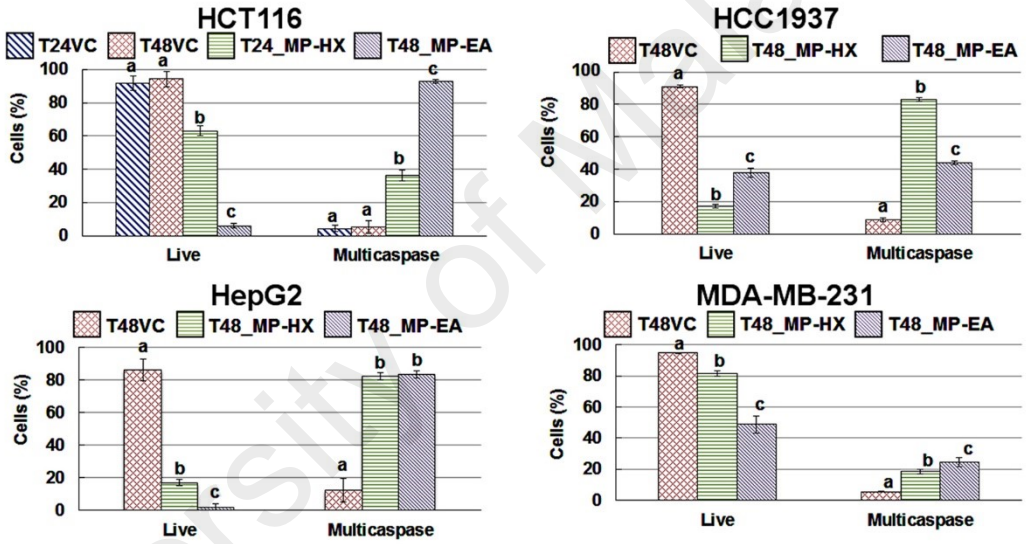

Figure 4.15: Bar charts of multicaspase enzyme activation assay. The bar charts depict the percentage of live cells and those with caspase activation. The concentration of the extracts used in each treatment was at ~IC_{50} value for the corresponding cell lines indicated. Values are mean ± SD (n=3). The means values with different letters (a-d) are significantly different, p <0.05. *T24/T48, 24 or 48 h treatment, respectively, VC, vehicle control.

4.3.4 Apoptosis induction activity

The results of the present study indicated that both MP-HX and MP-EA extracts were cytotoxic to the entire cancer cell lines tested, being able to significantly reduce viability of the cancer cells (**Figures 4.16** and **4.17**). In the HCT116 cells, treatments

with MP-HX and MP-EA significantly reduced cell viability to 28.81 ± 1.30 and 2.03 ± 0.18%, respectively. The treatments with MP-HX and MP-EA also markedly increased the percentage of late apoptotic cells in HCT116, which were 54.75 ± 0.10 and 90.23 ± 0.59%, respectively, compared to the corresponding vehicle controls, which were 18.95 ± 2.94 and 6.30 ± 1.06%, respectively. For the HCC1937 cells, treatments with MP-HX and MP-EA significantly reduced cell viability to 25.31 ± 0.89 and 4.90 ± 0.85%, respectively, compared to the corresponding vehicle control, which was 84.98 ± 1.61%. MP-HX also markedly increased the percentage of early apoptotic cells in HCC1937 to 18.50 ± 1.31%, compared to the corresponding vehicle control, which was only 2.21 ± 0.42%. The treatments with MP-HX and MP-EA also increased the percentage of late apoptotic cells in HCC1937, which were 52.13 ± 2.15 and 51.33 ± 0.43%, respectively, compared to the corresponding vehicle control, which was only 9.53 ± 1.07%.

For the HepG2 cells, treatments with MP-HX and MP-EA significantly reduced cell viability to 53.88 ± 2.37 and 10.11 ± 2.44%, respectively, compared to the corresponding vehicle control, which was 86.30 ± 0.74%. MP-HX also markedly increased the percentage of early apoptotic cells in HepG2 to 23.10 ± 1.18%, compared to the corresponding vehicle control, which was only 2.93 ± 1.40%. The treatments with MP-HX and MP-EA also increased the percentage of late apoptotic cells in HepG2, which were 19.38 ± 1.71 and 39.88 ± 2.54%, respectively, compared to the corresponding vehicle control, which was only 8.43 ± 1.00%.

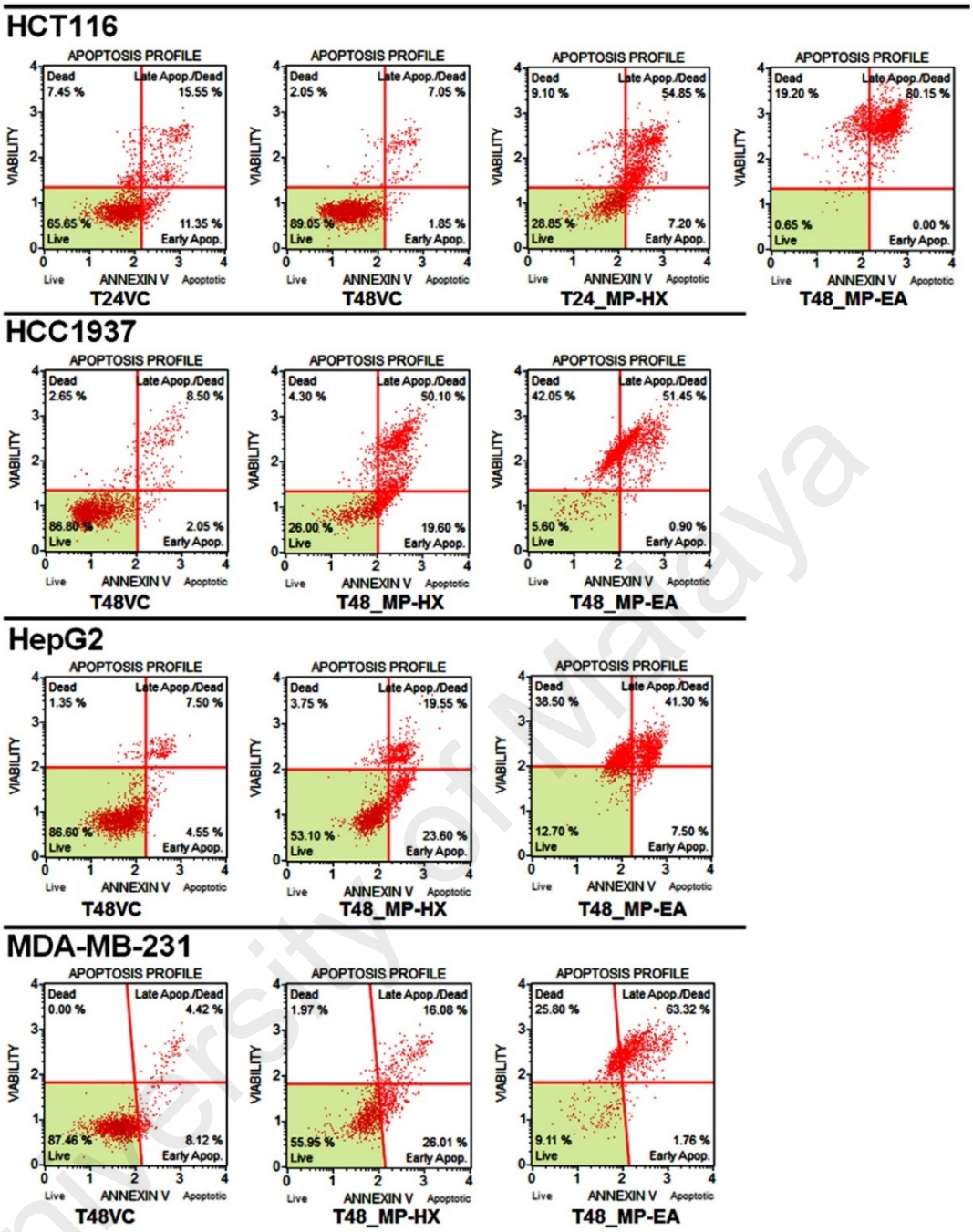

Figure 4.16: Plots of Annexin-V & Dead Cell (7-AAD) flow cytometry analysis. Apoptotic effect of MP-HX and MP-EA on HCT116, HCC1937, HepG2 and MDA-MB-231 cell lines. Each plot is a representative figure of the three replicates of each determination. The concentration of the extracts used in each treatment was at ~IC_{50} value for the corresponding cell lines indicated. *T24, 24 h treatment; T48, 48 h treatment; VC, vehicle control; L, live cells; EA, early apoptotic cells, LA, late apoptotic cells; D, dead cells.

For the MDA-MB-231 cells, treatments with MP-HX and MP-EA significantly reduced cell viability to 55.72 ± 1.28 and 7.17 ± 2.29%, respectively, compared to the

corresponding vehicle control, which was 82.14 ± 4.78%. MP-HX also markedly increased the percentage of early apoptotic cells in MDA-MB-231 to 25.79 ± 0.18%, compared to the corresponding vehicle control, which was only 12.29 ± 3.64%. The treatments with MP-HX and MP-EA also increased the percentage of late apoptotic cells in MDA-MB-231, which were 16.97 ± 1.12 and 63.81 ± 2.21%, respectively, compared to the corresponding vehicle control, which was only 5.52 ± 1.30%.

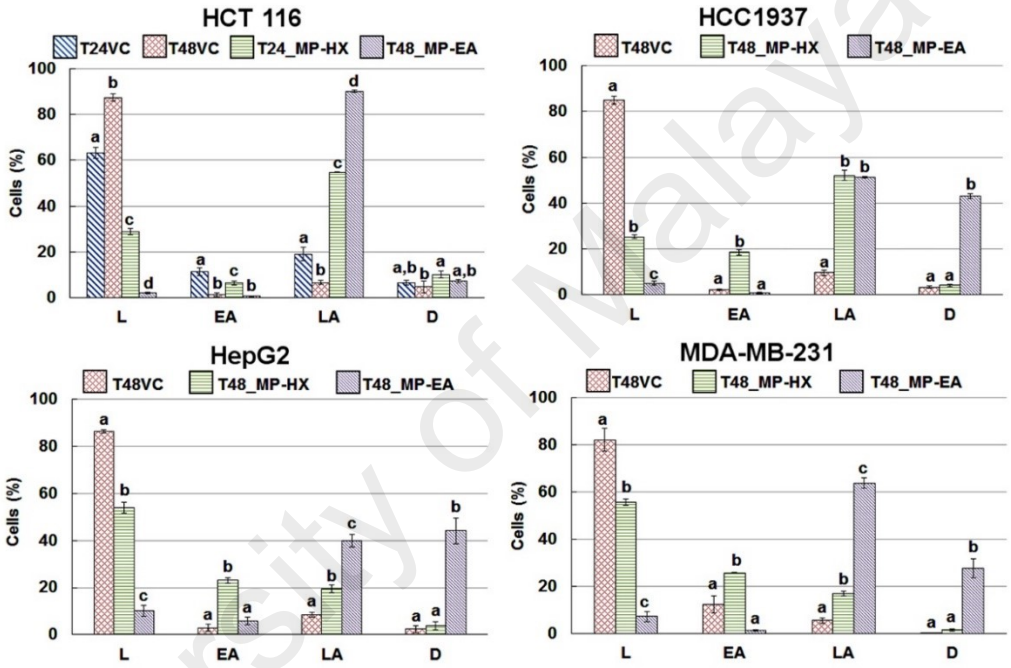

Figure 4.17: Bar charts of Annexin-V & Dead Cell (7-AAD) flow cytometry analysis. Apoptotic effect of MP-HX and MP-EA on HCT116, HCC1937, HepG2 and MDA-MB-231 cell lines. Bar charts depicting percentage of live, dead and apoptotic cells for the treatments on the corresponding cell lines. Values are mean ± SD (n=3). The mean values with different letters (a-d) are significantly different, p <0.05. The concentration of the extracts used in each treatment was at ~IC_{50} value for the corresponding cell lines indicated. T24, 24 h treatment; T48, 48 h treatment; VC, vehicle control. L, live cells; EA, early apoptotic cells, LA, late apoptotic cells; D, dead cells.

4.3.5 Caspase inhibition activity

This assay was performed to independently confirm that apoptosis induction of MP-HX and MP-EA extracts in the cancer cell lines was caspase dependent. The z-VAD-FMK (carbobenzoxy-valyl-alanyl-aspartyl-[O-methyl]-fluoromethylketone) reagent is a

cell-permeant pan caspase inhibitor that irreversibly binds to the catalytic site of caspase proteases, preventing apoptosis induction. The effect of the inhibitor on viability of the cancer cells in the presence and absence of MP-HX and MP-EA extracts are shown in **Figure 4.18**. The results indicated that z-VAD-FMK inhibitor (at 4 and 8 µM) was generally non-toxic to all of the cancer cell lines. As expected, treatments of all the cancer cell lines with MP-HX or MP-EA reduced cell viability. However, the viability was significantly and dose-dependently higher when z-VAD-FMK was added in the assay. This observation suggested that the cytotoxicity induced by the extracts was due to induction of apoptosis that was caspase dependent.

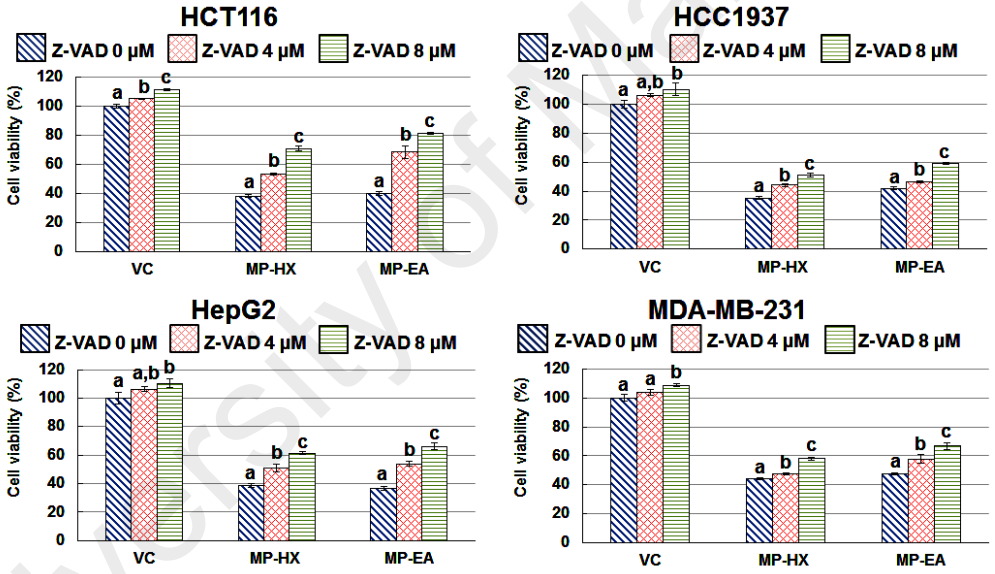

Figure 4.18: Pan caspase inhibitor assay. MTS cell viability assay (48 h) was employed using MP-HX or MP-EA extracts on the cell lines indicated, in the presence or absence of Z-VAD-FMK inhibitor. The concentration of the extracts used in each treatment was at ~IC_{50} value for the corresponding cell lines indicated. Values are mean ± SD (n=3). The mean values with different letters (a-c) are significantly different, p <0.05.

4.3.6 Cell cycle analysis

In the present study, flow cytometric analysis was carried out using Muse™ cell cycle kit. The flow cytometric assay profiles the percentages of cells in G_o/G_1, S and G_2/M phases of the cell cycle. The cell cycle assay results are shown in **Figures 4.19**

and **4.20**. In HCT116 cells, MP-HX and MP-EA significantly increased the percentage of cells in G_o/G_1, which were 33.6 and 39.7 percent higher than the vehicle control, respectively. MP-HX and MP-EA also significantly reduced the percentage of HCT116 cells in S phase, which were 15.4 and 20.4% lower than the vehicle control, respectively. Compared to the control, treatments of MP-HX and MP-EA on HCC1937 cells did not significantly alter the percentages of cells in different phases of the cell cycle. It is probable that the 24 h treatment in HCC1937 did not provide an ideal window of time-frame, to demonstrate the effect of the extracts on HCC1937 cell cycle. In comparison to the vehicle control, MP-HX treatment on HepG2 caused a significant increase (+19.4%) in the percentage of cells in G_o/G_1, and significant reduction in the percentages of cells in S (-11.7%) and G_2/M (-8.3%) phases. In comparison to the vehicle control, the treatment of HepG2 with MP-EA resulted 16.2% increase in G_o/G_1 while 10.2% and 5.3% decrease in S and G_2/M cells population, respectively, suggesting that MP-EA is able to disrupt HepG2 cell cycle at multiple phases.

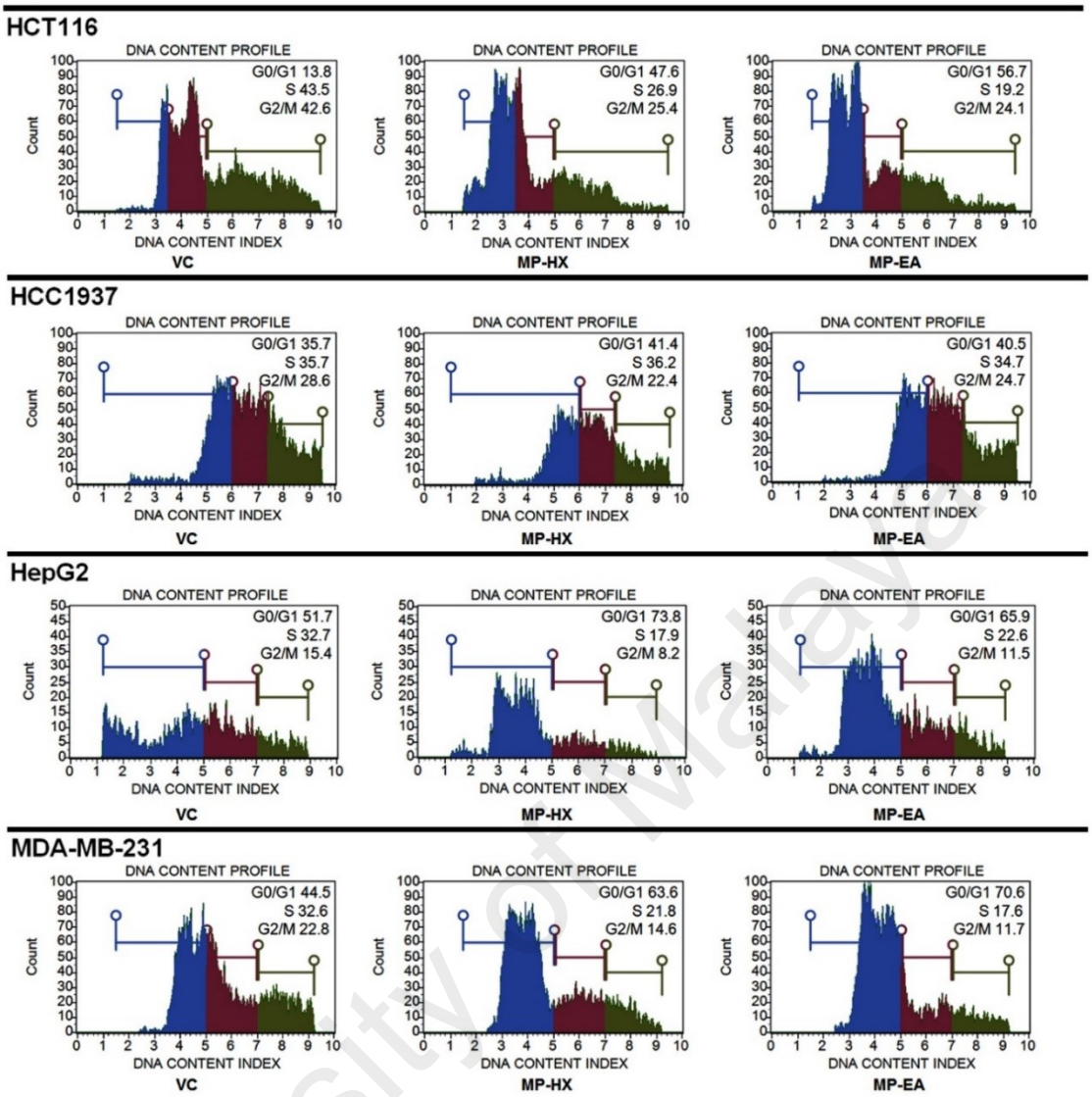

Figure 4.19: Effect of MP-HX and MP-EA on HCT116, HCC1937, HepG2 and MDA-MB-231 cell cycle distribution. The cells were treated for 24 h and the concentration of the extracts in each treatment was at ~IC_{50} value of the corresponding cell lines indicated. Each plot is a representative figure of the three replicates of each determination.

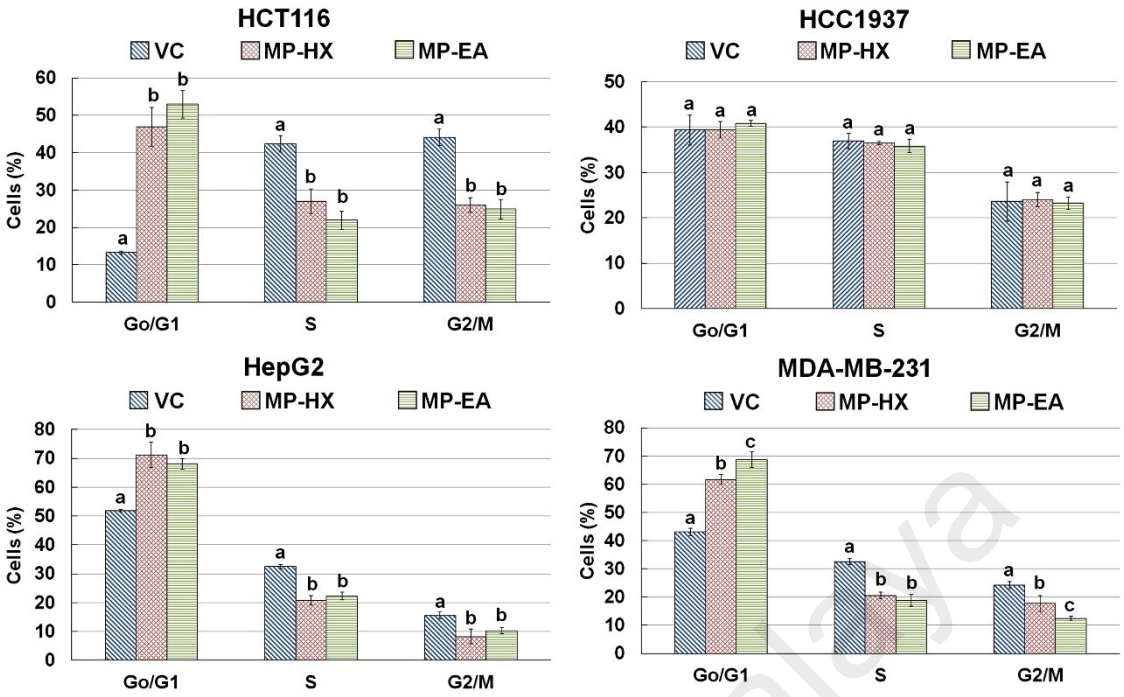

Figure 4.20: Bar charts of HCT116, HCC1937, HepG2 and MDA-MB-231 cell cycle distribution. The cells were treated with MP-HX and MP-EA for 24 h and the concentration of the extracts in each treatment was at ~IC_{50} value of the corresponding cell lines indicated. Bar charts depict the percentage of cells in the various stages of the cell cycle. Values are mean ± SD (n=3). The values with different letters (a-c) are significantly different, p <0.05.

Treatment of MDA-MB-231 with MP-HX resulted 18.6% increase in G_o/G_1 cell population while 12% and 6.5% reduction in S and G_2/M cells population respectively. This may have been sufficient to disrupt MDA-MB-231 cell cycle, resulting in MP-HX cytotoxic effect on the cells as observed earlier (**Figure 4.12** and **Table 4.4**). A similar effect was observed upon treatment with MP-EA. MP-EA significantly increased the percentage of cells in the G_o/G_1 phase (+25.6%) and significantly decreased the percentage of cells in S (-13.7%) and G_2/M (–11.8%) phases.

4.4 Molecular mechanism of anticancer activity of *Melicope ptelefolia*

4.4.1 Microarray data validation by RT-qPCR

The validation was performed by measuring the expression of 17 different genes (9 upregulated, 8 downregulated) through RT-qPCR. These genes were selected based on their roles in cell cycle progression, cellular proliferation and programmed cell death processes. Their up or downregulation likely made significant contribution towards MP-HX anticancer activity. The list of genes and a comparison of expression fold change (FC) between microarray and RT-qPCR techniques are shown in **Table 4.5** and **Figure 4.21**. The direction of gene expression FC for all of the genes (17/17) agree with the microarray data.

Table 4.5: Gene expression fold change induced by MP-HX in HCT116 and HepG2 cells. A comparison between microarray and RT-qPCR methods. A positive fold change value indicates upregulation, while negative value indicates downregulation. Values are mean ± SD for RT-qPCR fold change (n=3). Mean values with asterisks (*) were significantly different from the control (p <0.05). *MA_FC, fold change based on microarray data; RT-qPCR_FC, fold change based on real-time qPCR data.

Cell line	Gene symbol	Gene name	MA_FC	RT-qPCR_FC*
HCT116	BBC3	BCL-2 binding component 3	+2.93	+4.48±0.69
	CDKN1A	Cyclin-dependent kinase inhibitor 1A	+2.36	+4.44±0.33
	DDIT3	DNA-damage-inducible transcript 3	+8.36	+12.29±0.15
	GADD45A	Growth arrest and DNA-damage-inducible, alpha	+3.23	+5.49±0.49
	NDRG1	N-myc downstream regulated 1	+3.16	+6.52±0.83
	GABARAPL1	GABA(A) receptor-associated protein like 1	+3.74	+8.35±0.63
	JUN	Jun proto-oncogene	+4.53	+9.45±0.86
	CDKN2B	Cyclin-dependent kinase inhibitor 2B	+3.95	+9.82±0.21
	TP53	Tumor protein p53	+1.38	+2.01±0.04
	CCNA2	Cyclin A2	-4.21	-18.89±1.92
	GINS2	GINS complex subunit 2 (Psf2 homolog)	-7.03	-6.73±0.10
	HELLS	Helicase, lymphoid-specific	-6.15	-6.43±0.27
	RRM2	Ribonucleotide reductase M2	-3.80	-7.45±1.05
	PLK1	Polo-like kinase 1	-4.60	-19.52±0.87
	SKP2	S-phase kinase-associated protein 2	-4.86	-10.90±0.17
	MCM2	Minichromosome maintenance complex component 2	-4.70	-32.97±2.84
	MCM10	Minichromosome maintenance 10 replication initiation factor	-5.86	-23.99±3.78

Table 4.5, continued

Cell line	Gene symbol	Gene name	MA_FC	RT-qPCR_FC*
HepG2	BBC3	BCL-2 binding component 3	+2.71	+2.68±0.38
	CDKN1A	Cyclin-dependent kinase inhibitor 1A	+2.31	+2.03±0.14
	DDIT3	DNA-damage-inducible transcript 3	+5.21	+7.69±0.24
	GADD45A	Growth arrest and DNA-damage-inducible, alpha	+2.48	+2.12±0.07
	NDRG1	N-myc downstream regulated 1	+2.29	+5.69±1.70
	GABARAPL1	GABA(A) receptor-associated protein like 1	+4.87	+5.63±0.14
	JUN	Jun proto-oncogene	+5.06	+6.00±1.04
	CDKN2B	Cyclin-dependent kinase inhibitor 2B	+2.30	+3.52±0.59
	TP53	Tumor protein p53	+1.34	+1.41±0.05
	CCNA2	Cyclin A2	-2.66	-6.18±0.52
	GINS2	GINS complex subunit 2 (Psf2 homolog)	-2.37	-2.19±0.07
	HELLS	Helicase, lymphoid-specific	-4.03	-3.01±0.14
	RRM2	Ribonucleotide reductase M2	-2.19	-3.83±0.73
	PLK1	Polo-like kinase 1	-1.87	-14.94±2.33
	SKP2	S-phase kinase-associated protein 2	-3.65	-28.53±3.72
	MCM2	Minichromosome maintenance complex component 2	-1.59	-12.90±2.53
	MCM10	Minichromosome maintenance 10 replication initiation factor	-4.04	-21.03±1.00

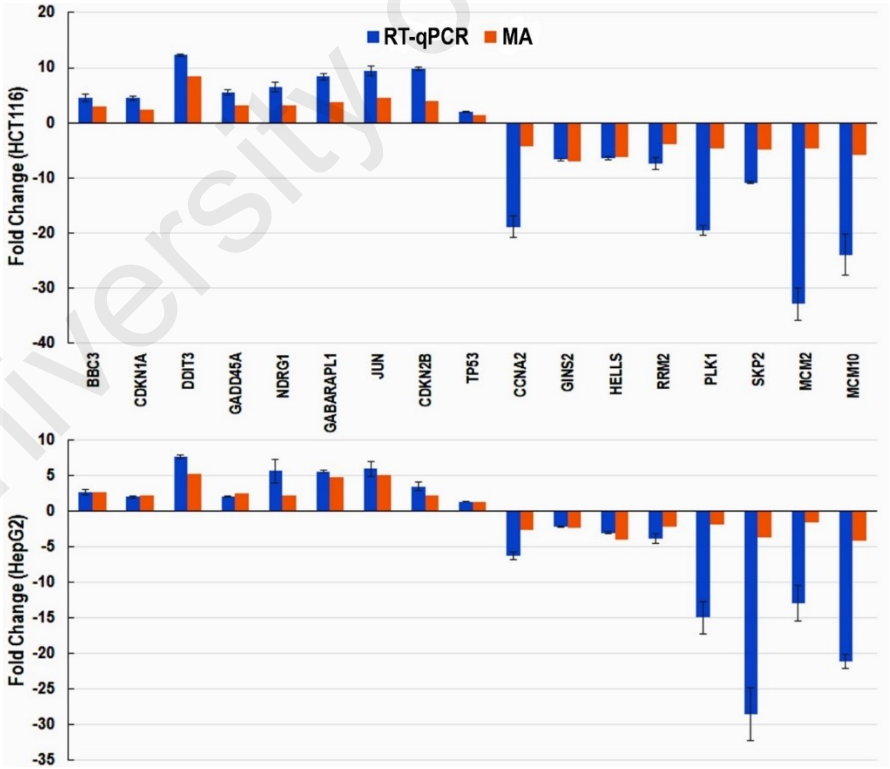

Figure 4.21: RT-qPCR validation of microarray data in HCT116 and HepG2 cells upon treatment with MP-HX. The bar chart shows gene expression fold changes obtained from microarray and RT-qPCR assays. For each RT-qPCR assay, the data was normalized to RPS29 expression and the value represent mean RT- qPCR_FC ± SD (n=3).

4.4.2 Microarray analysis

4.4.2.1 Analysis of microarray data using Transcriptome Analysis Console (TAC)

Using a cut-off fold change (FC) of ±2.00, 1290 and 1325 genes were noted to be differentially regulated in HCT116 and HepG2 cells, respectively. Among these genes, 437 were differentially regulated in both cell lines (**Figure 4.22**). Subjecting the genes (FC ≥ ±2.0) to TAC software analysis revealed a total of 130 and 164 Wikipathways (WPs) that were significantly regulated (p <0.05) in HCT116 and HepG2 cells, respectively. TAC ranked the WPs based on significance score. The significance score is calculated based on right tailed Fisher's exact test and the score is negative logarithm of Fisher's exact p-value. The higher the score, the more significant is the association of WPs with the differentially expressed genes.

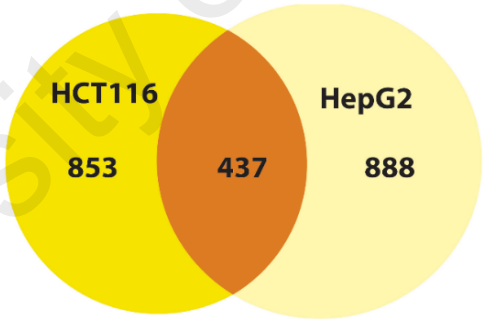

Figure 4.22: Number of differentially expressed genes (FC ≥ ±2.00) in HCT116 and HepG2 cells after treatment with MP-HX.

Among the WPs that were significantly regulated, "Retinoblastoma (RB) in cancer" (RIC-WP) ranked the highest in HCT116 and HepG2 cells, with significant scores of 36.09 and 22.82, respectively. In both cell lines, almost all of RIC-WP genes which promote cell cycle progression and proliferation were downregulated. This pathway interacted with 45 genes (1 upregulated, 44 downregulated) in HCT116 cells, and 35 genes (4 upregulated, 31 downregulated) in HepG2 cells (**Figures 4.23** and **4.24**). MP-

HX significantly downregulated E2F, CDK1, CDK2, CDK6, CCNA2, CCNB1, CCNB2, CCNE1 and CCNE2 in both cell lines.

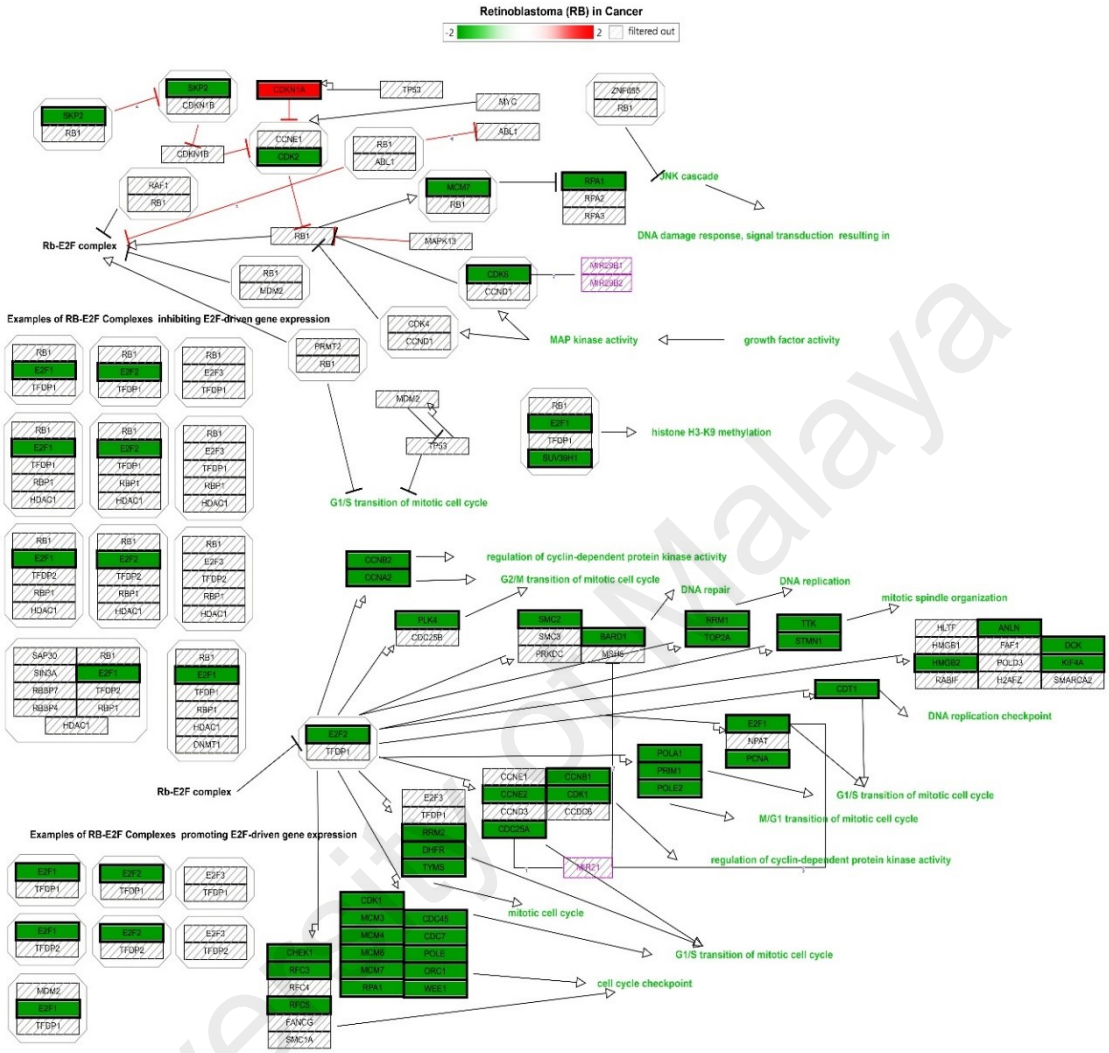

Figure 4.23: Modulation of "Retinoblastoma In Cancer" Wikipathway (RIC-WP) component genes by MP-HX in HCT116 cells. The figure shows component genes of RIC-WP that were differentially regulated by MP-HX in HCT116 cells. The genes in the pathway are colored red (MA_FC ≥ +2.0), or green (MA_FC ≥ -2.0), or grey hashed boxes (MA_FC < ±2).

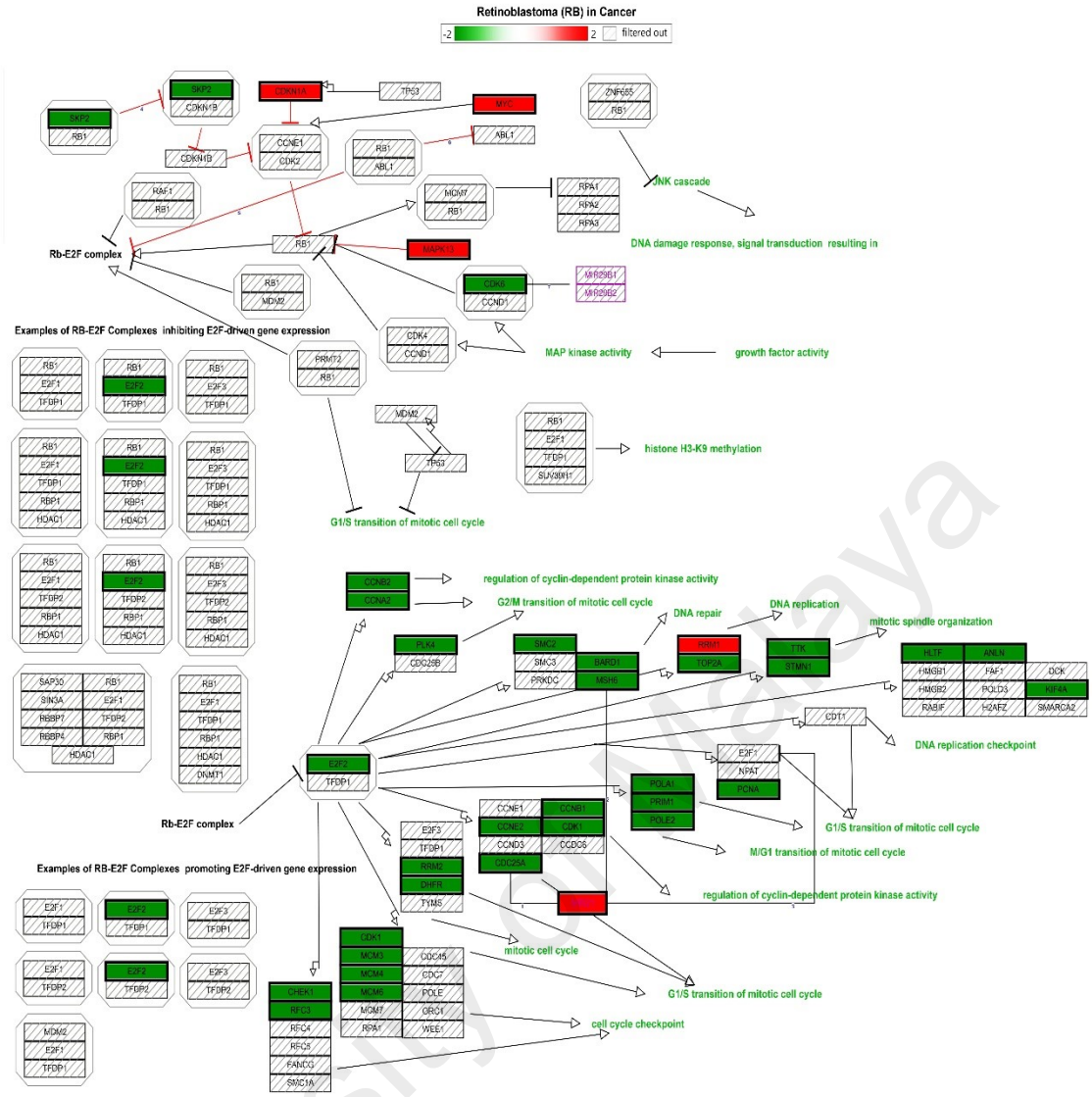

Figure 4.24: Modulation of "Retinoblastoma In Cancer" Wikipathway (RIC-WP) component genes by MP-HX in HepG2 cells. The figure shows component genes of RIC-WP that were differentially regulated by MP-HX in HepG2 cells. The genes in the pathway are colored red (MA_FC ≥ +2.0), or green (MA_FC ≥ -2.0), or grey hashed boxes (MA_FC < ±2).

The "G_1 to S cell cycle control" Wikipathway (G_1SCC-WP) demonstrated significant scores of 18.42 in HCT116 and 10.58 in HepG2 cells (**Figures 4.25** and **4.26**). Twenty-seven genes in G_1SCC-WP were modulated in HCT116 cells, 23 of which were downregulated. In HepG2 cells, 20 genes were modulated, 15 of which were downregulated. The G_1/S cell cycle transition is activated by cyclins, CDKs and E2F proteins. This transition can be inhibited by CDK inhibitors. From the figures, many genes in G_1SCC-WP which can promote proliferation were downregulated in both cell lines (CDC25A, CCNE2, PCNA, MCM3/5/6, POLE2, POLA2, CDK6, PRIM1, CDK1, CCNB1). In contrast, MP-HX upregulated GADD45A and CDK inhibitors p15 (CDKN2B) and p21 (CDKN1A) in both cell lines (**Figures 4.25** and **4.26**). (See figures of G_1SCC-WP modulated by MP-HX in HCT116 and HepG2 cells on the next pages).

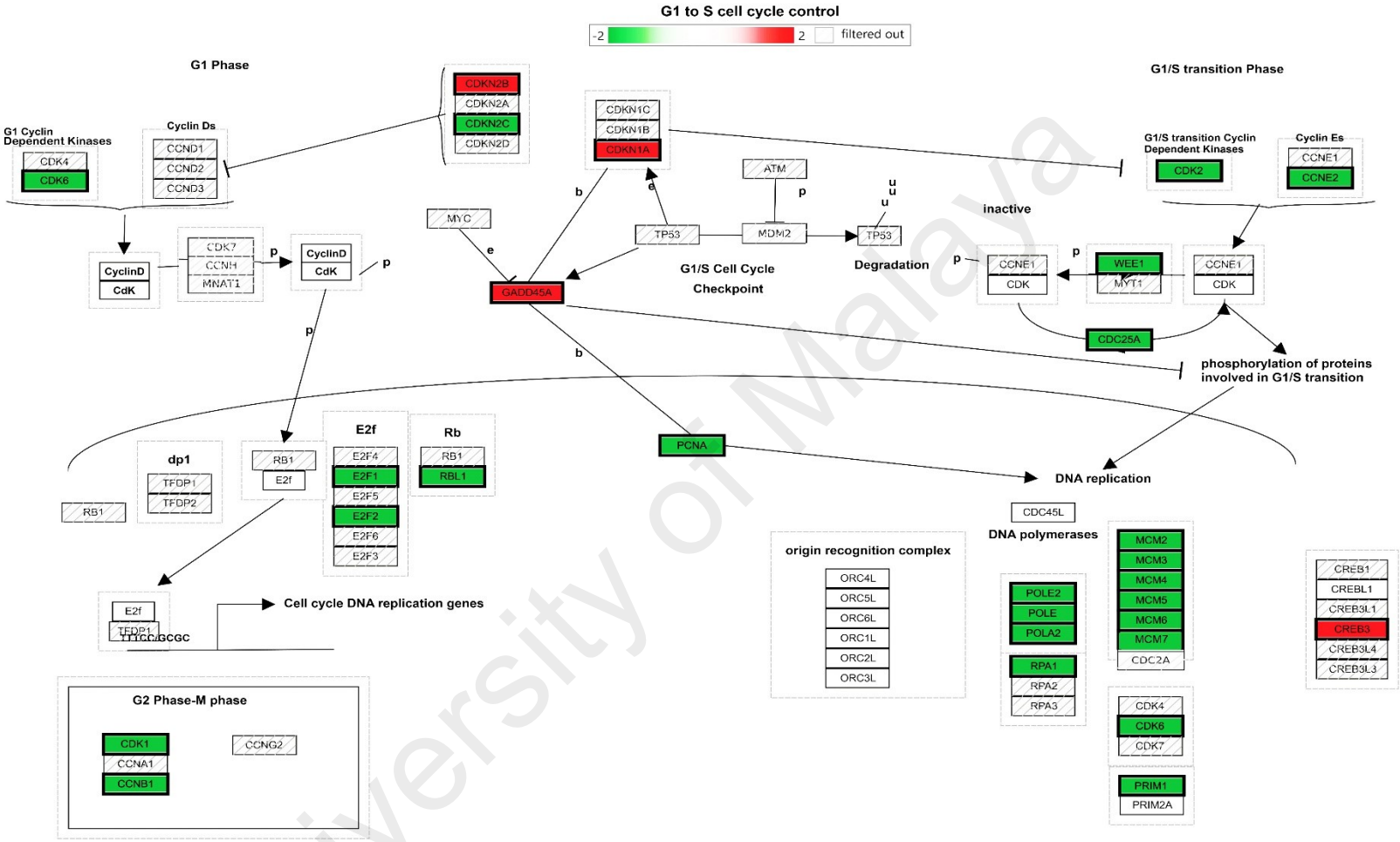

Figure 4.25: Modulation of "G1 to S Cell Cycle Control" Wikipathway (G1SCC-WP) component genes by MP-HX in HCT116 cells. The figure shows component genes of G_1SCC-WP that were differentially regulated by MP-HX in HCT116 cells. The genes in the pathway are colored red (MA_FC ≥ +2.0), or green (MA_FC ≥ -2.0), or grey hashed boxes (MA_FC < ±2).

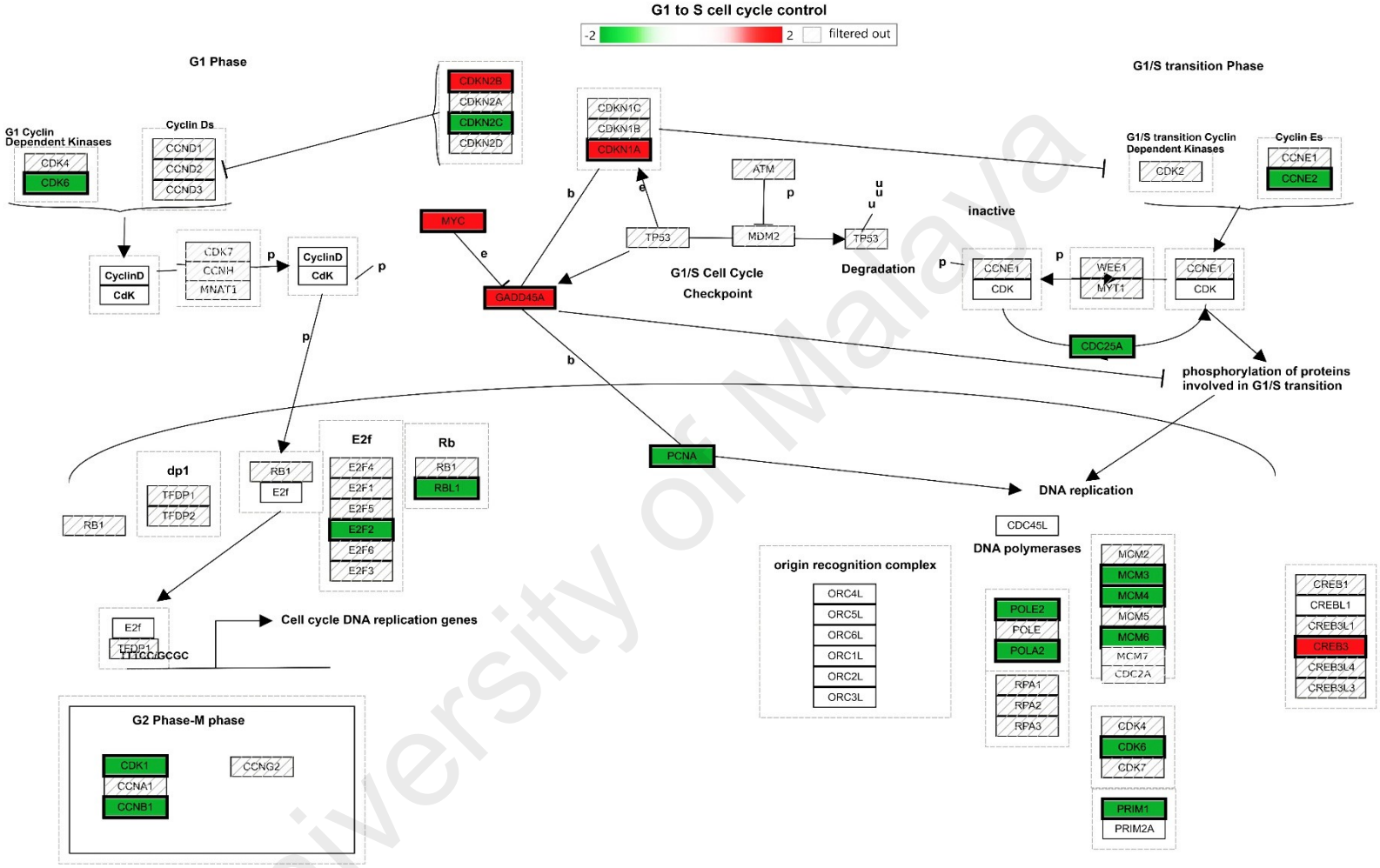

Figure 4.26: Modulation of "G1 to S Cell Cycle Control" Wikipathway (G1SCC-WP) component genes by MP-HX in HepG2 cells. The figure shows component genes of G_1SCC-WP that were differentially regulated by MP-HX in HepG2 cells. The genes in the pathway are colored red (MA_FC ≥ +2.0), or green (MA_FC ≥ -2.0), or grey hashed boxes (MA_FC < ±2).

The "Cell Cycle" WikiPathway (CC-WP) (**Figures 4.27** and **4.28)** had significant scores of 17.05 in HCT116 and 7.93 in HepG2. In HCT116, 31 genes were modulated, and they were all downregulated. In contrast, HepG2 cells showed modulation of 21 genes, 19 of which were downregulated and only 2 were upregulated. The dataset showed that MP-HX downregulated the expression of many cell cycle promoting proteins in CC-WP in both cell lines, and these include CCNA2, CCNB1, CCNB2, CCNE2, CDK1, CDK2 and CDK6 (**Figures 4.27** and **4.28**). MP-HX also significantly downregulated MCM2 and PLK1 in HCT116. Moreover, the expression of MCM10 was substantially downregulated in both cell lines. (See figures of CC-WP modulated by MP-HX in HCT116 and HepG2 cells on the next pages).

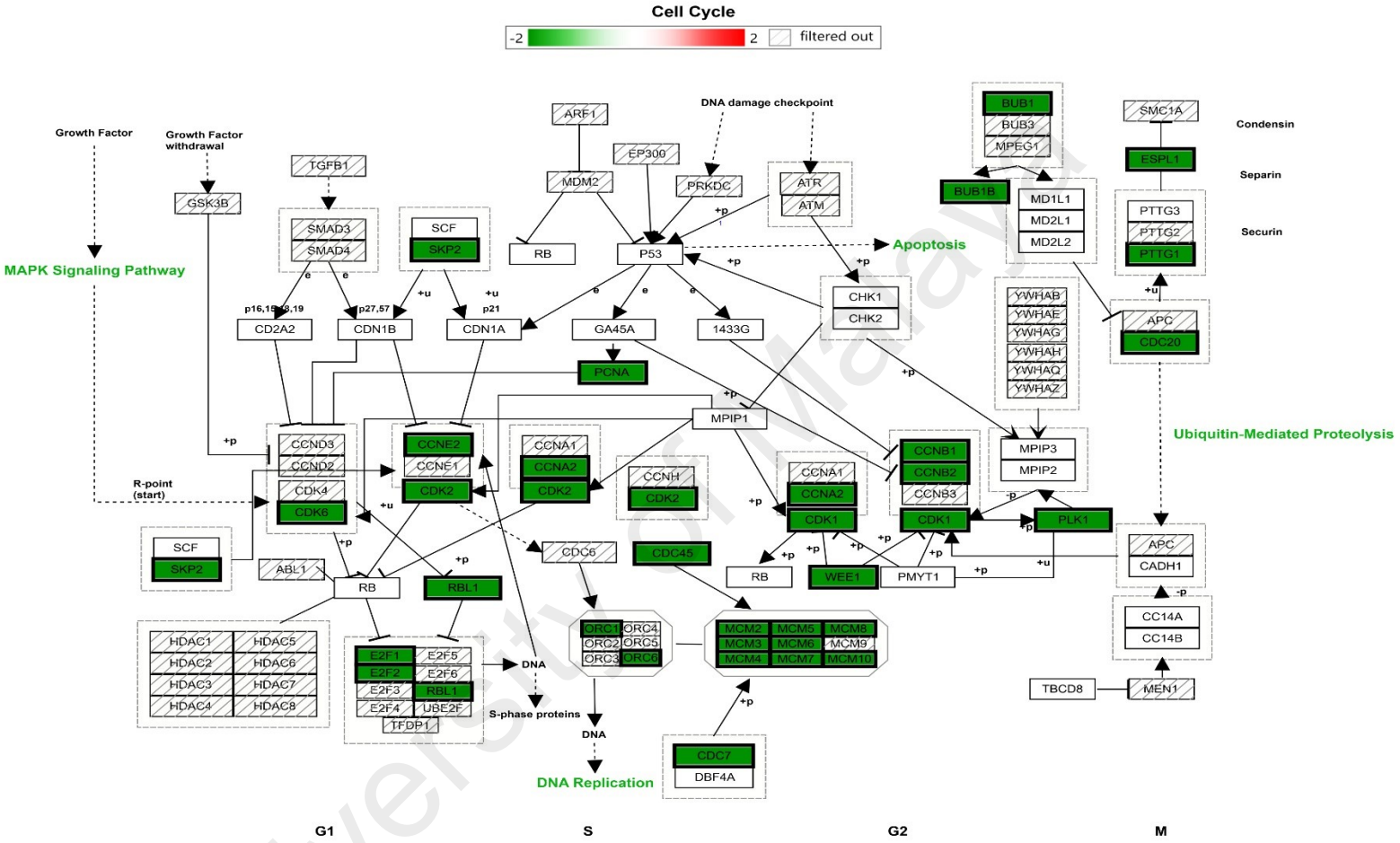

Figure 4.27: Modulation of "Cell Cycle" Wikipathway (CC-WP) component genes by MP-HX in HCT116 cells. The figure shows component genes of CC-WP that were differentially regulated by MP-HX in HCT116 cells. The genes in the pathway are colored red (MA_FC ≥ +2.0), or green (MA_FC ≥ -2.0), or grey hashed boxes (MA_FC < ±2).

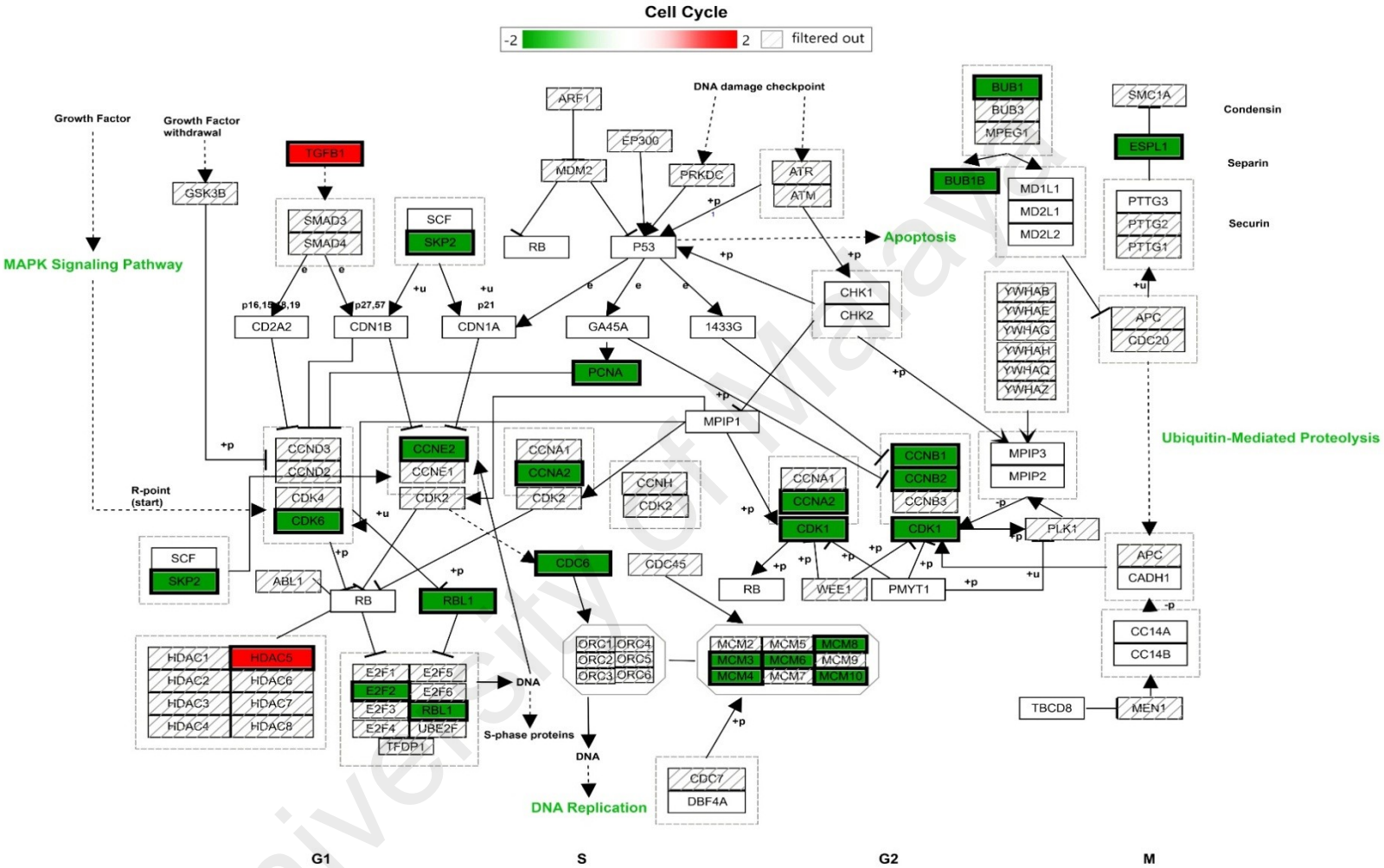

Figure 4.28: Modulation of "Cell Cycle" Wikipathway (CC-WP) component genes by MP-HX in HepG2 cells. The figure shows component genes of CC-WP that were differentially regulated by MP-HX in HepG2 cells. The genes in the pathway are colored red (MA_FC ≥ +2.0), or green (MA_FC ≥ -2.0), or grey hashed boxes (MA_FC < ±2).

The "DNA damage response" WikiPathway (DDR-WP) was also modulated by MP-HX, with significance score values of 6.67 and 6.38 in HCT116 and HepG2, respectively. In HCT116, 4 genes were upregulated, while 11 genes were downregulated (**Figure 4.29)**. In HepG2, 6 genes were upregulated, and 9 genes were downregulated (**Figure 4.30)**. MP-HX significantly downregulated CHEK1, RAD51, CDC25A, cyclins and CDKs expression, while upregulated CDKN1A, BBC3 and GADD45A in both cell lines. (See figures of DDR-WP modulated by MP-HX in HCT116 and HepG2 cells on the next pages).

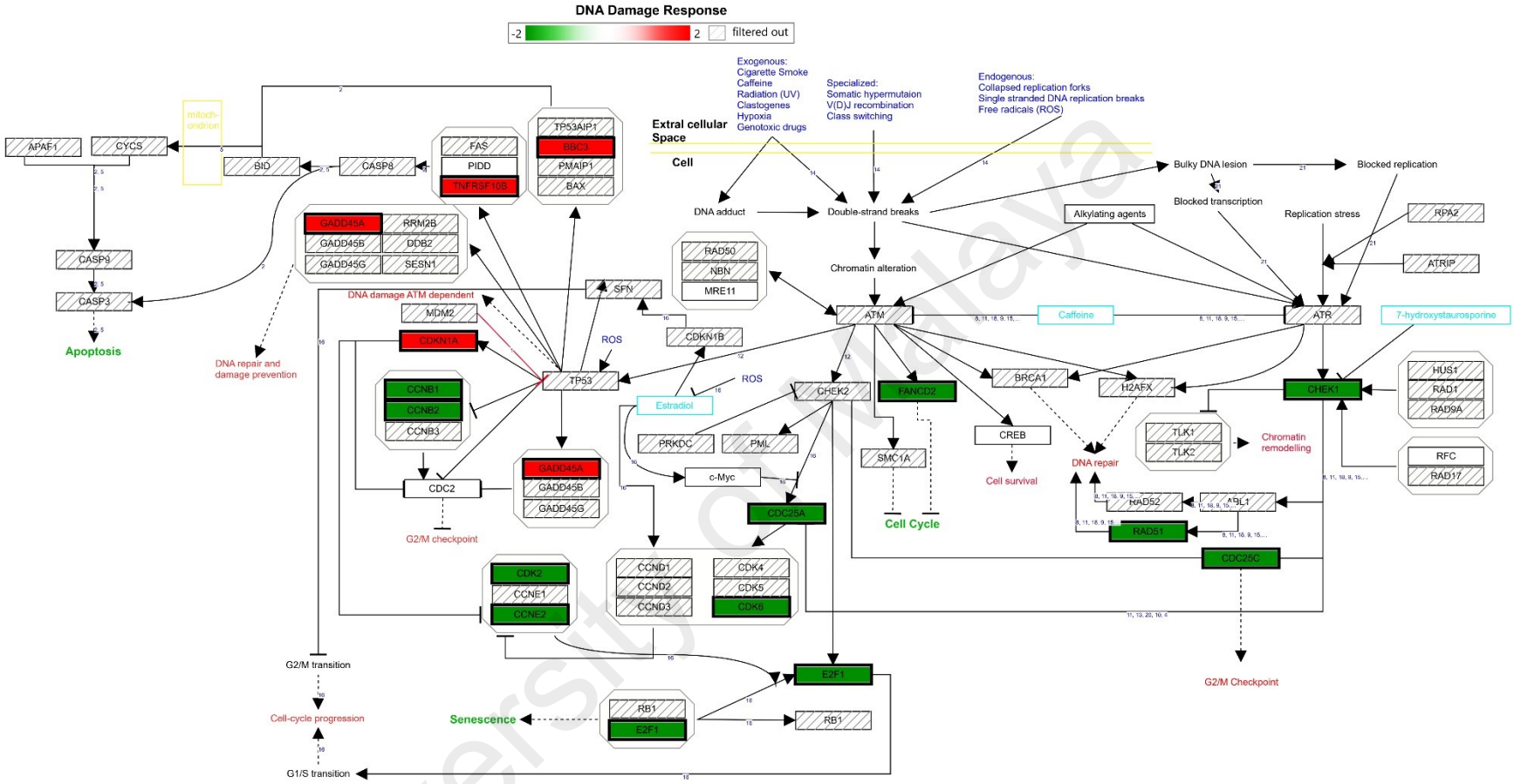

Figure 4.29: Modulation of "DNA Damage Response" Wikipathway (DDR-WP) component genes by MP-HX in HCT116 cells. The figure shows component genes of DDR-WP that were differentially regulated by MP-HX in HCT116 cells. The genes in the pathway are colored red (MA_FC ≥ +2.0), or green (MA_FC ≥ -2.0), or grey hashed boxes (MA_FC < ±2).

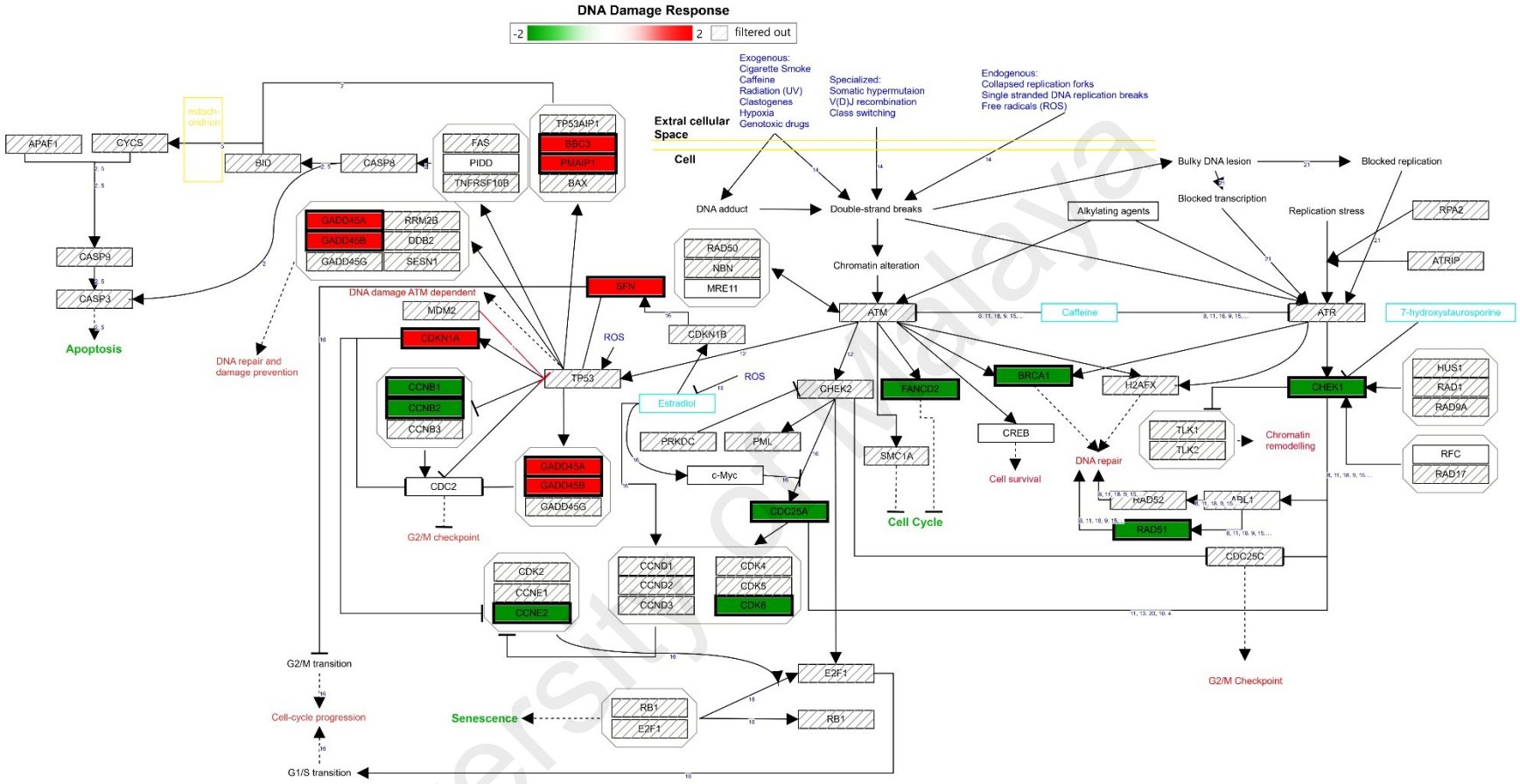

Figure 4.30: Modulation of "DNA Damage Response" Wikipathway (DDR-WP) component genes by MP-HX in HepG2 cells. The figure shows component genes of DDR-WP that were differentially regulated by MP-HX in HepG2 cells. The genes in the pathway are colored red (MA_FC ≥ +2.0), or green (MA_FC ≥ -2.0), or grey hashed boxes (MA_FC < ±2).

The "Apoptosis" Wikipathway (AP-WP) was modulated by MP-HX with **s**ignificance scores of 3.95 and 3.16 in HCT116 and HepG2 cells, respectively (**Figures 4.31** and **4.32)**. In HCT116, 10 genes were upregulated while 3 genes were downregulated. In HepG2, 12 genes were modulated and 7 of them were upregulated. MP-HX upregulated BBC3 and JUN while downregulated HELLS in both cell lines. BAK1 and PMAIP1 were also upregulated in HepG2 after treatment with MP-HX. On the other hand, BIRC5 was downregulated in HCT116 upon treatment with MP-HX. (See figures of AP-WP modulated by MP-HX in HCT116 and HepG2 cells on the next pages).

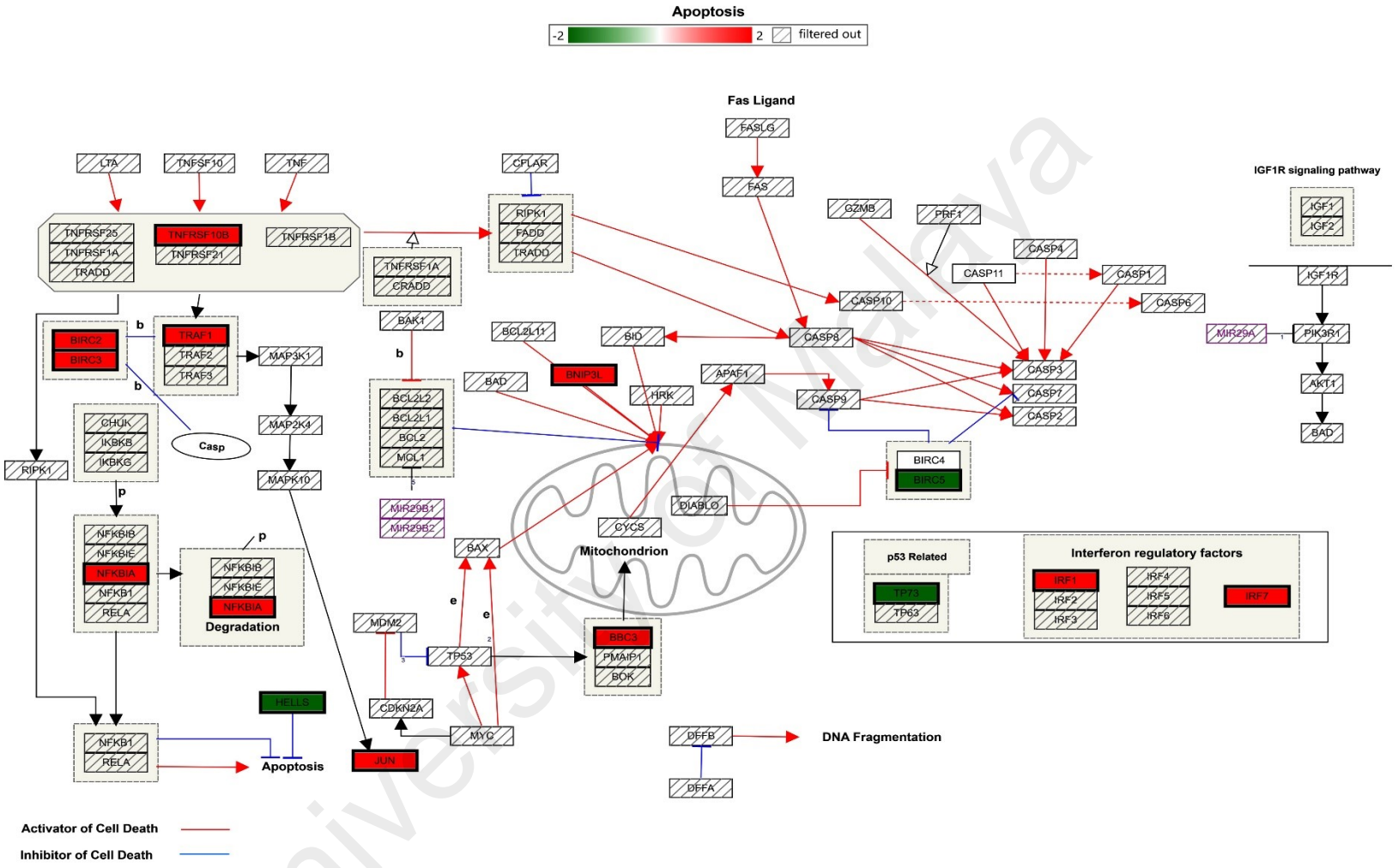

Figure 4.31: Modulation of "Apoptosis" Wikipathway (AP-WP) component genes by MP-HX in HCT116 cells. The figure shows component genes of AP-WP that were differentially regulated by MP-HX in HCT116 cells. The genes in the pathway are colored red (MA_FC ≥ +2.0), or green (MA_FC ≥ -2.0), or grey hashed boxes (MA_FC < ±2).

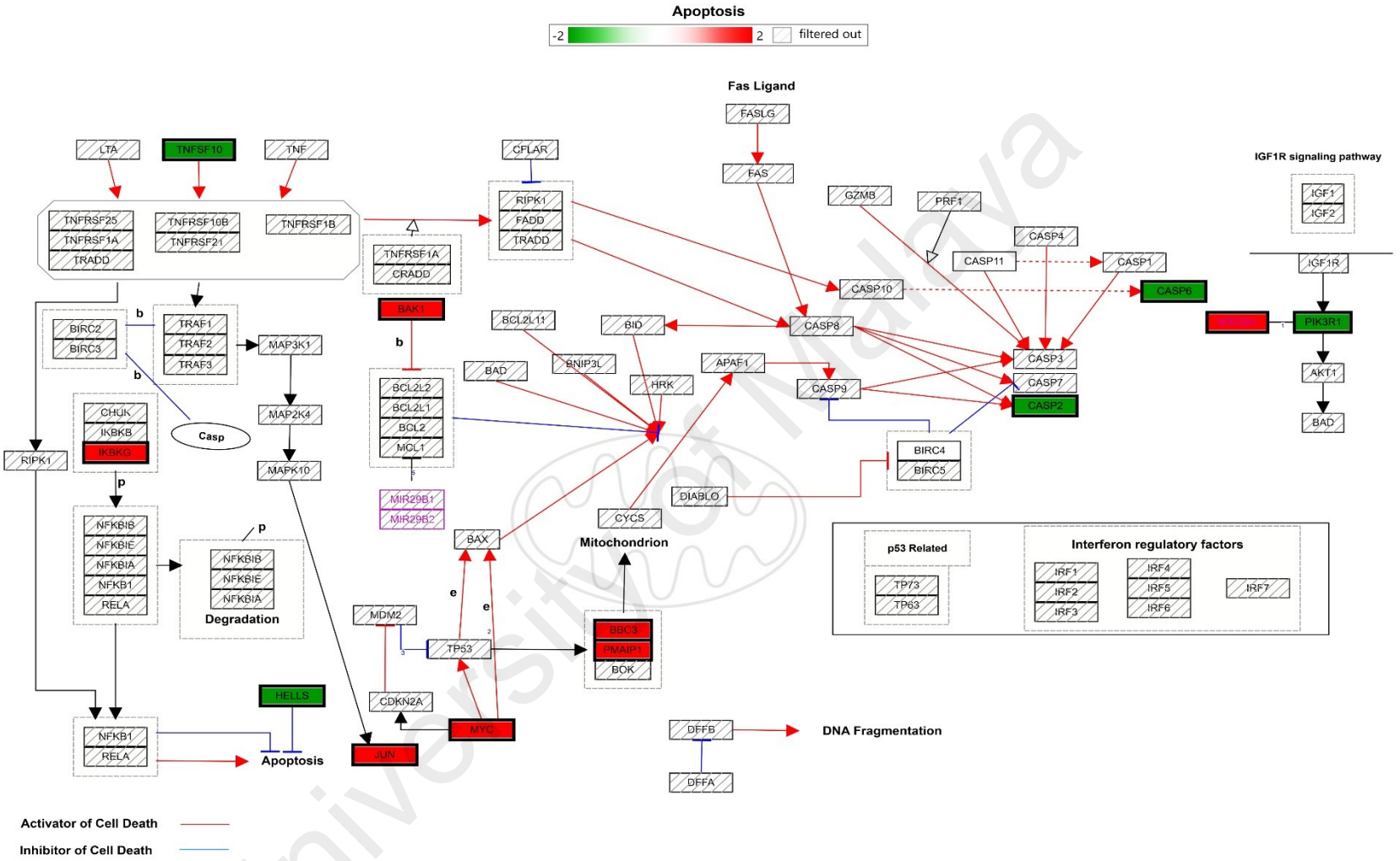

Figure 4.32: Modulation of "Apoptosis" Wikipathway (AP-WP) component genes by MP-HX in HepG2 cells. The figure shows component genes of AP-WP that were differentially regulated by MP-HX in HepG2 cells. The genes in the pathway are colored red (MA_FC ≥ +2.0), or green (MA_FC ≥ -2.0), or grey hashed boxes (MA_FC < ±2).

4.4.2.2 Ingenuity Pathway Analysis (IPA)

(a) ***Top canonical pathways modulated by MP-HX in HCT116 and HepG2 Cells***

A cut-off fold change (FC) of ±2.00 was used for Ingenuity pathway analysis (IPA). IPA enriched 55 and 135 canonical pathways (p <0.05) in HCT116 and HepG2, respectively. Canonical pathways (CPs) with -log (p-value) of 3.0 and above are shown in **Figures 4.33** and **4.34**. In HCT116, top most significant CPs included "cell cycle control of chromosomal replication", "role of BRCA1 in DNA damage response", "cell cycle: G_2/M DNA damage checkpoint regulation", "mitotic roles of polo-like kinase", "unfolded protein response", and "estrogen mediated S-phase entry" (**Figure 4.33**). In HepG2, top CPs were "hereditary breast cancer signaling", "NRF2-mediated oxidative stress response", "role of BRCA1 in DNA damage response", "ATM signaling", "cell cycle control of chromosomal replication", "estrogen mediated S-phase entry" and "GADD45 signaling" (**Figure 4.34**).

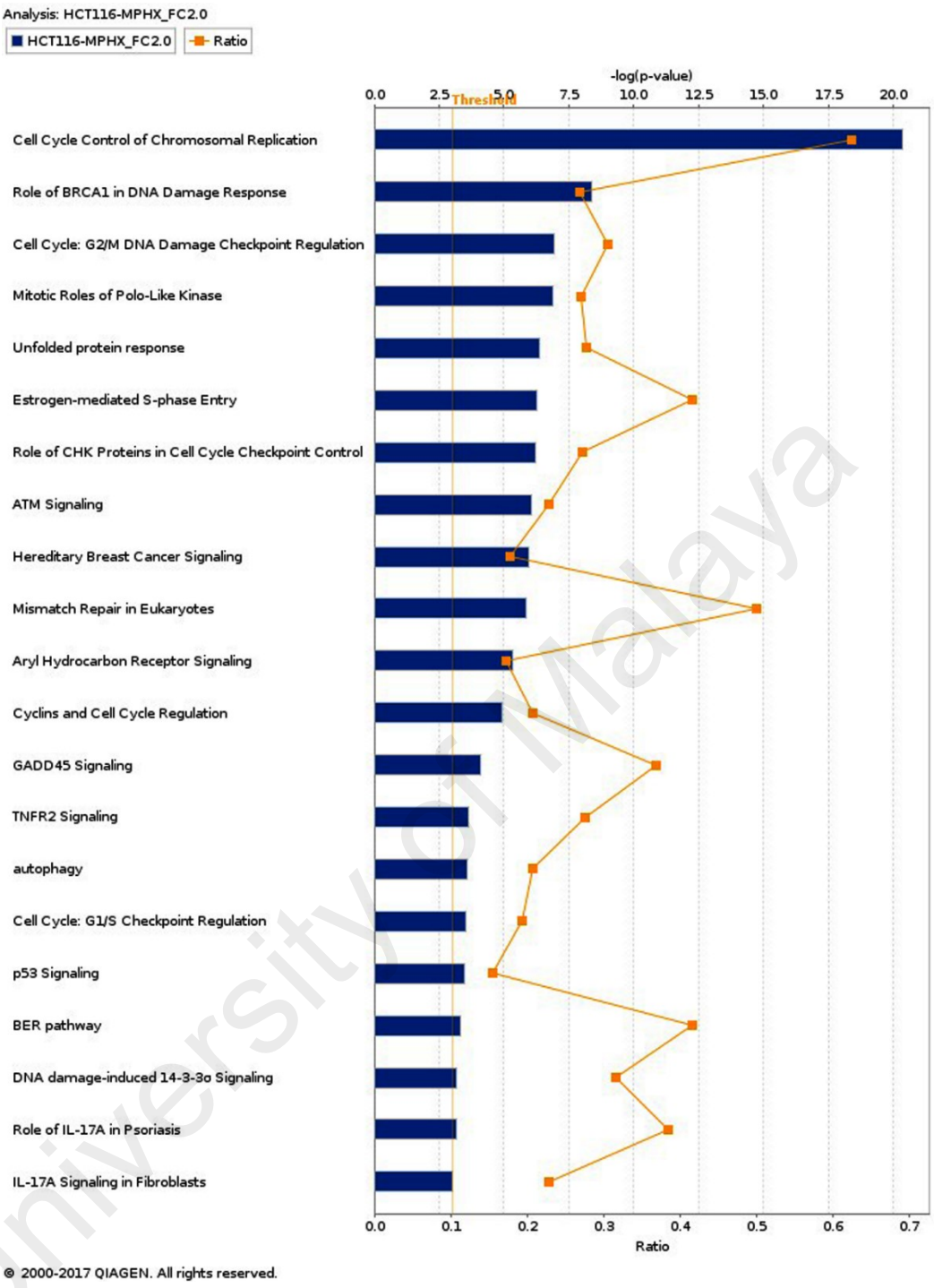

Figure 4.33: Top canonical pathways (CPs) enriched in HCT116 cells after MP-HX treatment. IPA software ranked the top CPs based on -log (*p*-value). Ratio value denotes the number of molecules in the dataset divided by the total number of molecules associated with the pathway.

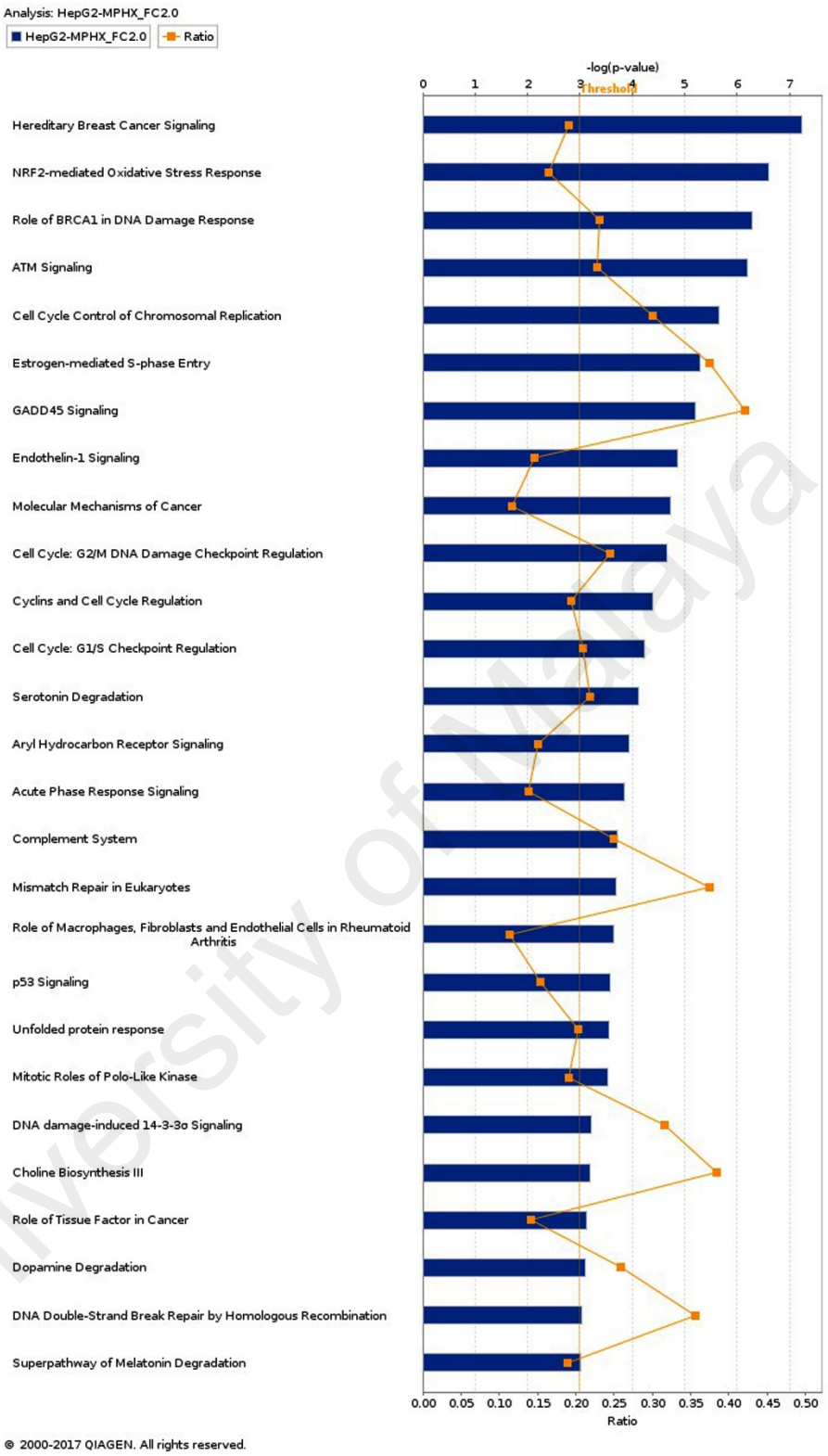

Figure 4.34: Top canonical pathways (CPs) enriched in HepG2 cells after MP-HX treatment. IPA software ranked the top CPs based on -log (*p*-value). Ratio value denotes the number of molecules in the dataset divided by the total number of molecules associated with the pathway.

A comparison of over-represented CPs in HCT116 and HepG2 are shown in **Table 4.6**. The CPs are ranked according to their respective -log (*p*-value). Based on the list, HCT116 showed a higher –log (*p*-value) for most of the CPs. In HepG2, only three CPs showed higher –log (*p*-value) than that of HCT116, and these include "hereditary breast cancer signaling", "ATM signaling" and "NRF2-mediated oxidative stress response". These observations could mean that although MP-HX may have exerted a similar anticancer effect in both cell lines, a subset of different effect or mechanism of action may have also occurred between the cell lines.

Table 4.6: Comparison of top canonical pathways in HCT116 and HepG2 cells based on -log (*p*-value).

Canonical Pathway	**-log (*p*-value)**	
	HCT116	**HepG2**
1. Cell Cycle Control of Chromosomal Replication	20.34	5.67
2. Role of BRCA1 in DNA Damage Response	8.36	6.28
3. Hereditary Breast Cancer Signaling	5.95	7.25
4. ATM Signaling	6.08	6.19
5. Cell Cycle: G2/M DNA Damage Checkpoint Regulation	6.96	4.66
6. Estrogen-mediated S-phase Entry	6.25	5.29
7. Mitotic Roles of Polo-Like Kinase	6.91	3.54
8. Unfolded protein response	6.35	3.55
9. NRF2-mediated Oxidative Stress Response	2.96	6.61
10. Mismatch Repair in Eukaryotes	5.84	3.68

(b) ***Diseases and functions modulated by MP-HX in HCT116 and HepG2 cells***

The top category of diseases and functions modulated in HCT116 and HepG2 cells by MP-HX include "cancer", "organismal injury and abnormalities", "gastrointestinal disease", "cell death and survival", "cell cycle", "cellular assembly and organization", "DNA replication, recombination and repair", "cellular development" and "cellular growth and proliferation" (**Figures 4.35** and **4.36)**.

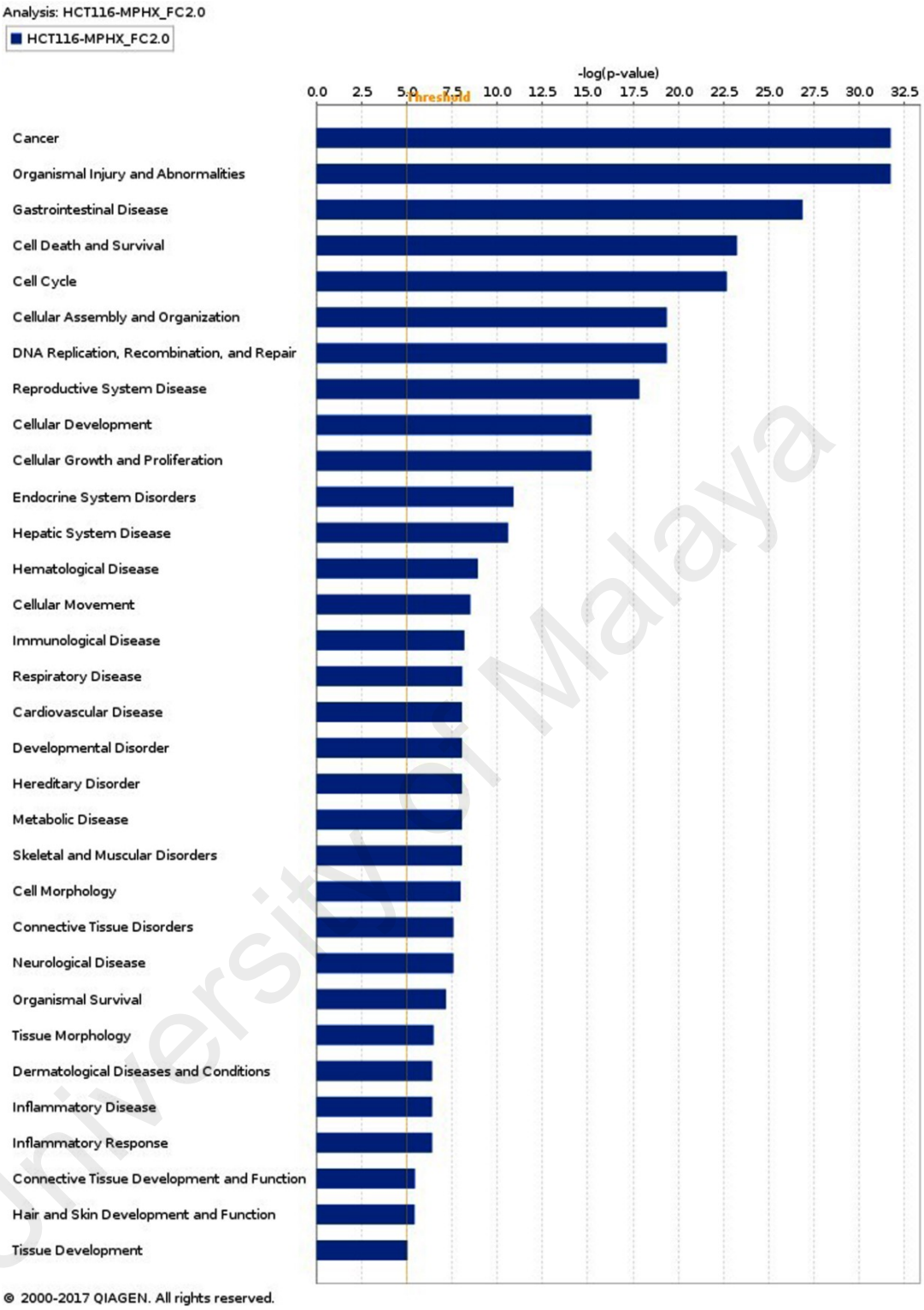

Figure 4.35: Modulation of diseases and biological functions by MP-HX in HCT116 cells. The figure shows top category of diseases and biological functions that were modulated by MP-HX (FC ≥ ±2.0) in HCT116 cells, and they were ranked by IPA software based on -log (*p*-value) ≥ 5.0.

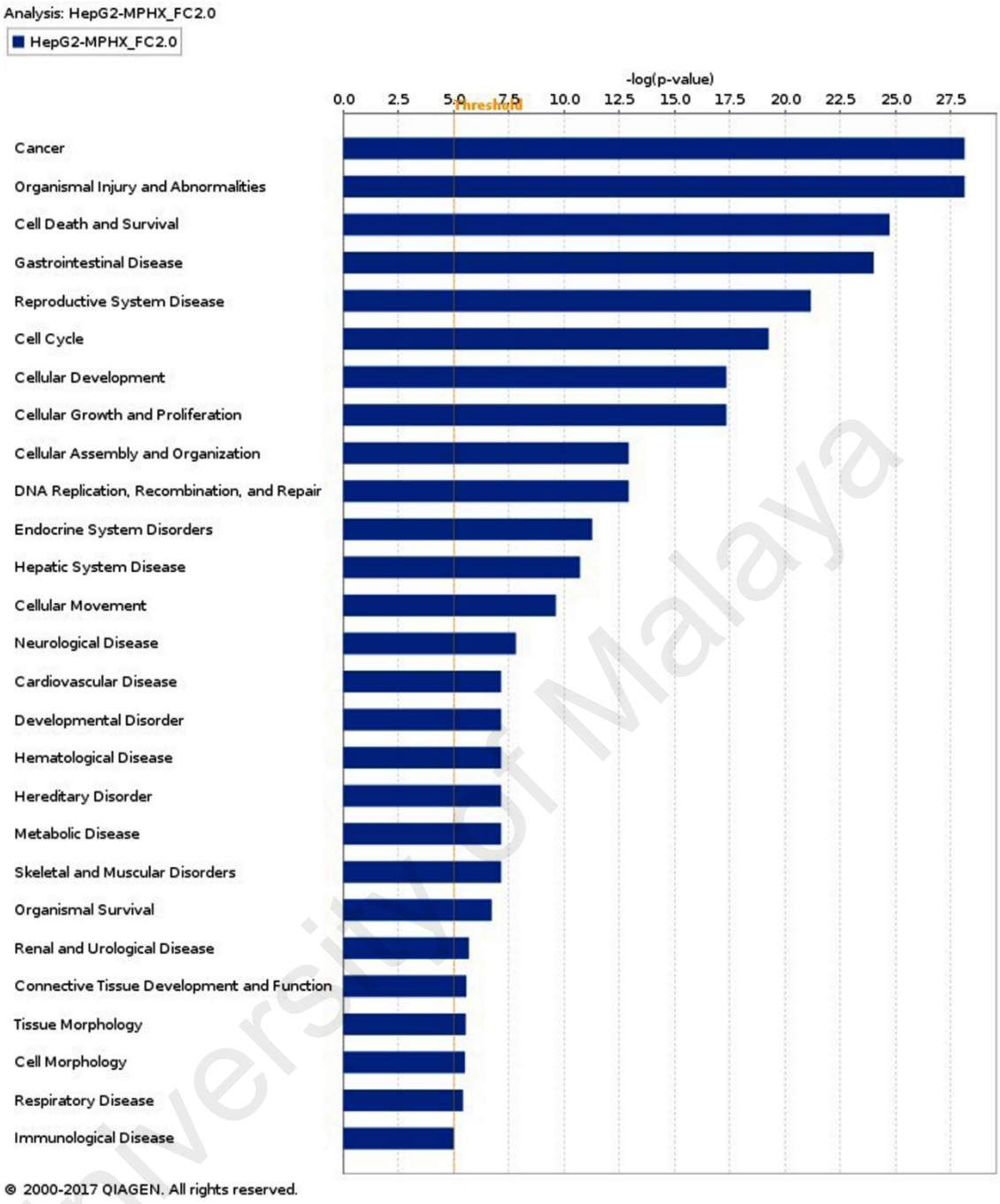

Figure 4.36: Modulation of diseases and biological functions by MP-HX in HepG2 cells. The figure shows top category of diseases and biological functions that were modulated by MP-HX (FC ≥ ±2.0) in HepG2 cells, and they were ranked by IPA software based on -log (*p*-value) ≥ 5.0.

In both HCT116 and HepG2 cells, the predicted activation z-scores appeared supportive of MP-HX activity, as the negative values are suggestive of inhibition of processes associated with cell growth, cell proliferation and cell cycle (**Table 4.7**).

Table 4.7: Diseases and functions modulated by MP-HX in HCT116 and HepG2 cells. The table shows the enriched terms corresponding to diseases or biological functions along with the number of associated genes in the experimental dataset, *p*-value and activation z-score. The z-score is calculated by the IPA software which predicts whether a specific disease or bio-function is increased (positive z-score) or decreased (negative z-score) based on the experimental dataset.

Cell line	Categories	Diseases or biological functions	*p*-value	z-score	# of genes in dataset
HCT116	Cellular development; cellular growth and proliferation	Cell proliferation of tumor cell lines	6.26E-16	-2.60	218
	DNA replication, recombination, and repair	DNA replication	3.48E-13	-2.07	27
	Cell cycle	S-phase	1.37E-11	-3.47	40
	Cell cycle	M-phase of tumor cell lines	5.02E-11	-2.00	28
	Cell cycle; DNA replication, recombination, and repair	Checkpoint control	6.93E-09	-2.55	15
	Cell death and survival	Cell death of cervical cancer cell lines	7.07E-08	+2.66	60
	Cell death and survival	Apoptosis of cervical cancer cell lines	1.71E-06	+3.37	47
	Cell cycle	G1-phase of tumor cell lines	4.41E-06	+2.39	35
	Cell cycle	Entry into interphase	7.87E-06	-2.30	17
	DNA replication, recombination, and repair	DNA damage	9.03E-06	+2.42	24
	Cell cycle	Entry into S-phase	1.42E-05	-2.57	16
	Cell death and survival	Cell viability of cervical cancer cell lines	3.01E-05	-2.18	34
	Cellular development; cellular growth and proliferation	Cell proliferation of breast cancer cell lines	3.58E-05	-2.94	61
HepG2	Cell death and survival	Apoptosis of cervical cancer cell lines	1.48E-08	+2.34	51
	Cell death and survival	Cell viability of cervical cancer cell lines	4.67E-05	-2.01	33
	Cell cycle	G1-phase of tumor cell lines	1.96E-04	+2.01	30
	Cell cycle	M-phase of tumor cell lines	2.17E-04	-2.34	17
	Cell cycle; DNA replication, recombination, and repair	Checkpoint control	5.56E-04	-2.38	9
	Cell death and survival; cellular development	Self-renewal of tumor cell lines	9.53E-04	-2.20	5

(c) ***Upstream Regulators Prediction in HCT116 and HepG2 Cells***

IPA upstream regulator analysis (URA) examines how many known targets of each transcriptional regulator (TR) are present in the dataset and compares their direction of change to what is expected from the literature to predict the likely relevant TRs. If the observed direction of change is mostly consistent with a particular activation state of the TR ("activated" or "inhibited"), then a prediction is computed about that activation state (z-score). This can provide insights on the underlying mechanism for the biological activities in the tissue/cells being studied.

Comparison of top upstream regulators between the HCT116 and HepG2 cells is depicted in **Figure 4.37**. The heatmap shows that most of the upstream regulators were modulated in the same direction in both cell lines, except IgG and ERBB2. There were only slight differences in the activation z-scores of AREG, SMARCA4, HDAC, CDKN1A, F7, IL1A, NFKB, E2F3 and TREM1 between the HCT116 and HepG2 cells. This observation suggests MP-HX exerted its effect by modulating a similar set of upstream regulators in both cell lines.

Figure 4.37: IPA software prediction of upstream regulators and their activation state in HCT116 and HepG2 cells after MP-HX treatment. IPA predicts modulation of regulators and ranked them based on the activation z-score. A positive score denotes activation, while a negative score denotes inhibition. The heatmap color intensity depicts relative value of activation z-score for the corresponding cell line. Upstream regulators were filtered based on -log (*p*-value) of 3.0 and activation z-score of 3.5. Orange color indicates activation whereas blue color indicates inhibition.

The top upstream regulators in HCT116 and HepG2 cells modulated by MP-HX are also listed in **Table 4.8**. NUPR1 was the most significant regulator in HCT116 and HepG2 with activation z-scores of +10.94 and +12.21, respectively. IPA also ranked TP53 as the second most significant upstream regulator in both cell lines, with activation z-scores of +7.16 and +6.22 in HCT116 and HepG2 cells, respectively. Another upstream regulator predicted by IPA was RABL6 (RAB, member RAS oncogene family like 6), which had activation z-scores of -6.25 and -4.80 in HCT116 and HepG2 cells, respectively.

Table 4.8: IPA software prediction of upstream regulators in HCT116 and HepG2 cells that were treated with MP-HX. IPA predicts modulation of upstream regulators and ranked them based on the activation z-score. A positive score denotes activation, while a negative score denotes inhibition. *UR, upstream regulators; MA_FC, fold change based on microarray data.

Cell line	Activation/ inhibition	UR	MA_FC	z-score	Overlap (*p*-value)
HCT116	Activated	NUPR1	+1.27	+10.94	8.34E-57
		TP53	+1.38	+7.16	3.07E-32
		TNF	+1.07	+4.81	1.15E-12
		KDM5B	+2.44	+4.79	9.05E-18
		IL1A	+2.74	+3.86	1.39E-08
		NFkB (complex)		+3.65	2.24E-12
		AR	+1.14	+3.61	4.8E-15
		CDKN1A	+2.36	+3.59	3.36E-10
		TGFB1	-1.20	+3.54	2.48E-21
		E2F6	+1.27	+3.46	1.01E-10
	Inhibited	RABL6	-1.28	-6.25	9.25E-37
		MITF	+1.12	-5.62	3.56E-26
		RARA	-1.24	-5.10	4.43E-11
		ESR1	-1.16	-4.91	9.74E-17
		FOXM1	-2.96	-4.89	2.09E-21
		TAL1	-1.21	-4.15	6.83E-08
		E2F3	-1.35	-3.71	1.99E-14
		MYC	-1.40	-3.67	3.23E-14
		ERBB2	-1.12	-3.54	7.77E-57
		E2F		-3.46	4.87E-19

Table 4.8, continued

Cell line	Activation/ inhibition	UR	MA_FC	z-score	Overlap (*p*-value)
HepG2	Activated	NUPR1	+2.40	+12.21	1.95E-73
		TP53	+1.34	+6.22	2.45E-27
		TGFB1	+2.29	+5.37	3.98E-17
		PDGF BB		+4.81	2.03E-14
		PRKCD	+1.63	+4.74	9.17E-11
		ERK		+4.68	3.94E-10
		SMARCA4	+1.06	+4.26	2.52E-10
		TREM1	+8.43	+3.75	1.56E-08
		TGM2	-1.34	+3.72	4.40E-03
		KDM5B	+1.08	+3.54	1.54E-13
	Inhibited	RABL6	-1.11	-4.80	1.15E-24
		RARA	+1.09	-4.40	1.22E-10
		MITF	+1.24	-4.19	7.93E-11
		ESR1	+1.08	-4.04	5.29E-17
		IgG		-3.84	6.49E-07
		26s Proteasome		-3.64	5.77E-14
		Hdac		-3.57	2.64E-08
		KIAA1524	-2.21	-3.26	7.02E-04
		FOXM1	-1.87	-3.20	6.48E-13
		TAL1	-1.22	-3.15	1.66E-06

(d) ***Networks enriched in HCT116 and HepG2 by MP-HX***

IPA network analyses display the interaction between molecules present in the dataset which reflects significance of biological function. The IPA software ranked top networks enriched in the microarray dataset based on 'network score' (**Table 4.9**). This analysis considers the number of network eligible molecules in the network, network size, total number of network eligible molecules analyzed and total number of network eligible molecules in the Ingenuity® Knowledge Base that could be included in the network. The network score is calculated based on right tailed Fisher's exact test and the presented network score is negative logarithm of Fisher's exact *p*-value. The higher the score, the more significant is the interaction between network eligible molecules.

Table 4.9: Modulation of networks in HCT116 and HepG2 cells by MP-HX. IPA software ranked top networks enriched in the microarray dataset based on the network score. *NI, network ID, FM, focus molecules.

Cell line	NI	Score	# of FM	Top disease and functions
HCT116	1	124	124	Cell Cycle, Cellular Assembly and Organization, DNA Replication, Recombination, and Repair
	2	114	119	Cellular Compromise, Cellular Function and Maintenance, Cancer
	3	73	94	Cell Death and Survival, Inflammatory Response, Cellular Development
	4	66	84	Cell Cycle, DNA Replication, Recombination, and Repair, Cell Death and Survival
	5	57	83	Cancer, Organismal Injury and Abnormalities, Respiratory Disease
HepG2	1	122	122	Cell Cycle, Cellular Assembly and Organization, DNA Replication, Recombination, and Repair
	2	110	116	Cell Death and Survival, Cell Morphology, Cellular Function and Maintenance
	3	68	90	Cell Death and Survival, Organismal Injury and Abnormalities, Cell Cycle
	4	61	85	Cell Cycle, Cancer, Organismal Injury and Abnormalities
	5	57	82	Cell Cycle, Cellular Assembly and Organization, DNA Replication, Recombination, and Repair

The top network (Network 1) in HCT116 had a network score (NS) of 124, and contains 124 focus molecules which include AURKA, AURKB, BBC3, CCNA2, CDK6, CDKN2B, E2F1, MCM2, MCM10, PLK1, POLA1, RAD51, RFC3, RRM2, TOP2A, TYMS (**Figure 4.38**). Many of the focus molecules in this network were downregulated. Network 2 (NS=73) in HCT116 has 119 focus molecules which include BIRF5, CCNB1, CDC25A, CDK2, CDKN1A, DDIT3, GADD45A, HMOX1, JUN, NDRG1, PCNA, while network 4 (NS=66) has 84 focus molecules which include AURKB, CCNA2, CDKN1A, GINS1, KIF11, MXD1, PLK1, POLE2, TP53. Although NUPR1 was not considered as a focus molecule in network 4 (due to its FC value of +1.27), IPA network analyses indicated NUPR1 interacted with many other focus

molecules in the network, and most of them were downregulated (**Figure 4.39),** an observation like that seen in HepG2 **(Figure 4.40)** (see below).

In HepG2, the top network (NS=122) has 122 focus molecules which include AURKA, BUB1, CCNA2, CDK6, CDKN2B, CHEK1, GINS2, GMNN, MCM3, MCM10, NUPR1, POLA2, RAD51, RFC3, RRM2, SKP2, TOP2A (**Figure 4.40**). The network figure shows NUPR1 (FC +2.40) interacted with many other focus molecules, and many of them were downregulated. Identification of NUPR1 as a focus molecule here is supportive of the earlier finding, i.e. upstream regulator analyses, where NUPR1 was predicted by IPA to be the top upstream regulator in both HepG2 and HCT116 cells. Network 2 (NS=110) in HepG2 has 116 focus molecules which include BBC3, DDIT4, ERN1, GABARAPL1, NDRG1, while network 3 (NS=68) has 90 focus molecules which include BAK1, CCNB1, CDK1, CDKN1A, DDIT3, DUSP1, GADD45B, HMOX1, JUN, PCNA.

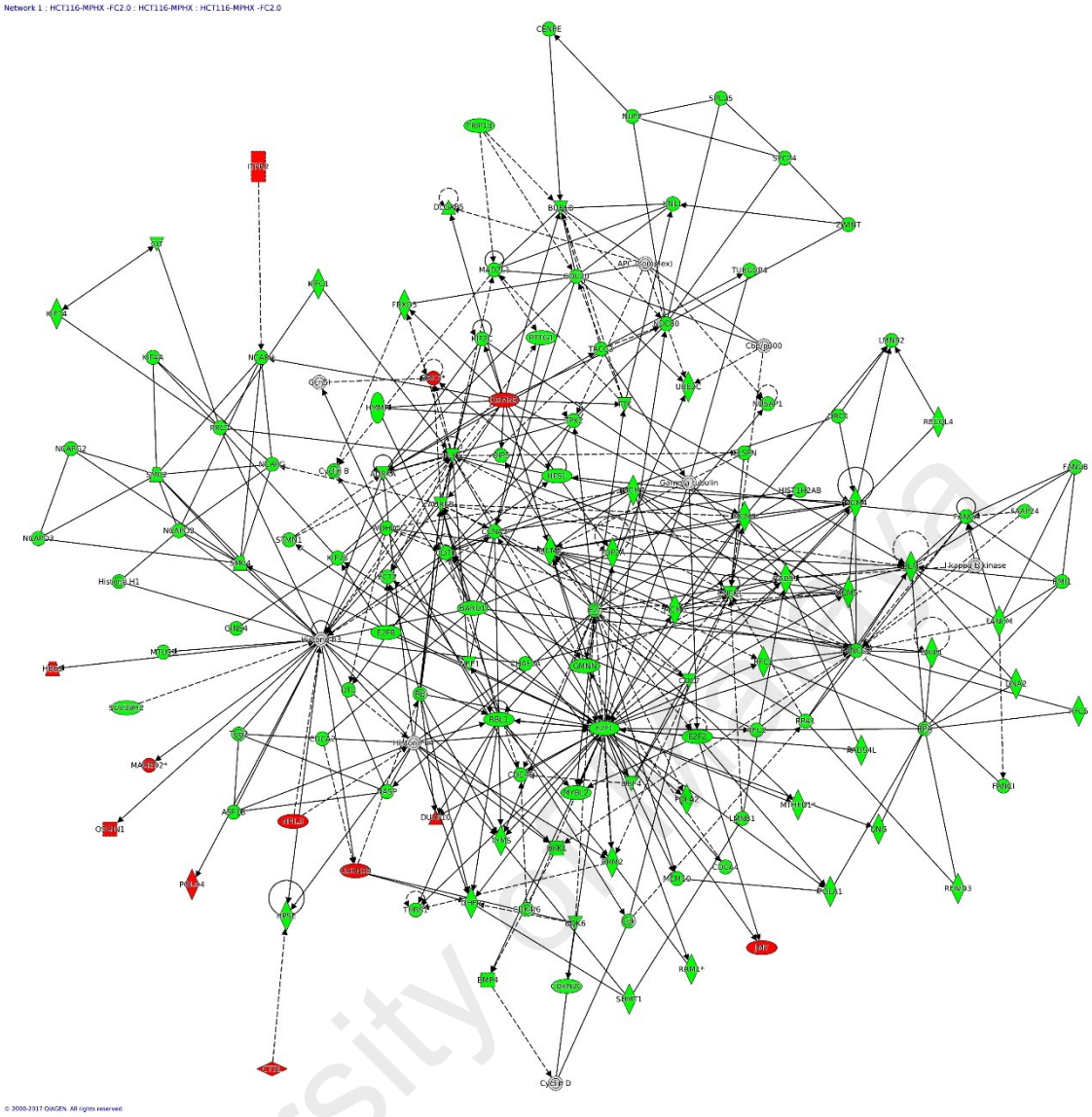

Figure 4.38: IPA network analysis: top ranked network shows annotated interactions between genes in HCT116 cells treated with MP-HX. The figure shows network 1 in HCT116, containing 124 focus molecules. Most of the focus molecules in this network were downregulated by MP-HX. Top diseases and functions associated with this network include processes related to cell proliferation, cell cycle and DNA replication. Molecules in the network are colored red (MA_FC ≥ +2.0), or green (MA_FC ≥ -2.0), or grey (MA_FC < ±2).

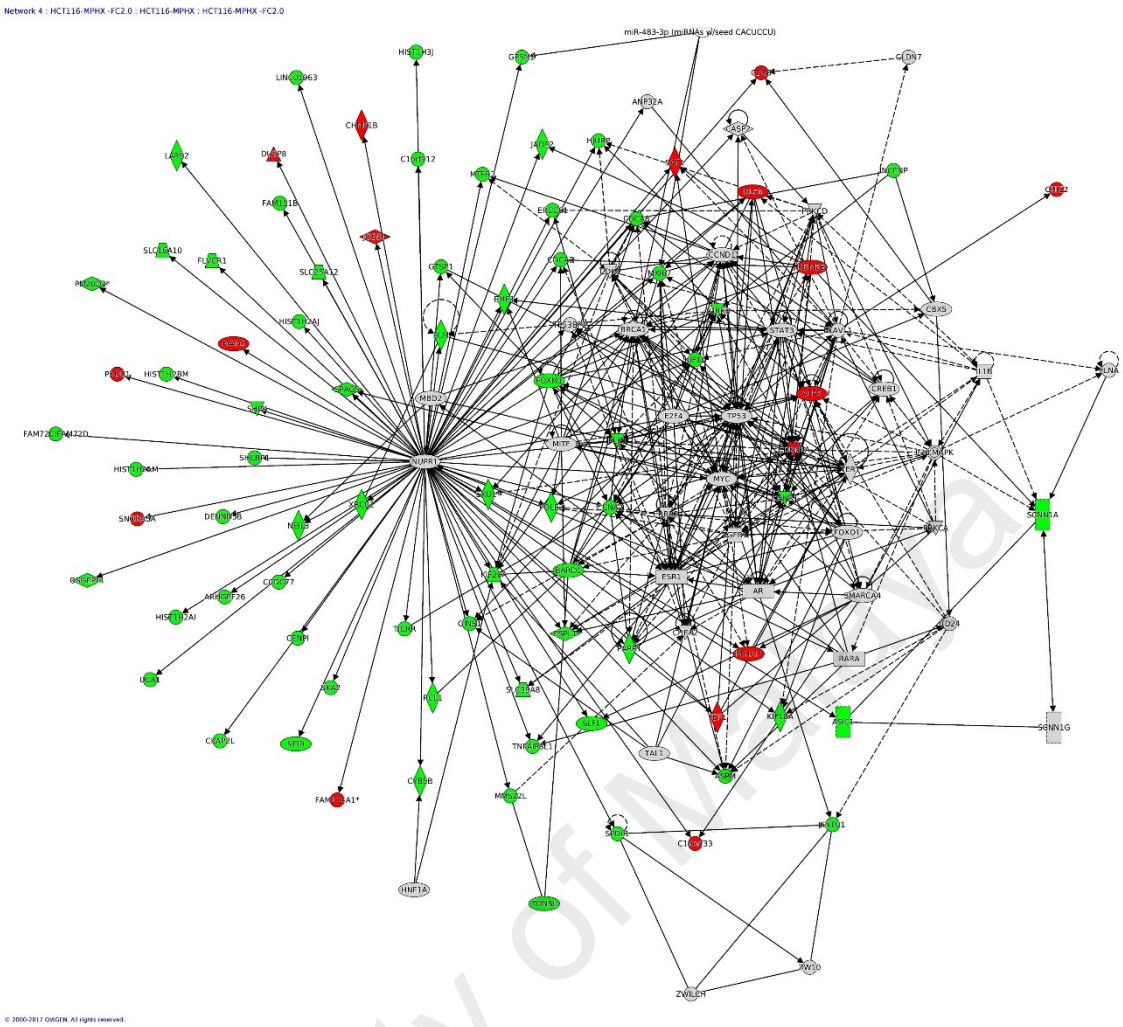

Figure 4.39: IPA network analysis: fourth ranked network shows annotated interactions between genes in HCT116 cells treated with MP-HX. The figure shows network 4 in HCT116, containing 84 focus molecules. NUPR1 shows interaction with many other focus molecules that show expression downregulation (MA_FC ≥ -2.0). Top diseases and functions associated with this network include processes related to cell cycle regulation, DNA replication and cell death/survival. Molecules in the network are colored red (MA_FC ≥ +2.0), or green (MA_FC ≥ -2.0), or grey (MA_FC < ±2).

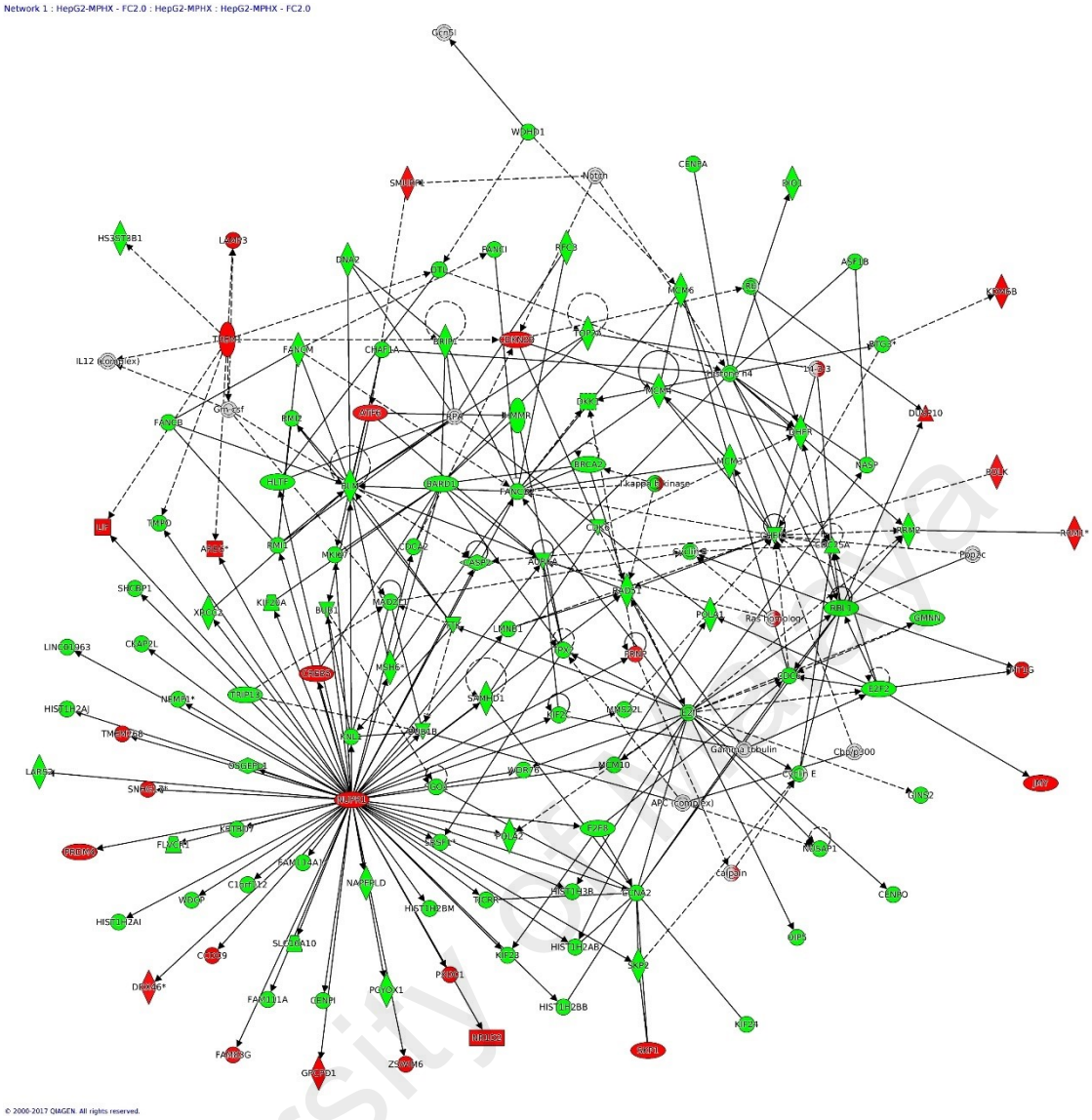

Figure 4.40: IPA network analysis: top ranked network shows annotated interactions between genes in HepG2 cells treated with MP-HX. The figure shows network 1 in HepG2 cells, containing 122 focus molecules. NUPR1 shows interaction with many other focus molecules that show expression downregulation (MA_FC ≥-2.0). Top diseases and functions associated with this network include processes related to cell cycle, cancer and DNA replication. Molecules in the network are colored red (MA_FC ≥ +2.0), or green (MA_FC ≥ -2.0), or grey (MA_FC < ±2).

4.5 Gene expression profiling in Hs27 cells treated with *Melicope ptelefolia*, quercetin and dexpanthenol

4.5.1 MTT cell viability assay

The effect of MP-HX, MP-EA, quercetin (QN) and dexpanthenol (DX) on Hs27 cell viability was evaluated through MTT assay.

4.5.1.1 Effect of MP-HX and MP-EA on Hs27 cell viability

At low concentration (15 µg/mL), MP-HX was able to increase the percentage of viable Hs27 cells (**Figure 4.41A**). At 15 µg/mL, MP-HX significantly increased the cell viability to 110.10 ± 1.49%. The cell viability was 101.77 ± 1.57% at 30 µg/mL of MP-HX. On the other hand, MP-EA was able to increase the percentage of viable Hs27 cells at lower range of concentrations (15 and 30 µg/mL) (**Figure 4.41B**). At 15 and 30 µg/mL, MP-EA significantly increased the percentage of viability to 126.97 ± 3.06 and 110.65 ± 2.11%, respectively. However, at 60 µg/mL, MP-HX and MP-EA reduced the viability of Hs27 to 83.08 ± 2.00% and 94.01 ± 1.15%, respectively. Considering these observations, 15 µg/mL was selected as the concentration of MP-HX and MP-EA for the microarray study.

4.5.1.2 Effect of quercetin and dexpanthenol on Hs27 cell viability

QN and DX demonstrated dose dependent effect on Hs27 cell viability (**Figures 4.41C** and **4.41D**). At 5 µg/mL, QN induced a significant increase in percentage of cell viability to 106.94 ± 2.93%. On the other hand, DX increased the percentage of cell viability to 105.99±1.66% at 10 mg/mL. From these observations, the concentrations of

QN and DX selected for the microarray study were 5 µg/mL and 10 mg/mL, respectively.

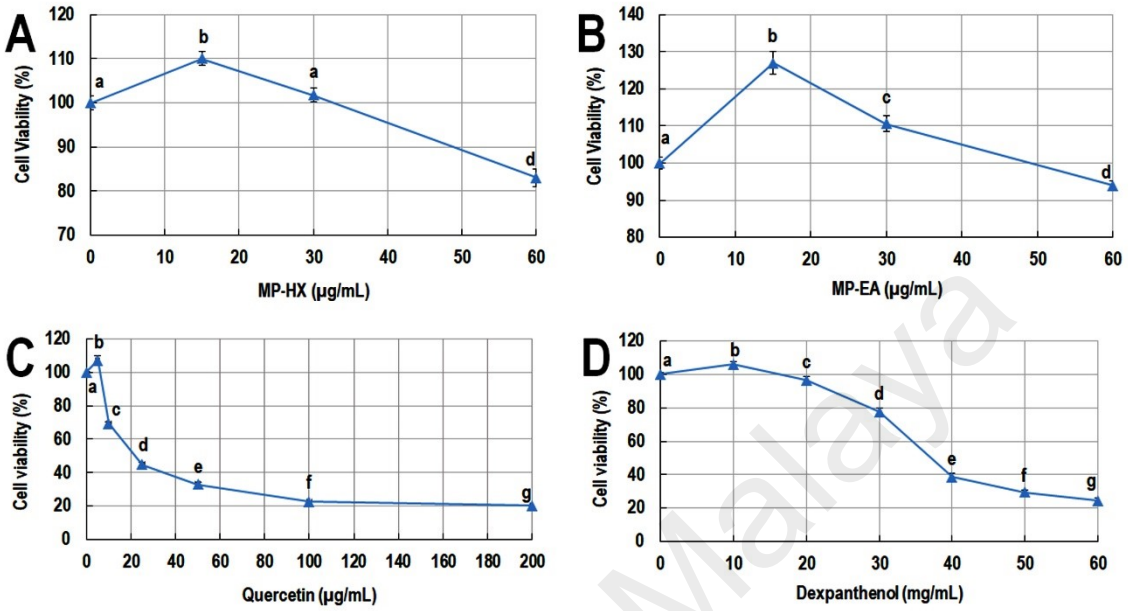

Figure 4.41: MTT cell viability assay. Effect of A) MP-HX, B) MP-EA, C) quercetin, and D) dexpanthenol on the cell viability of Hs27 cells (48 h treatment). Values are mean ± SD (n=3). Mean values with different letters (a-g) were significantly different from the control (p <0.05).

4.5.2 Microarray data validation by RT-qPCR

Real-time quantitative PCR was used to validate microarray data. Fifteen genes were selected for the validation. Among them, eight were upregulated (GSR, CAT, GSTP1, PCNA, RRM2B, HIRA, RRM2, HELLS), while seven were downregulated genes (GADD45A, GABARAPL1, FOS, HSPB2, CASP8, TNF, CDKN1C). RPS29 was used to normalize the gene expression data. The FC values obtained from RT-qPCR compared to that of microarray are shown in **Table 4.10**, **Figures 4.42** and **4.43**. The directions of gene expression fold change for all the genes were consistent with that of microarray.

Table 4.10: Gene expression fold change induced by MP-HX, MP-EA, QN and DX in Hs27 cells. A comparison between microarray and RT-qPCR methods. A positive fold change value indicates upregulation, while negative value indicates downregulation. Values are mean ± SD for RT-qPCR fold change (n=3). Mean values with asterisks (*) were significantly different from the control (p <0.05). *MA_FC, fold change based on microarray data; RT-qPCR_FC, fold change based on real-time PCR data.

Gene	MP-HX		MP-EA		QN		DX	
	MA_FC	RT-qPCR*_FC	MA_FC	RT-qPCR*_FC	MA_FC	RT-qPCR*_FC	MA_FC	RT-qPCR*_FC
GSR	+2.08	+4.70±0.09	+1.89	+3.71±0.24	+1.97	+3.78±0.24	+2.07	+4.24±0.40
CAT	+1.84	+2.43±0.12	+2.35	+2.49±0.10	+2.70	+3.21±0.07	+2.91	+3.48±0.06
GSTP1	+5.01	+8.46±0.42	+4.61	+5.68±1.06	+4.75	+5.37±1.06	+4.99	+5.43±0.77
PCNA	+1.28	+1.85±0.08	+1.98	+2.23±0.10	+2.16	+3.35±0.48	+1.55	+2.13±0.27
RRM2B	+2.09	+2.93±0.17	+1.97	+1.73±0.14	+2.05	+2.13±0.16	+1.72	+1.61±0.07
HIRA	+1.62	+3.82±0.10	+1.63	+1.81±0.17	+1.75	+3.22±0.48	+1.63	+2.39±0.24
RRM2	+1.50	1.53±0.12	+2.83	+2.71±0.30	+3.28	+3.52±0.37	+1.82	+1.53±0.34
HELLS	+1.89	+2.45±0.33	+2.71	+2.42±0.24	+3.73	+2.13±0.62	+2.05	+3.00±0.77
GADD45A	-1.75	-1.56±0.08	-1.39	-1.38±0.06	-1.21	-1.23±0.04	-1.51	-1.38±0.07
GABARAPL1	-2.92	-5.89±0.17	-2.67	-6.10±0.18	-2.16	-6.04±0.35	-2.49	-5.68±0.19
FOS	-1.76	-2.34±0.42	-1.92	-2.20±0.56	-1.71	-2.44±0.31	-1.48	-1.64±0.06
HSPB2	-1.53	-1.76±0.03	-1.65	-1.95±0.04	-1.64	-2.16±0.10	-1.41	-2.42±0.04
CASP8	-1.74	-2.29±0.05	-1.79	-2.31±0.04	-1.58	-2.26±0.07	-1.73	-2.00±0.38
TNF	-1.55	-5.24±0.93	-1.75	-6.37±1.17	-1.42	-2.6±0.48	-1.43	-2.88±0.90
CDKN1C	-1.55	-1.73±0.10	-1.46	-3.53±0.29	-1.78	-3.53±0.26	-1.74	-1.47±0.03

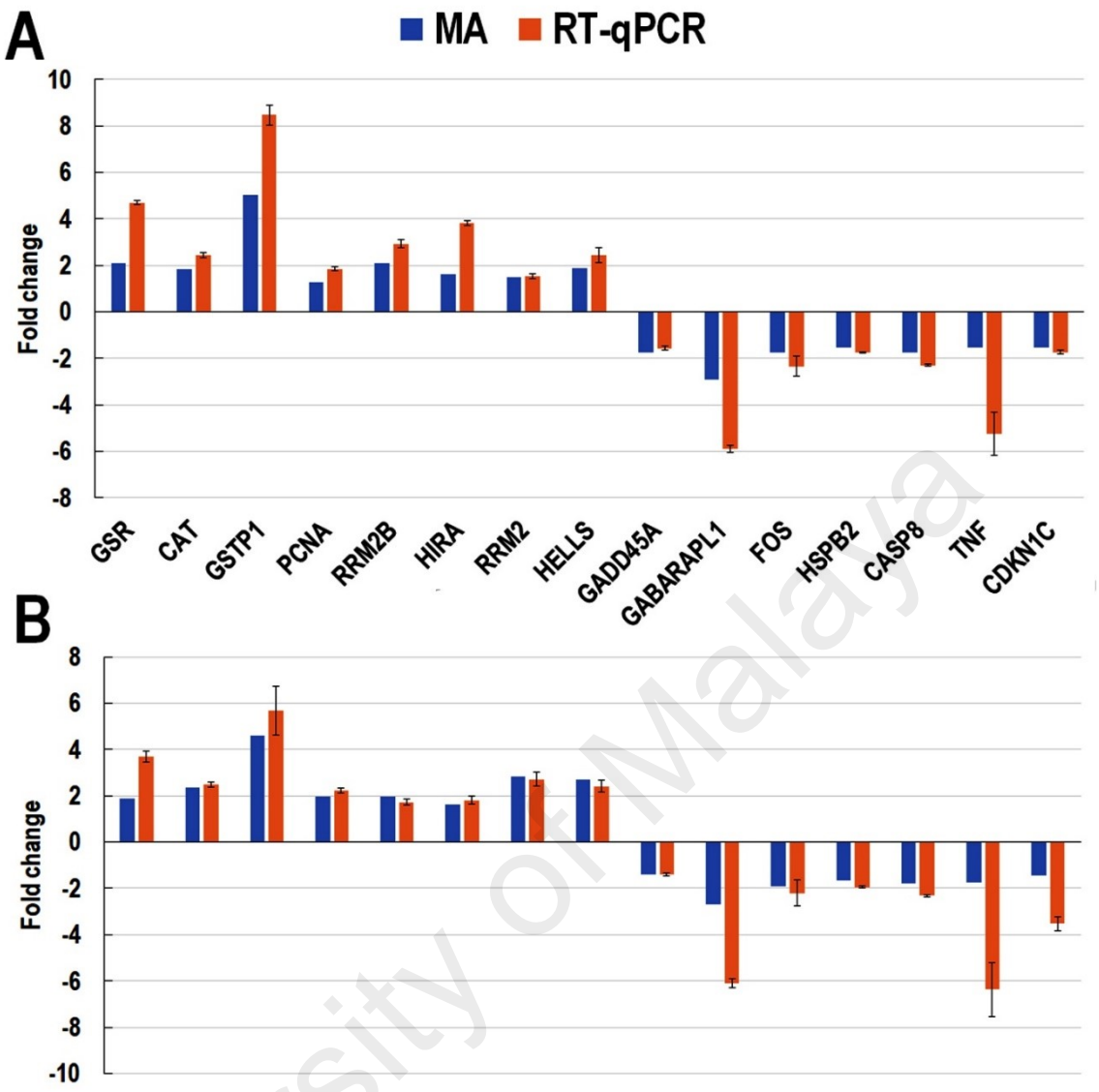

Figure 4.42: RT-qPCR validation of microarray data in Hs27 cells upon treatment with MP-HX and MP-EA. The bar chart shows gene expression fold change induced by A) MP-HX and B) MP-EA that was obtained from microarray and RT-qPCR assays. For each RT-qPCR assay, the data was normalized to RPS29 expression and the values represent mean RT-qPCR_FC ± SD (n=3).

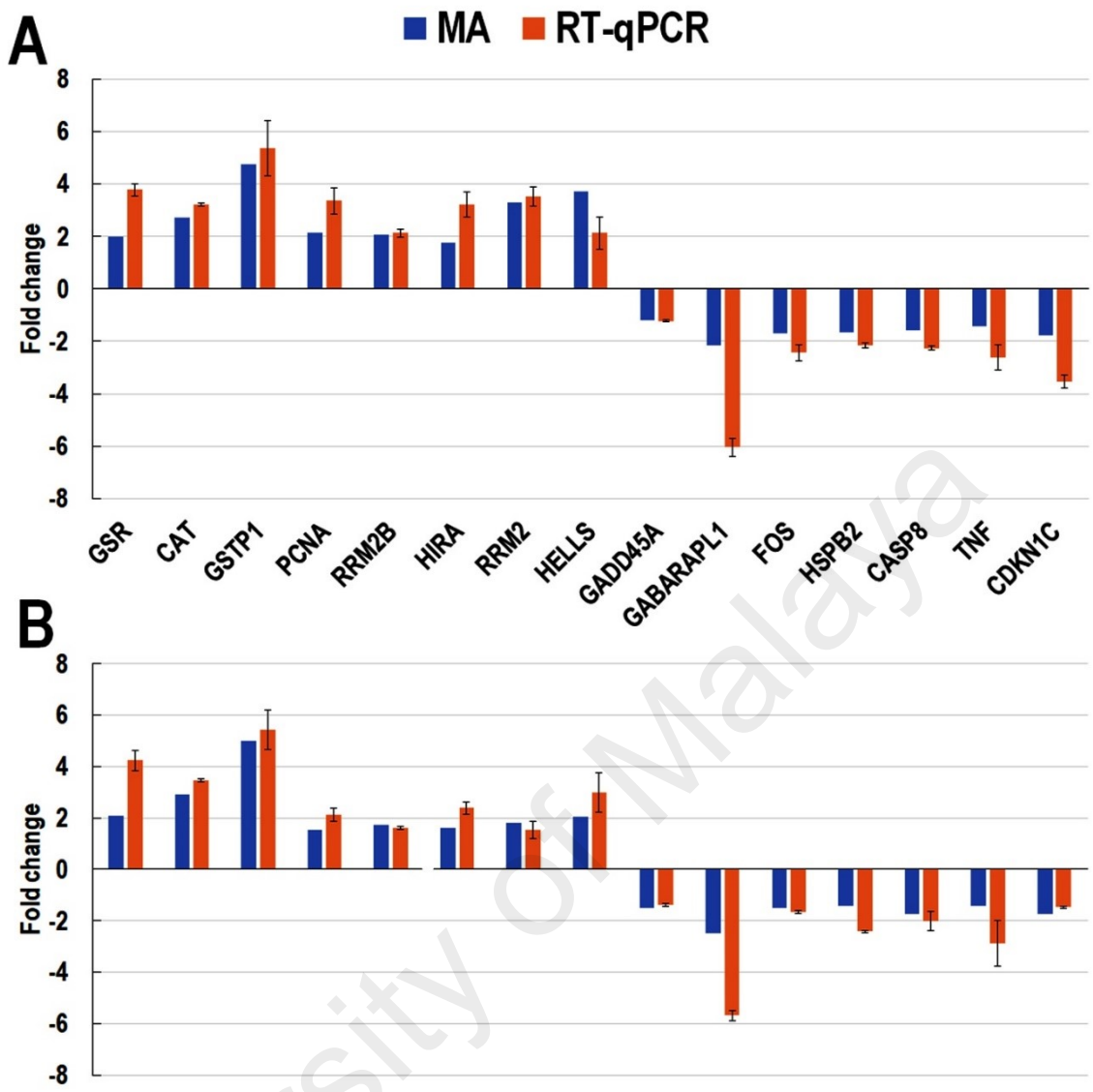

Figure 4.43: RT-qPCR validation of microarray data in Hs27 cells upon treatment with QN and DX. The bar chart shows gene expression fold change induced by A) QN and B) DX that was obtained from microarray and RT-qPCR assays. For each RT-qPCR assay, the data was normalized to RPS29 expression and the values represent mean RT-qPCR_FC ± SD (n=3).

4.5.3 Microarray analysis

4.5.3.1 Analysis of microarray data using Transcriptome Analysis Console (TAC)

Transcriptome analysis console (TAC) software (version 4.0) was used to identify differentially expressed genes (DEGs) induced by MP-HX, MP-EA, QN and DX in Hs27 cells. Using a cut-off fold change (FC) value of ±1.50, it was observed that MP-HX, MP-EA, QN and DX treatments in Hs27 cells resulted in differential expression of 15,529; 13,966; 15,097 and 13,842 genes, respectively (**Figure 4.44**). A comparison of DEGs among MP-HX, MP-EA, QN and DX gene dataset was performed using InteractiVenn (Heberle, Meirelles, da Silva, Telles, & Minghim, 2015) and the result is depicted in **Figure 4.45**. Comparing DEGs identified among MP-HX, MP-EA, QN and DX treatments, approximately 50% of the genes overlapped - they share 7,983 DEGs, and this account 51.4, 57.2, 52.9, 57.7% of DEGs for the corresponding treatment set, respectively. Of note, for each treatment, the number of up and downregulated genes were nearly equal, giving approximately 50% up and 50% downregulated genes.

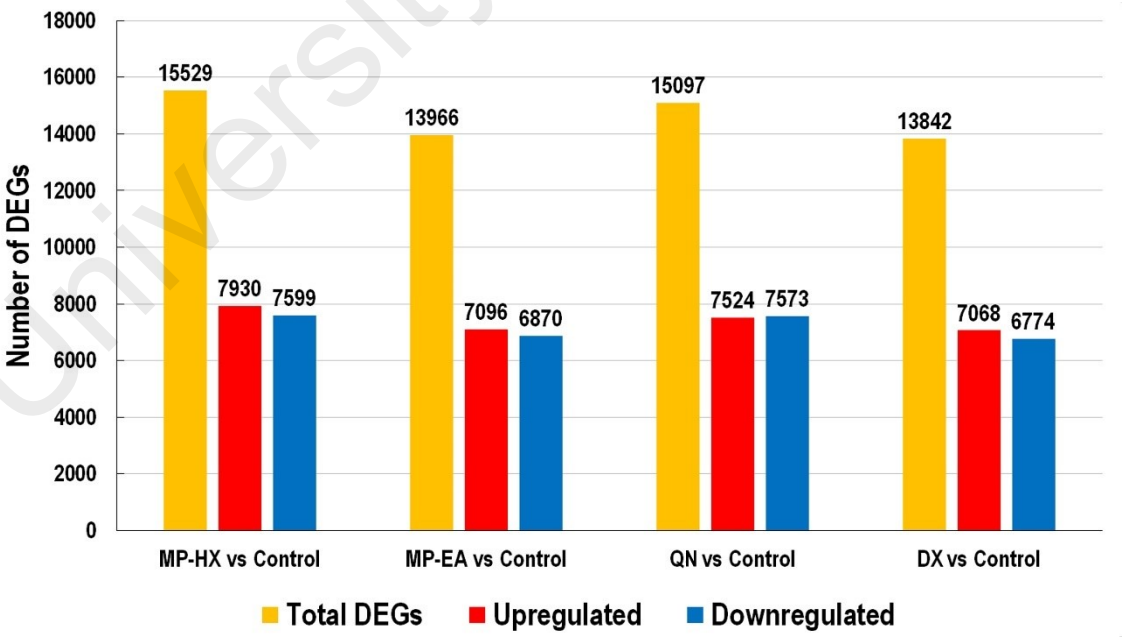

Figure 4.44: Number of differentially expressed genes (DEGs) (FC ≥ ±1.50) in Hs27 cells upon treatment with MP-HX, MP-EA, QN and DX.

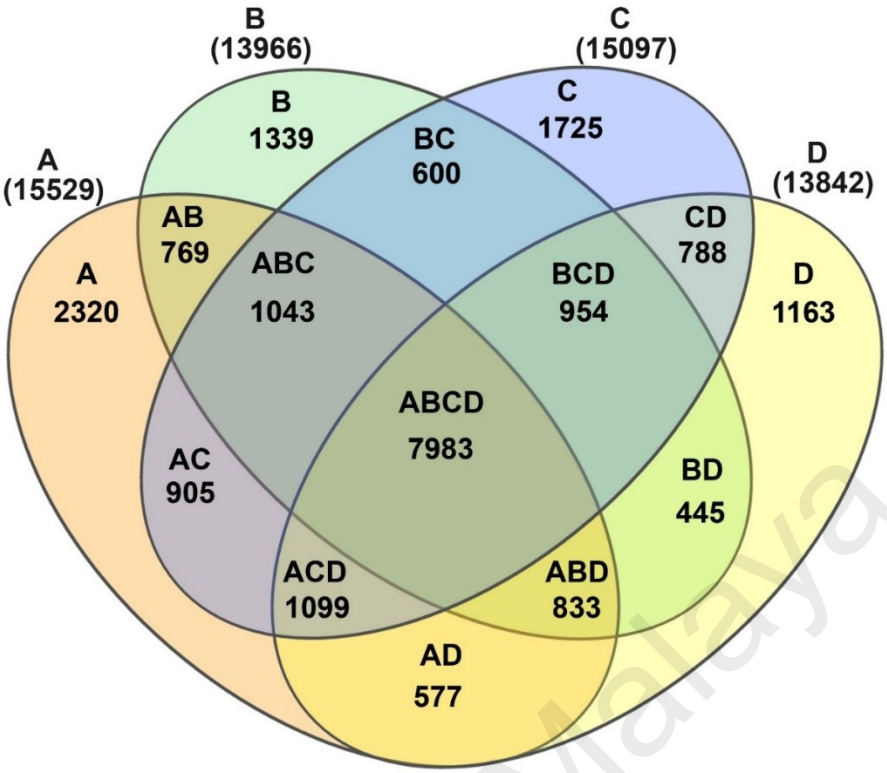

Figure 4.45: Venn diagram of differentially expressed genes (DEGs) (FC ≥ ±1.50) in Hs27 cells upon treatment with MP-HX, MP-EA, QN and DX. The Venn diagram shows comparison of DEGs among MP-HX, MP-EA, quercetin and dexpanthenol treatments. A, B, C and D indicate MP-HX vs control, MP-EA vs control, quercetin vs control and dexpanthenol vs control, respectively. The values indicate number of DEGs for the corresponding group(s).

As described earlier, MP-HX, MP-EA and QN showed potent cellular antioxidant activity in Hs27 cells (**Table 4.2**). Microarray gene expression profiling uncovered the gene expression changes associated with their antioxidant activity. It was noted that MP-HX, MP-EA, QN and DX upregulated numerous antioxidant genes in Hs27 cells. The list of significantly upregulated antioxidant genes in Hs27 upon MP-HX, MP-EA, QN and DX treatments is shown in **Table 4.11**.

Table 4.11: Expression fold change (FC) of representative antioxidant genes upregulated by MP-HX, MP-EA, QN and DX in Hs27 cells. Red colored FC values indicate upregulation of genes. The darker the color, the higher the expression of the relevant gene.

Gene ID	Gene name	MP-HX	MP-EA	QN	DX
CAT	Catalase	+1.84	+2.35	+2.70	+2.91
GPx1	Glutathione peroxidase 1	+1.52	+1.22	+1.28	+1.44
GPx5	Glutathione peroxidase 5	+1.57	+1.72	+2.03	+1.77
GPx7	Glutathione peroxidase 7	+2.60	+2.12	+2.06	+2.29
GPx8	Glutathione peroxidase 8	+2.80	+2.00	+1.67	+2.22
GSR	Glutathione-disulfide reductase	+2.08	+1.89	+1.97	+2.07
GSTK1	Glutathione S-transferase kappa 1	+1.23	+1.42	+1.80	+2.03
GSTP1	Glutathione S-transferase pi 1	+5.01	+4.61	+4.75	+4.99
GSTT1	Glutathione S-transferase theta 1	+1.29	+1.96	+1.78	+1.79
GSTT2	Glutathione S-transferase theta 2	+1.83	+1.47	+2.22	+1.51
MGST1	Microsomal glutathione S-transferase 1	+2.42	+2.15	+2.20	+2.44
NQO1	NAD(P)H quinone dehydrogenase 1	+1.59	+1.71	+1.50	+2.68
NXN	Nucleoredoxin	+1.20	+1.55	+2.16	+2.02
PRDX4	Peroxiredoxin 4	+1.92	+1.58	+1.59	+1.69
PRDX5	Peroxiredoxin 5	+2.13	+1.64	+1.38	+1.80
PRDX6	Peroxiredoxin 6	+1.75	+1.56	+1.99	+1.70
PTGS1	Prostaglandin-endoperoxide synthase 1	+1.90	+2.86	+3.72	+3.42
PXDN	Peroxidasin	+1.45	+1.76	+1.98	+2.30
SESN1	Sestrin 1	+2.61	+3.48	+3.77	+3.50
SOD2	Superoxide dismutase 2	+1.51	+1.50	+1.43	+1.55
TXNRD3	Thioredoxin reductase 3	+3.14	+3.22	+2.41	+2.59

GSTP1 (Glutathione S-transferase pi 1) was most significantly upregulated by MP-HX, MP-EA, QN and DX with FC values between +4.61 to +5.01. Other antioxidant genes such as CAT, GPx7, GPx8, GSR, MGST1, PTGS1, SESN1 and TXNRD3 were also highly upregulated (FC range: +1.84 to +3.77).

Genes related to aging (de Magalhaes, Curado, & Church, 2009) were also investigated. The result indicated that MP-HX, MP-EA, QN and DX modulated many

aging related genes in directions that could be said to be supportive of anti-aging activity (**Table 4.12**).

Table 4.12: Aging related genes modulated by MP-HX, MP-EA, QN and DX in Hs27 cells. *(de Magalhaes et al., 2009); **MA_FC, microarray gene expression fold change.

Aging Related Genes	MA_FC**			
Genes reported to be *upregulated* with age*	**MP-HX**	**MP-EA**	**Qn**	**Dx**
S100A6	-1.34	-1.36	-1.52	-1.20
GFAP	-1.86	-1.93	-2.44	-1.56
LGALS3	-2.29	-1.66	-1.76	-1.46
ANXA3	-2.04	-2.33	-1.98	-2.64
MPEG1	-2.03	-2.02	-1.98	-2.64
SPP1	-1.86	-1.52	-1.70	-1.55
HBA1	-2.73	-2.82	-2.49	-2.57
C1QA	-1.60	-1.63	-1.70	-1.55
Genes reported to be *downregulated* with age*				
TFRC	+1.79	+1.36	+1.34	+1.39
COL1A1	+2.33	+2.18	+1.83	+2.52
COL3A1	+1.28	+2.34	+1.67	+2.63
ATP5G3	+1.63	+1.93	+2.23	+1.97
NDUFB11	+2.13	+1.73	+2.06	+2.09
FABP3	+1.59	+1.67	+1.32	+1.34
GHITM	+1.76	+1.34	+1.39	+1.41
ACSS2	+1.93	+2.01	+1.93	+2.27
DIABLO	+1.75	+1.47	+1.48	+1.75

4.5.3.2 Analysis of microarray data using GATHER web-tool

The microarray gene expression data was also analysed using the web-based tool "Gene Annotation Tool to Help Explain Relationships" (GATHER) (http://changlab.uth.tmc.edu/gather/gather.py) (J. T. Chang & Nevins, 2006). GATHER categorizes statistically significant association between genes and biological processes. This could help reveal the biological functions associated with transcriptome profiles produced by the treatments. A cut-off FC value of ±1.50 was used to filter the list of DEGs, and the genes fulfilling the FC value were analysed using GATHER.

For MP-HX dataset, the GATHER revealed enrichment of GO categories which include "response to stress", "cell cycle", "DNA repair" (**Table 4.13, Figure 4.46**).

Table 4.13: GATHER analysis - GO categories enriched in MP-HX dataset. The list indicates biological processes that were significantly overrepresented in Hs27 upon treatment with MP-HX. *Count: gene number for the corresponding overrepresented biological process.

GO: biological process	Count	-log (*p*-value)
GO:0050875 [3]: cellular physiological process	3314	4.85
GO:0006950 [4]: response to stress	360	4.55
GO:0009581 [5]: detection of external stimulus	155	3.95
GO:0007154 [3]: cell communication	1108	3.37
GO:0009719 [4]: response to endogenous stimulus	102	2.73
GO:0006974 [5]: response to DNA damage stimulus	95	2.24
GO:0000086 [7]: G2/M transition of mitotic cell cycle	28	1.78
GO:0007049 [5]: cell cycle	286	1.68
GO:0006281 [6]: DNA repair	84	1.50
GO:0009605 [4]: response to external stimulus	390	1.48

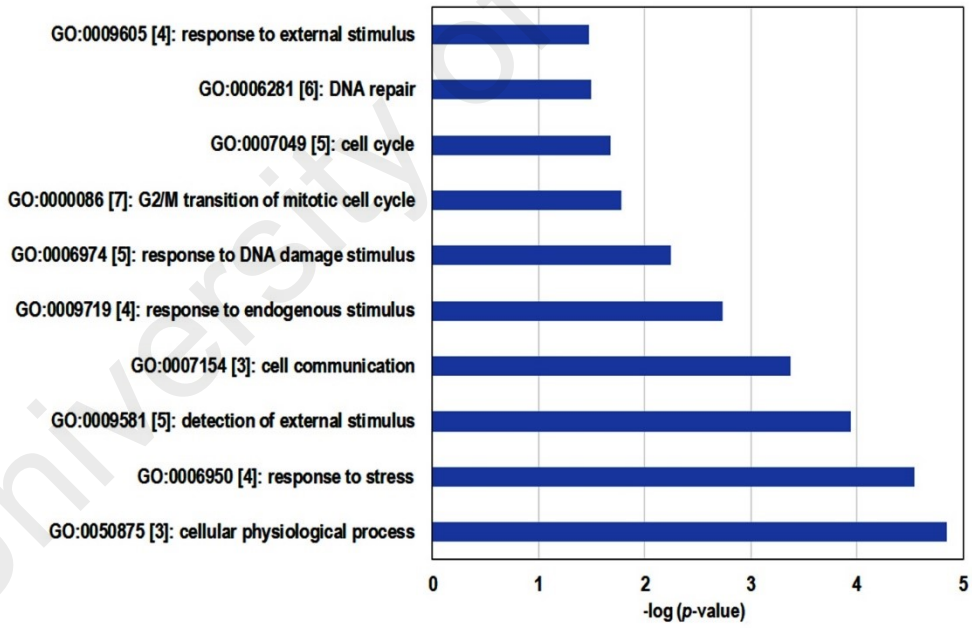

Figure 4.46: GATHER analysis - GO categories enriched in MP-HX dataset. The bar chart depicts significantly overrepresented GO categories in Hs27 cells after treatment with MP-HX.

The following GO categories were enriched in MP-EA dataset: "Cell proliferation", "Cell cycle", "Response to stress", "DNA repair" (**Table 4.14, Figure 4.47**).

Table 4.14: GATHER analysis - GO categories enriched in MP-EA dataset. The list indicates biological processes that were significantly overrepresented in Hs27 upon treatment with MP-EA. *Count: gene number for the corresponding overrepresented biological process.

GO: biological process	Count	-log (*p*-value)
GO:0008283 [4]: cell proliferation	401	4.85
GO:0007049 [5]: cell cycle	283	4.85
GO:0000074 [6]: regulation of cell cycle	166	4.55
GO:0000279 [6]: M phase	80	3.60
GO:0009719 [4]: response to endogenous stimulus	93	3.01
GO:0006974 [5]: response to DNA damage stimulus	87	2.64
GO:0006950 [4]: response to stress	305	2.41
GO:0000278 [6]: mitotic cell cycle	84	2.31
GO:0006281 [6]: DNA repair	78	2.06
GO:0000067 [6]: DNA replication and chromosome cycle	79	2.04
GO:0006955 [4]: immune response	268	2.02
GO:0006261 [7]: DNA-dependent DNA replication	38	2.02
GO:0000087 [7]: M phase of mitotic cell cycle	59	1.94
GO:0009581 [5]: detection of external stimulus	144	1.89
GO:0006260 [6]: DNA replication	63	1.76

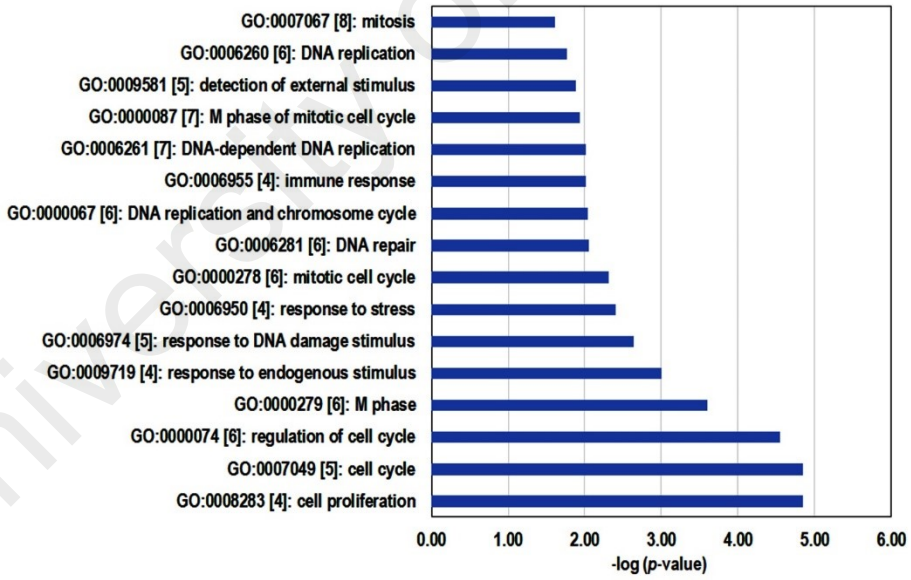

Figure 4.47: GATHER analysis - GO categories enriched in MP-EA dataset. The bar chart depicts significantly overrepresented GO categories in Hs27 cells after treatment with MP-EA.

The following GO categories were enriched in QN dataset: "Cell cycle", "Cell proliferation", "Response to stress", "DNA repair", "DNA replication" (**Table 4.15, Figure 4.48**).

Table 4.15: GATHER analysis - GO categories enriched in QN dataset. The list indicates biological processes that were significantly overrepresented in Hs27 upon treatment with QN. *Count: gene number for the corresponding overrepresented biological process.

GO: biological process	Count	-log (*p*-value)
GO:0007049 [5]: cell cycle	344	4.85
GO:0008283 [4]: cell proliferation	467	4.85
GO:0000074 [6]: regulation of cell cycle	196	4.85
GO:0006974 [5]: response to DNA damage stimulus	110	4.85
GO:0009719 [4]: response to endogenous stimulus	115	4.85
GO:0000279 [6]: M phase	94	4.85
GO:0006281 [6]: DNA repair	96	4.85
GO:0000067 [6]: DNA replication and chromosome cycle	97	4.85
GO:0000278 [6]: mitotic cell cycle	101	4.55
GO:0006260 [6]: DNA replication	78	4.37
GO:0006950 [4]: response to stress	353	4.07
GO:0009581 [5]: detection of external stimulus	152	4.07
GO:0000087 [7]: M phase of mitotic cell cycle	69	3.53
GO:0006261 [7]: DNA-dependent DNA replication	44	3.23
GO:0000075 [7]: cell cycle checkpoint	24	2.97
GO:0007067 [8]: mitosis	67	2.97
GO:0000910 [5]: cytokinesis	57	1.54
GO:0009605 [4]: response to external stimulus	385	1.50

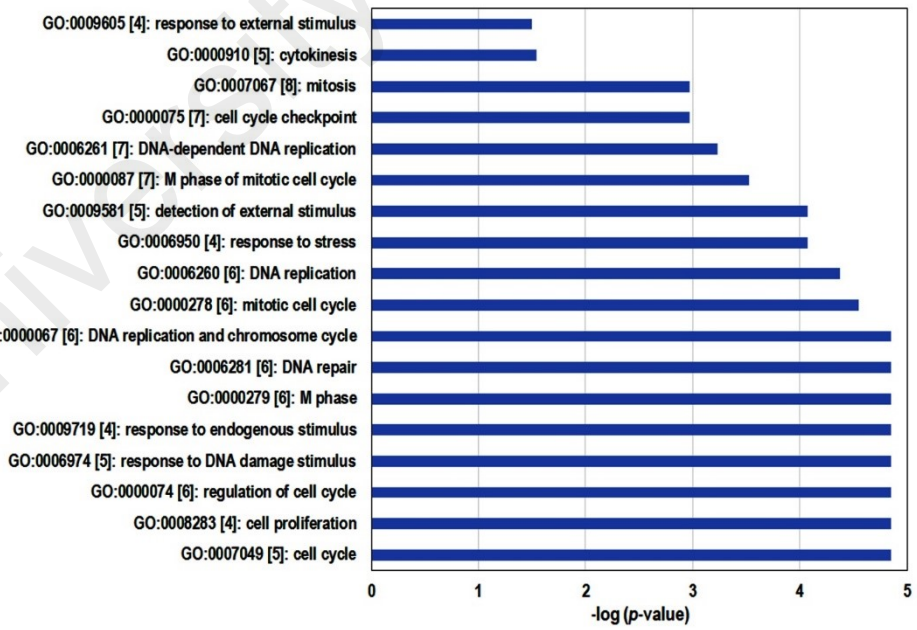

Figure 4.48: GATHER analysis - GO categories enriched in QN dataset. The bar chart depicts significantly overrepresented GO categories in Hs27 cells after treatment with QN.

The following GO categories were enriched in DX dataset: “Cell cycle”, “Response to stress”, “Cell proliferation” (**Table 4.16, Figure 4.49**).

Table 4.16: GATHER analysis - GO categories enriched in DX dataset. The list indicates biological processes that were significantly overrepresented in Hs27 upon treatment with DX. *Count: gene number for the corresponding overrepresented biological process.

GO: biological process	Count	-log (*p*-value)
GO:0000074 [6]: regulation of cell cycle	169	4.55
GO:0050875 [3]: cellular physiological process	2912	4.55
GO:0006412 [6]: protein biosynthesis	213	4.00
GO:0044237 [4]: cellular metabolism	2134	3.81
GO:0007049 [5]: cell cycle	270	3.37
GO:0006950 [4]: response to stress	316	3.34
GO:0008283 [4]: cell proliferation	381	2.70
GO:0009581 [5]: detection of external stimulus	143	2.54
GO:0009057 [5]: macromolecule catabolism	264	2.52
GO:0050794 [3]: regulation of cellular process	291	2.44
GO:0009719 [4]: response to endogenous stimulus	89	1.70
GO:0000082 [7]: G1/S transition of mitotic cell cycle	30	1.54

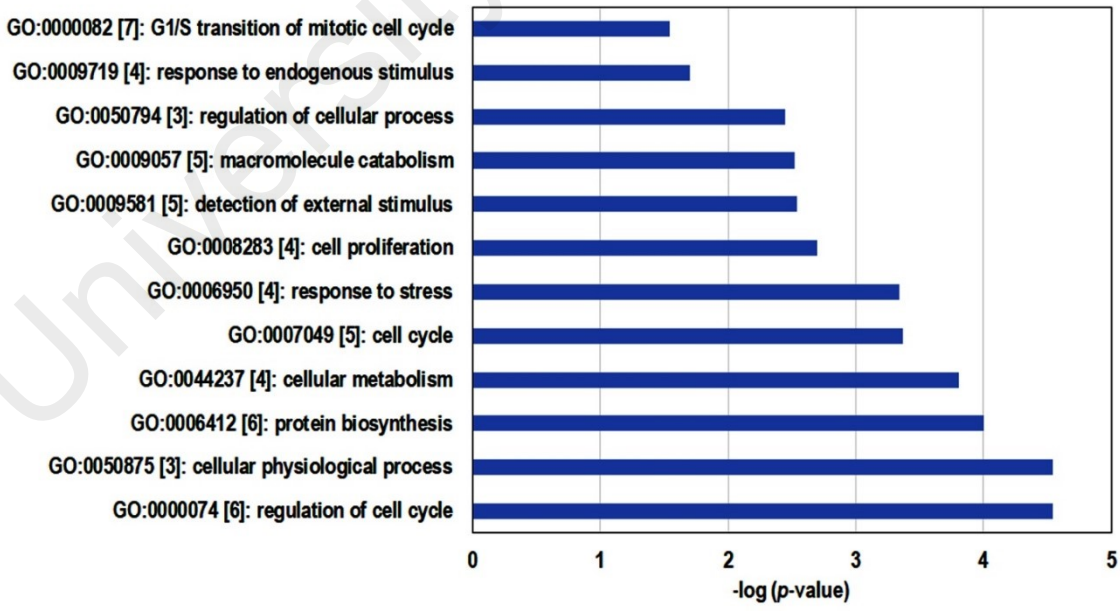

Figure 4.49: GATHER analysis - GO categories enriched in DX dataset. The bar chart depicts significantly overrepresented GO categories in Hs27 cells after treatment with DX.

The effect of MP-HX, MP-EA, QN and DX on genes governing cell cycle and cell proliferation was further evaluated using gene ontology categories (GO:0007049: Cell cycle) and (GO:0008283: Cell proliferation). Representative DEGs that are crucial for cell cycle and proliferation are listed in **Table 4.17**.

The most significantly upregulated genes by MP-HX include RPA2 followed by POLA2, CCNB1, E2F5 and CDK4. MP-EA, QN and DX treatments were noted to upregulate CCNB1 significantly. CDC7, CDK1, CCNB2, CDC6 and RRM2 were also highly upregulated by MP-EA, while QN highly upregulated the expression of CCNB2, PLK1, CDK1, PLK4 and CDC6. On the other hand, DX most highly upregulated genes include CDC25B, RPA2, CDC7 and POLA2.

Table 4.17: Expression fold change (FC) values of representative genes involved in cell cycle (GO:0007049) and cell proliferation (GO:0008283). FC values that are colored red indicate upregulation, while green FC values indicate downregulation. The darker red/green color, the higher FC value it represents, the lighter the red/green color the lower the FC value. If the FC value is ≤ ±1.10, it is assumed that gene expression modulation was absent.

Gene ID	Gene name	MP-HX	MP-EA	QN	DX
CCNB1	Cyclin B1	+2.44	+4.82	+11.51	+3.25
CCNB2	Cyclin B2	+1.49	+2.86	+6.31	+1.77
CCNE1	Cyclin E1	+1.59	+1.49	+1.62	+1.17
CCNE2	Cyclin E2	+1.06	+2.41	+2.96	+1.50
CDK1	Cyclin-dependent protein kinase	+1.59	+3.40	+5.06	+1.88
CDC25B	Cell division cycle 25B	+1.78	+2.42	+2.79	+2.60
CDC6	Cell division cycle 6	+1.36	+2.83	+4.46	+1.57
CDC7	Cell division cycle 7	+1.73	+3.42	+3.55	+1.99
CDK4	Cyclin dependent kinase 4	+2.41	+1.67	+1.85	+1.53
CDK7	Cyclin dependent kinase 7	+2.20	+1.59	+1.37	+1.67
CDKN1C	Cyclin dependent kinase inhibitor 1C	-1.55	-1.46	-1.78	-1.74
E2F4	E2F transcription factor 4	+2.21	+1.31	+2.03	+1.76
E2F5	E2F transcription factor 5	+2.43	+1.29	+1.39	+1.33
GADD45A	Growth arrest and DNA damage inducible alpha	-1.75	-1.39	-1.21	-1.51
MCM2	Minichromosome maintenance complex component 2	+1.89	+1.71	+2.53	+1.64
MCM3	Minichromosome maintenance complex component 3	+1.55	+1.62	+2.18	+1.20
MCM4	Minichromosome maintenance complex component 4	+1.56	+2.06	+2.00	+1.58
MCM6	Minichromosome maintenance complex component 6	+1.35	+1.75	+1.67	+1.30
MCM7	Minichromosome maintenance complex component 7	+1.18	+1.59	+2.97	+1.46
MDM2	MDM2 proto-oncogene	+1.56	+1.79	+1.43	+1.63
ORC1	Origin recognition complex subunit 1	+1.40	+1.86	+2.35	+1.20
PCNA	Proliferating cell nuclear antigen	+1.28	+1.98	+2.16	+1.55
PLK1	Polo like kinase 1	-1.03	+2.04	+5.21	+1.24
PLK4	Polo like kinase 4	+1.21	+2.05	+4.60	+1.47
POLA2	DNA polymerase alpha 2, accessory subunit	+ 2.97	+2.36	+2.79	+1.94
POLD3	DNA polymerase delta 3, accessory subunit	+1.82	+1.64	+1.87	+1.67
POLE2	DNA polymerase epsilon 2, accessory subunit	+1.14	+1.41	+2.24	+1.10

Table 4.17, continued

Gene ID	Gene name	MP-HX	MP-EA	QN	DX
PRIM1	DNA primase subunit 1	+1.14	+2.57	+2.86	+1.49
RFC4	Replication factor C subunit 4	+1.30	+1.37	+2.39	+1.26
RPA1	Replication protein A1	+1.36	+1.82	+2.14	+1.61
RPA2	Replication protein A2	+3.27	+2.27	+2.18	+2.18
RRM2	Ribonucleotide reductase regulatory subunit M2	+1.50	+2.83	+3.28	+1.82
RRM2B	Ribonucleotide reductase regulatory TP53 inducible subunit M2B	+2.09	+1.97	+2.05	+1.72
TTK	TTK protein kinase	+1.57	+2.33	+4.03	+1.60

4.5.3.3 Ingenuity Pathway Analysis (IPA)

Microarray gene expression data was evaluated using Ingenuity pathway analysis (IPA) software to identify canonical pathways, disease and functions, upstream regulators, and gene networks enriched in the datasets. A cut-off expression FC value of ±2.00 was used for the analysis.

(a) ***Top canonical pathways modulated by MP-HX, MP-EA, QN and DX in Hs27 cells***

IPA identified several canonical pathways (CPs) associated with MP-HX, MP-EA, QN and DX treatments. IPA uses Fisher's exact test to calculate the association of genes with the canonical pathways. Negative logarithm of Fisher's exact *p* value determines the significance of the pathway. The higher the -log (*p* value), the more significant the pathways are.

"EIF2 signaling", "Role of IL-17A in psoriasis", "Valine degradation I", "Telomere extension by telomerase" and "Sirtuin signaling pathway" were the top and statistically significant CPs in MP-HX dataset (**Figure 4.50**), while "IL-17 signaling", "Role of IL-17A in psoriasis", "Mitotic roles of polo-like kinase", "Role of IL-17A in arthritis" and "IL-17A signaling in fibroblast" were the top CPs in MP-EA dataset (**Figure 4.51**). For QN treatment, the top CPs include "Role of BRCA1 in DNA damage response", "Cell cycle: DNA damage checkpoint regulation", "Cell cycle control of chromosomal replication", "ATM signaling and mitotic roles of polo-like kinase" (**Figure 4.52**). On the other hand, top CPs modulated by DX treatment include "EIF2 signaling", "Autophagy", "Role of IL-17A in psoriasis", "Hepatic fibrosis" and "IL-1 signaling" pathways (**Figure 4.53**).

"EIF2 signaling" was the top CPs with the highest significance score upon MP-HX and DX treatment. "EIF2 signaling" was also one of the top statistically significant CPs

modulated by MP-EA and QN. IPA analysis also revealed that several of IL-17 related signaling pathways were modulated by all treatments. "IL-17 signaling" was significantly regulated by MP-EA, QN and DX while "IL-17A signaling in fibroblast" were significantly modulated by all treatments. "Mitotic roles of polo-like kinase" was one of the CPs for QN treatment. This pathway was also significantly enriched by MP-HX and MP-EA. The CP "Sirtuin signaling pathway" was also significantly modulated by MP-HX, QN and DX treatments. The representative genes for selected number of CPs are listed in **Table 4.18**.

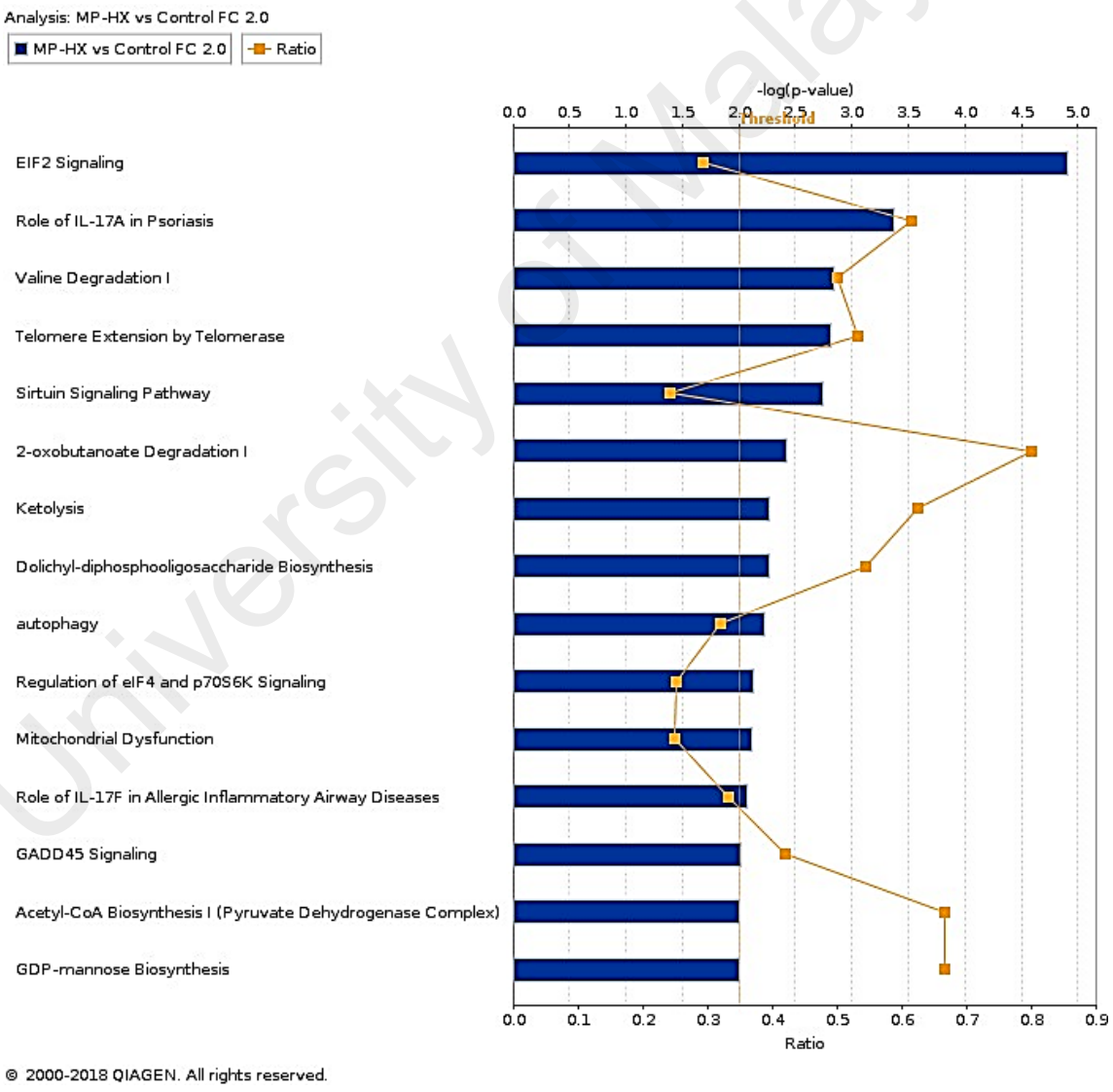

Figure 4.50: IPA analysis - top canonical pathways with -log (*p*-value) ≥ 2.0 as reported by IPA in Hs27 cells treated with MP-HX. Ratio value denotes the number of molecules in the dataset divided by total number of molecules associated with the pathway.

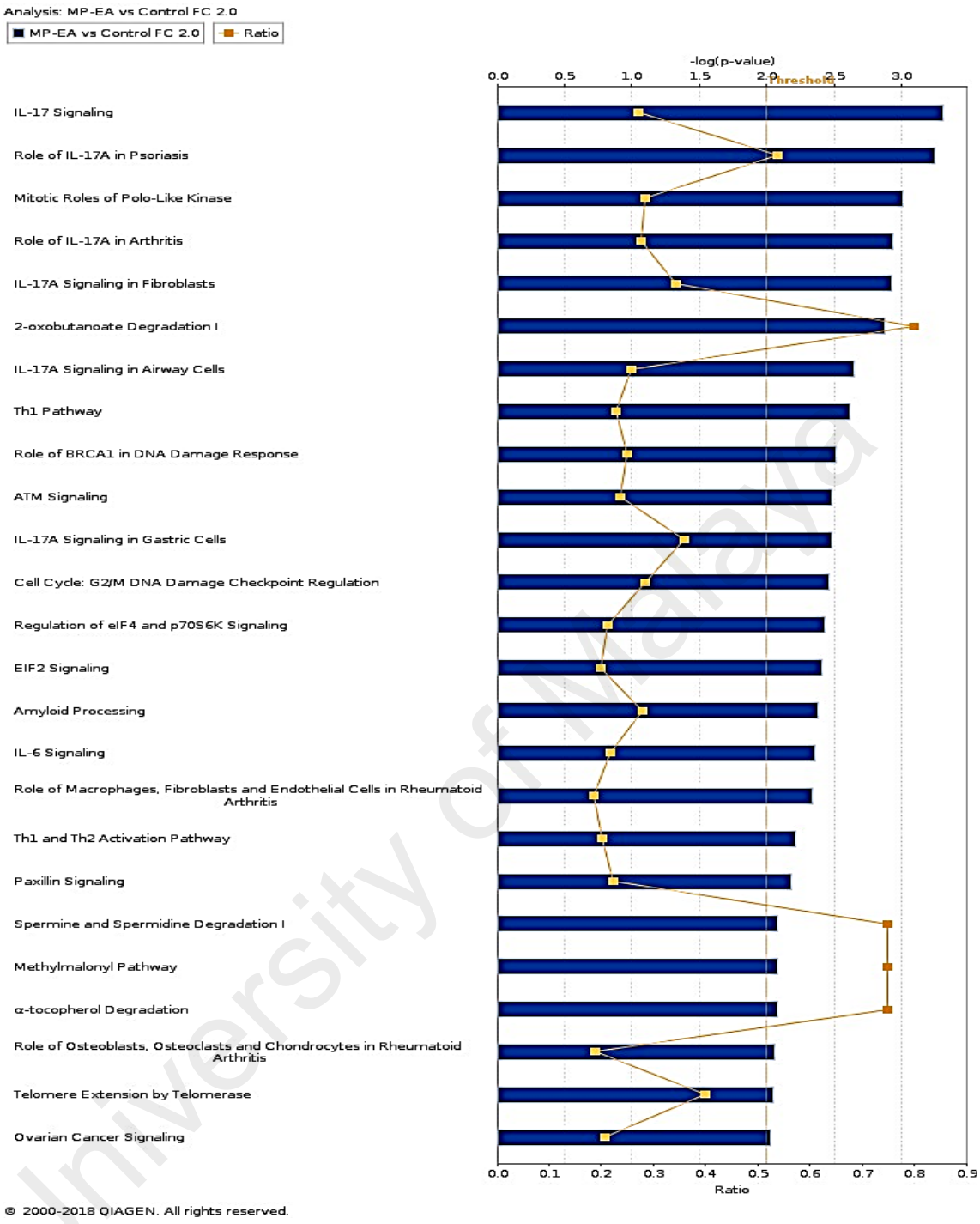

Figure 4.51: IPA analysis - top canonical pathways with -log (*p*-value) ≥ 2.0 in Hs27 cells treated with MP-EA. Ratio value denotes the number of molecules in the dataset divided by total number of molecules associated with the pathway.

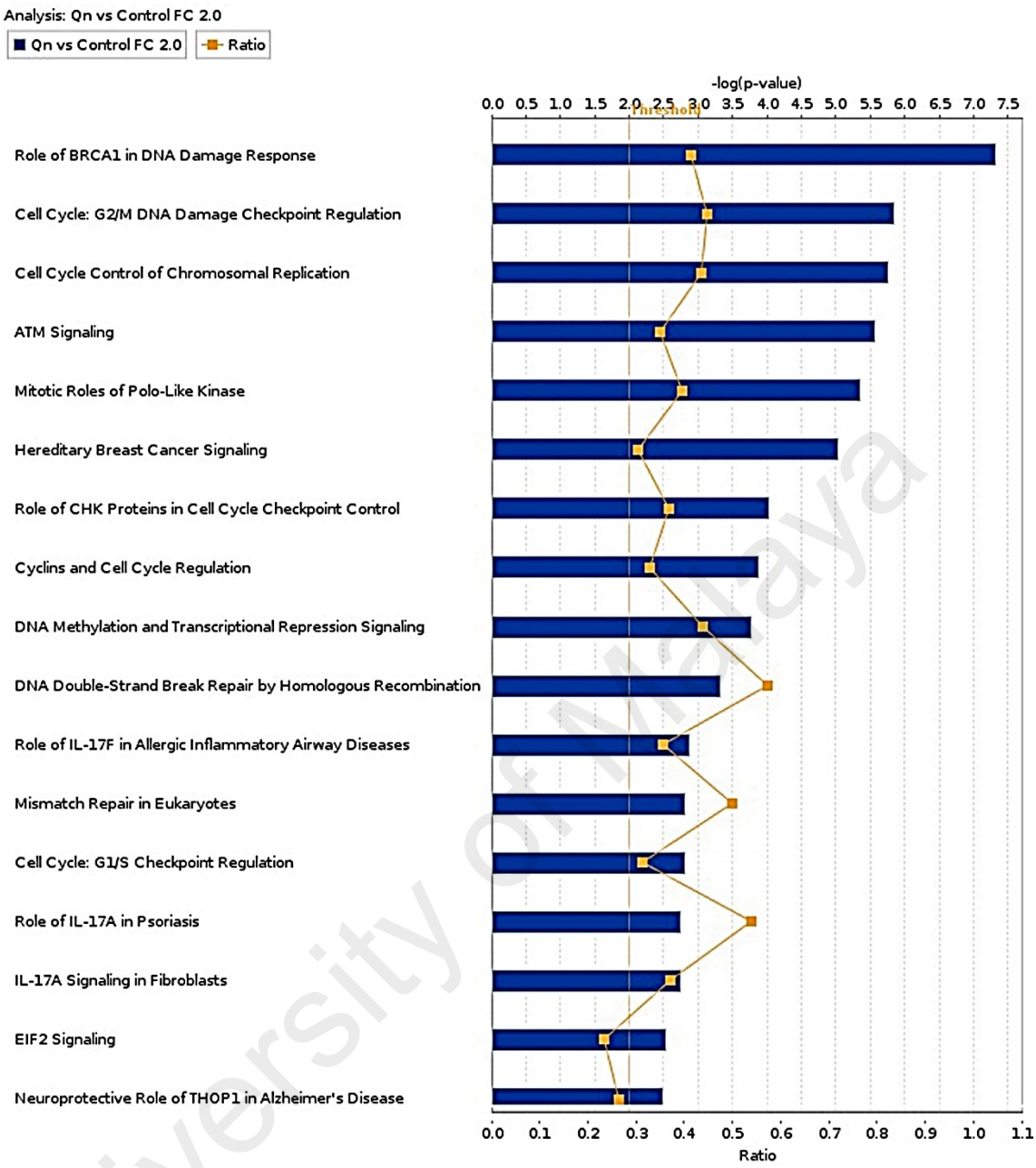

Figure 4.52: IPA analysis - top canonical pathways with -log (*p*-value) ≥ 2.5 in Hs27 cells treated with QN. Ratio value denotes the number of molecules in the dataset divided by total number of molecules associated with the pathway.

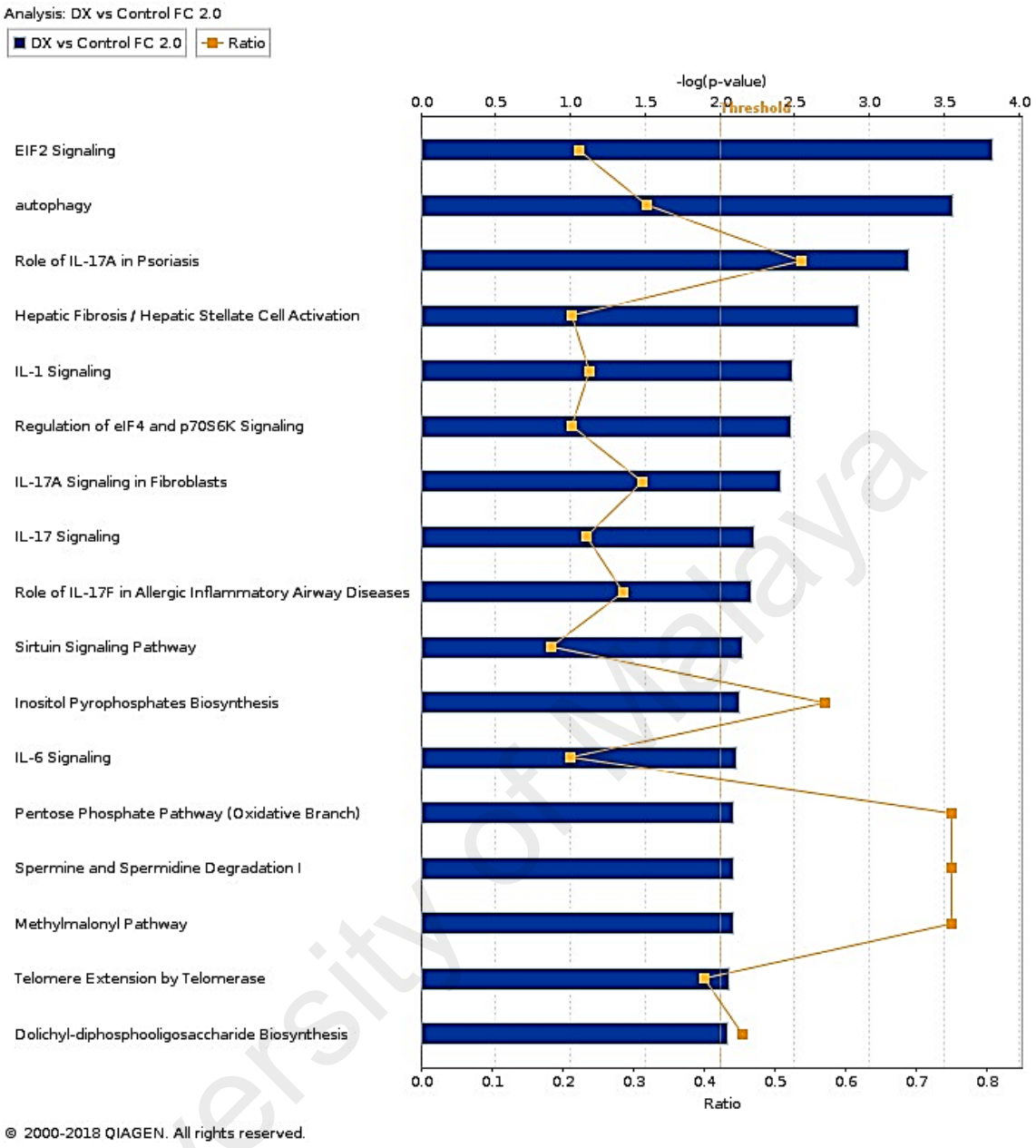

Figure 4.53: IPA analysis - top canonical pathways with -log (*p*-value) ≥ 2.0 in Hs27 cells treated with DX. Ratio value denotes the number of molecules in the dataset divided by total number of molecules associated with the pathway.

Table 4.18: Summary of selected top canonical pathways enriched in Hs27 cells after treatment with MP-HX, MP-EA, QN and DX. A number of selected representative genes involved in the canonical pathways are listed. *RG, representative genes; MA_FC, microarray gene expression fold change.

Pathway	-log (*p*-value)				RG	MA_FC			
	MP-HX	MP-EA	QN	DX		MP-HX	MP-EA	QN	DX
EIF2 signaling	4.91	2.41	2.54	3.83	EIF2S2	+3.40	+2.46	+2.60	+2.85
					EIF2AK1	+2.47	+1.65	+1.55	+1.66
					EIF2AK2	+1.97	+1.89	+1.83	+1.84
					EIF2AK3	+2.32	+1.27	+1.47	+1.09
					EIF2AK4	+1.88	+1.85	+2.01	+2.10
					ATF4	+2.22	+1.38	+1.92	+1.88
IL-17 signaling	0.87	3.31	1.65	2.23	IL17RA	+2.39	+2.46	+2.73	+2.98
					IL17RC	+4.01	+2.34	+2.71	+2.53
					TRAF3IP2	+1.95	+2.07	+2.12	+2.89
					NFKB2	+2.65	+1.78	+2.11	+2.30
					MAP2K6	+2.44	+3.16	+3.72	+3.66
					MAPK11	+1.43	+2.24	+1.96	+1.92
					MAPK13	+2.77	+2.28	+1.77	+1.79
					MAPK14	+2.10	+2.05	+2.29	+2.37
					IL6	+5.82	+5.81	+8.76	+7.06
					CXCL8	+3.54	+2.95	+6.49	+2.06
					IL19	+1.56	+2.81	+3.19	+2.43
					CCL2	+2.37	+2.89	+2.68	+2.75
					CCL11	+2.38	+10.69	+38.46	+4.82
					CXCL1	+12.42	+13.62	+16.43	14.54
					CXCL5	+3.27	+5.21	+11.04	+5.58
IL-17A Signaling in Fibroblasts	1.54	2.93	2.74	2.41	IL17RA	+2.39	+2.46	+2.73	+2.98
					IL17RC	+4.01	+2.34	+2.71	+2.53
					TRAF3IP2	+1.95	+2.07	+2.12	+2.89
					CCL2	+2.37	+2.89	+2.68	+2.75
					CEBPD	+3.01	+2.72	+2.81	+3.80
					IL6	+5.82	+5.81	+8.76	+7.06
					NFKB2	+2.65	+1.78	+2.11	+2.30

Table 4.18, continued

Pathway	-log (*p*-value)				RG	MA_FC			
	MP-HX	MP-EA	QN	DX		MP-HX	MP-EA	QN	DX
Mitotic roles of polo like kinase	1.46	3.01	5.34	1.21	SMC3	+2.00	+2.25	+2.35	+2.04
					PLK1	-1.03	+2.04	+5.21	+1.24
					PLK4	+1.21	+2.05	+4.60	+1.47
					FZR1	+2.05	+1.87	+1.85	+1.58
					ANAPC1	+2.48	+2.17	+2.42	+2.20
					ANAPC2	+2.28	+2.20	+2.11	+2.25
					ANAPC4	+2.60	+2.91	+3.07	+2.75
					ANAPC5	+2.16	+1.64	+1.78	+1.72
					CAPN1	-2.44	-1.87	-1.87	-1.84
					PKMYT1	-2.12	-1.57	-1.05	-1.68
					CDC16	+2.59	+1.84	+2.14	+2.05
Sirtuin signaling pathway	2.74	0.73	2.21	2.16	SIRT3	+2.04	+1.60	+1.87	+1.97
					PPARA	+2.12	+1.80	+2.73	+2.98
					GTF3C2	+3.46	+3.10	+3.24	+2.97
					NDUFB11	+2.13	+1.73	+2.06	+2.09
					ABCA1	+2.17	+3.42	+2.40	+2.60
					GABARAPL1	-2.92	-2.67	-2.16	-2.49
					GADD45B	-2.16	-1.81	-1.50	-1.78
					PARP1	+3.22	+2.51	+2.82	+2.27

(b) ***Diseases and functions modulated by MP-HX, MP-EA, QN and DX in Hs27 cells***

Among the top disease and functions (DFs) modulated by MP-HX include "Developmental disorder", "Inflammatory disease", "Inflammatory response", "Drug metabolism", "Organismal injury and abnormalities" and "Connective tissue disorder" (**Figure 4.54**). The top DFs most significantly regulated by MP-EA include "Cancer", "Organismal injury and abnormalities", "Gastrointestinal disease", "Dermatological disease and conditions" and "Inflammatory disease" (**Figure 4.55**). The top DFs affected by QN include "Cancer", "Organismal injury and abnormalities", "Cellular assembly and organization", "DNA replication", "Recombination and repair", and "Cell death and survival" (**Figure 4.56**). The top DFs modulated by DX include "Cancer", "Organismal injury and abnormalities", "Cellular development", "Cellular movement", "Dermatological disease and conditions", "Inflammatory disease" and "Cell growth and proliferation" (**Figure 4.57**). A list of diseases and functions that were either activated or inhibited by MP-HX and MP-EA are shown in **Table 4.19**. MP-HX activated "Proliferation of fibroblast cell lines", while it apparently inhibited "Senescence of cells". MP-EA activated "Repair of DNA", while it apparently inhibited "Apoptosis", "Necrosis", "Cell death". A list of DFs that were either activated or inhibited by QN and DX are shown in **Table 4.20**. QN and DX activated "Cell survival", "Cell viability", while they apparently inhibited "Cell death", "Necrosis", "Apoptosis".

Figure 4.54: Top category of diseases and functions with -log (*p*-value) ≥ 3.0 as reported by IPA in Hs27 cells treated with MP-HX.

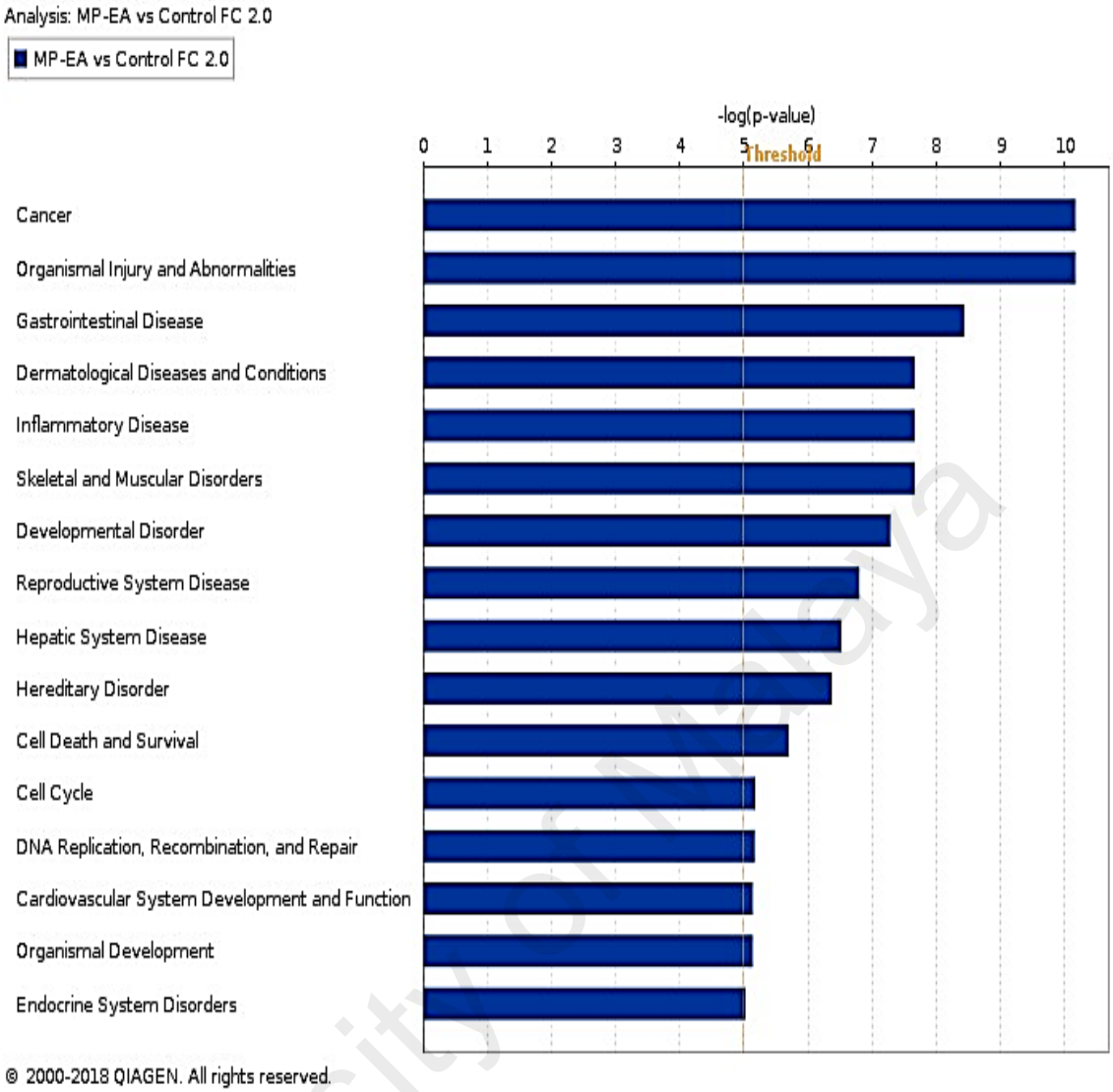

Figure 4.55: Top category of diseases and functions with -log (*p*-value) ≥ 5.0 as reported by IPA in Hs27 cells treated with MP-EA.

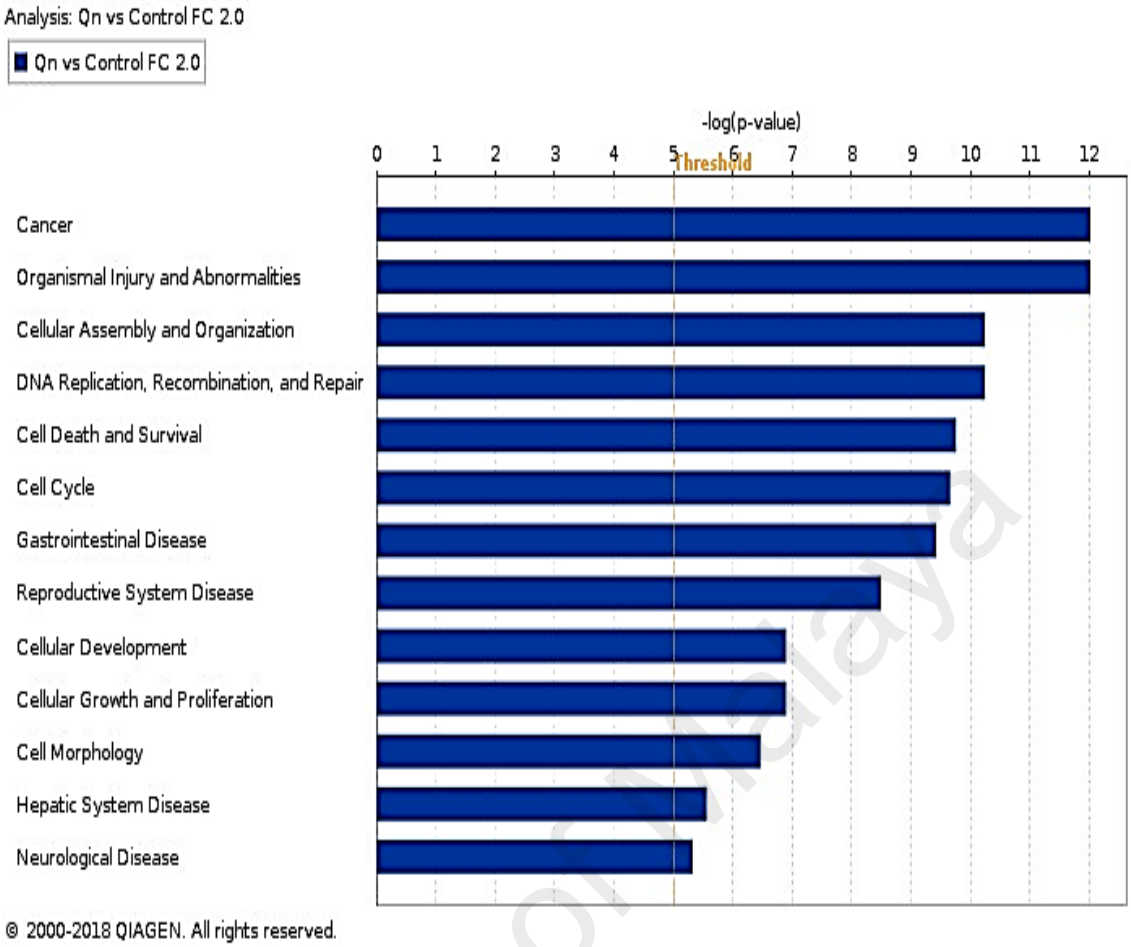

Figure 4.56: Top category of diseases and functions with -log (*p*-value) ≥ 5.0 as reported by IPA in Hs27 cells treated with QN.

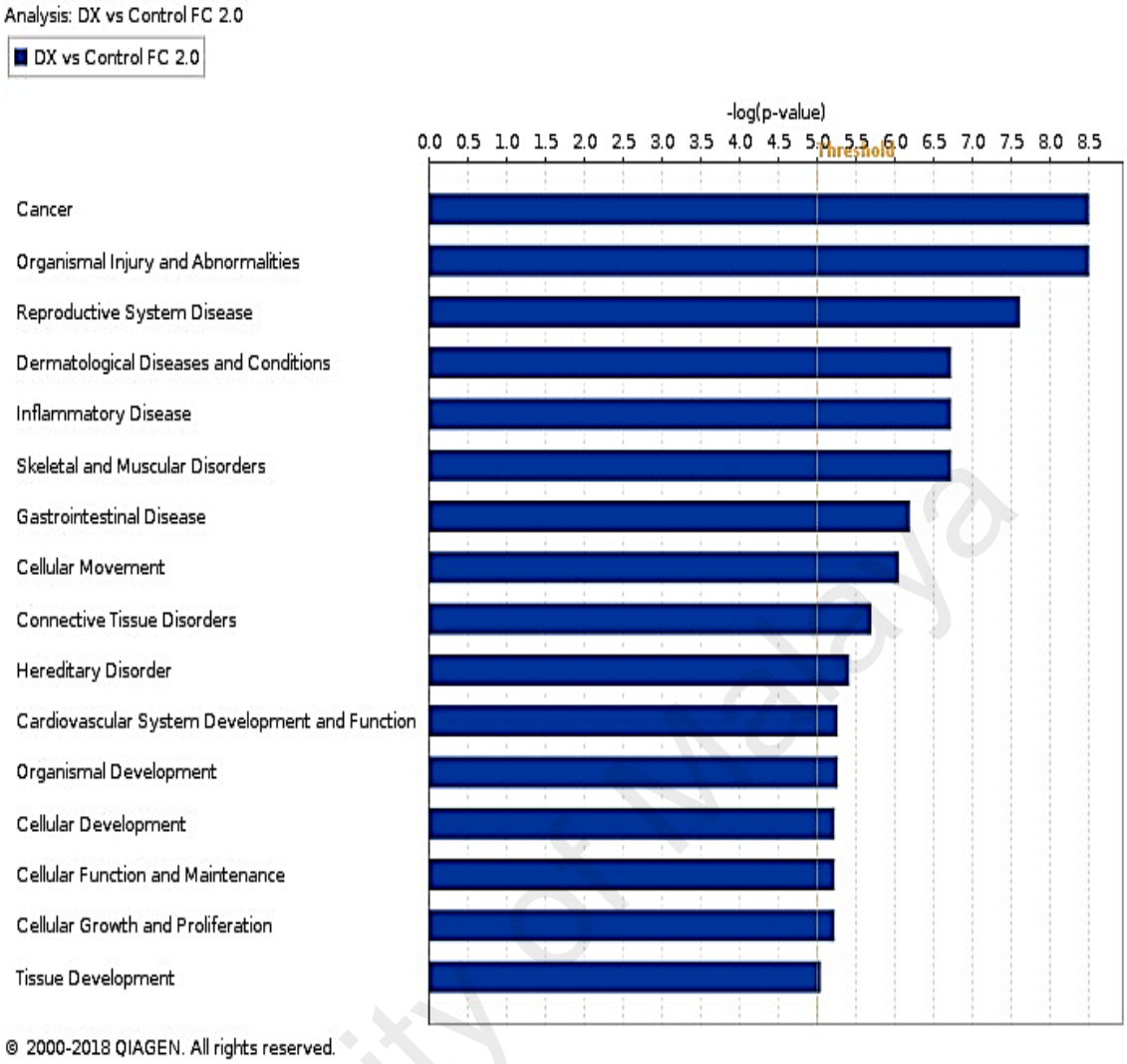

Figure 4.57: Top category of diseases and functions with -log (*p*-value) ≥ 5.0 as reported by IPA in Hs27 cells treated with DX.

Table 4.19: Diseases and functions modulated by MP-HX and MP-EA. The table shows the enriched terms corresponding to diseases or biological functions along with the number of associated genes in the experimental dataset, *p*-value and activation z-score. The z-score is calculated by the IPA software which predicts whether a specific disease or bio-function is increased (positive z-score) or decreased (negative z-score) based on the experimental dataset.

	Categories	**Diseases or biological functions**	***p*-value**	**z-score**	**# of genes in dataset**
MP-HX	Cell cycle; DNA Replication, Recombination, and Repair	Joining of DNA	1.19E-02	+2.60	7
	Cellular Development; Cellular Growth and Proliferation	Proliferation of fibroblast cell lines	4.00E-03	+2.17	24
	Cellular Growth and Proliferation	Stimulation of granulocytes	9.76E-03	+2.00	4
	Cellular Growth and Proliferation	Proliferation of bone marrow cell lines	1.76E-02	+1.98	5
	DNA Replication, Recombination, and Repair	DNA recombination	3.04E-02	+1.80	25
	DNA Replication, Recombination, and Repair	Chromosomal instability	3.28E-02	-1.75	7
	Cell Death and Survival	Apoptosis of gonadal cells	6.48E-03	-1.44	8
	Cell Cycle	Senescence of cells	2.34E-03	-1.43	56
MP-EA	DNA Replication, Recombination, and Repair	Repair of DNA	6.64E-03	+4.07	35
	Cellular Assembly and Organization	Association of chromatin	1.68E-03	+2.57	7
	Cellular Movement	Cell movement	1.88E-04	+2.50	271
	Cellular Growth and Proliferation	Stimulation of myeloid cells	5.62E-03	+2.24	5
	Cellular Growth and Proliferation	Stimulation of granulocytes	3.62E-03	+2.00	4
	Cellular Movement	Migration of cells	2.54E-03	+1.95	232
	Cell Cycle	M phase	1.16E-03	+1.86	32
	Cellular Growth and Proliferation	Cell proliferation of vascular endothelial cells	1.01E-03	+1.53	29
	Cell Death and Survival	Necrosis	1.57E-05	-2.73	398
	Cell Death and Survival	Apoptosis	1.13E-05	-2.42	336
	Cell Death and Survival	Cell death	1.97E-06	-2.05	446

Table 4.20. Diseases and functions modulated by QN and DX. The table shows the enriched terms corresponding to diseases or biological functions along with the number of associated genes in the experimental dataset, *p*-value and activation z-score. The z-score is calculated by the IPA software which predicts whether a specific disease or bio-function is increased (positive z-score) or decreased (negative z-score) based on the experimental dataset.

	Categories	**Diseases or biological functions**	***p*-value**	**z-score**	**# of genes in dataset**
QN	Cell Death and Survival	Cell survival	3.66E-07	+7.02	289
	Cell Death and Survival	Cell viability	1.56E-07	+6.81	281
	DNA Replication, Recombination, and Repair	Repair of DNA	5.16E-06	+4.62	51
	Cell Death and Survival	Cell viability of myeloma cell lines	2.66E-03	+4.10	28
	Tissue Development	Growth of epithelial tissue	3.21E-04	+2.36	68
	Cell Morphology; Cellular Function and Maintenance	Repair of cells	1.66E-04	+2.33	26
	Cell Death and Survival	Cell death	1.83E-09	-2.89	550
	Cell Death and Survival	Necrosis	1.65E-09	-2.84	501
	Cell Death and Survival	Apoptosis	1.93E-09	-2.41	423
	DNA Replication, Recombination, and Repair	DNA damage	1.13E-05	-1.89	45
DX	Cell Death and Survival	Cell viability	2.46E-03	+5.09	210
	Cell Death and Survival	Cell survival	5.13E-03	+4.92	215
	Cellular Movement	Cell movement	1.03E-05	+4.22	279
	Cellular Movement	Migration of cells	3.35E-05	+3.59	246
	Cellular Movement	Chemotaxis	1.57E-02	+2.96	57
	Cellular Development, Cellular Growth and Proliferation,	Cell proliferation of vascular endothelial cells	3.91E-03	+2.00	27
	Cell Death and Survival	Cell death	1.97E-06	-2.06	446
	Cell Death and Survival	Necrosis	8.04E-05	-2.10	389
	Cell Death and Survival	Apoptosis	2.53E-05	-1.87	331
	Cancer, Organismal Injury and Abnormalities	Neoplasia of epithelial tissue	6.95E-08	-1.56	490

(c) ***Upstream regulators prediction in Hs27 cells***

The upstream regulators (URs) were predicted by IPA based on the list of DEGs submitted for the analysis, and IPA ranked the URs according to their activation z-score. A positive z-score indicates activation while negative z-score specifies inhibition of the regulators.

The top upstream regulators predicted by IPA were ERBB2, TNF, IL17A, IL1B, EGFR, TGFB1 and PDGF BB were all activated while NUPR1 was inhibited in MP-HX, MP-EA, QN and DX dataset. **Figure 4.58** shows the comparison of upstream regulators among MP-HX, MP-EA, QN and DX. Orange color indicates activation while blue color indicates inhibition of the regulators. The top upstream regulators that were either activated or inhibited in the datasets are also summarized in **Table 4.21**.

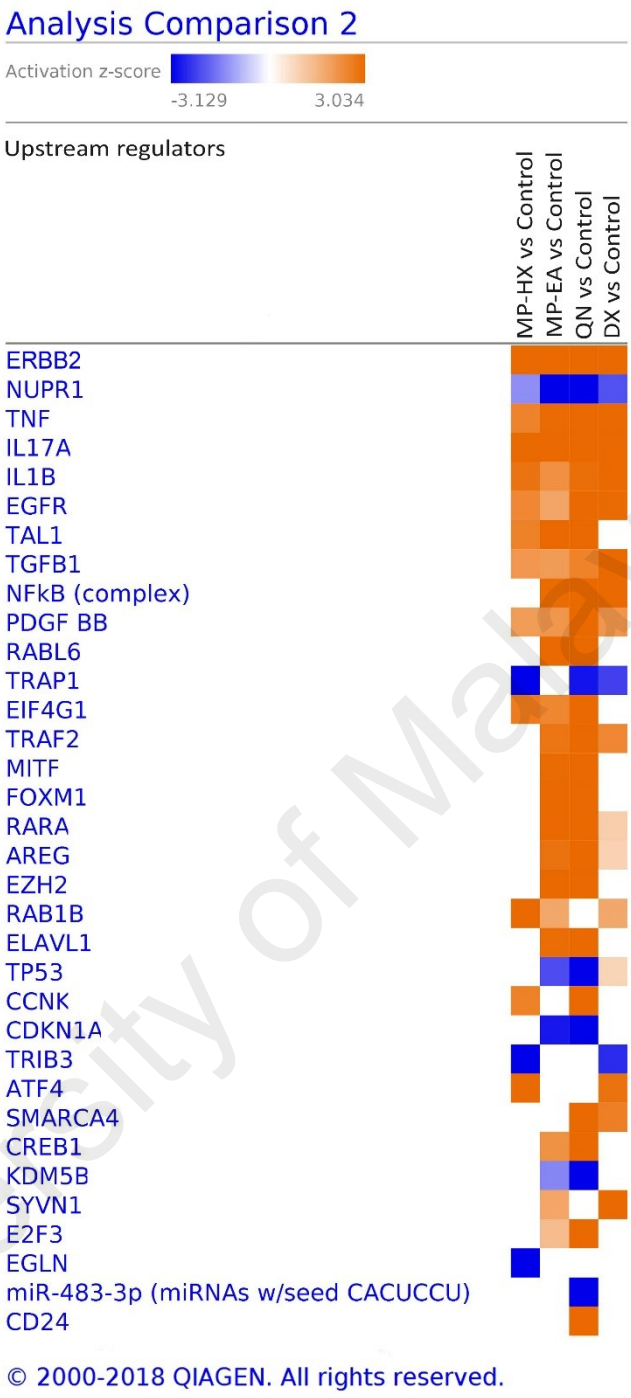

Figure 4.58: Prediction of upstream regulators and their activation z-score in Hs27 cells treated with MP-HX, MP-EA, QN and DX. The heatmap color intensity depicts relative value of activation z-score for the corresponding cell lines. Upstream regulators were filtered based on -log (*p*-value) of 1.30 and activation z-score of 3.0. Orange color indicates activation whereas blue color indicates inhibition.

Table 4.21: IPA analyses - top 5 upstream regulators ranked by activation z-score. The overlap *p*-value is a statistical measure to determine the statistical significance of overlap between the dataset genes and the genes that are regulated by a regulator molecule. *UR, upstream regulator; MA_FC, fold change based on microarray data.

Treatment	Activation/ inhibition	UR	MA_FC	z-score	Overlap (*p*-value)
MP-HX	Activated	ERBB2	-1.04	+3.56	1.96E-02
		RAB1B	+3.45	+3.33	1.05E-04
		IL17A	-1.12	+3.01	1.05E-02
		ATF4	+2.22	+3.01	4.07E-06
		EIF4G1	-1.07	+2.65	4.44E-02
	Inhibited	EGLN (complex)		-3.68	4.10E-03
		TRAP1	+2.76	-3.32	1.92E-02
		TRIB3	+2.35	-3.27	2.82E-06
		SPI1	-1.24	-2.60	1.65E-02
		BMP7	-1.47	-2.42	2.58E-02
MP-EA	Activated	ERBB2	-1.05	+4.40	4.98E-07
		RABL6	+1.32	+3.94	4.39E-06
		TAL1	-1.55	+3.71	1.89E-02
		FOXM1	+1.61	+3.02	1.36E-04
		IL17A	+1.14	+2.71	5.54E-05
	Inhibited	NUPR1	-1.27	-5.33	6.66E-08
		CDKN1A	-1.03	-2.84	1.35E-04
		HSF1	+1.1	-2.66	7.73E-04
		HCAR2	-1.52	-2.65	2.94E-04
		RBPJ	-2.07	-2.65	3.62E-02
QN	Activated	ERBB2	-1.06	+6.53	8.94E-18
		RABL6	+1.34	+5.49	8.92E-17
		MITF	+1.16	+5.37	2.39E-09
		FOXM1	+4.03	+4.69	2.16E-10
		TAL1	-1.26	+4.42	2.90E-02
	Inhibited	NUPR1	-1.11	-6.79	2.17E-19
		KDM5B	+1.49	-3.37	1.24E-06
		TP53	+2.38	-3.12	1.71E-11
		CDKN1A	-1.05	-3.09	5.12E-07
		TRAP1	+1.91	-2.89	3.39E-03
DX	Activated	ERBB2	+1.09	+3.86	1.90E-03
		TNF	-1.43	+3.81	1.20E-05
		TGFB1	+1.89	+3.78	6.30E-05
		NFkB (complex)		+3.39	3.81E-03
		IL1B	+1.96	+3.31	8.20E-05
	Inhibited	RBPJ	-2.18	-2.83	3.58E-02
		TRIB3	+1.37	-2.60	1.65E-03
		WISP2	+1.07	-2.36	4.64E-02
		TRAP1	+1.43	-2.33	2.32E-02
		COL18A1	+1.30	-2.17	4.07E-02

ERBB2 was the top upstream regulator that was activated in all of the treatment conditions. EGLN was another top upstream regulator inhibited by MP-HX. NUPR1 was the top upstream regulator inhibited by MP-EA and QN. The top upstream regulator inhibited in DX dataset was RBPJ.

(d) ***Networks enriched in Hs27 by MP-HX, MP-EA, QN and DX treatments***

The IPA network analysis evaluated the possible interactions among the DEGs in MP-HX, MP-EA, QN and DX dataset. IPA analysis connected the key genes and categorized them according to enriched disease and functions. Networks were ranked based on network score (NS) which is calculated by Fisher's exact test. The analysis result revealed that "Cell cycle", "Cellular growth and proliferation", "Cell death and survival", and "Cellular development" were the functions linked with many genes in the networks for MP-HX, MP-EA, QN and DX datasets. The top networks and their associated functions are shown in **Table 4.22**.

Table 4.22: Top networks enriched by IPA in Hs27 cells treated with MP-HX, MP-EA, QN and DX. *NI, network ID; FM, focus molecules.

Treatment	NI	Score	# of FM	Functions
MP-HX	1	72	120	Cellular Compromise, Cellular Function and Maintenance, Cell Death and Survival
	2	68	117	Cellular Movement, Cancer, Organismal Injury and Abnormalities
	3	68	117	Cell-To-Cell Signaling and Interaction, Cellular Assembly and Organization, Cancer
	4	54	107	Gene Expression, Cell Cycle, DNA Replication, Recombination, and Repair
	5	44	98	Cell Death and Survival, Cardiovascular System Development and Function, Organismal Development
MP-EA	1	103	130	Cancer, Gastrointestinal Disease, Organismal Injury and Abnormalities
	2	77	115	Cell Cycle, DNA Replication, Recombination, and Repair, Cell Death and Survival
	3	63	105	Cellular Movement, Cardiovascular Disease, Organismal Injury and Abnormalities
	4	45	90	Cellular Movement, Immune Cell Trafficking, Inflammatory Response
	5	37	82	Cancer, Organismal Injury and Abnormalities, Cell Death and Survival
QN	1	81	124	Cell Cycle, DNA Replication, Recombination, and Repair, Cellular Assembly and Organization
	2	76	121	Cardiovascular System Development and Function, Cellular Movement, Cell-To-Cell Signaling and Interaction
	3	71	118	Cellular Development, Cellular Growth and Proliferation, Hematological System Development and Function
	4	69	116	Cell Death and Survival, Cell Cycle, DNA Replication, Recombination, and Repair
	5	62	111	Cellular Development, Cellular Growth and Proliferation, Cell Cycle
DX	1	84	120	Post-Translational Modification, Protein Degradation, Protein Synthesis
	2	80	117	RNA Post-Transcriptional Modification, Gene Expression, Cellular Movement
	3	57	101	Cell Cycle, Cellular Development, Cellular Growth and Proliferation
	4	57	101	Cellular Development, Cellular Growth and Proliferation, Embryonic Development
	5	51	96	Cellular Function and Maintenance, Molecular Transport, Small Molecule Biochemistry

The first ranked network in MP-HX dataset (NS=72) is associated with the following functions: “Cellular Compromise”, “Cellular Function and Maintenance”, “Cell Death and Survival”. This network contains 120 focus molecules, including IFNGR1, NFE2L3, CCL8, IRF1, NFKB2, ATP5D, IL24, HSPA9, ATF4, EIF2AK3, NDUFAB1, NDUFB11, CEBPD, LPIN2, UBA52, TRAP1 and SYVN1 (**Figure 4.59**).

The forth ranked gene network (NS=45) in MP-EA dataset is associated with the following functions: “Cellular movement”, “Immune cell trafficking” and “Inflammatory response”. This network has a total of 90 focus molecules, including PDGFRA, CCL11, PDCD4, RPL23A, ACTA2, COL1A1, CDC42, PLAU, PI3K, VEGF, CD44, IKBKE, STAT6, HMOX1, CXCL1, IL1RN, CXCL8, CCL2, HGF, IL24, IRF1, CCL8, IL1R1, CXCL6 and IL10RB (**Figure 4.60**).

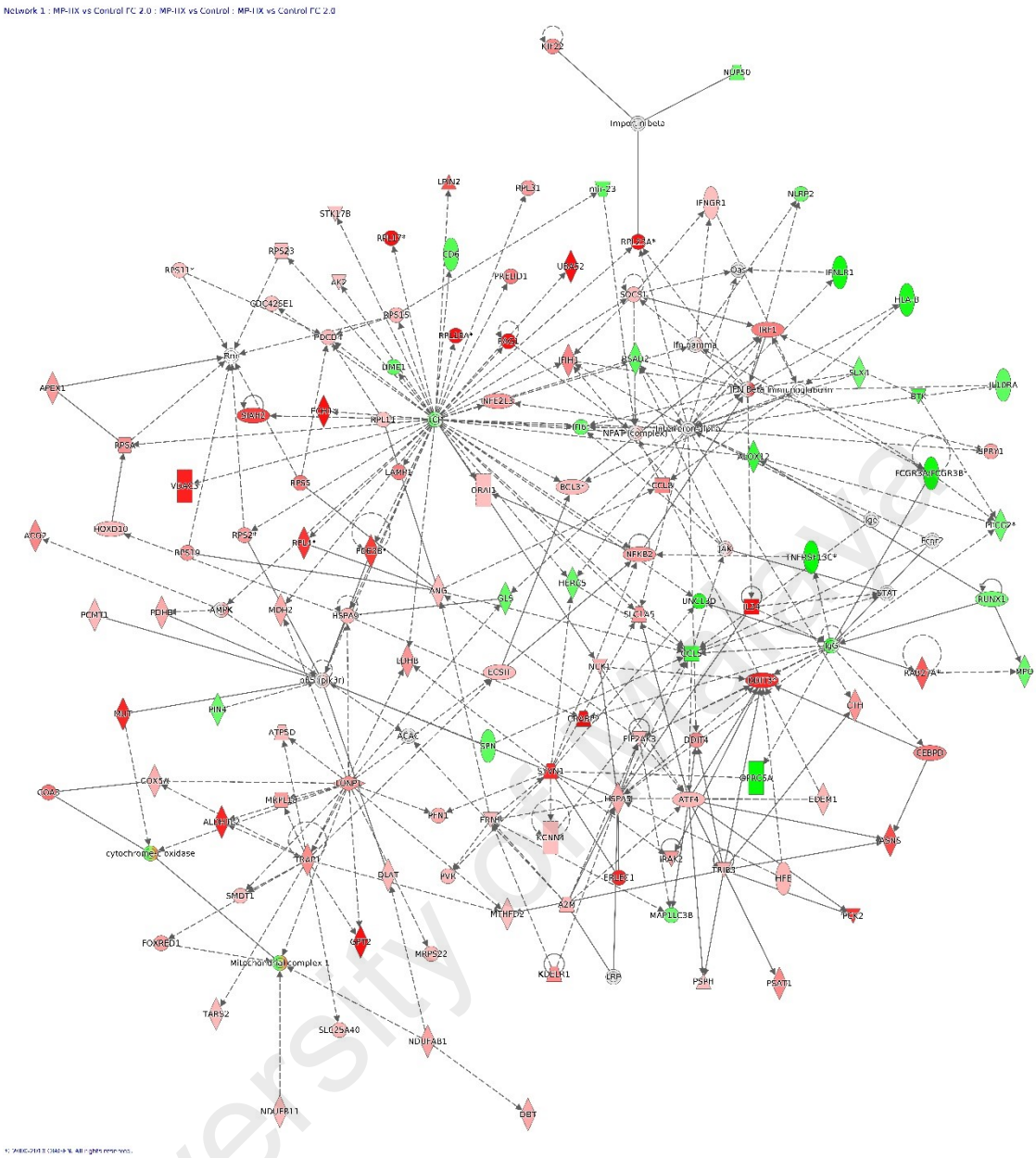

Figure 4.59: IPA network analysis: annotated interactions between genes in Hs27 cells treated with MP-HX. The figure shows network 1 and depicted interactions of 120 focus molecules. Molecules in the network are colored red (MA_FC ≥ +2.0), or green (MA_FC ≥ -2.0), or grey (MA_FC < ±2.0).

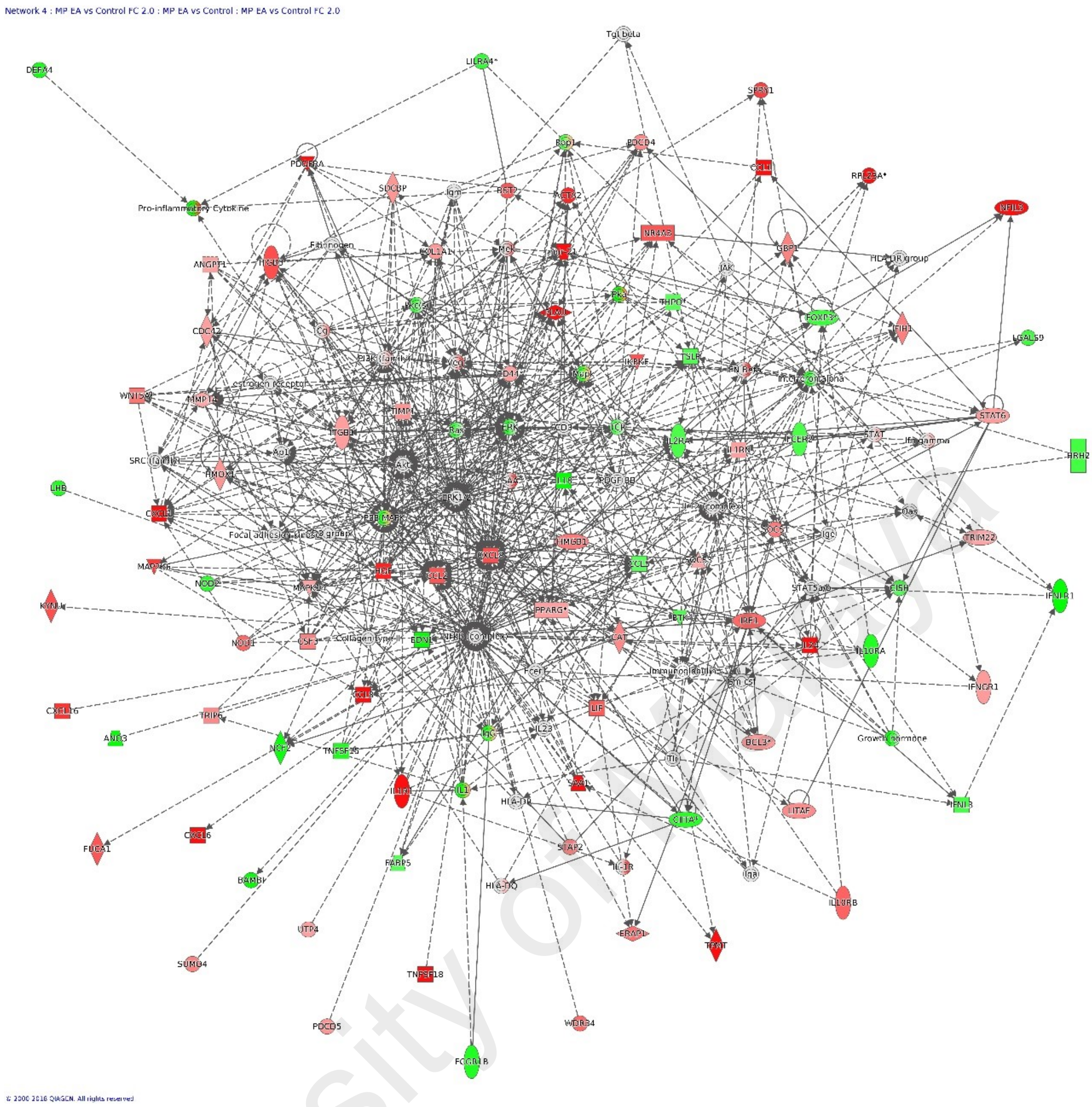

Figure 4.60: IPA network analysis: annotated interactions between genes in Hs27 cells treated with MP-EA. The figure shows network 4 and depicted interactions of 90 focus molecules. Molecules in the network are colored red (MA_FC ≥ +2.0), or green (MA_FC ≥ -2.0), or grey (MA_FC < ±2).

The third ranked gene network in QN dataset (network score: 71) is associated with the following functions: "Cellular development", "Cellular growth and proliferation", and "Hematological system development and function". This network has 118 focus molecules including CYFIP2, PSIP1, CDK16, TK1, SMARCD1, PLS3, MT1L, PRKX, MAP3K5, STAT6, SOCS1, PAG1, CCL11, IL13RA2, JPT1, LIMA1, MYL1 and others (**Figure 4.61**).

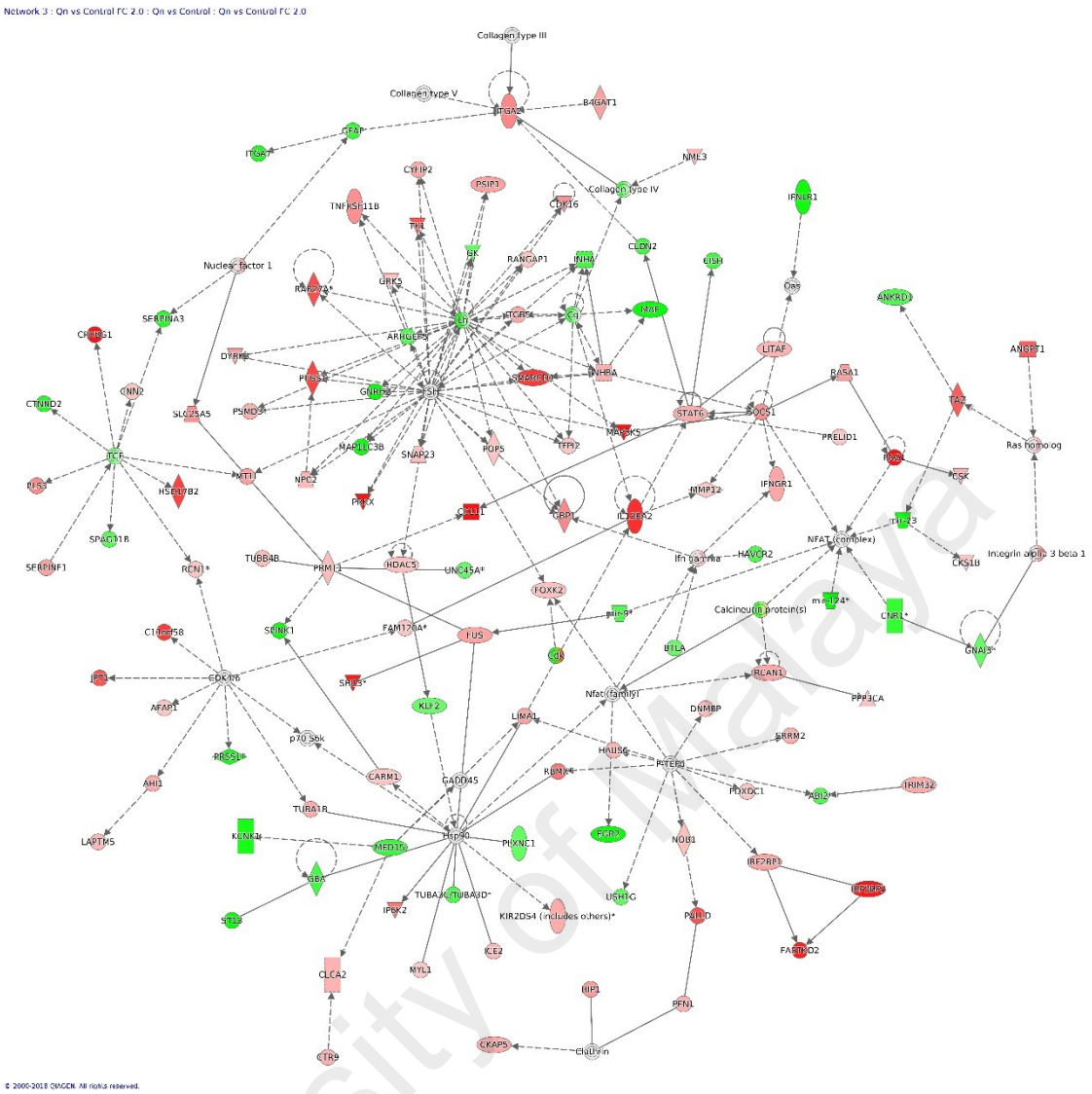

Figure 4.61: IPA network analysis: annotated interactions between genes in Hs27 cells treated with QN. The figure shows network 3 and depicted interactions of 118 focus molecules. Molecules in the network are colored red (MA_FC ≥ +2.0), or green (MA_FC ≥ -2.0), or grey (MA_FC < ±2).

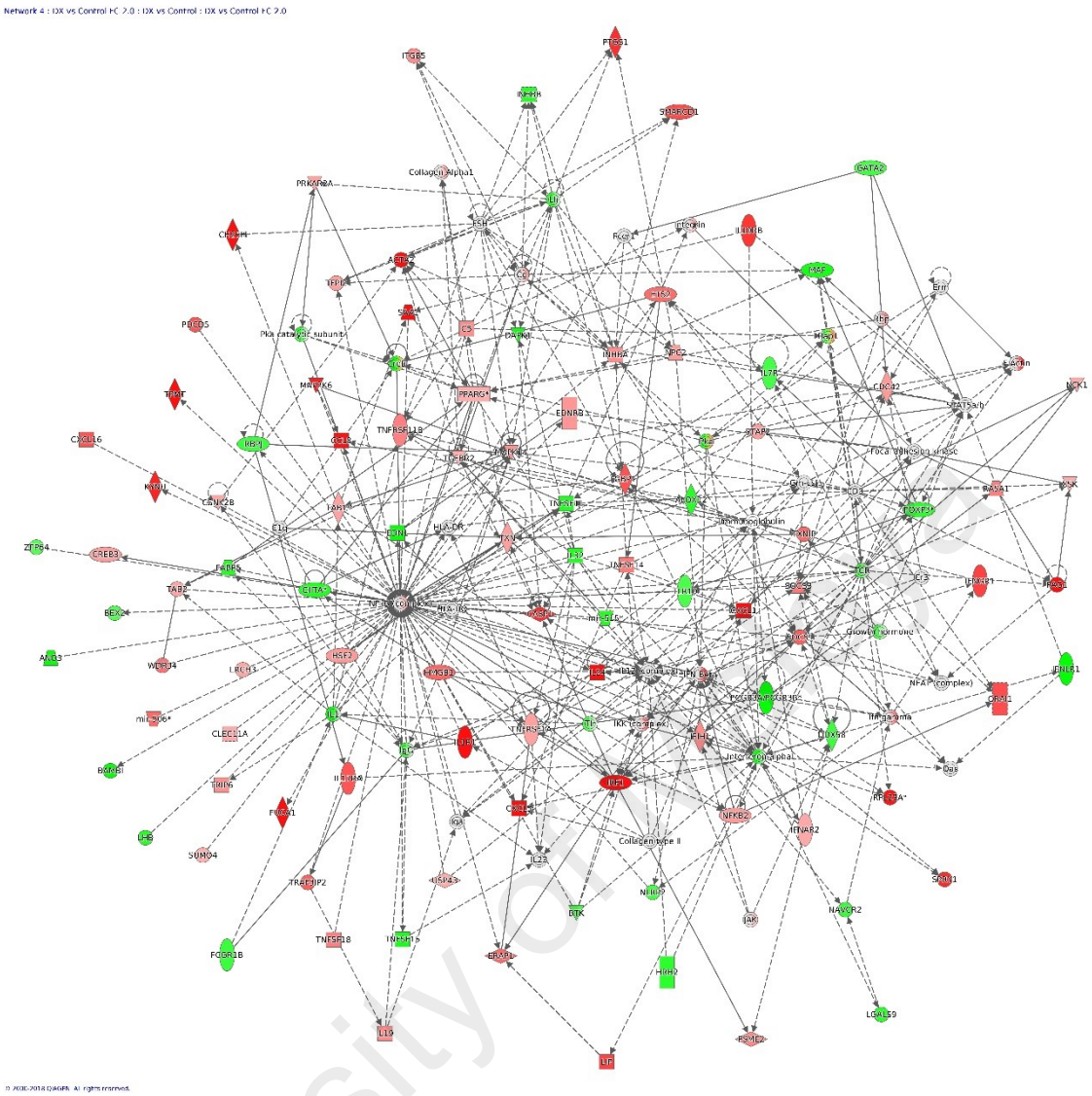

Figure 4.62: IPA network analysis: annotated interactions between genes in Hs27 cells treated with DX. The figure shows network 4 and depicted interactions of 101 focus molecules. Molecules in the network are colored red (MA_FC ≥ +2.0), or green (MA_FC ≥ -2.0), or grey (MA_FC < ±2).

The network that was ranked number 4 (NS=57) in DX dataset is associated with the following DFs: "Cellular development", "Cellular growth and proliferation" and "Embryonic development". This network has 101 focus molecules, including ITGB5, SMARCD1, IL10RB, ACTA2, PDCD5, ETS2, NPC2, MAP2K6, CCL8, CXCL16, TGFBR2, CDC42, TXN, TAB1, IL24, IL1R1, IRF1, CXCL5, NFKB2, SUMO4 and others are connected to this gene network (**Figure 4.62**).

4.6 Protective effect of *Melicope ptelefolia* from cadmium-induced cytotoxicity in Hs27 cells

4.6.1 Cytotoxicity of $CdCl_2$ in Hs27 cells

Cytotoxicity of $CdCl_2$ on Hs27 cells were assessed by MTT cell viability assay. $CdCl_2$ was noted to reduce the percentage of cell viability in a dose dependent manner (**Figure 4.63)**. At the highest dose (200 µM), $CdCl_2$ exerted pronounced cytotoxicity on Hs27 cells, reducing the percentage of viable cells to 5.03 ± 0.76%. Based on the dose-response curve, the IC_{50} value of $CdCl_2$ in Hs27 was 30.41 ± 1.32 µM.

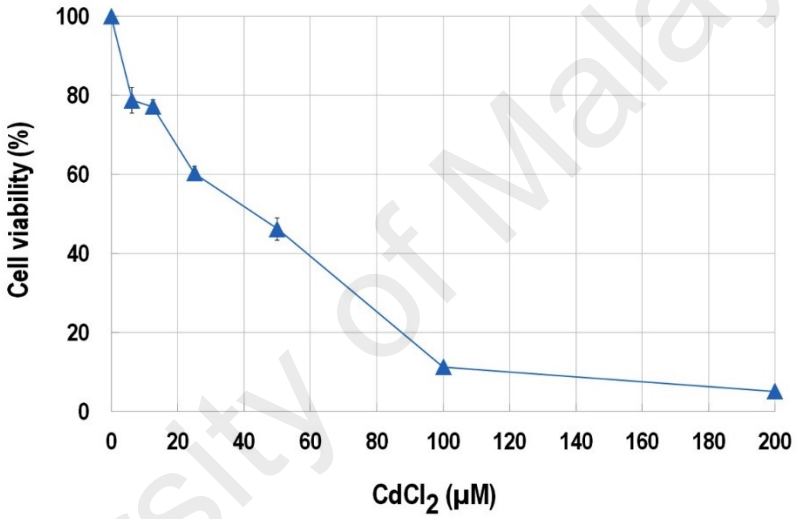

Figure 4.63: Cytotoxicity of $CdCl_2$ in Hs27 cells. Values are mean ± SD (n=3).

4.6.2 Protective effects of MP-HX and MP-EA against $CdCl_2$ -induced cytotoxicity in Hs27 cells

The MTT cell viability assay was used to evaluate the protective effect of MP-HX and MP-EA against $CdCl_2$-induced cytotoxicity in Hs27 cells. The cells were pretreated with MP-HX or MP-EA at various concentrations (60, 30, 15 and 0 µg/mL), prior to exposure with ~IC_{50} concentration of $CdCl_2$, which was at 30 µM. MP-HX pretreatment significantly reduced the cytotoxic effect of $CdCl_2$ (**Figure 4.64A**). The percentage of cell viability was increased from 64.02 ± 2.38% to 88.14 ± 2.32% and 99.91 ± 1.40% with 30 and 15 µg/mL of MP-HX pretreatment, respectively. A similar activity was

observed for MP-EA pretreatment (**Figure 4.64B**). In the presence of $CdCl_2$, the percentage of viable Hs27 cells was 64.02±2.38%, and this value increased to 86.82 ± 1.62 and 103.66 ± 1.41% after the cells were pretreated with 30 and 15 µg/mL of MP-EA, respectively. At 60 µg/mL, MP-HX did not protect Hs27 cells from $CdCl_2$-induced cytotoxicity. At this concentration, pretreatment with MP-HX resulted a reduction in percentage of cell viability to 51.96 ± 3.97%. On the other hand, MP-EA pretreatment at 60 µg/mL with and without $CdCl_2$ did not differ much, and the viability was around 94%. It is likely that at higher concentration of 60 µg/mL, MP-HX induced significant oxidative stress and this contributed to its failure in counteracting $CdCl_2$-induced cytotoxic effect. These results suggest that at low concentration of 15 µg/mL, MP-HX and MP-EA exerted cytoprotective effect on Hs27 cells from $CdCl_2$-induced cytotoxicity.

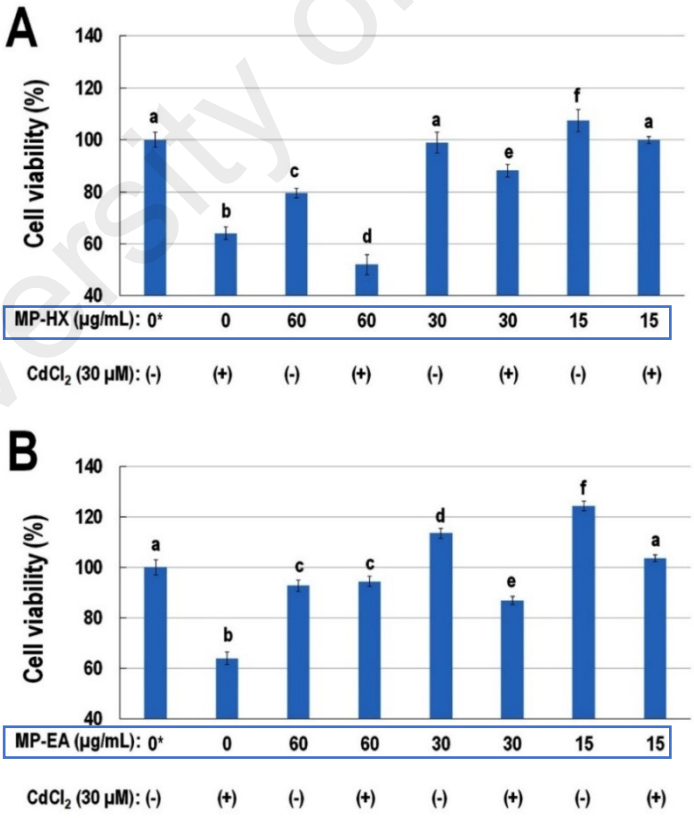

Figure 4.64: Protective effects of MP-HX and MP-EA from $CdCl_2$-induced cytotoxicity. Values are mean ± SD (n = 3). Mean values with different letters (a-f) are significantly different ($p < 0.05$). * denotes control set, without $CdCl_2$ or MP extracts.

4.6.3 Microarray data validation by RT-qPCR

The microarray gene expression data was validated through RT-qPCR assay. A total of 16 genes related to cell proliferation, apoptosis, DNA replication, DNA damage, DNA repair and stress response were selected for the analysis. Based on microarray data, eight of those genes were upregulated (DDIT3, GADD45A, JUN, FOS, PMAIP1, MYC, CDKN1C, HSPB2) and eight were downregulated (HIRA, MDM2, PCNA, RRM2B, NFKB1, PRKDC, RMI1, ARAF) by $CdCl_2$ treatment. The RT-qPCR data was normalized using RPS29 as the reference gene. The result is summarized in **Table 4.23** and **Figure 4.65**. The result indicates that the direction of gene expression (up or downregulation) obtained through RT-qPCR assay agreed with that of the microarray data.

Table 4.23: Gene expression fold change induced by $CdCl_2$, MP-HX+$CdCl_2$ and MP-EA+$CdCl_2$ in Hs27 cells. A comparison between microarray and RT-qPCR fold change values. A positive value indicates upregulation, while negative value indicates downregulation. Values are mean ± SD for RT-qPCR fold change (n=3). Mean values with asterisks (*) were significantly different from the control (p <0.05). *MA_FC, fold change based on microarray data; RT-qPCR_FC, fold change based on real-time qPCR data.

Gene	$CdCl_2$		MP-HX+$CdCl_2$		MP-EA+$CdCl_2$	
	MA_FC	RT-qPCR_FC	MA_FC	RT-qPCR_FC	MA_FC	RT-qPCR_FC
GADD45A	+2.84	+7.20±1.21*	+1.23	+2.43±0.11*	+2.30	+2.68±0.14*
DDIT3	+7.52	+7.86±1.23*	+2.88	+4.05±0.20*	+4.48	+3.78±0.21*
JUN	+5.38	+6.11±0.83*	+1.74	+1.96±0.07*	+2.67	+2.17±0.08*
FOS	+5.48	+35.17±4.00*	+1.87	+7.65±0.56*	+2.86	+6.92±0.52*
PMAIP1	+7.46	+7.91±0.49*	+1.69	+2.55±0.16*	+3.45	+3.49±0.11*
MYC	+2.05	+2.81±0.09*	-1.36	-1.20±0.04*	+1.21	+1.19±0.09*
CDKN1C	+7.38	+31.16±1.94*	+1.81	+6.49±0.09*	+3.85	+11.57±0.20*
HSPB2	+2.11	+2.36±0.19*	+1.07	+1.02±0.03	+1.24	+1.15±0.02*
HIRA	-3.61	-3.97±0.28*	+1.27	+1.13±0.22	-1.13	-1.11±0.07
MDM2	-3.61	-7.09±0.27*	+1.06	+1.17±0.02*	-1.66	-2.32±0.12*
PCNA	-2.17	-4.34±0.38*	-1.41	-1.22±0.02*	-1.40	-1.49±0.01*
RRM2B	-1.74	-3.07±0.21*	+1.66	+1.15±0.06*	-1.13	-1.53±0.04*
NFKB1	-3.42	-6.02±0.19*	-2.32	-1.48±0.09*	-2.77	-2.14±0.11*
PRKDC	-2.01	-3.64±0.30*	-1.06	-1.16±0.04*	-1.26	-1.51±0.05*
RMI1	-3.68	-2.95±0.36*	-2.48	-1.91±0.04*	-2.75	-2.12±0.10*
ARAF	-2.38	-2.78±0.21*	-1.25	-1.25±0.08*	-1.85	-1.47±0.09*

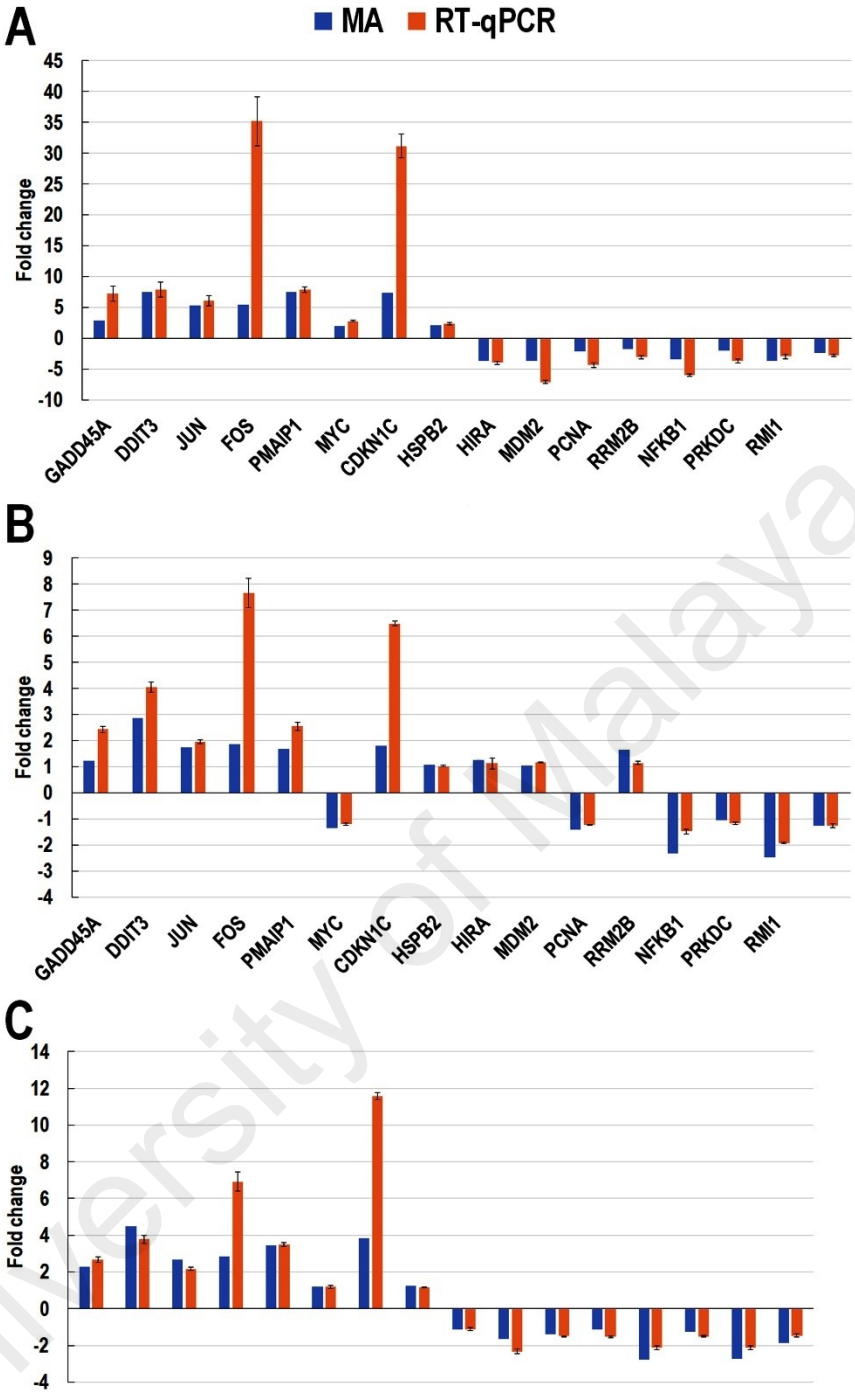

Figure 4.65: RT-qPCR validation of microarray data in Hs27 cells upon treatment with $CdCl_2$, MP-HX+$CdCl_2$ and MP-EA+$CdCl_2$. The bar chart shows gene expression fold change induced by A) $CdCl_2$, B) MP-HX+$CdCl_2$ and C) MP-EA+$CdCl_2$ that was obtained from microarray and RT-qPCR assays. For each RT-qPCR assay, the data was normalized to RPS29 expression and the values represent mean RT-qPCR_FC ± SD (n=3).

4.6.4 Microarray analysis

4.6.4.1 Analysis of microarray data using Transcriptome Analysis Console (TAC)

Using a cut-off fold change (FC) value of ±1.50 to filter the list of differentially expressed genes (DEGs), 10,594 genes were noted to be differentially regulated by $CdCl_2$ treatment. Among these, 3,914 (36.97%) genes were upregulated while 6,680 (63.03%) genes were downregulated (**Figure 4.66**). At a cut off FC value of ±1.50, TAC revealed differential expression of 10,127 and 9,407 genes in MP-HX+$CdCl_2$ and MP-EA+$CdCl_2$ datasets, respectively (**Figure 4.66**). For MP-HX+$CdCl_2$ dataset, 3,762 genes (37.15%) were upregulated while 6,365 (62.85%) genes were downregulated. On the other hand, 3,343 (35.53%) genes were upregulated while 6,064 (64.46%) genes were downregulated in MP-EA+$CdCl_2$. These seem to suggest that the number and percentage of up / downregulated genes induced by $CdCl_2$ alone or with MP-HX and MP-EA treatments were nearly similar.

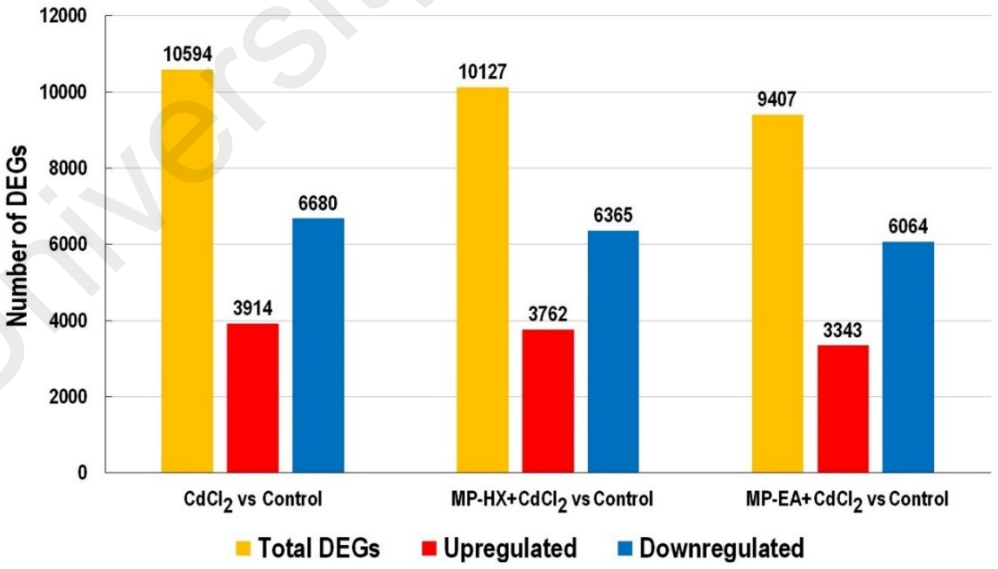

Figure 4.66: Number of differentially expressed genes (DEGs) (FC ≥ ±1.50) in Hs27 cells upon treatment with $CdCl_2$, MP-HX+$CdCl_2$ and MP-EA+$CdCl_2$. The bar chart shows the number of DEGs (FC ≥ ±1.50) modulated by the treatments.

A Venn diagram was constructed using TAC to further investigate the number of DEGs shared among the datasets. A total of 5,417 DEGs were noted to be shared between MP-HX+$CdCl_2$ and $CdCl_2$ treatments. For MP-EA+$CdCl_2$ and $CdCl_2$ treatment, 6,518 DEGs were shared between them. It was also noted that 4,339 DEGs were shared among the three datasets (**Fig. 4.67**).

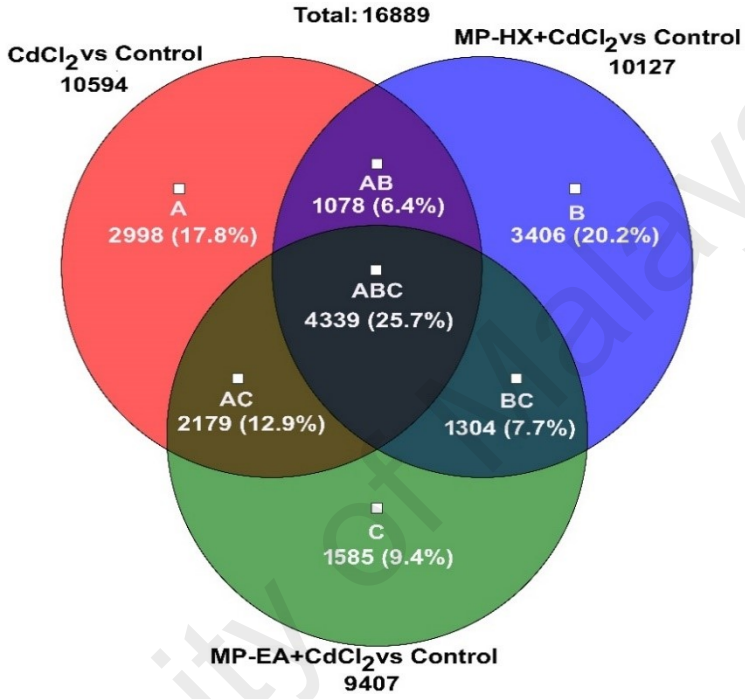

Figure 4.67: Venn diagram of differentially expressed genes (DEGs) (FC ≥ ±1.50) in Hs27 cells upon treatment with $CdCl_2$, MP-HX+$CdCl_2$ and MP-EA+$CdCl_2$. The Venn diagram shows comparison of DEGs among $CdCl_2$, MP-HX+$CdCl_2$ and MP-EA+$CdCl_2$ treatment. A, B, C indicates $CdCl_2$ vs control, MP-HX+$CdCl_2$ vs control, and MP-EA+$CdCl_2$ vs control, respectively.

The datasets revealed that many metallothionine (MT) and antioxidant genes were modulated by $CdCl_2$, MP-HX+$CdCl_2$ and MP-EA+$CdCl_2$ treatments. The expression FC values of MTs and selected antioxidant genes are shown in **Tables 4.24** and **4.25** respectively.

Table 4.24 shows that MT1A, MT1G, MT1H, MT1M were markedly upregulated by $CdCl_2$ in Hs27 cells with FC values of more than +100. In general, all of the MT genes were upregulated in the presence of $CdCl_2$ treatment. MT genes were also noted to be

upregulated in $CdCl_2$-exposed Hs27 cells, even with MP-HX and MP-EA pretreatments. However, the upregulation of MT1A, MT1G and MT1H, MT1M were noted to be significantly lower in the presence of MP-HX and MP-EA pretreatments.

Table 4.24: Gene expression fold change (FC) values for metallothionine genes after treatment with $CdCl_2$, MP-HX+$CdCl_2$ and MP-EA+$CdCl_2$ datasets. Microarray gene expression FC values with red color indicates upregulation of the gene. The more intense the color, the higher the FC value.

Gene	Microarray gene expression fold change		
	$CdCl_2$	MP-HX+$CdCl_2$	MP-EA+$CdCl_2$
MT1A	+458.33	+235.87	+416.64
MT1B	+7.06	+10.04	+8.06
MT1E	+6.52	+7.72	+7.34
MT1F	+26.30	+29.22	+25.28
MT1G	+438.95	+366.10	+414.22
MT1H	+172.08	+108.52	+163.84
MT1M	+101.66	+15.52	+20.63
MT1X	+34.41	+31.52	+32.77
MT1L	+18.55	+15.52	+20.63
MT2A	+2.55	+2.67	+2.49

In addition, the $CdCl_2$, MP-HX+$CdCl_2$ and MP-EA+$CdCl_2$ datasets showed modulation of several antioxidant genes in Hs27 cells (**Table 4.25**). In the presence of $CdCl_2$, the following antioxidant genes were downregulated: CAT, GPX4, GPX7, GPX8 (FC range: -1.74 to -2.25), while the expression of GPX1, GPX3, GSR, GSTO1, GSTO2, GSTP1, NQO1, PRDX1, TXNRD1, GCLM and GCLC were significantly upregulated (FC range: +1.54 to +2.80) (**Table 4.25**). MP-HX and MP-EA pretreatment also significantly upregulated many antioxidant genes (**Table 4.25**). The pretreatment with MP-HX/EA did not seem to show distinctive or marked difference in the pattern of expression compared to $CdCl_2$ dataset, for the antioxidant genes listed in **Table 4.25**.

Table 4.25: Gene expression fold change (FC) values for selected antioxidant genes after treatment with $CdCl_2$, MP-HX+$CdCl_2$ and MP-EA+$CdCl_2$. Microarray gene expression FC values with red color indicates upregulation while green color indicates downregulation. The more intense the color, the higher the FC value. If the FC value is $\leq \pm 1.10$, it is assumed that gene expression modulation was absent.

Gene	Microarray gene expression fold change		
	$CdCl_2$	MP-HX+$CdCl_2$	MP-EA+$CdCl_2$
CAT	-1.77	-1.40	-1.50
GPX1	+2.80	+2.07	+1.79
GPX3	+2.16	+2.37	+1.43
GPX4	-1.93	+1.50	+1.03
GPX7	-2.25	-1.23	-1.57
GPX8	-1.74	+1.19	-1.13
GSR	+2.40	+1.88	+2.36
GSTO1	+1.54	+1.17	+1.72
GSTO2	+1.66	+1.28	+1.49
GSTP1	+1.73	+1.47	+1.64
NQO1	+2.43	+1.30	+2.23
PRDX1	+1.78	+2.12	+1.89
PRDX3	-1.34	+1.02	-1.08
PRDX4	-1.26	+1.03	-1.08
PRDX5	-1.11	+2.04	+1.12
TXNRD1	+2.76	+2.23	+3.00
TXNRD3	-1.15	+1.29	+1.16
GCLM	+2.59	+1.45	+2.16
GCLC	+1.61	-1.09	+1.64

The $CdCl_2$, MP-HX+$CdCl_2$ and MP-EA+$CdCl_2$ datasets were noted to show modulation of many heat shock protein (HSP) genes (**Table 4.26**). In the presence of $CdCl_2$, following HSP genes were notably upregulated: DNAJB1, DNAJA4, HSPA6, HSPH1 and HSP90AA1 (FC range: +10.70 to +105.15) (**Table 4.26**). In contrast, MP-HX and MP-EA pretreatments were noted to have lesser degree of upregulation of DNAJA1, DNAJB1, DNAJA4, HSPA1L, HSPA6, HSPH1, HSP90AA1 (**Table 4.26**). MP-HX and MP-EA pretreatments also significantly downregulated HSPA2. In addition, the expression of HSPB2 was apparently unchanged after MP-HX pretreatment, while MP-EA pretreatment seems to have lessened the degree of HSPB2 upregulation (**Table 4.26**).

Table 4.26: Gene expression fold change (FC) values for selected heat shock protein genes after treatment with $CdCl_2$, MP-HX+$CdCl_2$ and MP-EA+$CdCl_2$. Microarray gene expression FC values with red color indicates upregulation while green color indicates downregulation. The more intense the color, the higher the FC value. If the FC value is ≤ ±1.10, it is assumed that gene expression modulation was absent.

Gene	Microarray gene expression fold change		
	$CdCl_2$	MP-HX+$CdCl_2$	MP-EA+$CdCl_2$
DNAJA1	+5.33	+3.72	+4.16
DNAJB1	+17.97	+5.93	+9.89
DNAJA4	+105.15	+30.46	+50.28
HSPA1L	+3.63	+1.37	+2.23
HSPA2	+1.37	-3.82	-1.57
HSPA6	+17.54	+4.79	+9.59
HSPB2	+2.11	+1.07	+1.24
HSPH1	+10.70	+6.20	+8.19
HSP90AA1	+14.57	+7.66	+11.21

The list of DEGs from all of the treatments were further analyzed using TAC software, to investigate the possible modulation of Wikipathways (WPs) by the treatments. This could reveal the possible genes networks and molecular pathways associated with the protective effect of MP-HX and MP-EA against $CdCl_2$-induced cytotoxicity. The following WPs were noted to be significantly modulated by $CdCl_2$, MP-HX+ $CdCl_2$, MP-EA+ $CdCl_2$ treatments: "Mitotic G_1-G_1/S phases", "S phase", "Mitotic G_2-G_2/M phases" and "Intrinsic pathway for apoptosis" (**Table 4.27**). TAC ranked WPs based on the significance score. The significance score is the negative logarithm of Fisher's exact *p*-value. The higher the score, the more significant is the association of WPs with the differentially expressed genes.

Table 4.27: Summary of the Wikipathways related to "cell cycle" and "apoptosis" that were modulated in Hs27 cells after treatment with $CdCl_2$, MP-HX+$CdCl_2$ and MP-EA+$CdCl_2$. The table list selected genes involved in the relevant WPs. Red color indicates upregulation of the genes while green color indicates downregulation. The darker the corresponding color, the higher the fold change (FC) of expression. If the FC value is ≤ ±1.10, it is assumed that gene expression modulation was absent. *RG, representative gene.

Wikipathway	Significance score			RG	Microarray gene expression fold change		
	$CdCl_2$	MP-HX +$CdCl_2$	MP-EA +$CdCl_2$		$CdCl_2$	MP-HX +$CdCl_2$	MP-EA+$CdCl_2$
Mitotic G_1-G_1/S phases	19.56	20.62	15.75	MYC	+2.05	-1.36	+1.21
				PCNA	-2.17	-1.41	-1.40
				CDK1	-1.60	-1.61	-1.08
S phase	12.81	15.33	13.07	GINS1	-1.69	-1.04	-1.01
				GINS2	-1.33	-1.08	+1.17
Mitotic G_2-G_2/M phases	18.91	16.73	17.56	CCNB2	-1.69	-1.73	-1.21
				CUL1	-1.85	-1.23	+1.41
				GTSE1	-1.53	-1.45	+1.13
				BORA	-1.18	+4.21	+1.32
Intrinsic pathway for apoptosis	4.66	4.06	5.78	PMAIP1	+7.46	+1.69	+3.45
				BBC3	+2.92	+1.06	+1.19
				BAD	-1.46	-1.26	-1.64

4.6.4.2 Analysis of the microarray data using GATHER web-tool

The microarray gene expression data was also analyzed using the web-based tool "Gene Annotation Tool to Help Explain Relationships" (GATHER) (http://changlab.uth.tmc.edu/gather/gather.py) (J. T. Chang & Nevins, 2006). GATHER categorizes statistically significant association between genes and biological processes. This could help reveal the biological functions associated with transcriptome profiles in the datasets. A cut-off fold change (FC) value of ±1.50 was used to filter the list of DEGs. This revealed 10,594; 10,127 and 9,407 DEGs for $CdCl_2$, MP-HX+$CdCl_2$ and MP-EA+$CdCl_2$ datasets, respectively. For $CdCl_2$ dataset, the following GO categories were overrepresented or enriched by GATHER: "regulation of cell cycle", "unfolded protein response", "cell proliferation", "cell cycle", "apoptosis", "cell death and response to DNA damage" (**Table 4.28, Figure 4.68)**.

Table 4.28: GATHER analysis - GO categories enriched in $CdCl_2$ dataset (FC ≥ ±1.50; 10,594 genes). The list indicates biological processes that were significantly overrepresented in Hs27 cells upon treatment with $CdCl_2$. *Count: enriched gene number in the GO: biological process.

GO: biological process	Count	-log (*p*-value)
GO:0000074 [6]: regulation of cell cycle	138	4.07
GO:0040008 [4]: regulation of growth	44	2.90
GO:0006986 [5]: response to unfolded protein	25	2.79
GO:0008283 [4]: cell proliferation	308	2.59
GO:0001558 [4]: regulation of cell growth	40	2.29
GO:0007049 [5]: cell cycle	214	2.24
GO:0040007 [3]: growth	58	2.20
GO:0016049 [4]: cell growth	48	2.02
GO:0006915 [6]: apoptosis	138	1.94
GO:0006974 [5]: response to DNA damage stimulus	70	1.74
GO:0006281 [6]: DNA repair	64	1.64
GO:0008219 [4]: cell death	144	1.64
GO:0016265 [3]: death	145	1.61
GO:0042127 [5]: regulation of cell proliferation	86	1.56

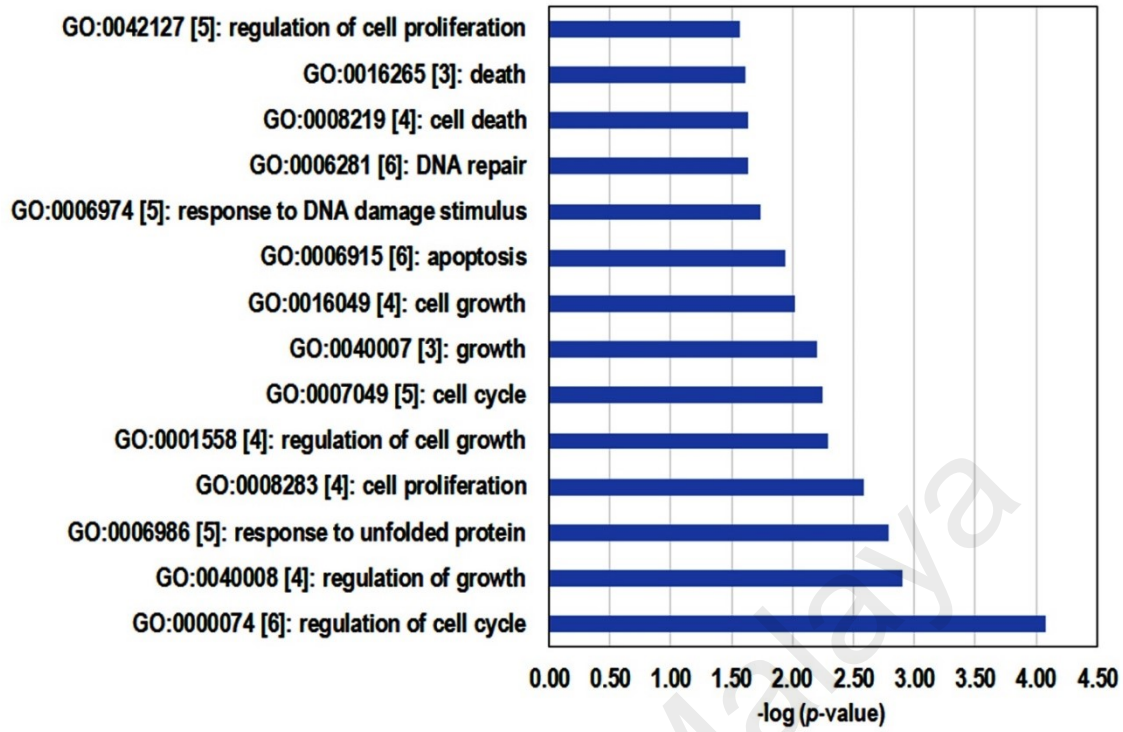

Figure 4.68. GATHER analysis - GO categories enriched in $CdCl_2$ dataset (FC ≥ ±1.50; 10,594 genes). The bar chart depicts significantly overrepresented GO categories in Hs27 cells after treatment with $CdCl_2$.

The following GO categories were enriched by MP-HX+$CdCl_2$ dataset: "regulation of cell cycle", "regulation of growth", "regulation of cellular process", "development and response to unfolded protein" (**Table 4.29, Figure 4.69)**.

Table 4.29: GATHER analysis - GO categories enriched in MP-HX+$CdCl_2$ dataset (FC ≥ ±1.50; 10,127 genes). The list indicates biological processes that were significantly overrepresented in Hs27 cells upon treatment with MP-HX+$CdCl_2$. *Count: enriched gene number in the GO: biological process.

GO: biological process	Count	-log (*p*-value)
GO:0050789 [2]: regulation of biological process	742	3.65
GO:0007155 [4]: cell adhesion	177	3.53
GO:0007275 [2]: development	478	3.37
GO:0000074 [6]: regulation of cell cycle	126	3.03
GO:0050794 [3]: regulation of cellular process	227	2.79
GO:0040008 [4]: regulation of growth	42	2.77
GO:0016055 [6]: Wnt receptor signaling pathway	37	2.62
GO:0050793 [3]: regulation of development	57	2.57
GO:0040007 [3]: growth	56	2.31
GO:0050791 [3]: regulation of physiological process	651	2.15
GO:0001558 [4]: regulation of cell growth	37	1.81
GO:0009653 [3]: morphogenesis	308	1.78
GO:0006986 [5]: response to unfolded protein	22	1.66

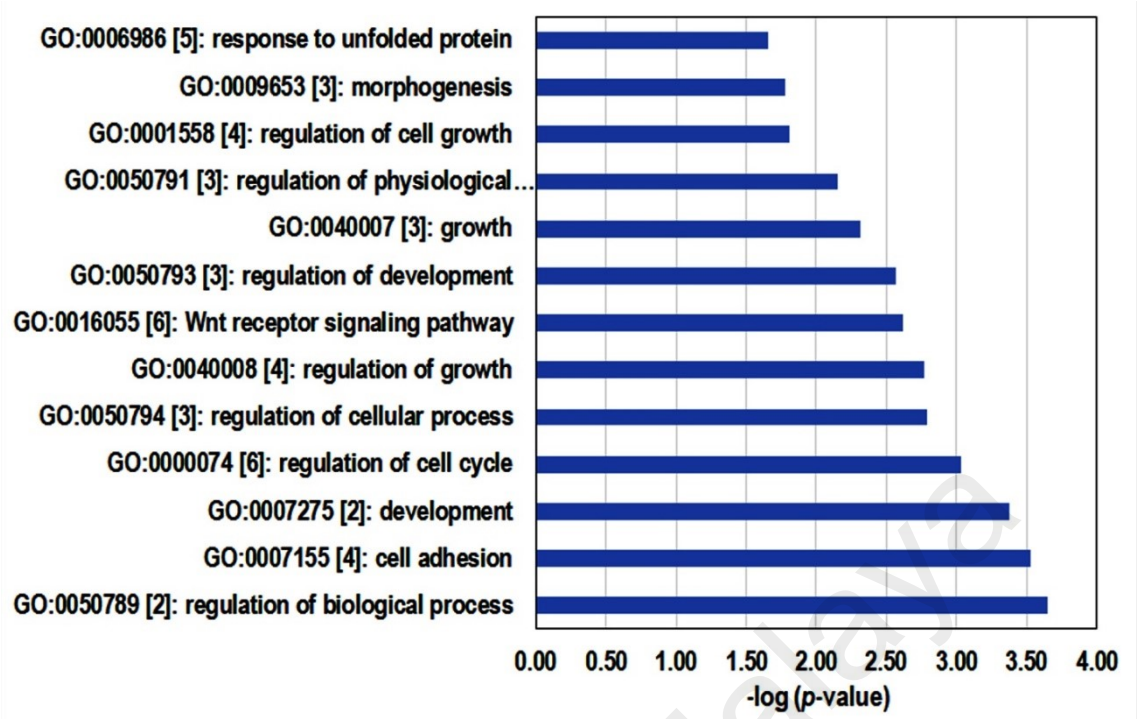

Figure 4.69: GATHER analysis - GO categories enriched in MP-HX+$CdCl_2$ dataset (FC ≥ ±1.50; 10,127 genes). The bar chart depicts significantly overrepresented GO categories in Hs27 cells after treatment with MP-HX+$CdCl_2$.

The GO categories enriched in MP-EA+$CdCl_2$ dataset include "regulation of cell cycle", "development, response to unfolded protein", "cell cycle", and "cell proliferation" (**Table 4.30, Figure 4.70)**.

Table 4.30: GATHER analysis - GO categories enriched in MP-EA+$CdCl_2$ dataset (FC≥ ±1.50; 9,407 genes). The list indicates biological processes that were significantly overrepresented in Hs27 cells upon treatment with MP-EA+$CdCl_2$. *Count: enriched gene number in the GO: biological process

GO: biological process	Count	-log (*p*-value)
GO:0000074 [6]: regulation of cell cycle	118	3.01
GO:0006350 [6]: transcription	483	2.94
GO:0006355 [7]: regulation of transcription, DNA-dependent	443	2.38
GO:0006351 [7]: transcription, DNA-dependent	455	2.34
GO:0006986 [5]: response to unfolded protein	22	2.17
GO:0007275 [2]: development	433	2.02
GO:0050794 [3]: regulation of cellular process	206	1.94
GO:0045860 [5]: positive regulation of protein kinase activity	20	1.83
GO:0008283 [4]: cell proliferation	266	1.81
GO:0001501 [5]: skeletal development	42	1.76
GO:0007049 [5]: cell cycle	184	1.50

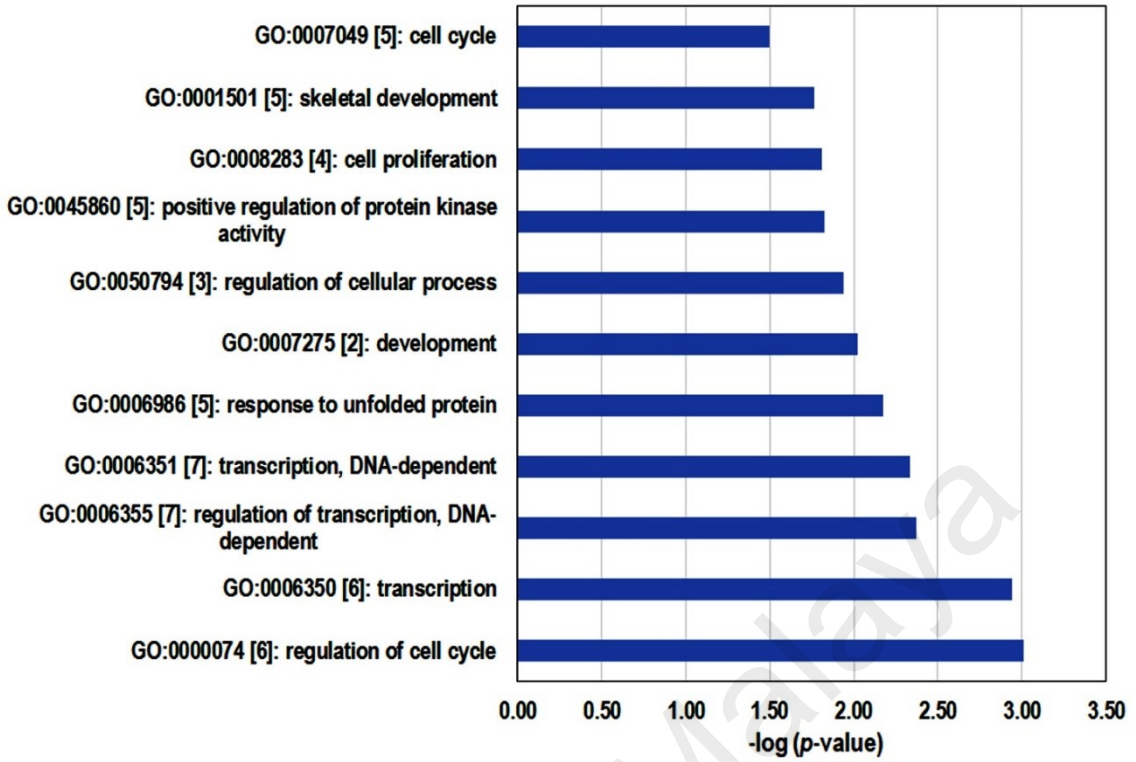

Figure 4.70: GATHER analysis – GO categories enriched in MP-EA+$CdCl_2$ dataset (FC ≥ ±1.50; 9,407 genes). The bar chart depicts significantly overrepresented GO categories in Hs27 cells after treatment with MP-EA+$CdCl_2$.

4.6.4.3 Analysis of microarray data with PANTHER classification system

The list of DEGs were further analyzed using "Protein Analysis Through Evolutionary Relationships" (PANTHER) (http://www.pantherdb.org/). PANTHER categorizes molecular functions and biological processes based on GO functional annotations (Mi & Thomas, 2009); (Mi et al., 2013); (Mi et al., 2017). A cut-off FC value of ±1.50 was used to filter the list of DEGs. A total of 10,594; 10,127 and 9,407 genes fulfilled the FC value criteria in $CdCl_2$, MP-HX+$CdCl_2$ and MP-EA+$CdCl_2$ datasets respectively and they were analysed using PANTHER. The DEGs were mapped onto PANTHER database to identify molecular function and biological processes that were enriched by the DEGs. PANTHER analysis indicated that the $CdCl_2$, MP-HX+$CdCl_2$ and MP-EA+$CdCl_2$ datasets enriched GO categories with molecular functions that were associated with "binding" and "catalytic activity" (**Figure 4.71**).

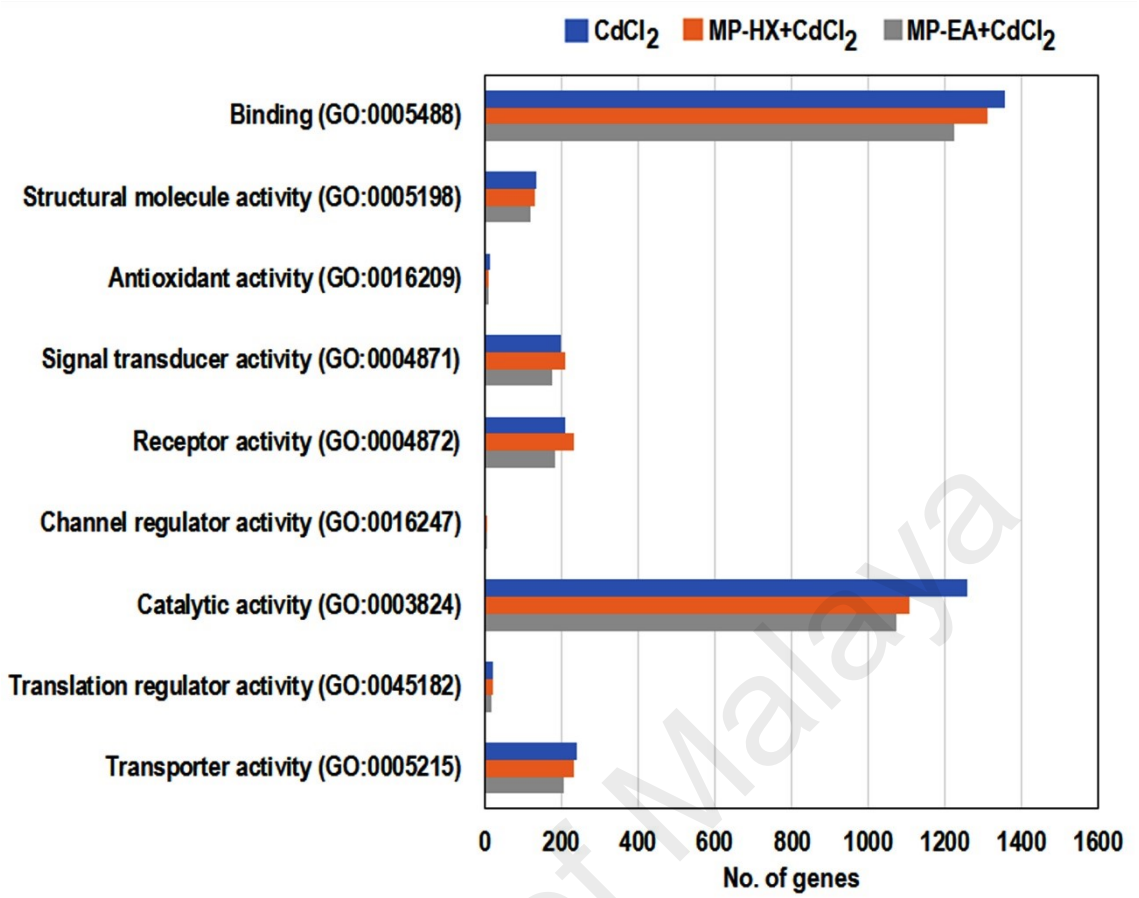

Figure 4.71: Functional categorization of DEGs by PANTHER based on molecular functions. GO categories with corresponding molecular functions that were enriched in $CdCl_2$ (FC ≥ ±1.50; 10,594 genes), MP-HX+$CdCl_2$ (FC ≥ ±1.50; 10,127 genes) and MP-EA+$CdCl_2$ datasets (FC ≥ ±1.50; 9,407 genes).

PANTHER analysis also indicated that the $CdCl_2$, MP-HX+$CdCl_2$ and MP-EA+$CdCl_2$ datasets enriched GO categories with biological functions that were associated with "cellular process", "metabolic process", "response to stimulus", "biological regulation" and "developmental process" (**Figure 4.72**).

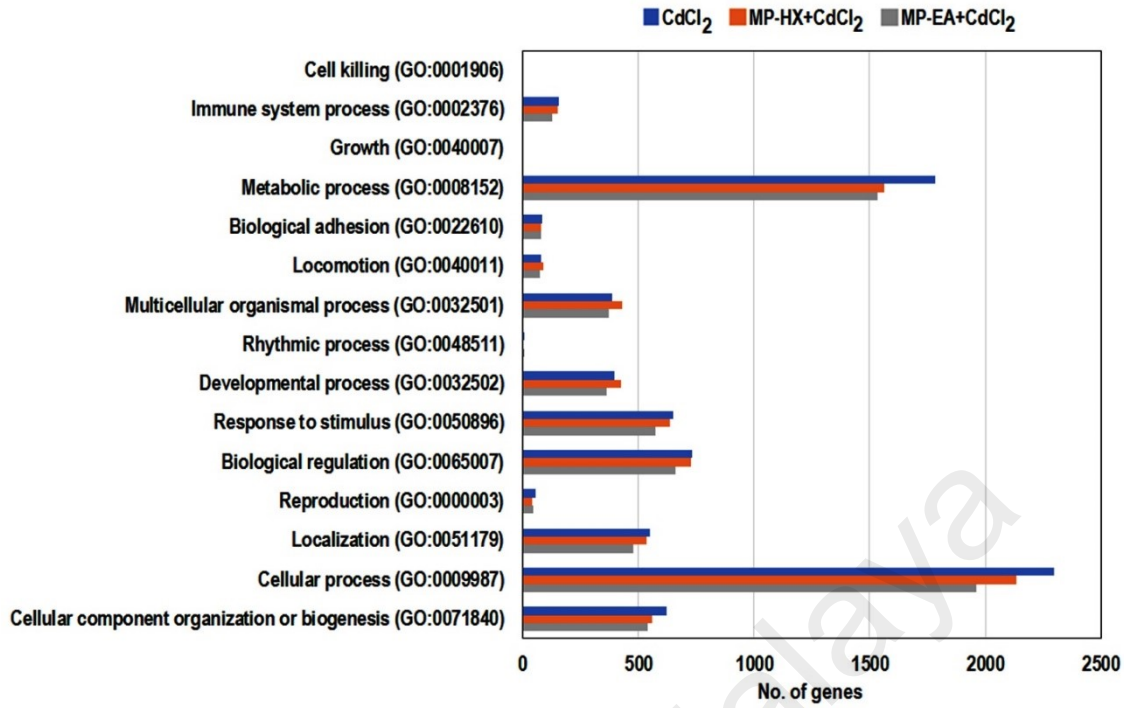

Figure 4.72: Functional categorization of DEGs by PANTHER based on biological functions. GO categories with corresponding biological functions that were enriched in $CdCl_2$ (FC ≥ ±1.50; 10,594 genes), MP-HX+$CdCl_2$ (FC ≥ ±1.50; 10,127 genes) and MP-EA+$CdCl_2$ datasets (FC ≥ ±1.50; 9,407 genes).

The GO terms "cellular process", "developmental process" and "response to stimulus" were further categorized to reveal the specific biological processes that were associated with the DEGs in Hs27 cells, after treatment with $CdCl_2$, MP-HX+$CdCl_2$ and MP-EA+$CdCl_2$. The subcategories for "cellular processes" (GO:0009987) were "cell communication", "cell growth", "cell proliferation", "cellular component and movement" and "cell cycle" (**Figure 4.73**). The subcategories for "developmental process" (GO:0032502) were "cell differentiation", "system development", "ectoderm development", "mesoderm development" and "death" (**Figure 4.74**). The subcategories for "response to stimulus" (GO:0050896) include "immune response", "cellular defense response", "response to endogenous stimulus", "response to external stimulus", "response to stress" and "response to biotic stimulus" (**Figure 4.75**).

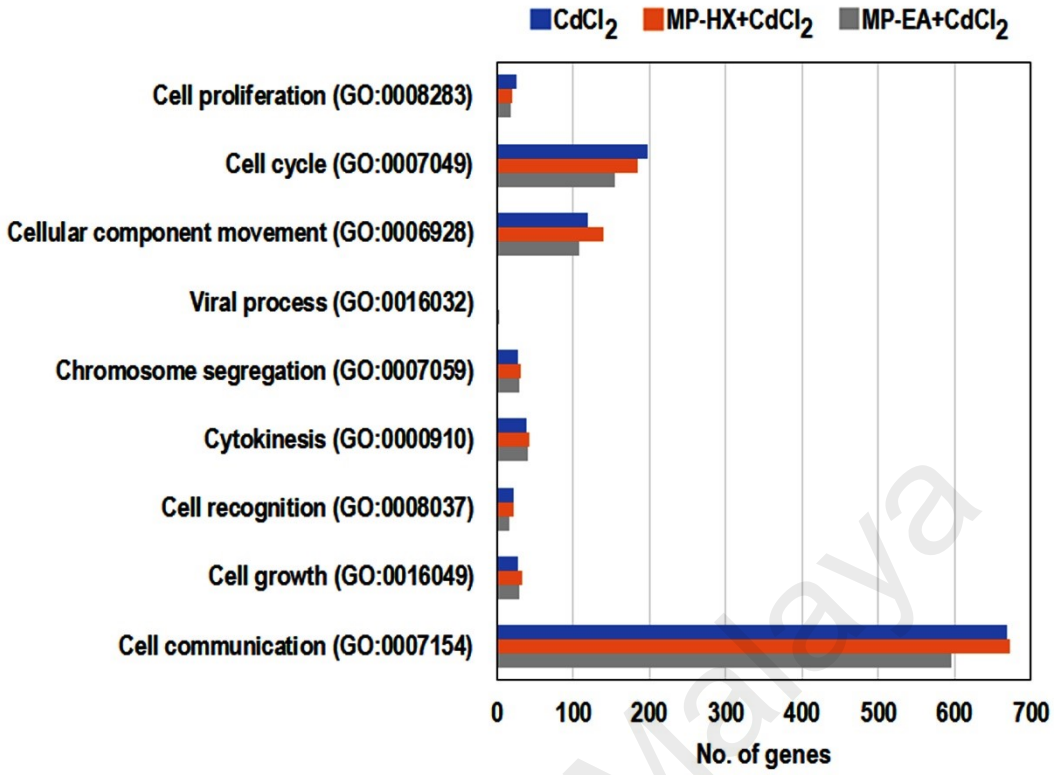

Figure 4.73: Functional categorization of DEGs by PANTHER based on "cellular process". GO categories for "cellular processes" that were enriched in $CdCl_2$ (FC ≥ ±1.50; 10,594 genes), MP-HX+$CdCl_2$ (FC ≥ ±1.50; 10,127 genes) and MP-EA+$CdCl_2$ datasets (FC ≥ ±1.50; 9,407 genes).

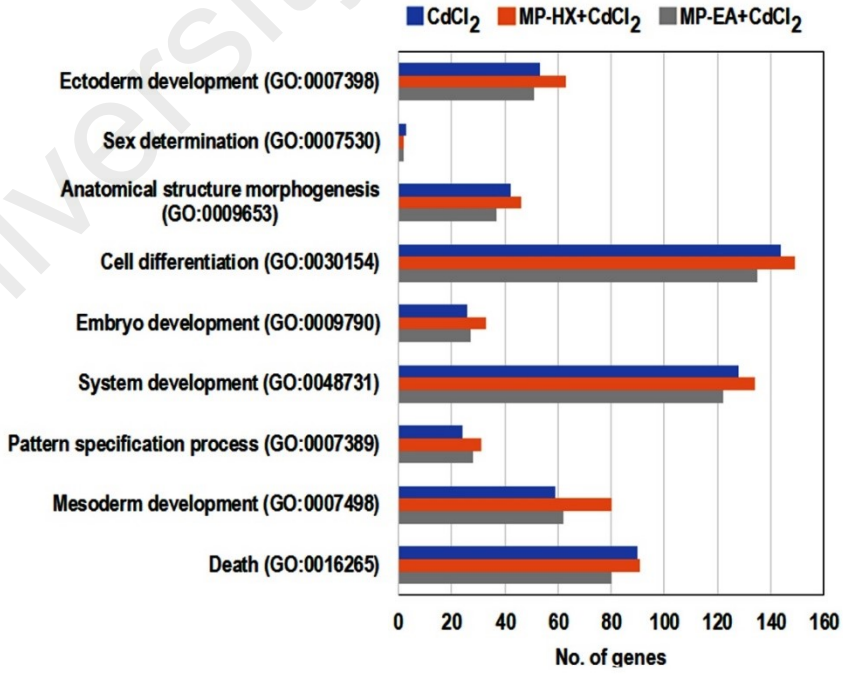

Figure 4.74: Functional categorization of DEGs by PANTHER based on "developmental process". GO categories for "developmental process" that were enriched in $CdCl_2$ (FC ≥ ±1.50; 10,594 genes), MP-HX+$CdCl_2$ (FC ≥ ±1.50; 10,127 genes) and MP-EA+$CdCl_2$ datasets (FC ≥ ±1.50; 9,407 genes).

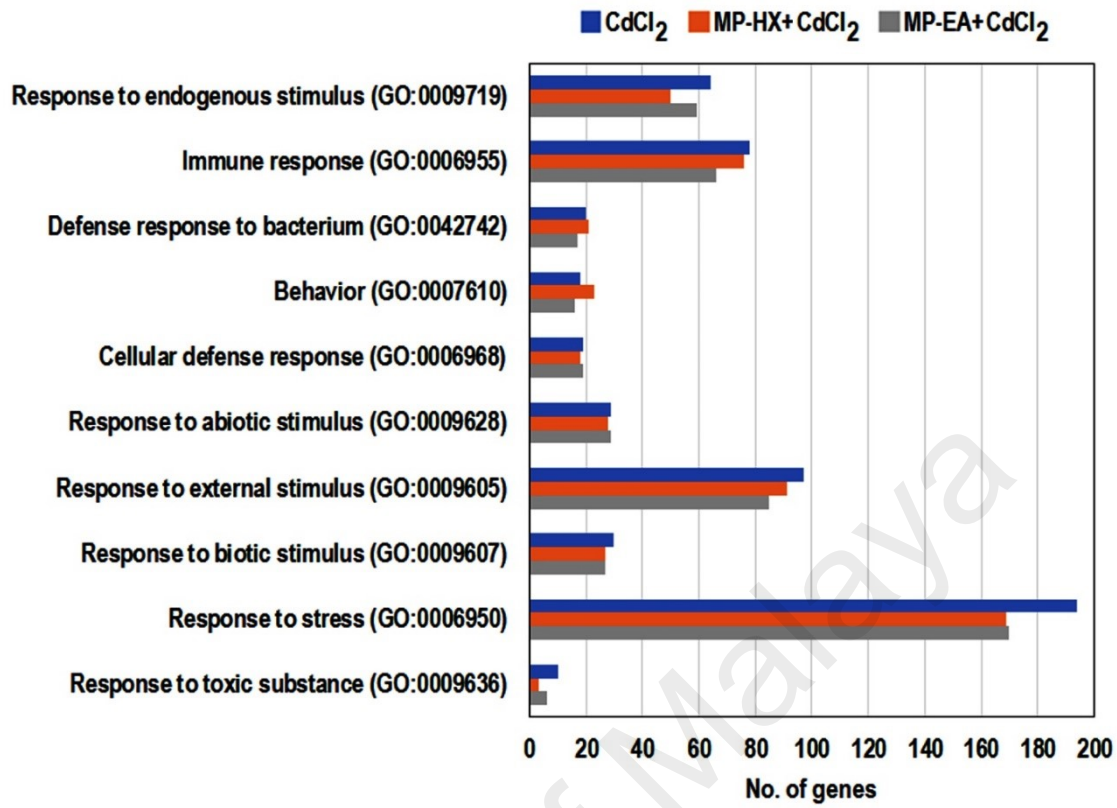

Figure 4.75: Functional categorization of DEGs by PANTHER based on "response to stimulus". GO categories for "response to stimulus" that were enriched in $CdCl_2$ (FC ≥ ±1.50; 10,594 genes), MP-HX+$CdCl_2$ (FC ≥ ±1.50; 10,127 genes) and MP-EA+$CdCl_2$ datasets (FC ≥ ±1.50; 9,407 genes).

4.6.4.4 Analysis of microarray data by STRING web-tool

An online protein-protein interaction analysis tool "Search Tool for the Retrieval of Interacting Genes" (STRING) (https://string-db.org) was also used to analyse the datasets. STRING is a network generation tool that uncovers physical, as well as functional interactions of differentially expressed genes (Szklarczyk et al., 2015). In STRING, false discovery rate (FDR) *p*-value is used to describe significance of functional enrichments. A list of DEGs was generated with FC value of ≥ ±2.50, comprising a total of 1,182; 927 and 768 genes respectively for $CdCl_2$, MP-HX+$CdCl_2$ and MP-EA+$CdCl_2$ datasets. These DEGs were submitted to STRING database for the generation of network and functional enrichments. STRING categorizes the interactions according to confidence of association. The higher the confidence value the higher the

interaction between genes. Confidence value of 0.15, 0.4, 0.7 and 0.9 indicates low, medium, high and highest interaction respectively (**Figure 4.76**).

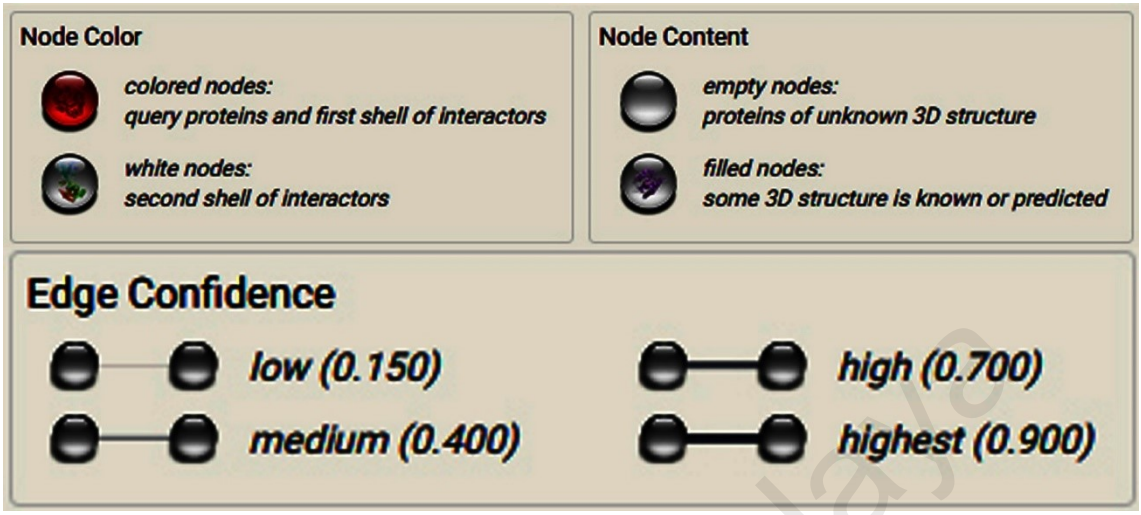

Figure 4.76: Legend for STRING network analysis. Network nodes represent proteins while edges represent protein-protein interactions.

A total of 801 (67.8%) of the DEGs (out of 1,182) showed interaction for $CdCl_2$ dataset, with 3,113 interactions (confidence value: ≥ 0.4) were predicted among them. The DEGs in the network significantly enriched several biological processes including "cellular response to metal ion", "response to unfolded protein", "cellular response to cadmium ion", "regulation of cell death", "cellular response to stress" and others (**Table 4.31**).

Table 4.31: STRING network analysis of $CdCl_2$ dataset. Biological processes enriched in the network (threshold confidence value: 0.4) of $CdCl_2$ dataset (FC ≥ ±2.50). The list indicates biological processes that were significantly overrepresented in Hs27 for $CdCl_2$ dataset. *Count: enriched gene number in the GO: biological process; FDR, false discovery rate.

GO: biological process	Count	FDR (*p*-value)
GO.0071248: cellular response to metal ion	21	9.11E-06
GO.0006986: response to unfolded protein	23	2.35E-05
GO.0071276: cellular response to cadmium ion	8	2.72E-05
GO.0010941: regulation of cell death	88	0.000317
GO.0046686: response to cadmium ion	10	0.000403
GO.0042127: regulation of cell proliferation	87	0.000448
GO.0036499: PERK-mediated unfolded protein response	6	0.00053
GO.0006950: response to stress	167	0.000716
GO.0010038: response to metal ion	28	0.000785
GO.0080135: regulation of cellular response to stress	51	0.000785
GO.0033554: cellular response to stress	91	0.0016
GO.0070059: intrinsic apoptotic signaling pathway in response to endoplasmic reticulum stress	7	0.0126
GO.0012501: programmed cell death	62	0.0131
GO.0016265: death	64	0.0131
GO.0008219: cell death	63	0.0175
GO.0006915: apoptotic process	60	0.0247
GO.0008285: negative regulation of cell proliferation	41	0.0256
GO.0051726: regulation of cell cycle	54	0.0302
GO.0045926: negative regulation of growth	19	0.0309

The network of DEGs with highest confidence value (≥ 0.9) is shown in **Figure 4.77**. There was a close relationship among the DEGs. Numerous genes including CDKN1C, NEDD4L, E2F7, SKP2, PMAIP1, BBC3, ERN1, HSPA6, HSPA5, HSPA1L, HSPA8, DNAJA4, DNAJA9, MDM2, NFKB1, NFKBIA, RIPK1, JUN, JUNB, JUND, FOS, FOSB, FOSL1, ATF3, RMI1, IL8, DDIT3, GADD45A, GADD45B, GADD45G, TNFRSF9, TNFSF9 and histone cluster genes were connected to this network. The functional clusters, "GO.0071248: cellular response to metal ion", "GO.0006986: response to unfolded protein", "GO.0010941: regulation of cell death", "GO.0008285: negative regulation of cell proliferation", "GO.0006950: response to stress" and

"GO.0006915: apoptotic process", were selected to show the members of the clusters in the network (**Figure 4.77**).

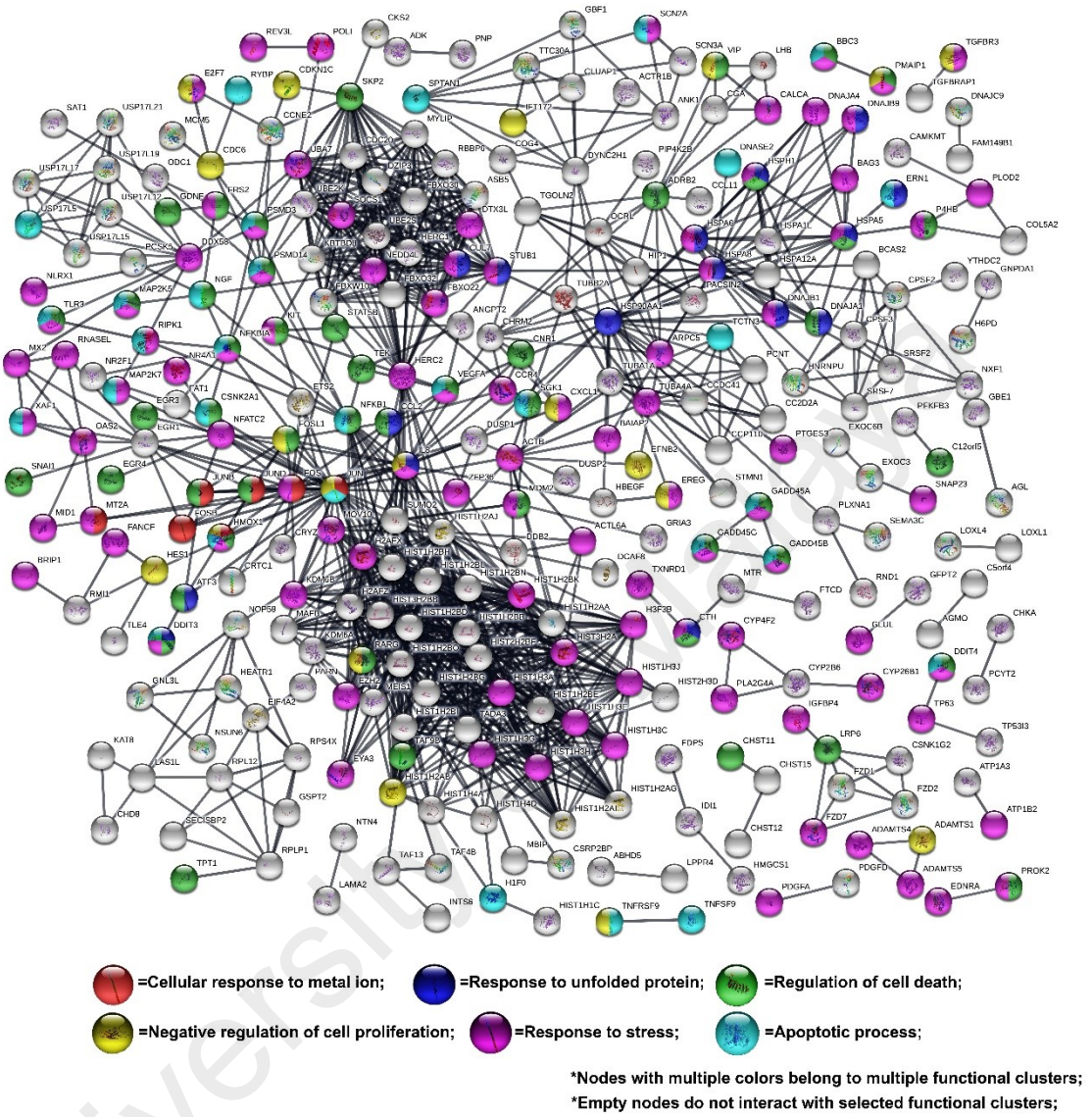

Figure 4.77: STRING network analysis of $CdCl_2$ dataset (FC ≥ ±2.50). The figure illustrates the network and interactions among the 300 DEGs that were predicted by STRING. The interaction figure was generated using the highest confidence value (≥ 0.9). The functional clusters, "cellular response to metal ion", "response to unfolded protein", "regulation of cell death", "negative regulation of cell proliferation", "response to stress" and "apoptotic process", were identified in the network.

In MP-HX+$CdCl_2$ dataset, a total of 653 (70.4%) of the DEGs (out of 927) interacted in the network and 1,518 interactions (confidence value: ≥ 0.4) were predicted among them. The DEGs in this network showed functional enrichment of several biological processes including "cellular response to cadmium ion", "response to unfolded protein",

"cellular response to metal ion", "regulation of growth", "positive regulation of cell proliferation", and others (**Table 4.32**).

Table 4.32: STRING network analysis of MP-HX+$CdCl_2$ dataset. Biological processes enriched in the network (threshold confidence value: 0.4) of MP-HX+$CdCl_2$ dataset (FC ≥ ±2.50). The list indicates biological processes that were significantly overrepresented in Hs27 for MP-HX + $CdCl_2$ dataset. *Count: enriched gene number in the GO: biological process; FDR, false discovery rate.

GO: biological process	Count	FDR (*p*-value)
GO.0071276: cellular response to cadmium ion	8	3.45E-06
GO.0043067: regulation of programmed cell death	77	1.57E-05
GO.0010941: regulation of cell death	80	1.94E-05
GO.0006986: response to unfolded protein	19	8.56E-05
GO.0071248: cellular response to metal ion	15	0.000683
GO.0040008: regulation of growth	40	0.000867
GO.0008284: positive regulation of cell proliferation	45	0.00319
GO.0042127: regulation of cell proliferation	70	0.00345
GO.0060548: negative regulation of cell death	49	0.00359
GO.2000377: regulation of reactive oxygen species metabolic process	15	0.00372
GO.0050673: epithelial cell proliferation	11	0.00541
GO.0048468: cell development	73	0.00759
GO.0012501: programmed cell death	54	0.00787
GO.0080135: regulation of cellular response to stress	40	0.00818
GO.0008219: cell death	55	0.00912
GO.0034620: cellular response to unfolded protein	12	0.0114
GO.0090594: inflammatory response to wounding	3	0.0281

The network of DEGs with highest confidence value (≥ 0.9) is shown in **Figure 4.78**. The DEGs were very closely related in the network. **Figure 4.78** shows that many genes including ATF3, DDIT3, EIF4A3, DNAJA4, HSPA2, HSPA5, HSPA6, HSPA9, HSPA13, IL8, POLD2, HSP90AA1, GADD45B, GADD45G, SKP2, USP17L12, collagens and histone cluster genes were connected to this network.

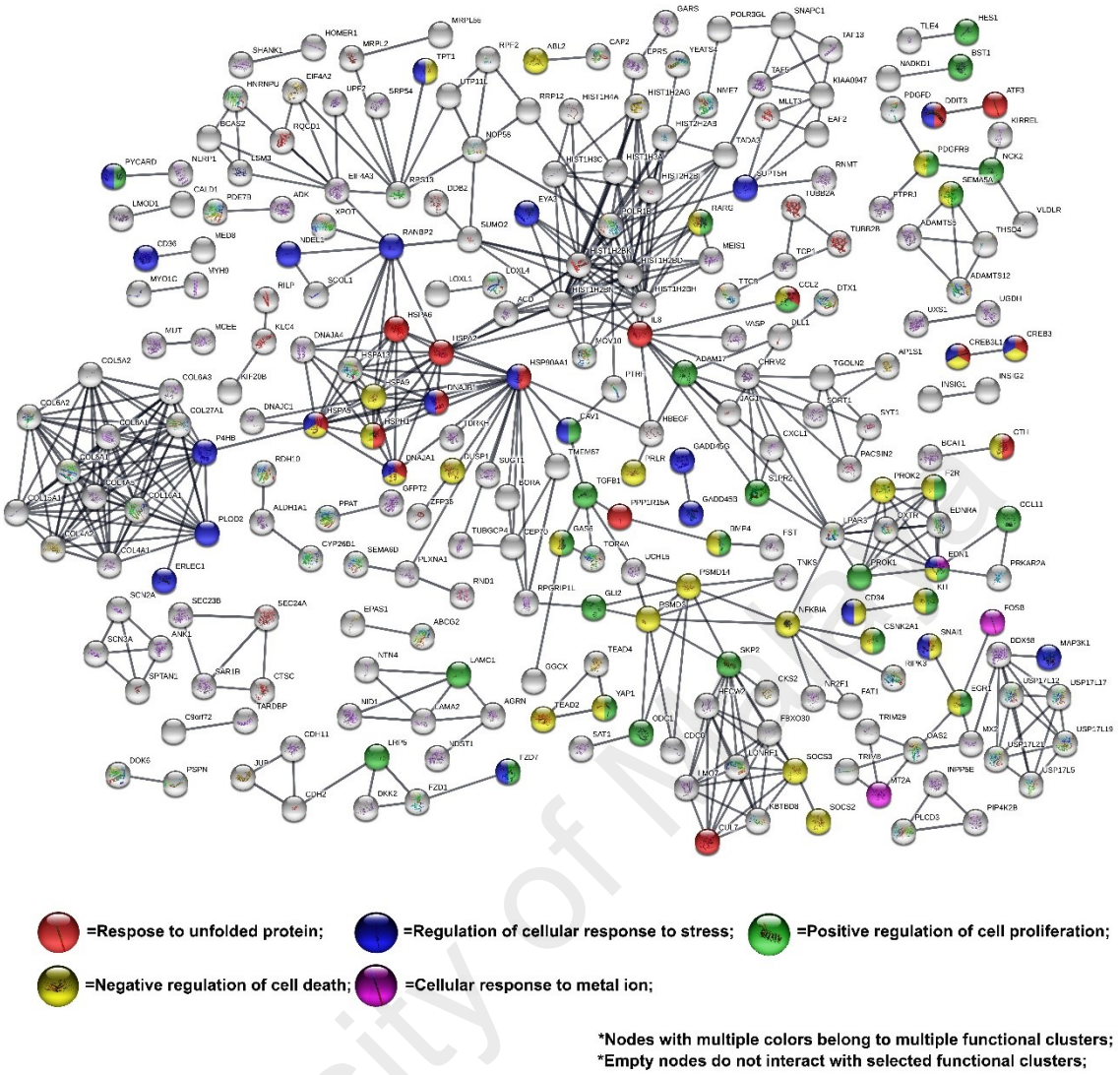

Figure 4.78: STRING network analysis of MP-HX+$CdCl_2$ dataset (FC ≥ ±2.50). The figure illustrates the networks and interactions among the 253 DEGs that were predicted by STRING. The interaction figure was generated using the highest confidence value (≥ 0.9). The functional clusters, "response to unfolded protein", "regulation of cellular response to stress", "positive regulation of cell proliferation", "negative regulation of cell death", and "cellular response to metal ion", were identified in the network.

The functional clusters, "GO.0006986: response to unfolded protein", "GO.0080135: regulation of cellular response to stress", "GO.0008284: positive regulation of cell proliferation", "GO.0060548: negative regulation of cell death", and "GO.0071248: cellular response to metal ion", were selected to show the members of the clusters in the network.

In MP-EA+$CdCl_2$ dataset, a total of 504 (65.6%) of the DEGs (out of 768) interacted in the network and 1,094 interactions (confidence value: ≥ 0.4) were predicted among them. The DEGs in this network showed functional enrichment of several biological processes including "cellular response to cadmium ion", "cellular response to metal ion", "response to unfolded protein", "positive regulation of cell proliferation", "response to stimulus", "response to metal ion", "response to oxidative stress", regulation of cell cycle" and others (**Table 4.33**).

Table 4.33: STRING network analysis of MP-EA+$CdCl_2$ dataset. Biological processes enriched in the network (threshold confidence value: 0.4) of MP-EA+$CdCl_2$ dataset (FC ≥ ±2.50). The list indicates biological processes that were significantly overrepresented in Hs27 for MP-EA+$CdCl_2$ dataset. *Count: enriched gene number in the GO: biological process; FDR, false discovery rate.

GO: biological process	Count	FDR (*p*-value)
GO.0071276: cellular response to cadmium ion	8	2.37E-06
GO.0071248: cellular response to metal ion	17	7.09E-06
GO.0006986: response to unfolded protein	19	9.12E-06
GO.0046686: response to cadmium ion	9	0.000169
GO.2001233: regulation of apoptotic signaling pathway	27	0.000199
GO.0042981: regulation of apoptotic process	57	0.00159
GO.0008284: positive regulation of cell proliferation	39	0.00174
GO.0006950: response to stress	111	0.00261
GO.0033554: cellular response to stress	63	0.00268
GO.0034620: cellular response to unfolded protein	12	0.00268
GO.0010038: response to metal ion	20	0.00297
GO.0010941: regulation of cell death	58	0.00318
GO.0050896: response to stimulus	192	0.00347
GO.0006979: response to oxidative stress	21	0.0064
GO.0000302: response to reactive oxygen species	14	0.00812
GO.0051726: regulation of cell cycle	40	0.0116
GO.0071495: cellular response to endogenous stimulus	42	0.0116
GO.2001020: regulation of response to DNA damage stimulus	11	0.0266
GO.0043066: negative regulation of apoptotic process	35	0.029
GO.0060548: negative regulation of cell death	36	0.0445

The network of DEGs with highest confidence value (≥ 0.9) is shown in **Figure 4.79**. There is a strong interaction among the DEGs and they are very closely related. This network linked many genes including SKP2, CDKN1C, GADD45B, GADD45G, DNAJA1, DNAJA4, HSP90AA1, HSPA5, HSPA6, COL15A1, COL5A2, IL8, JUN, FOS, ATF3, DDIT3, HMOX1, BBC3, PMAIP1 and histone cluster genes (**Figure 4.79**). The functional clusters, "GO.0071248: cellular response to metal ion", "GO.0006986: response to unfolded protein", "GO.0008284: positive regulation of cell proliferation", "GO.0043066: negative regulation of apoptotic process", "GO.0060548: negative regulation of cell death", "GO.0000302: response to reactive oxygen species" and "GO.0033554: cellular response to stress", were selected to show the members of the clusters in the network.

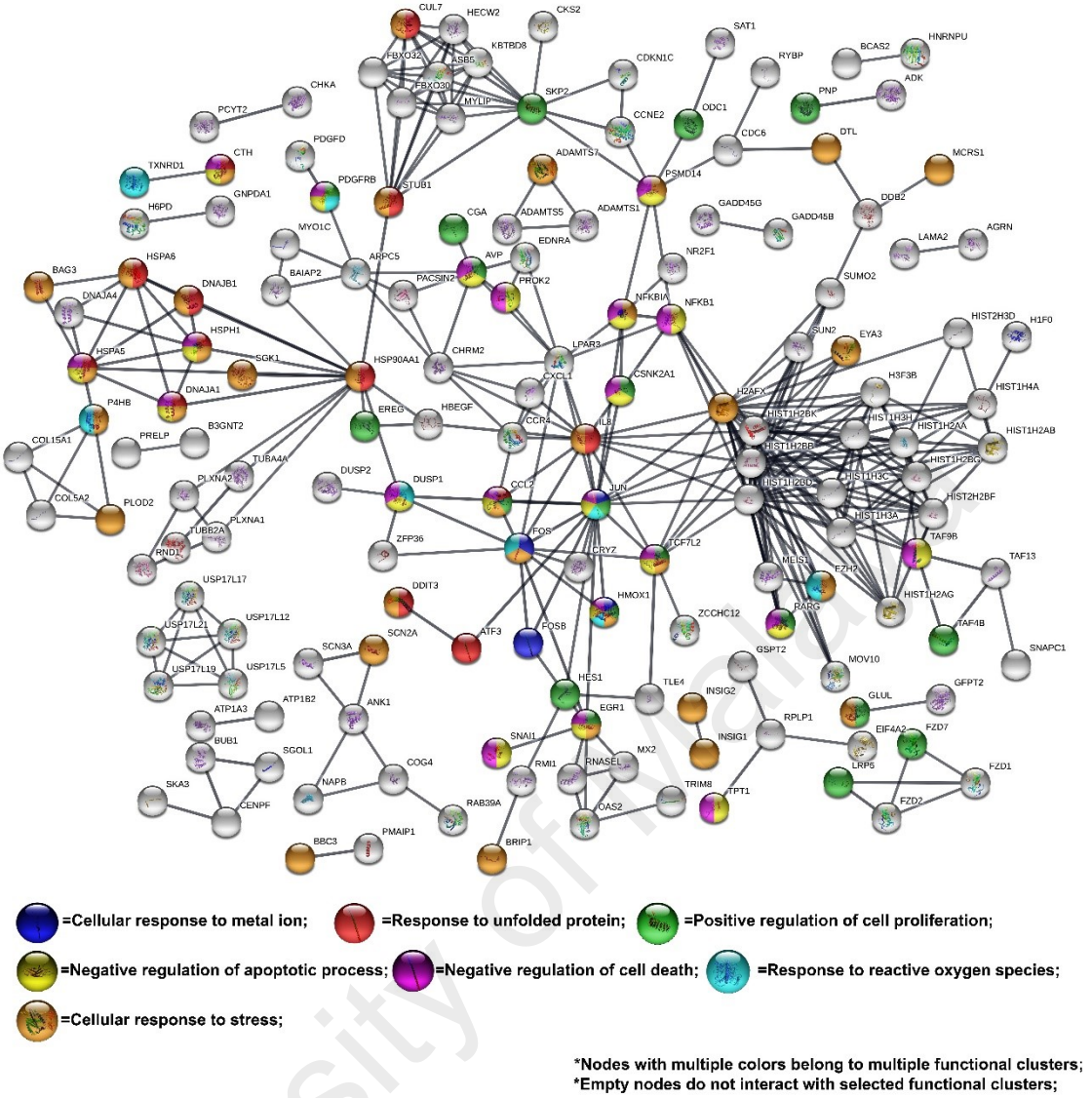

Figure 4.79: STRING network analysis of MP-EA+$CdCl_2$ dataset (FC ≥ ±2.50). The figure illustrates the networks and interactions among the 159 DEGs that were predicted by STRING. The interaction figure was generated using the highest confidence value (≥ 0.9). The functional clusters, "cellular response to metal ion", "response to unfolded protein", "positive regulation of cell proliferation", "negative regulation of apoptotic process", "negative regulation of cell death", "response to reactive oxygen species" and "cellular response to stress", were identified in the network.

CHAPTER 5: DISCUSSION

5.1 Extraction yield

The yield for the extraction of plant materials is generally dependent on the extraction methods, the types of solvent used, as well as physical and chemical properties of plant phytochemicals (J. Dai & Mumper, 2010). In the present study, sequential extraction was employed to obtain MP leaf extracts using solvents of varying polarity. This may help separate the phytochemical constituents according to their polarity. The use of solvents of varying polarity may also provide a broader coverage of extraction conditions and this could lead to higher mass transfer of plant phytochemicals. In present study, the extraction yield was increased with increasing polarity of the solvent and polar solvents (water and methanol) had the yield of approximately 80% (**Table 4.1**). This indicates that MP leaves contain mainly polar compounds.

5.2 Antioxidant activity of *Melicope ptelefolia*

Phenolic compounds are the major constituents responsible for antioxidant activities in plants. They act as free radical scavengers, metal chelating agents and chain breaking antioxidants (Pereira, Valentão, Pereira, & Andrade, 2009). The varying TPC values demonstrated by the extracts suggest that MP leaves contained phenolics of varying polarities. The present study indicated that MP leaves contain predominantly polar phenolic compounds, although substantial amount of semi-polar and non-polar phenolic compounds was also detected in the leaves, as reflected by MP-HX and MP-EA TPC values (**Figure 4.2, Table 4.1**).

The estimation of flavonoids content in plant extracts is of significance for the assessment of its nutraceutical value, since flavonoids are phytonutrients that are

renowned for their antioxidant activity. Flavonoids could prevent oxidative stress through the modulation of ROS generating enzymes activity, scavenging of free radicals and chelation of metal ions. Flavonoids also exhibit various health promoting bioactivities, which include anticancer, antimicrobial, anti-inflammatory and hepatoprotective activities (M. Abbas et al., 2017); (Tapas, Sakarkar, & Kakde, 2008). A similar observation as TPC was found for TFC. Data showed that MP extracts contained flavonoid compounds of varying polarities. About 46% of them were semi-polar and non-polar flavonoids (**Figure 4.4, Table 4.1**).

Several chemical antioxidant assays namely $DPPH^{\bullet}$ and $ABTS^{\bullet+}$ radical scavenging and FRAP were employed to evaluate antioxidant activity of MP extracts. $DPPH^{\bullet}$ radical-scavenging assay is the most widely used *in vitro* antioxidant assay for evaluation of antioxidant activity. $DPPH^{\bullet}$ is a purple-colored radical which can be reduced by antioxidants to form a yellow-colored 2,2-diphenyl-1-picrylhydrazine, and this reaction can cause a decrease in absorbance value at 517 nm (Sharma & Bhat, 2009). This assay is suitable for measuring radical-scavenging activity of both hydrophilic and lipophilic phytochemicals (Cheng, Moore, & Yu, 2006). In the present study, MP-HX and MP-EA demonstrated potent $DPPH^{\bullet}$ radical scavenging activity (**Figure 4.7, Table 4.2**). In $ABTS^{\bullet+}$ assay, the oxidation of ABTS reagent by potassium persulfate ($K_2S_2O_8$) results in the formation of ABTS radical cations ($ABTS^{\bullet+}$), characterized by a blue-green colored solution. The $ABTS^{\bullet+}$ concentration can be monitored through spectrophotometric measurement at 734 nm (Re et al., 1999). A decrease in absorbance value is observed when $ABTS^{\bullet+}$ is scavenged by antioxidant molecules that are present in the extracts. Data obtained in the present study showed that MP-HX and MP-EA significantly scavenged $ABTS^{\bullet+}$ radicals (**Figure 4.6, Table 4.2**). In FRAP assay, antioxidants can cause the reduction of the yellow-colored ferric-2,4,6-tripyridyl-s-triazine complex (Fe^{3+} -TPTZ) to the ferrous form (Fe^{2+}-TPTZ),

forming a blue-colored product that can be spectrophotometrically monitored at 593 nm (Benzie & Strain, 1996). The amount of Fe^{2+}-TPTZ complex is correlated to the amount antioxidant molecules present in the extract, introduced into the reaction mixture. All the MP extracts showed potent ferric reducing power (**Table 4.2**).

To further verify antioxidant activity of MP extracts, cellular antioxidant activity was assessed in Hs27 cells. CAA assay is generally considered to be more accurate in evaluating the antioxidant potential of phytochemicals or plant extract, as compared to *in vitro* antioxidant assays. This is because the assay utilizes a cell-based model that takes into account of the complex biological processes of a living system, such as the absorption, distribution, metabolism and bioavailability of phytochemicals. These are among the crucial factors that can greatly affect antioxidant capacity (Wolfe & Liu, 2007); (R. H. Liu & Finley, 2005). In comparison to common fruits and vegetables, the findings in the present study indicated that the MP extracts exhibited a more pronounced cellular antioxidant activity (**Figures 4.8** and **4.10, Table 4.2**). The EC_{50} value of MP extracts in Hs27 were ~31 to 956 times lower than blueberry (EC_{50} in HepG2 = 10.81 ± 0.44 mg/mL), and they were ~338 to 10,176 times lower than broccoli (EC_{50} in HepG2 = 115 ± 15 mg/mL) (Wolfe & Liu, 2007); (W. Song et al., 2010). It was found that MP-HX and MP-EA had strong cellular antioxidant activity in Hs27 cells and the observation was in agreement with $DPPH^{\bullet}$ and $ABTS^{\bullet+}$ radical scavenging assays.

Various antioxidant assays are routinely used to evaluate antioxidant potential of food/plant extracts, but they do not necessarily provide consistent picture when compared against each other, due to differences in their antioxidant activity assessment mechanism. Thus, correlation analysis between antioxidant components and antioxidant activities of MP extracts was done to examine the relationships between them (**Table**

4.3). Antioxidant assays were strongly correlated with one another but there was very weak correlation of TPC with DPPH• radical scavenging and CAA assay. In contrast, DPPH• radical scavenging and CAA assay were negatively correlated with TFC. These observations suggest that polyphenols may not be the major constituents that are responsible for the antioxidant activity of MP.

5.3 Anticancer activity of *Melicope ptelefolia*

The present study investigated the anticancer potential of MP extracts towards renowned ATCC cancer cell lines, namely HCT116 (colon cancer), HCC 1937, MDA-MB-231 (breast cancers) and HepG2 (liver cancer). The cell viability assay results indicate that MP-HX and MP-EA contain phytochemicals that are cytotoxic towards the entire cancer cell lines tested. These extracts showed promising antiproliferative activity, as their IC_{50} values were less than 100 μg/mL in almost all of the cancer cell lines tested, except for MP-EA in HepG2 cells, with an IC_{50} value of about 131 μg/mL (**Table 4.4**). MP-HX and MP-EA were also selectively more cytotoxic towards the cancer cells, as they showed higher IC_{50} values (>300 μg/mL) towards non-cancerous cell lines CCD841 and Hs27 (**Table 4.4**). The notable antiproliferative activity demonstrated by MP-HX and MP-EA on the cancer cell lines suggested that apoptosis could be a mechanism of this activity. To investigate the mechanism of antiproliferation activity, apoptosis induction ability of MP-HX and MP-EA was evaluated. Apoptosis is a form of programmed cell death with essential roles in removal of damaged or abnormal cells from the body. Apoptosis is characterized by morphological and cellular changes which include PS extrusion (Van Engeland, Nieland, Ramaekers, Schutte, & Reutelingsperger, 1998), cellular shrinkage and DNA fragmentation (Richardson, Sethi, Lee, & Malek, 2016). Perturbation of apoptosis could arise from overexpression of anti-

apoptotic and/or down regulation of pro-apoptotic proteins, and such scenarios could lead to the development of chronic conditions such as cancer and neurodegenerative diseases (Elmore, 2007). In many types of human cancers, apoptosis is often dysregulated. Thus, when screening for new anticancer drugs, the candidate drug should ideally demonstrate selective cytotoxicity, by its preferential induction of apoptosis in cancer cells with minimal toxicity on non-cancerous or normal cells (Bai & Wang, 2014).

In the present study, the ability of MP-HX and MP-EA to induce apoptosis was evaluated through four different assays, which include measurements of caspase 3/7 activity, multicaspase activity, caspase enzyme inhibition and Annexin-V/7-AAD staining. Caspases (cysteinyl aspartases) are a family of proteolytic enzymes which play a key role in the induction of apoptosis (Li & Yuan, 2008). They are classified as initiator caspases (-2, -8, -9. -10) and executioner caspases (-3, -6, -7) (Riedl & Shi, 2004). Initiator caspases can be activated by the intrinsic or extrinsic pathways, which themselves can activate the executioner caspases and leading to apoptosis induction. Activation of caspase-3/7 is an important biomarker for the detection of apoptosis (Riedl & Shi, 2004). Phosphatidylserine (PS) is a component of a cell membrane that is normally restricted in the inner leaflet of the membrane. During the early stage of apoptosis, PS is extruded to the outer leaflet of the membrane (Van Engeland et al., 1998). Annexin-V is a calcium dependent phospholipid binding protein with a high binding affinity towards PS. The event of annexin-V binding with the PS molecules that are extruded in early apoptotic cells can be detected by flow cytometric analysis. The 7-AAD dye is used to detect the cell membrane structural integrity, as the dye is only permeable to the membrane of dead cells, but impermeable to live and healthy cells, as well as early apoptotic cells. Overall, the results of these assays indicate that MP-HX and MP-EA were able to induce apoptosis in the four cancer cell lines tested. Both

extracts induced activation of multiple caspases in all of the cancer cell lines (**Figures 4.13, 4.14** and **4.15**). The extracts were also able to increase the percentage of apoptotic cells as revealed by annexin-v/7-AAD flow cytometry assay (**Figures 4.16** and **4.17**). The apoptosis induction was also confirmed through pan-caspase inhibitor (z-VAD-FMK) assay. The inhibitor was able to reduce the cytotoxicity of MP-HX and MP-EA in all of the cancer cell lines tested, in a dose-dependent manner, validating their apoptosis induction ability (**Figure 4.18**).

Cell cycle distribution of the cells were also investigated. The cell cycle is composed of Go, G_1, S, G_2 and M phases and a dysregulation in cell cycle is often observed in cancer development (Vermeulen, Van Bockstaele, & Berneman, 2003). Chemotherapeutic drugs may exert anticancer effect through the inhibition of cancer cell proliferation by disrupting selected phases of the cell cycle (G. I. Shapiro & Harper, 1999). The cell cycle assay results suggest that MP-EA and MP-HX had the potential to disrupt cell cycle progression in three (HCT116, HepG2 and MDA-MB-231) of the four cancer cell lines (**Figures 4.19** and **4.20**).

5.4 Molecular mechanism of anticancer activity of *Melicope ptelefolia*

In the present study, the anticancer activity of MP-HX against HepG2 and HCT116 cells was characterised through microarray gene expression profiling followed by bioinformatics analysis using TAC and IPA softwares. The microarray data was validated by performing RT-qPCR assay on selected genes that were differentially regulated. The direction of gene expression changes for the 17 genes selected for RT-qPCR assay was in agreement with the microarray data.

TAC software analysis revealed that MP-HX significantly regulated many Wikipathways (WP) associated with cell cycle, cell proliferation and cell death. The pathways that were modulated include "retinoblastoma (RB) in cancer", "G_1 to S cell cycle control", "cell cycle", "DNA damage response" and "apoptosis".

The "Retinoblastoma in cancer" Wikipathway (RIC-WP) was the top pathway that was significantly regulated in both cell lines **(Figures 4.23** and **4.24)**. The RIC-WP mainly consists of Rb family protein pRb (also known as RB1), cyclin dependent kinases (CDKs), cyclin dependent kinase inhibitors and E2F proteins. The pRb protein acts as a tumor suppressor by inhibiting the function of E2F transcription factors, leading to inhibition of cell cycle progression (Giacinti & Giordano, 2006). The presence of CDKs in the G_1 phase of the cell cycle inactivates pRb through phosphorylation, allowing the cells to enter S-phase and initiate DNA replication (Henley & Dick, 2012). The phosphorylation of pRb by CDKs are prevented by CDK inhibitors INK4 (p15, p16, p18, and p19) and Cip/Kip (p21, p27 and p57) (Asghar, Witkiewicz, Turner, & Knudsen, 2015). In both cell lines, the concomitant decrease in the expression of E2F, CDK1, CDK2, CDK6, CCNA2, CCNB1, CCNB2, CCNE1 and CCNE2 as observed in the dataset may have conferred a synergistic effect, leading to MP-HX antiproliferative activity.

Cyclin dependent kinase inhibitor 1A (CDKN1A) (also known as p21) is an inhibitor of CDK in RIC-WP. CDKN1A expression was upregulated in both HCT116 and HepG2 (**Table 4.5**). CDKN1A is a sensor and effector of multiple antiproliferative signals and capable of inducing cell cycle arrest (T. Abbas & Dutta, 2009). MP-HX also induced downregulation of E2F and CDKs expression in both HepG2 and HCT116 **(Figures. 4.23** and **4.24)**. These facts are in accordance with CDKN1A upregulation as

noted above, and these events are likely to contribute to the inhibition of G_1/S transition, leading to antiproliferative effect by MP-HX in both cell lines.

Cyclin A2 (CCNA2) is a component of RIC-WP. CCNA2 was downregulated by MP-HX in both HCT116 and HepG2 (**Table 4.5**). This gene is widely expressed in many tissues with important roles in mediating G_1-S and G_2/M transitions (Hochegger, Takeda, & Hunt, 2008). Cyclin A2 promotes DNA replication during S-phase by activating CDK2. It also activates CDK1 to induce mitotic entry (Wolgemuth, 2008); (Hochegger et al., 2008). CCNA2 overexpression has been reported in numerous types of cancers (Uhlen et al., 2010).

Ribonucleotide Reductase Regulatory Subunit-M2 (RRM2) is another component of RIC-WP that was downregulated by MP-HX in both HCT116 and HepG2 (**Table 4.5**). RRM2 is a subunit of ribonucleotide reductase (RNR). It catalyzes conversion of NDP to dNDP, which is pivotal for the supply of nucleotides for DNA synthesis and cell proliferation. RRM2 can be classified as an oncogene as its overexpression in transgenic mice promoted tumour development (Furuta, Okuda, Kobayashi, & Watabe, 2010). RRM2 overexpression in epithelial ovarian carcinoma (EOC) cases predicts a shorter overall survival. Knockdown of RRM2 in EOC cell lines inhibited its proliferation and triggers cellular senescence (Aird, Li, Xin, Konstantinopoulos, & Zhang, 2014).

MP-HX also modulated "G_1 to S cell cycle control" Wikipathway (G_1SCC-WP) in both cell lines **(Figures 4.25** and **4.26)**. Cyclin Dependent Kinase Inhibitor 2B (CDKN2B) is a component of G_1SCC-WP that was upregulated after treatment with MP-HX in HCT116 and HepG2 (**Table 4.5**). CDKN2B encodes a cyclin-dependent kinase inhibitor, which can form a complex with CDK4 or CDK6, and prevents the activation of the CDK kinases (Santo, Siu, & Raje, 2015). CDKN2B is capable of inhibiting CDK4/6 activity by preventing them from hyperphosphorylating RB proteins,

leading to G_1 cell cycle arrest (W. Y. Kim & Sharpless, 2006). CDKN2B was reported to be deleted in a wide variety of human tumors (W. Y. Kim & Sharpless, 2006). Inactivation of this gene promoted carcinogenesis in hepatocellular and colorectal carcinoma (Ren et al., 2015); (Ishiguro et al., 2006).

GADD45A is another component gene in G_1SCC-WP that was upregulated by MP-HX in HCT116 and HepG2 (**Table 4.5**). This gene is a member of growth arrest and DNA damage (GADD) family of proteins. GADD45A upregulation is often induced by DNA damage and other stress signals associated with growth arrest and apoptosis (Salvador, Brown-Clay, & Fornace, 2013). GADD45A interactions with CDK1, cyclin B1 and p21 can inhibit cell cycle progression and induce apoptotic cell death through JNK/p38 pathway (Zhan, 2005). During G_2/M checkpoint, GADD45A can arrest cell cycle progression by inhibiting cyclin-B1 and CDC2 interaction, preventing entry into M-phase. Repression of GADD45A expression alleviated G_2/M arrest (Rosemary Siafakas & Richardson, 2009).

The "Cell cycle Wikipathway" (CC-WP) was also significantly modulated by MP-HX treatment in both cell lines **(Figures 4.27 and 4.28)**. The CC-WP member genes include cyclins and CDKs proteins, which are responsible for the promotion of cell cycle progression. These proteins are frequently overexpressed in numerous types of cancer (Asghar et al., 2015). In both cell lines, MP-HX downregulated many of the cyclins and CDKs genes, including CCNA2, CCNB1, CCNB2, CCNE2, CDK1, 2 and 6. Downregulation of these genes likely contributed to MP-HX inhibition of cell cycle progression in the cancer cells. Many anticancer drugs have been reported to exert anticancer effect by arresting cell cycle progression at G_1/S and G_2/M transition points, and this is achieved through the inhibition of key proteins that promote cell cycle progression (Santo et al., 2015); (Dominguez-Brauer et al., 2015).

The CC-WP also include minichromosome maintenance (MCM), S-phase kinase-associated protein 2 (SKP2) and Polo-like kinase 1 (PLK1) genes. These genes were also downregulated by MP-HX in both cell lines. The MCM family of proteins play important roles in replication, transcription, checkpoint response and cancer progression (Forsburg, 2004); (Deegan & Diffley, 2016). MCM2 was markedly downregulated by MP-HX treatment in HCT116 and HepG2 (**Table 4.5**). MCM2 is a component member of Mcm2-7 complex. The complex unwinds parental DNA to form single-stranded DNA template during replication (Simon & Schwacha, 2014). MCM2 overexpression has been reported in colorectal, glioma and oral squamous cell carcinomas (Guzińska-ustymowicz, Pryczynicz, Kemona, & Czyżewska, 2009); (Razavi, Jafari, Heidarpoor, & Khalesi, 2015); (Hua, Zhao, Li, & Bie, 2014). MCM10 was also significantly downregulated by MP-HX treatment in HCT116 and HepG2 (**Table 4.5**). MCM10 is thought to be essential for activating MCM2-7 helicase activity, since the unwinding of origins of replication is defective in the absence of MCM10 (Deegan & Diffley, 2016). MCM10 and MCM2 overexpression have been reported in urothelial and cervical cancers (W.-M. Li et al., 2016); (Das et al., 2013). Of note, MP-HX also downregulated other MCMs, which include MCM3 (MA_FC: -4.15, -2.90) and MCM7 (MA_FC: -2.79, -1.53) in HCT116 and HepG2, respectively.

SKP2 is a component of ubiquitin–proteasome system (UPS), which plays vital roles in regulating the degradation of various cellular proteins (Z. Wang et al., 2012). This gene was downregulated in both HCT116 and HepG2 (**Table 4.5**). SKP2 is a subunit in SKP1–Cullin1–F-box (SCF) E3 ligase complex. SKP2 is a F-box protein of the SCF complex SCF^{SKP2} E3 ligase, which targets many tumor suppressor proteins (eg. p27, p21, p57, TOB1, FOXO1) for degradation. For this reason, it is not surprising that overexpression of SKP2 is observed in diverse type of human cancers (Z. Wang et al., 2012).

Polo-like kinase 1 (PLK1) is a member of polo-like kinase family. PLK1 was also downregulated in HCT116 and HepG2 (**Table 4.5**). PLK1 roles include regulation of mitotic entry, centrosome separation and maturation, kinetochore attachment and cytokinesis (Schmucker & Sumara, 2014). PLK1 was reported to be overexpressed in various cancers and thought to confer tolerance of cells to cancer associated cellular stress (Strebhardt, 2010). Inhibition of PLK1 was also reported to induce anticancer effect in hepatocellular carcinoma and retinoblastoma cell lines (Xu et al., 2017); (Schwermer et al., 2017). Up to this point, it is interesting to note that in both cell lines, MP-HX downregulated all six top-ranked genes (PLK1, MCM2, MCM3, MCM7, MCM10 and SKP2) that were proposed to be cancer-associated (C. Wu, Zhu, & Zhang, 2012).

MP-HX also modulated many components genes of "DNA damage response Wikipathway" (DDR-WP) in both cell lines (**Figures 4.29** and **4.30**). The expression of genes in DDR-WP can be induced by genotoxic agents or environmental stress such as UV and ionizing radiation, and the response could lead to induction of cell cycle arrest and mobilisation of DNA repair mechanisms to circumvent DNA damage (O'Connor, 2015). In both HCT116 and HepG2, MP-HX downregulated some of the genes in DDR-WP, which include CHEK1, RAD51, CDC25A, cyclins and CDKs expression, while CDKN1A, BBC3 and GADD45A expression were upregulated. With regards to their functions, CHEK1, RAD51 and CDC25A have been suggested to promote tumor development, while GADD45A can act as a tumor suppressor (Hosoya & Miyagawa, 2014); (Broustas & Lieberman, 2014). CDKN1A, as discussed earlier, can induce cell cycle arrest through inhibition of cyclins and CDKs. BBC3 is a pro-apoptotic protein which is capable of suppressing cancer development (Yu & Zhang, 2008), and a more detailed description of its role is discussed below.

MP-HX treatment also modulated "Apoptosis Wikipathway" (AP-WP) in both cell lines (**Figures 4.31** and **4.32**). Apoptosis is a form of programmed cell death, characterized by chromatin condensation, cytoplasmic shrinkage, membrane blebbing and nuclear fragmentation (Wong, 2011). Many types of cancers are known to evade apoptosis for their survival (Hanahan & Weinberg, 2011). Apoptotic signaling is modulated by BCL-2 anti-apoptotic and pro-apoptotic family proteins, inhibitor of apoptosis proteins (IAP), p53 tumor suppressor, caspases and death receptor signaling (Wong, 2011). The Bcl-2 family of proteins is one of the major regulators of apoptosis, namely the intrinsic pathway of apoptosis. This family contains pro-apoptotic and anti-apoptotic (or pro-survival) protein members (Delbridge & Strasser, 2015). An imbalance in the amount of BCL-2 family of proteins, overexpression of IAP proteins, inhibition of caspases, reduced p53 function and impaired death receptor signaling are responsible for the development of cancer and chemoresistance (Pistritto, Trisciuoglio, Ceci, Garufi, & D'Orazi, 2016). Therefore, targeting proteins which modulate apoptosis is of key interest in cancer therapy (Goldar, Khaniani, Derakhshan, & Baradaran, 2015). Apoptosis modulating drugs may inhibit BCL-2 anti-apoptotic proteins, IAP proteins or activate BCL-2 pro-apoptotic proteins, caspase enzymes and p53 functions to confer anticancer effect (Wong, 2011).

MP-HX treatment induced upregulation of BBC3 in HCT116 and HepG2 (**Table 4.5**). BBC3 is a pro-apoptotic gene of the BCL-2 family. At the same time, MP-HX treatment induced downregulation of BIRC5, which is an inhibitor of apoptosis (IAP) protein, in HCT116 (MA_FC: -3.44) and HepG2 (MA_FC: -1.82). BBC3 is known to facilitate p53-dependent or independent apoptosis (Yu & Zhang, 2008) while BIRC5 was reported to be overexpressed in various type of cancers (R. J. Kelly, Lopez-Chavez, Citrin, Janik, & Morris, 2011). BBC3 antagonizes anti-apoptotic members of BCL-2 to promote cell death. BBC3 colocalizes in mitochondrial membrane to inhibit anti-

apoptotic BCL-2 family members, while activating pro-apoptotic BAX/BAK, causing outer mitochondrial membrane permeabilization and leading the initiation of mitochondrial pathway of apoptosis. Inhibition or deletion of BBC3 impairs apoptosis and contributing to the development of cancer and chemo-resistance (Hikisz & Kilianska, 2012).

MP-HX also induced the upregulation of another AP-WP member, PMAIP1 (NOXA) in HCT116 (MA_FC: +1.69) and HepG2 (MA_FC: +3.10). In HepG2 cells, MP-HX upregulated pro-apoptotic gene BAK1 (MA_FC: +2.14), another member of AP-WP. NOXA is capable of inactivating anti-apoptotic members of BCL-2 family, allowing BAK and BAX to interact with pro-apoptotic members of BCL-2 and leading to apoptosis (Hata, Engelman, & Faber, 2015); (Albert, Brinkmann, & Kashkar, 2014).

Helicase, lymphoid specific (HELLS) is another component member of AP-WP that was downregulated by MP-HX in both HCT116 and HepG2 (**Table 4.5**). HELLS demonstrated diverse functions, which include epigenetics regulation of development, co-activator of E2F to stimulate cell growth and DNA repair (Mjelle et al., 2015). HELLS can promote cancer, as it enhances growth, migration, and invasion of nasopharyngeal carcinoma cell lines (He et al., 2016). Overexpression of HELLS was also reported in prostate and oropharyngeal squamous cell carcinomas (von Eyss et al., 2012); (Janus et al., 2011). Increased HELLS expression was associated with poor prognosis in patients with renal cell carcinoma (D. Chen et al., 2017).

JUN (also known as c-JUN) is another component member of AP-WP that was upregulated by MP-HX in HCT116 and HepG2 (**Table 4.5**). JUN proto-oncogene is a component of the AP-1 transcription factor that demonstrated cancer promoting, as well as apoptotic induction activities (Eferl et al., 2003); (Fan & Chambers, 2001); (Dhanasekaran & Reddy, 2008); (Bossy-Wetzel, Bakiri, & Yaniv, 1997). In glioma cells

treated with temozolomide and nimustine, apoptosis was achieved through c-JUN mediated activation of BIM (BCL-2 interacting mediator of cell death) (Tomicic et al., 2015). The anticancer activity of tylophorine, an alkaloid from *Tylophora indica* was also demonstrated to be mediated by c-JUN in HONE-1, NUGC-3 and HepG2 carcinoma cells. The upregulation of c-JUN by tylophorine resulted in cyclin A2 transcriptional repression, leading to G_1 cell cycle arrest (C. W. Yang et al., 2013). The induction of pro-apoptotic and downregulation of anti-apoptotic genes suggests that MP-HX promoted network signaling or transcriptome profile favoring apoptosis induction. This finding is consistent with the previous sections, which described apoptosis induction of MP-HX on four different cancer cell lines (**Sections 4.3** and **5.3**).

IPA software analysis also revealed that MP-HX modulated many canonical pathways, biological functions and gene networks linked to cell cycle, cell proliferation, DNA replication, DNA damage, cell death and apoptosis in both HepG2 and HCT116 cell lines. IPA ranked nuclear protein 1 (NUPR1) as the top upstream regulator that was activated in both cell lines by MP-HX treatment. The microarray data also showed that MP-HX upregulated NUPR1 expression in both HCT116 (MA_FC +1.27) and HepG2 (MA_FC +2.40) cell lines. NUPR1 is a transcription factor that has been reported to show tumor inhibiting and promoting activities. NUPR1 was able to inhibit tumor progression in brain and prostate cancers, as well as being overexpressed in several other cancers (Goruppi & Iovanna, 2010). A recent study reported NUPR1 acted as a negative regulator of tumor repopulating cells (TRCs) growth (Q. Jia et al., 2016). The above observations suggest NUPR1 had a significant role in mediating MP-HX anticancer activity. Future study could investigate this hypothesis by silencing NUPR1 expression in MP-HX treated cells.

IPA analysis also predicted tumor protein 53 (TP53) as another top upstream regulator that was activated in both cell lines. TP53 is a classical tumor suppressor gene which is frequently mutated in cancers (Leroy et al., 2014). TP53 and its target genes are renowned for their involvement in cell cycle arrest, DNA repair and apoptosis (Fischer, 2017). IPA also predicted RABL6 (RAB, member RAS oncogene family like 6) as another top upstream regulator that was modulated by MP-HX treatment, although it was predicted to be inhibited in both cell lines. The microarray data showed that RABL6 was mildly downregulated in HepG2 and HCT116 (MA_FC of -1.11 and -1.28, respectively). RABL6 has been reported to promote proliferation of osteosarcoma and pancreatic neuroendocrine tumor through inhibition of retinoblastoma 1 (pRb) (Tang et al., 2016); (Hagen et al., 2014). RABL6 also enhanced MDM2-induced TP53 degradation (Lui et al., 2013). These highlight RABL6 tumor promoting properties. The activation or inhibition of the above transcriptional regulators in both cell lines likely played significant roles in modulating the antiproliferative effect induced by MP-HX, and a more detailed investigation on their contributions could be explored in future studies.

IPA software network analysis suggested N-myc Downstream Regulated 1 (NDRG1) as a focus molecule in both HCT116 (network 2) and HepG2 (network 2) cells. NDRG1 expression was upregulated by MP-HX in both HCT116 and HepG2 cells (**Table 4.5**). NDRG1 demonstrated anti-oncogenic function and was proposed to be a metastasis suppressor in diverse type of cancers (Fang et al., 2014). NDRG1 is capable of blocking metastasis by activating cell adhesion molecules (E-cadherin, β-catenin), and inhibiting snail/slug, Wnt signaling and ROCK1/pMLC2 pathways (Bae et al., 2013). GINS complex subunit 2 (GINS2) is another focus molecule highlighted by IPA network analysis. GINS2 is a component member of network 1 in HepG2 and network 5 in HCT116 cells, and its expression was downregulated in both HCT116 and HepG2 cell

lines (**Table 4.5**). GINS2 is a component of 'GINS complex', a tetrameric complex with crucial roles in the initiation of DNA replication, including correct assembly and maintenance of DNA replication forks and its progression during replication (Gambus et al., 2006). GINS2 upregulation was associated with poor prognosis and reduced survival in early-stage cervical cancer (F. Ouyang et al., 2017). In breast cancer patients, elevated GINS2 transcript level was associated with poor relapse-free and distant metastasis-free survival (Zheng et al., 2014).

5.5 Gene expression analysis – transcriptome profiles induced by *Melicope ptelefolia*, quercetin and dexpanthenol in Hs27 cells

The present study was conducted to investigate the effect of MP extracts (MP-HX and MP-EA), QN and DX on human skin fibroblast cells (Hs27) proliferation and gene expression profile. The two extracts were previously shown to contain appreciable polyphenols content and demonstrated notable antioxidant activity (**Tables 4.1** and **4.2**). On the other hand, QN and DX are well known phytochemical and topical drug agent, respectively. The effect of these agents on skin fibroblast proliferation and gene expression profile may provide insights on their beneficial use in skin health or cosmetic and dermatological applications.

In the present study, MP extracts, QN and DX treatments were noted to induce differential expression of approximately 14-15,000 genes (FC $\geq \pm 1.50$) in Hs27 cells, of which approximately 50% of the genes were upregulated and 50% were downregulated in each of the cases (**Figure 4.44**). Furthermore, approximately half of the DEGs (totalling 7983 genes) were shared among the four datasets (**Figure 4.45**). Numerous antioxidant genes including CAT, GPx (GPx1, GPx5, GPx7, GPx8), SOD2, GSR, GST

(GSTK1, GSTP1, GSTT1, GSTT2, MGST1), PRDX (PRDX 4, PRDX 5, PRDX 6) were commonly upregulated by the four treatments (**Table 4.11**).

Catalase (CAT) is a well-known antioxidant enzyme, which can neutralize hydrogen peroxide (H_2O_2) by reducing it into water. This could prevent excessive accumulation of H_2O_2, protecting the cells against H_2O_2-induced oxidative stress. Although CAT is considered as a housekeeping gene, its expression can be activated by transcription factors such as SP1, NF-Y, XBP1, FOXO1, FOXO3a, FoxM1 and PPARγ (Glorieux, Zamocky, Sandoval, Verrax, & Calderon, 2015). Certain polymorphisms in the DNA sequence of CAT could lead to its reduced expression, and this is associated with several diseases including diabetes, hypertension, asthma, vitiligo and cancer. Abnormal expression of CAT has been reported in cancer, however, depending on the types of cancers, the expression may be lower or higher (Glorieux et al., 2015).

Glutathione-disulfide reductase (GSR) was also upregulated by all treatments (**Table 4.11**). GSR is an enzyme that is needed for regenerating glutathione (GSH). GSH is a thiol containing antioxidant molecule that is involved in processes such as redox homeostasis, detoxification, cellular signaling, proliferation, apoptosis and DNA repair (Kalinina et al., 2014). Although GSR plays important roles in cellular homeostasis, its overexpression may promote cancer, as its overexpression has been reported to induce glioblastoma resistance against chemodrug-induced oxidative stress (Zhu et al., 2018).

GSTP1 was also significantly upregulated in Hs27 cells by all of the treatments (**Table 4.11**). GSTP1 is a member of glutathione S-transferases (GST) family. The GST family is composed of isoenzymes that neutralize electrophiles by conjugating it with glutathione and this contributes to GSH antioxidant function (Kalinina et al., 2014). The expression of GSTP1 is regulated by specificity protein 1 (SP1), activator protein 1 (AP-1), nuclear factor kappa-light-chain-enhancer of activated B cells (NF-κB) and

GATA binding protein 1 (GATA1) (Schnekenburger, Karius, & Diederich, 2014). GSTP1 mediated conjugation of hydroperoxides and catecholamines to GSH prevents oxidative stress (Kalinina et al., 2014). GSTP1 also plays important roles in the regulation of oxidative stress that can be activated by JNK1, ERK1/ERK2 and TRAF2 cell death signaling (Schnekenburger et al., 2014).

IPA analysis indicated that "EIF2 signaling" was one of the most significant canonical pathways (CPs) enriched by all treatments. EIF2S1 (also known as EIF2, EIF2α) was noted to be upregulated in all of the datasets (FC induced by MP-HX: +1.71, MP-EA: +1.54, QN: +1.74, DX: +1.62). Consistent with IPA finding, the dataset for all treatments showed that components of EIF2 signaling were upregulated – the expression of EIF2S2 (also known as EIF2β), EIF2AK1 (also known as HRI), EIF2AK3 (also known as PERK), EIF2AK4 (also known as GCN2) and ATF4 were upregulated by MP-HX, MP-EA, QN and DX (**Table 4.18**). The four datasets also showed significant upregulation of EIF2AK2 (also known as PKR) with FC values of +1.97, +1.89, +1.83 and +1.84, respectively.

Eukaryotic translation initiation factor 2 (EIF2, EIF2α) is required for the initiation of translation or protein synthesis (Bellato & Hajj, 2016); (Baird & Wek, 2012). EIF2α kinases are a family of serine-threonine kinases, comprising PKR-like ER kinase (PERK), general control non-derepressible-2 (GCN2), heme-regulated inhibitor (HRI) and protein kinase double-stranded RNA-dependent (PKR). These kinases determine the functional status of EIF2α (Donnelly, Gorman, Gupta, & Samali, 2013). During various stress conditions, such as oxidative stress, endoplasmic reticulum (ER) stress, viral infection and nutrient deprivation, the α subunit of EIF2 (EIF2α) is phosphorylated by EIF2α kinases, and this generally lead to the inhibition of protein translation (Baird & Wek, 2012). However, phosphorylated EIF2α could also result in the enhancement of

ATF4, which is a stress-related transcription factor, facilitating an integrated stress response which restores cellular homeostasis (Baird & Wek, 2012); (Pakos-Zebrucka et al., 2016). EIF2α mediated ATF4 activation protects the cells against oxidative stress, facilitate detoxification and promote cellular growth (Ameri & Harris, 2008); (Donnelly et al., 2013). *In vivo* study showed that phosphorylation of EIF2α reduced oxidative stress in pancreatic beta cells (Back et al., 2009). Consistent with this observation, it has been reported that impaired phosphorylation of EIF2α resulted in oxidative stress, while adequate EIF2α phosphorylation protected mouse embryonic fibroblasts from oxidative damage (Lewerenz & Maher, 2009). It has also been reported that activation of EIF2 signaling in mouse fetal liver (FL) cells inhibited oxidative stress via HRI and ATF4 mediated upregulation of antioxidant genes HO-1, GST-μ, NQO1 and SOD2 (Suragani et al., 2012). In contrast, deletion of HRI and ATF4 enhanced oxidative stress in mouse FL cells (Suragani et al., 2012). The upregulation of EIF2 kinases and ATF4 as observed in the present study suggest that "EIF2 signaling" is activated by all treatments. This CP might be involved in the modulation of oxidative status and upregulation of antioxidant genes as observed in MP-HX, MP-EA, QN and DX datasets.

The gene ontology terms "Cell cycle" (GO:0007049) and "Cell proliferation" (GO:0008283) were investigated to evaluate the modulation of genes related to cell cycle progression and proliferation in Hs27 cells by MP-HX, MP-EA, QN and DX treatments. This could shed insights to help identify relevant genes responsible for induction of cell cycle and proliferation in Hs27 cells. The analysis revealed that MP-HX, MP-EA, QN and DX treatments significantly upregulated numerous cell cycle genes, including cyclins B (CCNB1, CCNB2), cyclin E (CCNE1), CDKs (CDK1, CDK4, CDK7) and E2F transcription factors (E2F4, E2F5) (**Table 4.17**). Other genes notably upregulated were member of MCM genes (MCM2, MCM3, MCM4, MCM6,

MCM7), ORC1, PCNA, DNA polymerases (POLA2, POLD3, POLE2), replication proteins (RPA1, RPA2) and other cell cycle regulatory genes (**Table 4.17**). Furthermore, polo-like kinases (PLK1, PLK4) were significantly upregulated by MP-EA, QN and DX (**Table 4.17**) and. A more detailed role of these genes is discussed below.

Cyclin-dependent kinases (CDKs), principally CDK1, CDK2, CDK4 and CDK6 and their binding partner cyclins (cyclin A, B, D, E) play crucial roles in various stages of the cell cycle to regulate cell cycle progression (Lopez-Mejia & Fajas, 2015). The binding of cyclin D with CDK4/6 and cyclin E with CDK2 results in the phosphorylation of Rb family proteins (pRb, pRb1, pRb2) in the G_1 stage of the cell cycle (Duronio & Xiong, 2013), and this could result in cell cycle activation. Hyperphosphorylated Rb protein is permissive for E2F transcription factors activation, allowing induction of genes necessary for G_1/S transition (Duronio & Xiong, 2013). The replication of DNA occurs in the S-phase of the cell cycle, which is an essential requirement prior to mitotic phase entry. The replication of DNA starts at the origin of replication and involves several steps, including selection of replication origin, assembly of pre-replication complex (pre-RC), activation of pre-RC, recruitment of replication proteins to origins and firing of origins for DNA synthesis (L. Wu, Liu, & Kong, 2014). During G_1/S transition, the assembly of pre-replicative components (CDC6, MCM, ORC and CDT1 proteins) are stimulated by CDK (cyclin dependent kinase) and Dbf4-dependent protein kinase (DDK) which is followed by association of RPA, primase-POLA, PCNA, topoisomerase, CDC45 and DNA polymerase (POLD, POLE) to start DNA replication (L. Wu et al., 2014); (Barnum & O'Connell, 2014). PCNA takes important part in DNA synthesis, DNA damage bypass, DNA repair, cell survival, gene transcription and chromatin assembly (S. C. Wang, 2014). During mitosis, CDK1 interacts with cyclin B to promote cell division. The association of

CDK1 with CCNB1 induces nuclear breakdown, condensation of chromosome and mitotic spindle assembly. CDK1 also binds with CCNB2 to promote mitotic reorganization of Golgi apparatus (Satyanarayana & Kaldis, 2009). Polo-like kinases were also noted to be upregulated, and these have important roles in mitotic cell division (Schmucker & Sumara, 2014); (G. Wang, Jiang, & Zhang, 2014).

In contrast, cell cycle inhibitor CDKN1C and GADD45A was downregulated upon treatment with MP-HX, MP-EA, QN and DX (**Table 4.17**). CDKN1C (p57KIP2) is a Cip/Kip family member of cyclin dependent kinase (CDK) inhibitor (S. Lim & Kaldis, 2013). It inhibits cell cycle progression, regulates apoptosis, and prevents invasion, metastasis and angiogenesis (Kavanagh & Joseph, 2011). GADD45A promotes p53 mediated cell cycle arrest and apoptosis (Siafakas & Richardson, 2009). This gene interacts with CDK1, cyclin B1 and P21 to suppress cell cycle and activates apoptosis through JNK/P38 pathway (Zhan, 2005).

The presents study noted that caspase-8 (CASP8) expression was downregulated by MP-HX, MP-EA, QN and DX (**Table 4.10**). CASP8 is required to induce extrinsic pathway of apoptosis through death receptor (DR) signaling (Holland, 2014). In extrinsic pathway, binding of DR with death ligand leads to formation of FADD (Fas associated protein with death domain) which in turn activates CASP8 (Crowder & El-Deiry, 2012). CASP8 facilitates the activation of CASP3 ('executioner caspase') to induce apoptotic cell death (Crowder & El-Deiry, 2012). Interaction of CASP8 with BCL-2 (pro-apoptotic member BID) contributes indirectly to the intrinsic pathway of apoptosis (Holland, 2014). In the present study, the FC range of CASP3 and BID were +1.02 to -1.17 and -1.05 to -1.28, respectively. This suggests that CASP8 mediated apoptosis was likely not operational or inhibited by MP-HX, MP-EA, QN and DX. FOS (Fos proto-oncogene, ap-1 transcription factor subunit) expression was also noted to be

downregulated by MP-HX treatment (**Table 4.10**), and this gene is known to play important role in cell death. It has been demonstrated that vanadium sulfate triggered apoptosis in human keratinocyte cell line through upregulation of FOS (Markopoulou et al., 2009). Furthermore, *Centella asiatica* was reported to promote DNA damage and apoptosis in HepG2 cells by upregulating FOS (Hussin, Eshkoor, Rahmat, Othman, & Akim, 2014). The autophagy marker GABARAPL1 was noted to be significantly downregulated in Hs27 cells treated with MP-HX, MP-EA, QN and DX (**Table 4.10**). GABARAPL1 belongs to the family of GABA type A receptor associated protein (GABARAP), which can facilitate autophagic cell death (Le Grand et al., 2011). GABARAPL1 has been reported to suppress Wnt/β-catenin signaling to induce autophagic cell death (Y. Zhang et al., 2011). Furthermore, overexpression of GABARAPL1 was reported to inhibit cellular growth (Berthier et al., 2010). TNF-α (also known as TNF) was also downregulated by all treatments (**Table 4.10**). TNF is known to induce apoptotic and necrotic cell death (Chu, 2013). It has been reported that TNF can activate apoptosis through induction of oxidative stress (J. J. Kim, Lee, Park, & Yoo, 2010) and CASP8 (L. Wang, Du, & Wang, 2008).

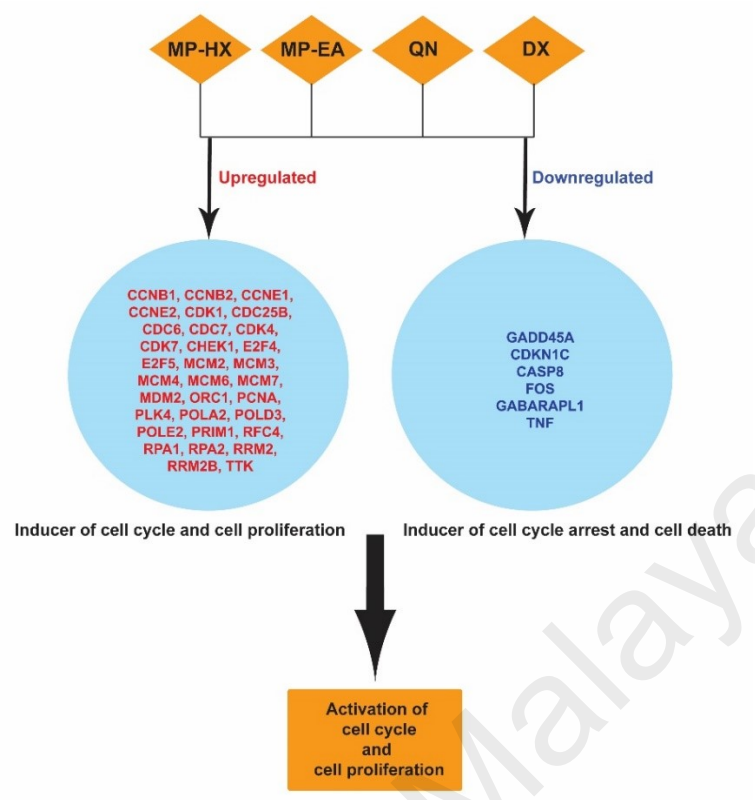

Figure 5.1: Promotion of cell cycle and cell proliferation in Hs27 cells by MP-HX, MP-EA, QN and DX.

The treatments upregulated several genes associated with cell cycle activation and cell proliferation, while they downregulated the genes involved in cell cycle arrest and cell death (**Figure 5.1**). This could explain why MP-HX, MP-EA, QN and DX treatments promoted cellular proliferation in Hs27 cells.

IPA analysis indicated that "Mitotic roles of polo-like kinase" was one of the top CPs modulated by MP-HX, MP-EA and QN treatments (**Table 4.18**). Polo-like kinases are a family of cell cycle kinase consisting of PLK1, PLK2, PLK3, PLK4 and PLK5 (Malumbres, 2011). PLKs exert various roles during cell cycle including DNA replication, chromosome condensation, centriole duplication, cytokinesis, mitotic and anaphase entries. The datasets obtained in the present study indicated that PLK1 and PLK4 were significantly upregulated by MP-EA and QN while PLK4 was slightly upregulated by MP-HX (**Table 4.18)**. DX also upregulated PLK1 and PLK4 (**Table**

4.18). PLK1 is particularly important for mitotic entry, centrosome separation and maturation, kinetochore attachment and cytokinesis (Schmucker & Sumara, 2014). During mitotic entry, BORA (Aurora kinase A activator) is phosphorylated by CDK1 at serine-252 site and promotes PLK1/BORA interaction (Asteriti, De Mattia, & Guarguaglini, 2015). BORA and AURKA interact together to activate PLK1 (Asteriti et al., 2015). Centrosome duplication is required for chromosome separation and maintenance of genomic stability (Lerit & Poulton, 2016). During mitotic phase, PLK1 promotes centriole disengagement and centrosome separation while PLK4 initiates procentriole formation and centrosome duplication (G. Wang et al., 2014). Furthermore, PLK1 recovers cells from DNA damage through inhibition of p53 and induction of Topors, GTSE1 and MDM2 (Hyun, Hwang, & Jang, 2014). In the present study, CDK1 was upregulated by each of the treatment conditions (**Table 4.18)**. Moreover, the expression of BORA (FC by MP-HX: +6.65, MP-EA: +2.49, QN: +4.69, DX: +1.53) and MDM2 (FC by MP-HX: +1.56, MP-EA: +1.79, QN: +1.43, DX: +1.63) was significantly increased by all treatment. MP-EA and QN also upregulated GTSE1 with a FC value of +1.59 and +3.21 respectively. The observations in the present study suggest that polo-like kinases are involved in mediating cell cycle and growth of Hs27 cells for MP-HX, MP-EA, QN and DX treatments.

The skin is the outermost organ which covers our body. It acts as a protective barrier against UV radiation, pathogens and various harmful stimuli. The continuous exposure of skin to external injuries could lead to the loss of skin barrier function and resulting in infection. Skin damage can be repaired through the process of wound healing. Wound healing mainly consists of three sequential steps: inflammation, cellular proliferation and remodeling (Wild, Rahbarnia, Kellner, Sobotka, & Eberlein, 2010). Inflammation is the first response for wound healing to take place, where several cytokines (such as IL-1A, IL-1B, IL-18 and IL-33) and chemokines are released to promote inflammation, and

this event is followed by stimulation of immune function (Kasuya & Tokura, 2014). In the present study, "IL-17 signaling" was one of the top CPs that was modulated by MP-EA, QN and DX, while "IL-17A signaling in fibroblast" was one of the top CPs that was significantly modulated by all treatments (**Table 4.18)**. Interleukin-17 (IL-17) is a family of cytokines containing six members, namely IL-17A, IL-17-B, IL-17C, IL-17D, IL-17E and IL-17F (Iwakura, Ishigame, Saijo, & Nakae, 2011). IL17A (also known as IL-17, IL-17A) is the central member of IL-17 family that is produced mainly by Th17 (T helper 17) cells and plays key roles in host defense against microbial infection and inducing inflammation (X. Song & Qian, 2013b). IL17A is capable of promoting the inflammatory phase of wound healing (Brockmann, Giannou, Gagliani, & Huber, 2017). IL17A acts on immune cells, epithelial cells, fibroblasts, endothelial cells and keratinocytes (X. Song & Qian, 2013b). IL17A binding to IL-17 receptors (IL17RA and IL17RC) facilitates the recruitment ACT1, which is an IL17A mediator (X. Song & Qian, 2013a). ACT1 activates NF-κB, MAPK and C/EBP signaling with the help of TRAF6, to induce inflammatory response (X. Song & Qian, 2013a). The present study shows that IL-17 receptors (IL17RA, IL17RC), TRAF3IP2 (ACT1), NFKB2, MAPKs (MAP2K6, MAPK11, MAPK13, MAPK14), cytokines (IL6, IL9) and chemokines (CCL2, CCL11, CXCL1, CXCL5, CXCL8) were upregulated in all four datasets (**Table 4.18**). CEBPA was also upregulated by MP-HX, MP-EA, QN and DX with a FC of +1.52, +1.23, +1.46 and +1.27 respectively. IL1A (FC by MP-HX: +1.48, MP-EA: +1.37, QN: +1.54, DX: +1.09) and IL1B (FC by MP-HX: +2.33, MP-EA: +2.25, QN: +2.45, DX: +1.96) were also upregulated by the treatments. CEBPA expression was reported to be repressed in diabetes, and this contributes to chronic inflammation that could lead to complications associated with diabetic wound (Wicks et al., 2015). The above observations suggest that inflammatory phase of wound healing may be promoted

by MP-HX, MP-EA, QN and DX treatments without unfavorable outcome, since CEBPA expression was not downregulated.

During the cell proliferation phase of wound healing, several growth factors (including TGF-β, PDGF, bFGF and IGF-1) are stimulated, to promote granular tissue formation (Wild et al., 2010). Growth factors has many functions in wound healing which include inflammation, angiogenesis, granular tissue formation, collagen synthesis and remodeling (Barrientos, Stojadinovic, Golinko, Brem, & Tomic-Canic, 2008); (Behm, Babilas, Landthaler, & Schreml, 2012). Macrophages, fibroblasts, granulocytes, capillaries and collagen bundles are the main components of granular tissue. Fibroblast synthesizes collagen III and extracellular matrix at the end of cell proliferation phase (Reinke & Sorg, 2012). In the present study, the growth factor TGFB1 was upregulated by MP-EA, QN and DX with a FC of +1.35, +1.96, +1.89 respectively. Collagen III (COL3A1) was also upregulated (FC by MP-HX: +1.28, MP-EA: +2.34, QN: +1.67, DX: +2.63). In addition, several genes involved in cell proliferation and cell cycle activation were upregulated by the treatments (**Table 4.17**). Overall, the findings indicated above suggest that MP-HX, MP-EA, QN and DX could promote wound healing as they induced the upregulation of genes that could promote cell proliferation and inflammatory phases of wound healing.

During remodeling, collagen III is converted to collagen I, while myofibroblast contributes to the contraction of wounds through its association with collagen I (Reinke & Sorg, 2012). As a result, recovery from wound is achieved. The present study noted that COL1A1 was significantly upregulated by MP-HX, MP-EA, QN and DX with a FC of +2.33, +2.18, +1.83 and +2.52 respectively. Topical use of *Delonix elata* extract and its constituent, quercetin-3-rhamnopyranosyl-(1-6) glucopyranoside were reported to improve wound healing in rats by promoting wound contraction through the

upregulation of COL1A1 (Krishnappa, Venkatarangaiah, Venkatesh, Shimoga Rajanna, & Kayattukandy Balan, 2016). The upregulation of cytokines, chemokines, growth factors and collagens indicate that MP-HX, MP-EA, QN and DX could facilitate wound healing by modulating genes involved in inflammatory, cell proliferation and remodeling phases (Kasuya & Tokura, 2014); (Barrientos et al., 2008); (Behm et al., 2012); (Reinke & Sorg, 2012).

Aging is characterized by oxidative stress, unfolded and damaged proteins, damaged cellular components, telomere shortening, loosely associated chromatin, epigenetic alterations, dysregulation in signaling pathways (the insulin and IGF-1 signaling pathway, mTOR, AMPK and sirtuin signaling), mitochondrial dysfunction, cellular senescence, stem cell exhaustion and altered intercellular communication (DiLoreto & Murphy, 2015); (Lopez-Otin, Blasco, Partridge, Serrano, & Kroemer, 2013). Aging is normally caused by physiological, molecular and genetic changes that unfold as we get older. Aging can also be induced from degenerative diseases and unhealthy lifestyles (Kolovou, Kolovou, & Mavrogeni, 2014). Excessive oxidative stress and oxidative damage of biomolecules could also cause aging, and these are responsible for the development of age-related diseases (Bokov, Chaudhuri, & Richardson, 2004); (Kregel & Zhang, 2007); (D. F. Dai, Chiao, Marcinek, Szeto, & Rabinovitch, 2014). Human lifespan could possibly be extended through several approaches, such as calorie restriction, epigenetic modulation, inhibition of IGF signaling, and activation of sirtuins (Longo et al., 2015).

"Sirtuin signaling pathway" was one of the top CPs modulated by MP-HX, QN and DX (**Table 4.18**). In the present study, SIRT3 was noted to be upregulated in all four treatments (**Table 4.18**). MP-HX, MP-EA, QN and DX also upregulated SIRT4 with a FC of +1.93, +1.77, +1.55 and +1.57, respectively. SIRT1 was also mildly upregulated

(FC by MP-HX: +1.38, MP-EA: +1.22, QN: +1.14, DX: +1.12). Sirtuins are members of NAD-dependent histone deacetylases family, consisting of SIRT1 to 7. SIRT1 exerts roles in cell survival, apoptosis, autophagy, metabolism, while SIRT2, 3 and 4 have roles in oxidative phosphorylation, ROS synthesis, urea-cycle, ATP synthesis and apoptosis. The roles of SIRT6 include chromatin association and inflammation while SIRT7 has a role in RNA polymerase I dependent gene transcription (Pillai, Sundaresan, & Gupta, 2014). Sirtuins expression are induced by calorie restriction and they are crucial for the extension of lifespan and preventing age related diseases such as cardiac disease, Alzheimer's disease, Parkinson's disease, Huntington's disease and amyotrophic lateral sclerosis (Cencioni et al., 2015); (Roth, Wang, & Chen, 2013); (Mazucanti et al., 2015). Under calorie depletion, sirtuins inhibit AKT and IGF signaling pathways, causing deacetylations of FOXO1 and FOXO3 and this is thought to slow down aging process (Pillai et al., 2014). MP-HX, MP-EA, QN and DX also downregulated IGF1R expression, with FC of -2.28, -1.65, -1.37 and -1.84, respectively. Sirtuins activation is anti-senescence, anti-apoptotic and pro-survival and these activities are thought to contribute towards improvement of lifespan i.e. longevity (Kyrylenko & Baniahmad, 2010). In the present study, it was also noted growth suppressor GADD45B and autophagy marker GABARAPL1 were downregulated by all treatments (**Table 4.18**).

Supplementation of natural antioxidants have been suggested to extend lifespan in many experimental models (Sadowska-Bartosz & Bartosz, 2014). Plant extracts and phytochemicals could exert anti-aging effect and they have been proposed to help increase lifespan by upregulating antioxidant genes such as CAT, SOD1, SOD2 (Peng et al., 2014). In the present study, numerous antioxidants genes including CAT and SOD2 were significantly upregulated by MP-HX, MP-EA, QN and DX (**Table 4.11**).

A meta-analysis to identify aging related genes signature revealed that S100A6, GFAP, LGALS3, ANXA3, MPEG1, SPP1, HBA1 and C1QA were among the genes upregulated with age, while TFRC, COL1A1, COL3A1, ATP5G3, NDUFB11, FABP3, GHITM, ACSS2 and DIABLO were noted to be downregulated with age (de Magalhaes et al., 2009). The datasets in the present study showed that MP-HX, MP-EA, QN and DX significantly downregulated S100A6, GFAP, LGALS3, ANXA3, MPEG1, SPP1, HBA1 and C1QA, while at the same time, they upregulated the expression of TFRC, COL1A1, COL3A1, ATP5G3, NDUFB11, FABP3, GHITM ACSS2 and DIABLO (**Table 4.12**). This finding shows that the treatments apparently reversed the expression profile of a subset of genes associated with aging. This suggests that the agents used in the present study are able to modulate the expression pattern of genes associated with aging in directions that support anti-aging effect.

In the present study, IPA predicted the following upstream regulators to be activated in all four datasets: ERBB2, EGFR, IL17A, IL1B, TNF, PDGF BB, and TGFB1 (**Figure 4.58**). ERBB2 (also known as HER2) and EGFR (also known as ERBB1, HER1) are the members of epidermal growth factor receptor (EGFR) family (Wee & Wang, 2017). ERBB2 and EGFR promote cell cycle, cell proliferation and cell survival (Iqbal & Iqbal, 2014). The cytokines IL17A, IL1B and TNF promote inflammatory phase of the wound healing (Brockmann et al., 2017); (Kasuya & Tokura, 2014); (Barrientos et al., 2008). On the other hand, the growth factor PDGF BB is a member of PDGF family (Kaltalioglu & Coskun-Cevher, 2015) while TGFB1 (also known as TGF-β) is a member of TGF-β family (Poniatowski et al., 2015). PDGF (platelet derived growth factor) and TGF-β (transforming growth factor beta) play vital roles in inflammatory, cell proliferation and remodeling phases of the wound healing (Behm et al., 2012).

The present study shows that MP-HX, MP-EA, QN and DX induced transcriptome profiles in Hs27 cells that modulate many components genes that were associated cell cycle progression, cellular proliferation, antioxidant defense, wound healing, aging and sirtuin signaling pathway in Hs27 cells. These findings are supportive for the use of MP-HX, MP-EA, QN and DX in skin-health, cosmetic and dermatological applications.

5.6 Protective effect of *Melicope ptelefolia* from cadmium-induced cytotoxicity

Cadmium (Cd) is a known cytotoxic agent as it can cause oxidative stress (Rahimzadeh et al., 2017) and denature various proteins including enzymes (Banfalvi, 2011). In the present study, the protective effect of MP-HX and MP-EA against Cd-induced cytotoxicity in Hs27 cells was studied. Hs27 cells was exposed to Cd and cell viability was evaluated using MTT assay, in the presence and absence of MP-HX and MP-EA. The results showed that Hs27 cells pretreated with MP-HX and MP-EA at 15 µg/mL protected Hs27 cells from Cd-induced cytotoxicity, as the percentage of viable Hs27 cells was near 100%, similar to that of the control (**Figure 4.64**). This suggests that MP extracts were able to protect Hs27 cells against Cd-induced cytotoxicity.

It is likely that MP extracts antioxidant activity contributed to the protection of Hs27 cells from Cd-induced oxidative stress, preserving the viability of Hs27 cells, even in the presence of Cd. Cd-induced cytotoxicity in rat liver cells have also been reported to be counteracted by the antioxidant N-acetylcysteine (NAC) (Odewumi et al., 2011). Garlic extracts have also been reported to exert protective effect on the viability of human embryonic kidney cells upon Cd exposure (Boonpeng et al., 2014).

To uncover the possible molecular mechanisms exerted by MP extracts against Cd-induced cytotoxicity in Hs27 cells, microarray analysis was performed. The treatment

using $CdCl_2$, MP-HX+$CdCl_2$ and MP-EA+$CdCl_2$ were noted to modulate numerous genes linked to cell cycle, cell proliferation, cell growth and antioxidant defense.

$CdCl_2$ treatment was noted to have upregulated the expression of many members of metallothionine (MT) genes in Hs27 cells (**Table 4.24**). Metallothionines (MTs) are known to play crucial roles in cadmium detoxification (Klaassen, Liu, & Diwan, 2009). MTs are metal binding proteins which demonstrate high affinity on divalent heavy metals, including cadmium and they play vital roles for the detoxification of heavy metals. MT proteins contain sulfhydryl (-SH) groups that can bind and chelate cadmium, reducing its bioavailability and this could protect the body from Cd toxicity. Cadmium is eliminated through urine as metallothionine (MT) bound complex (CdMT) (Hodgson & Levi, 2004). The members of MTs genes include MT1A, MT1B, MT1E, MT1F, MT1H, MT1G, MT1M, MT1X and MT2A. The MTs synthesis are induced by oxidative stress, growth factors and presence of heavy metals, including Cd. MT1E, MT1X and MT2A expression were reported to be upregulated in MCF10 breast epithelial cells, while MT1F and MT1G were upregulated in HB2 breast epithelial cells upon Cd exposure (Luparello et al., 2011). In agreement with these observations, the present study observed that the expression of MTs in Hs27 cells were markedly upregulated after $CdCl_2$ exposure, and this observation suggests Hs27 cells also used MTs a defense mechanism to prevent $CdCl_2$ cytotoxicity. The induction MTs by $CdCl_2$ in human skin fibroblast cells has never been reported. Besides chelating Cd to prevent toxicity, the MTs are also able to inhibit oxidative damage that could be induced by Cd presence. The MTs are able to scavenge free radicals such as superoxide and hydroxyl radicals (Thirumoorthy, Manisenthil Kumar, Shyam Sundar, Panayappan, & Chatterjee, 2007); (Ruttkay-Nedecky et al., 2013) and this can exert cytoprotective effect.

In general, the pretreatment using MP extracts did not markedly reduce or reverse MT gene upregulation in Hs27 cells, that were noted to be induced by Cd, but some expression differences were observed. The degree of MT1A, MT1G, MT1H and MT1M upregulation were noted to be significantly lower in the presence of MP-HX and MP-EA pretreatments (**Table 4.24**). The polyphenols or antioxidant phytochemicals in MP-HX and MP-EA likely exerted antioxidant effect inside Hs27 cells (**Table 4.2**), leading to oxidative stress reduction and thus, a lesser degree of upregulation was observed for the relevant MT genes.

In the present study, the $CdCl_2$ treatment in Hs27 cells was noted to have modulated the expression of genes related to glutathione synthesis (GPx1, GPx3, GSR, GSTO1, GSTO2, GSTP1, GCLM and GCLC) and the upregulation of antioxidant genes PRDX1, NQO1 and TXNRD1 (**Table 4.25**). In the Cd-exposed Hs27 cells, MP-HX pretreatment was noted to have upregulated the expression of antioxidant genes GPX3, GPX4, GPX8, PRDX1, PRDX5 and TXNRD3, while MP-EA pretreatment resulted in the upregulation of GSTO1, PRDX1, PRDX5, TXNRD1 and TXNRD3 (**Table 4.25**). It is conceivable that the modulation/upregulation of these genes are relevant responses by Hs27 cells to counteract the oxidative stress induced by Cd (Nair et al., 2015).

The present study also noted that $CdCl_2$ treatment resulted in the upregulation of MYC proto-oncogene (MYC), FOS proto-oncogene (FOS), and JUN proto-oncogene (JUN) in Hs27 cells (**Table 4.23**). In contrast, the same Cd exposure with MP-HX pretreatment induced MYC downregulation, while MP-EA pretreatment resulted in a lesser degree of upregulation of MYC. Although FOS and JUN were also upregulated in MP-HX and MP-EA pretreated cells, the upregulation was at lesser degrees than that seen in $CdCl_2$ treatment (**Table 4.23**). MYC, FOS and JUN are known immediate early response genes (IERGs) that are induced by cadmium exposure (Waisberg et al., 2003).

MYC is known to promote cell cycle arrest and apoptosis in normal cells (Gabay, Li, & Felsher, 2014). In keratinocyte cell lines, apoptosis induction was reported to be associated with FOS upregulation (Markopoulou et al., 2009). JUN was also reported to induce apoptosis by activating BIM (Tomicic et al., 2015). In addition, cadmium was found to reduce proliferation of human renal mesangial cells through upregulation of both FOS and JUN and induction of JNK signaling pathway (X. Chen et al., 2016). The above observations suggest that MP-HX and MP-EA pretreatments modulated the expression of the above mentioned IERGs and such modulation likely contributed to the protection of Hs27 cells from Cd-induced cytotoxicity.

The present study also noted that $CdCl_2$ treatment in Hs27 cells resulted in the downregulation of DNA damage responsive genes, which were ATM and ATR with MA_FC values of -1.17 and -1.50, respectively. In contrast, MP-HX pretreatment significantly upregulated both ATM and ATR, with MA_FC values of +1.71 and +2.18, respectively. MP-EA pretreatment also upregulated ATM with MA_FC value of +1.30 while the expression of ATR remained unchanged. During DNA damage, ATM and ATR activate DNA repair process to prevent further damage (Surova & Zhivotovsky, 2013). On the other hand, if the damage is not repairable, ATM and ATR induce cell death proteins to activate necrosis, apoptosis and autophagy (Surova & Zhivotovsky, 2013). A defect in the DNA repair mechanisms can cause genomic instability (Heijink, Krajewska, & van Vugt, 2013). Cd has been reported to inhibit multiple DNA repair mechanisms which can lead to genomic instability (Filipic, 2012).

The present study also noted that $CdCl_2$ significantly downregulated DNA repair genes RRM2B, PRKDC and RMI1 (**Table 4.23**). On the other hand, MP-HX pretreatment upregulated RRM2B, while at the same time, it lessened the degree of $CdCl_2$-induced downregulation of PRKDC and RMI1 (**Table 4.23**). MP-EA

pretreatment also lessened $CdCl_2$-induced downregulation RRM2B, PRKDC and RMI1 (**Table 4.23**). RRM2B is a subunit of ribonucleotide reductase (RNR). RNR enzyme is essential for the synthesis of dNTPs (deoxynucleoside triphosphate) during DNA replication and repair (Guarino, Salguero, & Kearsey, 2014). RRM2B plays vital role in DNA replication and repair of quiescent cells (Pontarin, Ferraro, Bee, Reichard, & Bianchi, 2012). Furthermore, RRM2B can protect cells from oxidative stress (X. Liu, Xue, & Yen, 2008). PRKDC (also known as 'protein kinase, DNA-activated, catalytic subunit') is a DNA dependent protein kinase involved in the repair of DSB (DNA double strand breaks) through non-homologous end-joining and homologous recombination repair mechanism (Goodwin & Knudsen, 2014). PRKDC has been proposed to be a cellular growth regulator through its activation of PKB/AKT enzyme system (Kong, Shen, Jiang, Fei, & Mi, 2011). RecQ mediated genome instability 1 (RMI1) plays important role in DNA repair through its interaction with TOP3A and BLM (Croteau, Popuri, Opresko, & Bohr, 2014). RMI1 was reported to enhance DNA replication fork progression and this could help cells to recover from replication stress (J. Yang, O'Donnell, Durocher, & Brown, 2012). Functional characterisation of RMI1 function using RMI1 knockout mice indicated that the gene was essential for embryonic development and tumor suppression (H. Chen, You, Jiang, Wang, & Li, 2011). The findings in the present study indicated that Cd toxicity may have resulted in deficiency in DNA damage repair mechanisms, which could lead to cytotoxic effect and genomic instability. The modulation of several DNA damage responsive and DNA repair genes by MP extracts in Hs27 likely have significant roles in mediating the protective effect of the extracts against Cd-induced cytotoxicity in Hs27 cells.

Analysis using TAC software revealed that "mitotic G_1-G_1/S phases" (MG_1-G_1SP), "S-phase" (SP), "mitotic G_2-G_2/M phases" (MG_2-G_2MP) and "Intrinsic pathway for

apoptosis" (IntPA) Wikipathways (WPs) were significantly modulated by $CdCl_2$, MP-HX+$CdCl_2$ and MP-EA+$CdCl_2$ treatments (**Table 4.27**).

For MG_1-G_1SP-WP, $CdCl_2$ treatment resulted in downregulation of PCNA and CDK1 (**Table 4.27**). The degree of PCNA downregulation was lesser in the presence of MP-HX and MP-EA pretreatments (**Table 4.27**). On the other hand, the expression of CDK1 was relatively unchanged in MP-EA pretreated cells. CDK1 promotes G_1/S transition by phosphorylating pRb protein (Duronio & Xiong, 2013), while PCNA initiates DNA replication by activating pre-replicative components CDC6, MCM, ORC and CDT1 (L. Wu et al., 2014); (Barnum & O'Connell, 2014). The $CdCl_2$ treatment was also noted to cause a significant downregulation of GINS1, which is a component member of SP-WP. In contrast, GINS1 expression was relatively unchanged in MP-HX and MP-EA pretreated Hs27 cells (**Table 4.27**). GINS1 (also known as PSF1) is a member of GINS complex, with essential roles in DNA replication and cell growth (Aparicio, Ibarra, & Mendez, 2006). GINS2 is another member of GINS complex, and this gene was mildly downregulated by $CdCl_2$ treatment. In contrast, MP-EA pretreatment resulted in mild upregulation of GINS2 (**Table 4.27**).

Four component members of MG_2-G_2MP-WP (CCNB2, CUL1, GTSE1 and BORA) were noted to be downregulated by $CdCl_2$ treatment (**Table 4.27**). In contrast, MP-HX pretreatment induced upregulation of BORA, while it lessened the degree of $CdCl_2$-induced downregulation of CUL1 and GTSE1 (**Table 4.27**). On the other hand, MP-EA pretreatment induced the upregulation of CUL1, GTSE1 and BORA, while it lessened $CdCl_2$-induced downregulation of CCNB2 (**Table 4.27**). The modulation of cell cycle genes by MP extracts in Hs27 cells likely contributed to the promotion Hs27 cells viability (**Figure 4.64**), and this was achieved by reducing the negative impact of Cd on the expression of selected members of MG_2-G_2MP-WP.

The present study also showed that $CdCl_2$ and MP extracts significantly modulated IntPA-WP (**Table 4.27**). Two of the components of IntPA-WP (BBC3 and PMAIP1) were noted to be significantly upregulated by $CdCl_2$ treatment (**Table 4.27**). MP-HX pretreatment noticeably lessened the degree of PMAIP1 upregulation, while BBC3 expression was relatively unchanged (**Table 4.27**). On the other hand, MP-EA pretreatment significantly lessened $CdCl_2$-induced upregulation of both BBC3 and PMAIP1 (**Table 4.27**). In response to cellular stress, pro-apoptotic BBC3 and PMAIP1 are able to stimulate BAX and BAK to release cytochrome c (Jendrossek, 2012), to induce apoptosis. Cytochrome c facilitates the formation of apoptosome complex, and this could lead to the activation of effector caspases (caspase-3,6,7), leading to apoptosis induction (Jendrossek, 2012). The pattern of BBC3 and PMAIP1 modulation by MP-HX and MP-EA suggested that they are capable of minimizing apoptosis pathway activity that was induced by $CdCl_2$. This observation provided further evidence on the protective role of MP-HX and MP-EA against Cd-induced cytotoxicity in Hs27 cells (**Figure 4.64**).

The dataset was also analysed using GATHER web-tool. The DEGs for $CdCl_2$ dataset were noted to be significantly enriched for biological processes related to "cell cycle", "cell growth", "apoptosis" and "cell death" (**Table 4.28, Figure 4.68**). On the other hand, the DEGs from MP-HX+$CdCl_2$ and MP-EA+$CdCl_2$ datasets were significantly enriched with "cell cycle" and "cell growth" related biological processes (**Tables 4.29** and **4.30; Figures 4.69** and **4.70**). PANTHER analysis also revealed that the DEGs in $CdCl_2$, MP-HX+$CdCl_2$ and MP-EA+$CdCl_2$ datasets were associated with "cell growth", "cell cycle", "cell proliferation", "death" and "stress response" (**Figures 4.72, 4.73, 4.74** and **4.75**). The biological processes uncovered by GATHER and PANTHER analyses are consistent with TAC software output, whereby the Wikipathways uncovered by TAC were "cell cycle" and "apoptosis" WPs (**Table 4.27**).

The findings in the present study indicate that "cell cycle", "cell proliferation" and "cell growth" processes are likely positively modulated by MP-HX and MP-EA pretreatments, and this resulted in enhancement of cell viability despite $CdCl_2$ exposure in the Hs27 cells (**Figure 4.64**).

The datasets were also analysed using STRING web-tool, to analyse the enrichment of network functions. The STRING output results showed that biological processes such as "cellular response to cadmium ion", "cellular response to metal ion" and "response to unfolded protein" were enriched in the networks of $CdCl_2$, MP-HX+$CdCl_2$ and MP-EA+$CdCl_2$ datasets (**Tables 4.31, 4.32** and **4.33**). "Apoptotic process", "negative regulation of cell proliferation" and "negative regulation of cell growth" were also significantly associated with the network in $CdCl_2$ dataset (**Table 4.31**). On the other hand, "positive regulation of cell proliferation" and "negative regulation of cell death" were significantly associated with the networks in MP-HX+$CdCl_2$ (**Table 4.32**). The network in MP-EA+$CdCl_2$ dataset was significantly associated with "positive regulation of cell proliferation", "negative regulation of apoptotic process" and "negative regulation of cell death" (**Table 4.33**).

STRING indicated that several genes such as JUN, FOS, BBC3 and PMAIP1 formed network interactions in $CdCl_2$, MP-HX+$CdCl_2$ and MP-EA+$CdCl_2$ datasets (**Figures 4.77, 4.78** and **4.79**). JUN was associated with "cellular response to metal ion", "negative regulation of cell proliferation" and "apoptotic process". On the other hand, FOS was associated with "cellular response to metal ion" and "response to stress". The pro-apoptotic genes BBC3 and PMAIP1 were associated with "regulation of cell death" and "response to stress". BBC3 was also associated with "apoptotic process" while PMAIP1 was associated with "negative regulation of cell proliferation. As discussed earlier, JUN, FOS, BBC3 and PMAIP1 were notably upregulated by $CdCl_2$ in Hs27

cells while MP-HX and MP-EA pretreatments significantly lessened $CdCl_2$-induced upregulation of these genes (**Table 4.23**). The modulation of these genes likely contributed significant role in reducing Cd-induced cytotoxicity.

Furthermore, GADD45B and GADD45G showed interactions in the network for $CdCl_2$, MP-HX+$CdCl_2$ and MP-EA+$CdCl_2$ datasets (**Figures 4.77, 4.78** and **4.79**). GADD45A, CDKN1C and MDM2 also formed network of interactions in $CdCl_2$ dataset (**Figure 4.77**). The GADD45 family genes are associated with "regulation of cell death", "apoptotic process" and "response to stress". The members of GADD45 family (GADD45A, GADD45B and GADD45G) were also substantially upregulated by $CdCl_2$ with MA-FC values of +2.84, +15.88 and +47.20 respectively. In contrast, MP-HX pretreatment significantly lessened $CdCl_2$-induced upregulation of the corresponding genes, with MA_FC value of +1.23, +3.77 and +8.22, respectively. A similar effect was observed in the presence of MP-EA. MP-EA pretreatment lessened $CdCl_2$-induced upregulation of GADD45A, GADD45B and GADD45G with MA_FC values of +2.30, +10.57 and +22.16, respectively. GADD45 family members demonstrated diverse roles in cell cycle arrest and apoptosis processes (Liebermann & Hoffman, 2007). CDKN1C was associated with "negative regulation of cell proliferation" while MDM2 was associated with "regulation of cell death". $CdCl_2$ significantly upregulated cell cycle inhibitor CDKN1C expression, while it downregulated cell proliferation inducer MDM2 (**Table 4.23**). In contrast, MP-HX and MP-EA pretreatments significantly lessened $CdCl_2$-induced upregulation of CDKN1C (**Table 4.23).** MP-HX pretreatment upregulated MDM2 while MP-EA pretreatment lessened $CdCl_2$-induced downregulation of MDM2 (**Table 4.23**). CDKN1C ($p57^{KIP2}$) is a Cip/Kip family member of CDK inhibitor (S. Lim & Kaldis, 2013) which suppresses cell cycle progression by inhibiting of CDKs (Kavanagh & Joseph, 2011). On the other hand, MDM2 promotes cell proliferation through modulation of cell cycle, apoptosis, DNA

repair and angiogenesis (Nag et al., 2014). MDM2 is able to degrade p53, CDK inhibitor (p21) and pro-apoptotic FOXO3a by its ubiquitin ligase activity. Conversely, it can enhance the activation of E2F transcription factor and anti-apoptotic XIAP protein (Nag et al., 2014). As a result, MDM2 is able to stimulate cell cycle progression and cell proliferation. These observations indicate that MDM2 is a negative regulator of cell death. Consistent with this notion, downregulation of MDM2 has been reported to be associated with reduction in cell proliferation (Yoou, Kim, & Jeong, 2015). The above observations suggest that MP-HX and MP-EA pretreatments modulated the expression of GADD45A, GADD45B, GADD45G, CDKN1C and MDM2 and such modulation likely played a significant role in counteracting $CdCl_2$-induced cytotoxicity in Hs27 cells.

The present study also noted that several heat shock protein (HSP) genes were modulated (**Table 4.26**) and showed interaction for the network in $CdCl_2$, MP-HX+$CdCl_2$ and MP-EA+$CdCl_2$ datasets (**Figures 4.77, 4.78** and **4.79**). This finding is not surprising, as Cd exposure are known to induce HSP genes expression to prevent Cd-induced cytotoxicity (Sandbichler & Hockner, 2016); (Waisberg et al., 2003). STRING network analysis indicated that HSP genes were associated with many biological processes including "response to unfolded protein", "response to stress", "regulation of cellular response to stress" and "cellular response to stress". $CdCl_2$ was noted to have upregulated many HSP genes such as DNAJA1, DNAJB1, DNAJA4, HSPA1L, HSPA2, HSPA6, HSPB2, HSPH1 and HSP90AA1 (**Table 4.26**). In contrast, MP-HX and MP-EA pretreatments significantly downregulated HSPA2, while they lessened $CdCl_2$-induced upregulation of DNAJA1, DNAJB1, DNAJA4, HSPA1L, HSPA6, HSPH1 and HSP90AA1 (**Table 4.26**). The expression of HSPB2 remained unchanged after pretreatment with MP-HX, while MP-EA lessened $CdCl_2$-induced upregulation of HSPB2 (**Table 4.26**). The differences in the modulation of HSP genes

between the datasets were likely due to the reduction of oxidative stress by MP-HX and MP-EA pretreatments.

In summary, MP-HX and MP-EA pretreatments preserved Hs27 cells viability despite $CdCl_2$ exposure and this was achieved by the extracts cytoprotective actions in modulating cell proliferation, cell death, DNA repair, antioxidant defense and stress response in Hs27 cells.

CHAPTER 6: CONCLUSION

The present study reports bioactivities of MP leaf extracts, including antioxidant, anticancer, gene expression modulation and its protective activity against cadmium-induced cytotoxicity. Based on the *in vitro* and cellular antioxidant assays, MP-HX demonstrated the most notable antioxidant activity. Since MP-HX did not have remarkable phenolic and flavonoid contents, it is likely that polyphenols were not the main component responsible for the observed antioxidant activity. The present study is the first report to show anticancer activities of MP leaf extracts. MP-HX and MP-EA extracts were able to exert antiproliferative activity on four different cancer cell lines, which include human colorectal (HCT116), breast (HCC1937, MDA-MB-231) and hepatocellular carcinoma (HepG2) cell lines.

MP-HX and MP-EA exhibited promising antiproliferative activity as the IC_{50} values obtained for the four cancer cell lines tested were mostly below 100 μg/mL. The cytotoxicity effect of MP-HX and MP-EA appeared to be selective towards the cancer cells, as the IC_{50} values of the extracts on normal colon (CCD841) and fibroblast (Hs27) cell lines and were significantly higher (> 300 μg/mL) than those of the cancer cells. Furthermore, caspase enzyme assays using flow cytometry and fluorometric assays indicated that MP-HX and MP-EA were able to induce caspase enzymes activation in all four cancer cell lines tested, indicating that the cytotoxicity effect on the cancer cells was induced through apoptosis programmed cell death. Flow cytometry assay also showed that MP-HX and MP-EA were able to alter the cell cycle distribution in three of the four cancer cell lines.

The present study is the first to demonstrate the anticancer potential of MP. To date, none of the previous studies on MP have reported (or evaluated) its anticancer potential. Previous bioactivity studies have either used polar (eg. ethanol and methanol) MP

extracts (Sulaiman et al., 2010); (Mahadi et al., 2016); (Abas et al., 2010a); (Shaari, Zareen, et al., 2011) or pure phytochemical compound (tHGA), which was isolated from methanol extract of MP (Lee et al., 2017); (Ji Wei Tan et al., 2017); (Chong et al., 2016). Thus, the lack of report on MP anticancer activity may have been due to non-polar extract of MP being overlooked.

The present study also showed that MP-HX conferred its anticancer activity in HCT116 and HepG2 cell lines by modulating the expression of various key genes regulating DNA replication, cell cycle progression, cell growth/proliferation and programmed cell death in a direction favoring anticancer effect. The transcriptome profiles induced by MP-HX includes upregulation of pro-apoptotic, cell cycle arresting and metastasis suppression genes and downregulation of genes that promote anti-apoptotic effect, cell cycle progression, tumor development and progression. MP-HX also downregulated the expression of many members of minichromosome maintenance genes, which have critical roles in DNA replication. MP-HX likely contain phytochemical(s) that can downregulate multiple MCM genes and this activity is very useful for cancer therapy (Simon & Schwacha, 2014). MP-HX also downregulated the six top-ranked genes that were proposed to be cancer-associated (PLK1, MCM2, MCM3, MCM7, MCM10 and SKP2) in both cell lines (C. Wu et al., 2012).

Microarray gene expression profiling in Hs27 cells treated with MP-HX and MP-EA showed that the extracts were able to upregulate the expression of genes governing cellular antioxidant function, proliferation and cell cycle progression. In Hs27 cells treated with MP extracts, an upregulation of genes involved in wound healing were also noted and these genes are known to be involved in releasing cytokines, chemokines and growth factors. In addition, MP-HX and MP-EA modulated the expression of several aging-related genes in Hs27 cells, in a direction or pattern of expression that could

promote cellular longevity. These observations suggest that MP-HX and MP-EA contain phytochemicals that may help improve cellular redox homeostasis, induce molecular pathways which promote Hs27 proliferation, support fibroblast function in wound healing and anti-aging activities.

The present study also showed that MP extracts were able to exert cytoprotective effect on Hs27. When Hs27 cells were challenged with $CdCl_2$ treatment, the percentage of viable Hs27 cells was increased in the presence of MP-HX or MP-EA pretreatments. Microarray gene expression profiling showed that MP-HX and MP-EA significantly changed the expression pattern of many genes that were modulated by $CdCl_2$ exposure. Many of the genes that were modulated are involved in biological processes such as cell proliferation, apoptosis, DNA replication, DNA damage, DNA repair and stress response.

The results from the present study project MP as a source of phytochemical compounds with notable antioxidant and anti-cancer activities. The extracts also likely contain phytochemical compounds that are useful for cosmetic and dermatological applications. The findings in the present study provide novel insights on the bioactivity and medicinal values of MP. Further research is warranted, to isolate and characterise the phytochemical compound(s) from MP that is/are responsible for the bioactivities.

REFERENCES

Ab. Karim, M., Nasouddin, S., Othman, M., Mohd Adzahan, N., & Hussin, S. (2011). Consumers' knowledge and perception towards Melicope ptelefolia (Daun Tenggek Burung): A preliminary qualitative study. *International Food Research Journal, 18*(4), 1481-1488.

Abas, F., Shaari, K., Israf, D., Syafri, S., Zainal, Z., & Lajis, N. H. (2010a). LC–DAD–ESI-MS analysis of nitric oxide inhibitory fractions of tenggek burung (Melicope ptelefolia Champ. ex Benth.). *Journal of food composition and analysis, 23*(1), 107-112.

Abas, F., Shaari, K., Israf, D. A., Syafri, S., Zainal, Z., & Lajis, N. H. (2010b). LC–DAD–ESI-MS analysis of nitric oxide inhibitory fractions of tenggek burung (Melicope ptelefolia Champ. ex Benth.). *Journal of food composition and analysis, 23*(1), 107-112. doi: 10.1016/j.jfca.2009.03.009

Abbas, M., Saeed, F., Anjum, F. M., Afzaal, M., Tufail, T., Bashir, M. S., . . . Suleria, H. A. R. (2017). Natural polyphenols: An overview. *International Journal of Food Properties, 20*(8), 1689-1699. doi: 10.1080/10942912.2016.1220393

Abbas, T., & Dutta, A. (2009). p21 in cancer: intricate networks and multiple activities. *Nat Rev Cancer, 9*(6), 400-414. doi: 10.1038/nrc2657

Aburjai, T., & Natsheh, F. M. (2003). Plants used in cosmetics. *Phytother Res, 17*(9), 987-1000. doi: 10.1002/ptr.1363

Afzal, O., Kumar, S., Haider, M. R., Ali, M. R., Kumar, R., Jaggi, M., & Bawa, S. (2015). A review on anticancer potential of bioactive heterocycle quinoline. *Eur J Med Chem, 97*, 871-910. doi: 10.1016/j.ejmech.2014.07.044

Aird, K. M., Li, H., Xin, F., Konstantinopoulos, P. A., & Zhang, R. (2014). Identification of ribonucleotide reductase M2 as a potential target for pro-senescence therapy in epithelial ovarian cancer. *Cell Cycle, 13*(2), 199-207. doi: 10.4161/cc.26953

Akbik, D., Ghadiri, M., Chrzanowski, W., & Rohanizadeh, R. (2014). Curcumin as a wound healing agent. *Life Sci, 116*(1), 1-7. doi: 10.1016/j.lfs.2014.08.016

Akerele, O. (1993). Nature's medicinal bounty: don't throw it away. *World Health Forum, 14*(4), 390-395.

Albert, M.-C., Brinkmann, K., & Kashkar, H. (2014). Noxa and cancer therapy. *Molecular & Cellular Oncology, 1*(1), e29906. doi: 10.4161/mco.29906

Alok, S., Jain, S. K., Verma, A., Kumar, M., Mahor, A., & Sabharwal, M. (2014). Herbal antioxidant in clinical practice: a review. *Asian Pac J Trop Biomed, 4*(1), 78-84. doi: 10.1016/s2221-1691(14)60213-6

Alshatwi, A. A., Hasan, T. N., Alqahtani, A. M., Syed, N. A., Shafi, G., Al-Assaf, A. H., & Al-Khalifa, A. S. (2014). Delineating the anti-cytotoxic and anti-genotoxic potentials of catechin hydrate against cadmium toxicity in human peripheral blood lymphocytes. *Environ Toxicol Pharmacol, 38*(2), 653-662. doi: 10.1016/j.etap.2014.07.013

Aman, R. (2006). *Tumbuhan liar berkhasiat ubatan* (Cet. 1. ed.). Kuala Lumpur: Dewan Bahasa dan Pustaka.

Ameri, K., & Harris, A. L. (2008). Activating transcription factor 4. *Int J Biochem Cell Biol, 40*(1), 14-21. doi: 10.1016/j.biocel.2007.01.020

Anand David, A. V., Arulmoli, R., & Parasuraman, S. (2016). Overviews of Biological Importance of Quercetin: A Bioactive Flavonoid. *Pharmacognosy Reviews, 10*(20), 84-89. doi: 10.4103/0973-7847.194044

Anand, P., Kunnumakara, A. B., Sundaram, C., Harikumar, K. B., Tharakan, S. T., Lai, O. S., . . . Aggarwal, B. B. (2008). Cancer is a Preventable Disease that Requires Major Lifestyle Changes. *Pharmaceutical Research, 25*(9), 2097-2116. doi: 10.1007/s11095-008-9661-9

Antignac, E., Nohynek, G. J., Re, T., Clouzeau, J., & Toutain, H. (2011). Safety of botanical ingredients in personal care products/cosmetics. *Food Chem Toxicol, 49*(2), 324-341. doi: 10.1016/j.fct.2010.11.022

Aparicio, T., Ibarra, A., & Mendez, J. (2006). Cdc45-MCM-GINS, a new power player for DNA replication. *Cell Div, 1*, 18. doi: 10.1186/1747-1028-1-18

Arruebo, M., Vilaboa, N., Sáez-Gutierrez, B., Lambea, J., Tres, A., Valladares, M., & González-Fernández, Á. (2011). Assessment of the Evolution of Cancer Treatment Therapies. *Cancers, 3*(3), 3279-3330. doi: 10.3390/cancers3033279

Asghar, U., Witkiewicz, A. K., Turner, N. C., & Knudsen, E. S. (2015). The history and future of targeting cyclin-dependent kinases in cancer therapy. *Nat Rev Drug Discov, 14*(2), 130-146. doi: 10.1038/nrd4504

Asteriti, I. A., De Mattia, F., & Guarguaglini, G. (2015). Cross-Talk between AURKA and Plk1 in Mitotic Entry and Spindle Assembly. *Front Oncol, 5*, 283. doi: 10.3389/fonc.2015.00283

Atanasov, A. G., Waltenberger, B., Pferschy-Wenzig, E. M., Linder, T., Wawrosch, C., Uhrin, P., . . . Stuppner, H. (2015). Discovery and resupply of pharmacologically active plant-derived natural products: A review. *Biotechnol Adv, 33*(8), 1582-1614. doi: 10.1016/j.biotechadv.2015.08.001

Azab, A., Nassar, A., & Azab, A. N. (2016). Anti-Inflammatory Activity of Natural Products. *Molecules, 21*(10). doi: 10.3390/molecules21101321

Back, S. H., Scheuner, D., Han, J., Song, B., Ribick, M., Wang, J., . . . Kaufman, R. J. (2009). Translation attenuation through eIF2alpha phosphorylation prevents oxidative stress and maintains the differentiated state in beta cells. *Cell Metab, 10*(1), 13-26. doi: 10.1016/j.cmet.2009.06.002

Bae, D. H., Jansson, P. J., Huang, M. L., Kovacevic, Z., Kalinowski, D., Lee, C. S., . . . Richardson, D. R. (2013). The role of NDRG1 in the pathology and potential treatment of human cancers. *J Clin Pathol, 66*(11), 911-917. doi: 10.1136/jclinpath-2013-201692

Bai, L., & Wang, S. (2014). Targeting apoptosis pathways for new cancer therapeutics. *Annu Rev Med, 65*, 139-155. doi: 10.1146/annurev-med-010713-141310

Baird, T. D., & Wek, R. C. (2012). Eukaryotic initiation factor 2 phosphorylation and translational control in metabolism. *Adv Nutr, 3*(3), 307-321. doi: 10.3945/an.112.002113

Banfalvi, G. (2011). Heavy Metals,Trace Elements and Their Cellular Effects. In G. Banfalvi (Ed.), *Cellular Effects of Heavy Metals* (pp. 3-28). Netherlands: Springer.

Barnum, K. J., & O'Connell, M. J. (2014). Cell cycle regulation by checkpoints. *Methods Mol Biol, 1170*, 29-40. doi: 10.1007/978-1-4939-0888-2_2

Barrientos, S., Stojadinovic, O., Golinko, M. S., Brem, H., & Tomic-Canic, M. (2008). Growth factors and cytokines in wound healing. *Wound Repair Regen, 16*(5), 585-601. doi: 10.1111/j.1524-475X.2008.00410.x

Baskar, A. A., Ignacimuthu, S., Paulraj, G. M., & Al Numair, K. S. (2010). Chemopreventive potential of β-Sitosterol in experimental colon cancer model - an In vitro and In vivo study. *BMC Complement Altern Med, 10*, 24-24. doi: 10.1186/1472-6882-10-24

Baskar, R., Lee, K. A., Yeo, R., & Yeoh, K. W. (2012). Cancer and radiation therapy: current advances and future directions. *Int J Med Sci, 9*(3), 193-199. doi: 10.7150/ijms.3635

Beckenbach, L., Baron, J. M., Merk, H. F., Loffler, H., & Amann, P. M. (2015). Retinoid treatment of skin diseases. *Eur J Dermatol, 25*(5), 384-391. doi: 10.1684/ejd.2015.2544

Behm, B., Babilas, P., Landthaler, M., & Schreml, S. (2012). Cytokines, chemokines and growth factors in wound healing. *J Eur Acad Dermatol Venereol, 26*(7), 812-820. doi: 10.1111/j.1468-3083.2011.04415.x

Bellato, H. M., & Hajj, G. N. (2016). Translational control by eIF2alpha in neurons: Beyond the stress response. *Cytoskeleton (Hoboken), 73*(10), 551-565. doi: 10.1002/cm.21294

Belpomme, D., Irigaray, P., Hardell, L., Clapp, R., Montagnier, L., Epstein, S., & Sasco, A. J. (2007). The multitude and diversity of environmental carcinogens. *Environ Res, 105*(3), 414-429. doi: 10.1016/j.envres.2007.07.002

Benzie, I. F. F., & Strain, J. J. (1996). The ferric reducing ability of plasma (FRAP) as a measure of "antioxidant power": The FRAP assay. *Analytical Biochemistry, 239*, 70-76.

Berna, G., Oliveras-Lopez, M. J., Jurado-Ruiz, E., Tejedo, J., Bedoya, F., Soria, B., & Martin, F. (2014). Nutrigenetics and nutrigenomics insights into diabetes etiopathogenesis. *Nutrients, 6*(11), 5338-5369. doi: 10.3390/nu6115338

Berthier, A., Seguin, S., Sasco, A. J., Bobin, J. Y., De Laroche, G., Datchary, J., . . . Descotes, F. (2010). High expression of gabarapl1 is associated with a better outcome for patients with lymph node-positive breast cancer. *Br J Cancer, 102*(6), 1024-1031. doi: 10.1038/sj.bjc.6605568

Bokov, A., Chaudhuri, A., & Richardson, A. (2004). The role of oxidative damage and stress in aging. *Mech Ageing Dev, 125*(10-11), 811-826. doi: 10.1016/j.mad.2004.07.009

Boonpeng, S., Siripongvutikorn, S., Sae-Wong, C., & Sutthirak, P. (2014). The antioxidant and anti-cadmium toxicity properties of garlic extracts. *Food Sci Nutr, 2*(6), 792-801. doi: 10.1002/fsn3.164

Bossy-Wetzel, E., Bakiri, L., & Yaniv, M. (1997). Induction of apoptosis by the transcription factor c-Jun. *EMBO J, 16*(7), 1695-1709. doi: 10.1093/emboj/16.7.1695

Brockmann, L., Giannou, A. D., Gagliani, N., & Huber, S. (2017). Regulation of TH17 Cells and Associated Cytokines in Wound Healing, Tissue Regeneration, and Carcinogenesis. *Int J Mol Sci, 18*(5). doi: 10.3390/ijms18051033

Brooks, A. N., Kilgour, E., & Smith, P. D. (2012). Molecular pathways: fibroblast growth factor signaling: a new therapeutic opportunity in cancer. *Clin Cancer Res, 18*(7), 1855-1862. doi: 10.1158/1078-0432.ccr-11-0699

Broustas, C. G., & Lieberman, H. B. (2014). DNA damage response genes and the development of cancer metastasis. *Radiat Res, 181*(2), 111-130. doi: 10.1667/RR13515.1

Bureau, G., Longpre, F., & Martinoli, M. G. (2008). Resveratrol and quercetin, two natural polyphenols, reduce apoptotic neuronal cell death induced by neuroinflammation. *J Neurosci Res, 86*(2), 403-410. doi: 10.1002/jnr.21503

Burns, J., Yokota, T., Ashihara, H., Lean, M. E., & Crozier, A. (2002). Plant foods and herbal sources of resveratrol. *J Agric Food Chem, 50*(11), 3337-3340. doi: 10.1021/jf0112973

Burotto, M., Chiou, V. L., Lee, J. M., & Kohn, E. C. (2014). The MAPK pathway across different malignancies: a new perspective. *Cancer, 120*(22), 3446-3456. doi: 10.1002/cncr.28864

Bylka, W., Znajdek-Awizen, P., Studzinska-Sroka, E., Danczak-Pazdrowska, A., & Brzezinska, M. (2014). Centella asiatica in dermatology: an overview. *Phytother Res, 28*(8), 1117-1124. doi: 10.1002/ptr.5110

Carter, L. G., D'Orazio, J. A., & Pearson, K. J. (2014). Resveratrol and cancer: focus on in vivo evidence. *Endocrine-Related Cancer, 21*(3), R209-R225. doi: 10.1530/ERC-13-0171

Cencioni, C., Spallotta, F., Mai, A., Martelli, F., Farsetti, A., Zeiher, A. M., & Gaetano, C. (2015). Sirtuin function in aging heart and vessels. *J Mol Cell Cardiol, 83*, 55-61. doi: 10.1016/j.yjmcc.2014.12.023

César, F., Carnevale Neto, F., Porto, G. S., & Campos, P. M. (2017). Patent analysis: a look at the innovative nature of plant-based cosmetics. *Química Nova, 40*(7), 840-847.

Chahar, M. K., Sharma, N., Dobhal, M. P., & Joshi, Y. C. (2011). Flavonoids: A versatile source of anticancer drugs. *Pharmacogn Rev, 5*(9), 1-12. doi: 10.4103/0973-7847.79093

Chang, C.-C., Yang, M.-H., Wen, H.-M., & Chern, J.-C. (2002). Estimation of total flavonoid content in propolis by two complementary colorimetric methods. *Journal of Food and Drug Analysis, 10*(3), 178-182.

Chang, J. T., & Nevins, J. R. (2006). GATHER: a systems approach to interpreting genomic signatures. *Bioinformatics, 22*(23), 2926-2933. doi: 10.1093/bioinformatics/btl483

Chen, D., Maruschke, M., Hakenberg, O., Zimmermann, W., Stief, C. G., & Buchner, A. (2017). TOP2A, HELLS, ATAD2, and TET3 Are Novel Prognostic Markers in Renal Cell Carcinoma. *Urology, 102*, 265 e261-265 e267. doi: 10.1016/j.urology.2016.12.050

Chen, H., You, M. J., Jiang, Y., Wang, W., & Li, L. (2011). RMI1 attenuates tumor development and is essential for early embryonic survival. *Mol Carcinog, 50*(2), 80-88. doi: 10.1002/mc.20694

Chen, H. Z., Tsai, S. Y., & Leone, G. (2009). Emerging roles of E2Fs in cancer: an exit from cell cycle control. *Nat Rev Cancer, 9*(11), 785-797. doi: 10.1038/nrc2696

Chen, J., O'Donoghue, A., Deng, Y. F., Zhang, B., Kent, F., & O'Hare, T. (2014). The effect of lycopene on the PI3K/Akt signalling pathway in prostate cancer. *Anticancer Agents Med Chem, 14*(6), 800-805.

Chen, X., Li, J., Cheng, Z., Xu, Y., Wang, X., Li, X., . . . Liu, J. (2016). Low Dose Cadmium Inhibits Proliferation of Human Renal Mesangial Cells via Activation of the JNK Pathway. *Int J Environ Res Public Health, 13*(10), 990. doi: 10.3390/ijerph13100990

Chen, X., Li, J., Cheng, Z., Xu, Y., Wang, X., Li, X., . . . Liu, J. (2016). Low Dose Cadmium Inhibits Proliferation of Human Renal Mesangial Cells via Activation of the JNK Pathway. *Int J Environ Res Public Health, 13*(10). doi: 10.3390/ijerph13100990

Cheng, Z., Moore, J., & Yu, L. (2006). High-throughput relative DPPH radical scavenging capacity assay. *J Agric Food Chem, 54*(20), 7429-7436. doi: 10.1021/jf0611668

Chin, Y. T., Hsieh, M. T., Yang, S. H., Tsai, P. W., Wang, S. H., Wang, C. C., . . . Davis, P. J. (2014). Anti-proliferative and gene expression actions of resveratrol in breast cancer cells in vitro. *Oncotarget, 5*(24), 12891-12907. doi: 10.18632/oncotarget.2632

Chinnam, M., & Goodrich, D. W. (2011). RB1, development, and cancer. *Curr Top Dev Biol, 94*, 129-169. doi: 10.1016/b978-0-12-380916-2.00005-x

Chong, Y. J., Musa, N. F., Ng, C. H., Shaari, K., Israf, D. A., & Tham, C. L. (2016). Barrier protective effects of 2,4,6-trihydroxy-3-geranyl acetophenone on lipopolysaccharides-stimulated inflammatory responses in human umbilical vein endothelial cells. *J Ethnopharmacol, 192*, 248-255. doi: 10.1016/j.jep.2016.07.032

Chu, W.-M. (2013). Tumor necrosis factor. *Cancer Lett, 328*(2), 222-225. doi: 10.1016/j.canlet.2012.10.014

Cikos, S., Bukovska, A., & Koppel, J. (2007). Relative quantification of mRNA: comparison of methods currently used for real-time PCR data analysis. *BMC Mol Biol, 8*, 113. doi: 10.1186/1471-2199-8-113

Cleeland, C. S., Allen, J. D., Roberts, S. A., Brell, J. M., Giralt, S. A., Khakoo, A. Y., . . . Skillings, J. (2012). Reducing the toxicity of cancer therapy: recognizing needs, taking action. *Nat Rev Clin Oncol, 9*(8), 471-478. doi: 10.1038/nrclinonc.2012.99

Cooper, G. M., & Hausman, R. E. (2007). *The Cell: A Molecular Approach* (4th ed.). Washington, D.C., USA: ASM Press.

Cope, W. G., Leidy, R. B., & Hodgson, E. (2004). Classes of Toxicants: Use Classes. In E. Hodgson (Ed.), *A Textbook of Modern Toxicology* (3rd ed., pp. 49-74). New Jersey, USA: John Wiley & Sons, Inc.

Couteau, C., & Coiffard, L. (2016). Overview of Skin Whitening Agents: Drugs and Cosmetic Products. *Cosmetics, 3*(3). doi: 10.3390/cosmetics3030027

Cragg, G. M., & Newman, D. J. (2013). Natural products: a continuing source of novel drug leads. *Biochim Biophys Acta, 1830*(6), 3670-3695. doi: 10.1016/j.bbagen.2013.02.008

Croteau, D. L., Popuri, V., Opresko, P. L., & Bohr, V. A. (2014). Human RecQ helicases in DNA repair, recombination, and replication. *Annu Rev Biochem, 83*, 519-552. doi: 10.1146/annurev-biochem-060713-035428

Crowder, R. N., & El-Deiry, W. S. (2012). Caspase-8 regulation of TRAIL-mediated cell death. *Exp Oncol, 34*(3), 160-164.

D'Andrea, G. (2015). Quercetin: A flavonol with multifaceted therapeutic applications? *Fitoterapia, 106*, 256-271. doi: 10.1016/j.fitote.2015.09.018

Dai, D. F., Chiao, Y. A., Marcinek, D. J., Szeto, H. H., & Rabinovitch, P. S. (2014). Mitochondrial oxidative stress in aging and healthspan. *Longev Healthspan, 3*, 6. doi: 10.1186/2046-2395-3-6

Dai, J., & Mumper, R. J. (2010). Plant phenolics: extraction, analysis and their antioxidant and anticancer properties. *Molecules, 15*(10), 7313-7352. doi: 10.3390/molecules15107313

Dang, T. S., Walker, M., Ford, D., & Valentine, R. A. (2014). Nutrigenomics: the role of nutrients in gene expression. *Periodontol 2000, 64*(1), 154-160. doi: 10.1111/prd.12001

Das, M., Prasad, S. B., Yadav, S. S., Govardhan, H. B., Pandey, L. K., Singh, S., . . . Narayan, G. (2013). Over expression of minichromosome maintenance genes is clinically correlated to cervical carcinogenesis. *PLoS One, 8*(7), e69607. doi: 10.1371/journal.pone.0069607

de Jonge, H. J. M., Fehrmann, R. S. N., de Bont, E. S. J. M., Hofstra, R. M. W., Gerbens, F., Kamps, W. A., . . . ter Elst, A. (2007). Evidence Based Selection of Housekeeping Genes. *PLoS One, 2*(9), e898. doi: 10.1371/journal.pone.0000898

de Klerk, E., den Dunnen, J. T., & 't Hoen, P. A. C. (2014). RNA sequencing: from tag-based profiling to resolving complete transcript structure. *Cellular and Molecular Life Sciences, 71*(18), 3537-3551. doi: 10.1007/s00018-014-1637-9

de Magalhaes, J. P., Curado, J., & Church, G. M. (2009). Meta-analysis of age-related gene expression profiles identifies common signatures of aging. *Bioinformatics, 25*(7), 875-881. doi: 10.1093/bioinformatics/btp073

Deegan, T. D., & Diffley, J. F. (2016). MCM: one ring to rule them all. *Curr Opin Struct Biol, 37*, 145-151. doi: 10.1016/j.sbi.2016.01.014

Delaney, G., Jacob, S., Featherstone, C., & Barton, M. (2005). The role of radiotherapy in cancer treatment: estimating optimal utilization from a review of evidence-based clinical guidelines. *Cancer, 104*(6), 1129-1137. doi: 10.1002/cncr.21324

Delbridge, A. R., & Strasser, A. (2015). The BCL-2 protein family, BH3-mimetics and cancer therapy. *Cell Death Differ, 22*(7), 1071-1080. doi: 10.1038/cdd.2015.50

Dhanasekaran, D. N., & Reddy, E. P. (2008). JNK signaling in apoptosis. *Oncogene, 27*(48), 6245-6251. doi: 10.1038/onc.2008.301

Dias, V., Junn, E., & Mouradian, M. M. (2013). The role of oxidative stress in Parkinson's disease. *J Parkinsons Dis, 3*(4), 461-491. doi: 10.3233/jpd-130230

DiLoreto, R., & Murphy, C. T. (2015). The cell biology of aging. *Mol Biol Cell, 26*(25), 4524-4531. doi: 10.1091/mbc.E14-06-1084

Dominguez-Brauer, C., Thu, K. L., Mason, J. M., Blaser, H., Bray, M. R., & Mak, T. W. (2015). Targeting Mitosis in Cancer: Emerging Strategies. *Mol Cell, 60*(4), 524-536. doi: 10.1016/j.molcel.2015.11.006

Donnelly, N., Gorman, A. M., Gupta, S., & Samali, A. (2013). The eIF2alpha kinases: their structures and functions. *Cell Mol Life Sci, 70*(19), 3493-3511. doi: 10.1007/s00018-012-1252-6

Duronio, R. J., & Xiong, Y. (2013). Signaling pathways that control cell proliferation. *Cold Spring Harb Perspect Biol, 5*(3), a008904. doi: 10.1101/cshperspect.a008904

Dzamko, N., Geczy, C. L., & Halliday, G. M. (2015). Inflammation is genetically implicated in Parkinson's disease. *Neuroscience, 302*, 89-102. doi: 10.1016/j.neuroscience.2014.10.028

Ebner, F., Heller, A., Rippke, F., & Tausch, I. (2002). Topical use of dexpanthenol in skin disorders. *Am J Clin Dermatol, 3*(6), 427-433.

Eferl, R., Ricci, R., Kenner, L., Zenz, R., David, J. P., Rath, M., & Wagner, E. F. (2003). Liver tumor development. c-Jun antagonizes the proapoptotic activity of p53. *Cell, 112*(2), 181-192.

Elmore, S. (2007). Apoptosis: A review of programmed cell death. *Toxicol Pathol., 35*(4), 495-516.

Faes, S., & Dormond, O. (2015). PI3K and AKT: Unfaithful Partners in Cancer. *Int J Mol Sci, 16*(9), 21138-21152. doi: 10.3390/ijms160921138

Fan, M., & Chambers, T. C. (2001). Role of mitogen-activated protein kinases in the response of tumor cells to chemotherapy. *Drug Resist Updat, 4*(4), 253-267. doi: 10.1054/drup.2001.0214

Fang, B. A., Kovacevic, Z., Park, K. C., Kalinowski, D. S., Jansson, P. J., Lane, D. J., . . . Richardson, D. R. (2014). Molecular functions of the iron-regulated metastasis suppressor, NDRG1, and its potential as a molecular target for cancer therapy. *Biochim Biophys Acta, 1845*(1), 1-19. doi: 10.1016/j.bbcan.2013.11.002

Fenech, M., El-Sohemy, A., Cahill, L., Ferguson, L. R., French, T. A., Tai, E. S., . . . Head, R. (2011). Nutrigenetics and nutrigenomics: viewpoints on the current status and applications in nutrition research and practice. *J Nutrigenet Nutrigenomics, 4*(2), 69-89. doi: 10.1159/000327772

Ferlay, J., Soerjomataram, I., Dikshit, R., Eser, S., Mathers, C., Rebelo, M., . . . Bray, F. (2015). Cancer incidence and mortality worldwide: sources, methods and major patterns in GLOBOCAN 2012. *Int J Cancer, 136*(5), E359-386. doi: 10.1002/ijc.29210

Filipic, M. (2012). Mechanisms of cadmium induced genomic instability. *Mutat Res, 733*(1-2), 69-77. doi: 10.1016/j.mrfmmm.2011.09.002

Fischer, M. (2017). Census and evaluation of p53 target genes. *Oncogene, 36*(28), 3943-3956. doi: 10.1038/onc.2016.502

Flora, S. J. S., & Pachauri, V. (2010). Chelation in Metal Intoxication. *Int J Environ Res Public Health, 7*(7), 2745-2788. doi: 10.3390/ijerph7072745

Forsburg, S. L. (2004). Eukaryotic MCM Proteins: Beyond Replication Initiation. *Microbiology and Molecular Biology Reviews, 68*(1), 109-131. doi: 10.1128/mmbr.68.1.109-131.2004

Frey, F. M., & Meyers, R. (2010). Antibacterial activity of traditional medicinal plants used by Haudenosaunee peoples of New York State. *BMC Complement Altern Med, 10*, 64. doi: 10.1186/1472-6882-10-64

Furuta, E., Okuda, H., Kobayashi, A., & Watabe, K. (2010). Metabolic genes in cancer: their roles in tumor progression and clinical implications. *Biochim Biophys Acta, 1805*(2), 141-152. doi: 10.1016/j.bbcan.2010.01.005

Gabay, M., Li, Y., & Felsher, D. W. (2014). MYC activation is a hallmark of cancer initiation and maintenance. *Cold Spring Harb Perspect Med, 4*(6). doi: 10.1101/cshperspect.a014241

Gambus, A., Jones, R. C., Sanchez-Diaz, A., Kanemaki, M., van Deursen, F., Edmondson, R. D., & Labib, K. (2006). GINS maintains association of Cdc45 with MCM in replisome progression complexes at eukaryotic DNA replication forks. *Nat Cell Biol, 8*(4), 358-366. doi: 10.1038/ncb1382

Ghazvini, P., Pagan, L. C., Rutledge, T. K., & Goodman, H. S., Jr. (2010). Atopic dermatitis. *J Pharm Pract, 23*(2), 110-116. doi: 10.1177/0897190009360634

Ghosh, P. K., & Gaba, A. (2013). Phyto-extracts in wound healing. *J Pharm Pharm Sci, 16*(5), 760-820.

Giacinti, C., & Giordano, A. (2006). RB and cell cycle progression. *Oncogene, 25*(38), 5220-5227. doi: 10.1038/sj.onc.1209615

Glorieux, C., Zamocky, M., Sandoval, J. M., Verrax, J., & Calderon, P. B. (2015). Regulation of catalase expression in healthy and cancerous cells. *Free Radic Biol Med, 87*, 84-97. doi: 10.1016/j.freeradbiomed.2015.06.017

Goel, H. L., & Mercurio, A. M. (2013). VEGF targets the tumour cell. *Nat Rev Cancer, 13*(12), 871-882. doi: 10.1038/nrc3627

Goldar, S., Khaniani, M. S., Derakhshan, S. M., & Baradaran, B. (2015). Molecular Mechanisms of Apoptosis and Roles in Cancer Development and Treatment. *Asian Pacific Journal of Cancer Prevention, 16*(6), 2129-2144. doi: 10.7314/apjcp.2015.16.6.2129

Goodwin, J. F., & Knudsen, K. E. (2014). Beyond DNA repair: DNA-PK function in cancer. *Cancer Discov, 4*(10), 1126-1139. doi: 10.1158/2159-8290.cd-14-0358

Goruppi, S., & Iovanna, J. L. (2010). Stress-inducible protein p8 is involved in several physiological and pathological processes. *J Biol Chem, 285*(3), 1577-1581. doi: 10.1074/jbc.R109.080887

Govindarajan, R., Duraiyan, J., Kaliyappan, K., & Palanisamy, M. (2012). Microarray and its applications. *Journal of Pharmacy & Bioallied Sciences, 4*(Suppl 2), S310-S312. doi: 10.4103/0975-7406.100283

Guarino, E., Salguero, I., & Kearsey, S. E. (2014). Cellular regulation of ribonucleotide reductase in eukaryotes. *Semin Cell Dev Biol, 30*, 97-103. doi: 10.1016/j.semcdb.2014.03.030

Gurib-Fakim, A. (2006). Medicinal plants: traditions of yesterday and drugs of tomorrow. *Mol Aspects Med, 27*(1), 1-93. doi: 10.1016/j.mam.2005.07.008

Guzińska-ustymowicz, K., Pryczynicz, A., Kemona, A., & Czyżewska, J. (2009). Correlation between Proliferation Markers: PCNA, Ki-67, MCM-2 and Antiapoptotic Protein Bcl-2 in Colorectal Cancer. *Anticancer Res, 29*(8), 3049-3052.

Hagen, J., Muniz, V. P., Falls, K. C., Reed, S. M., Taghiyev, A. F., Quelle, F. W., . . . Quelle, D. E. (2014). RABL6A promotes G1-S phase progression and pancreatic neuroendocrine tumor cell proliferation in an Rb1-dependent manner. *Cancer Res, 74*(22), 6661-6670. doi: 10.1158/0008-5472.CAN-13-3742

Halliwell, B. (2007). Biochemistry of oxidative stress. *Biochem Soc Trans, 35*(Pt 5), 1147-1150. doi: 10.1042/bst0351147

Halliwell, B. (2011). Free radicals and antioxidants - quo vadis? *Trends Pharmacol Sci, 32*(3), 125-130. doi: 10.1016/j.tips.2010.12.002

Halliwell, B. (2012). Free radicals and antioxidants: updating a personal view. *Nutr Rev, 70*(5), 257-265. doi: 10.1111/j.1753-4887.2012.00476.x

Hamid, A., Aiyelaagbe, O., Usman, L., Ameen, O., & Lawal, A. (2010). Antioxidants: Its medicinal and pharmacological applications. *African Journal of pure and applied Chemistry, 4*(8), 142-151.

Hanahan, D., & Weinberg, R. A. (2011). Hallmarks of cancer: the next generation. *Cell, 144*(5), 646-674. doi: 10.1016/j.cell.2011.02.013

Haque, T., Rahman, K. M., Thurston, D. E., Hadgraft, J., & Lane, M. E. (2015). Topical therapies for skin cancer and actinic keratosis. *Eur J Pharm Sci, 77*, 279-289. doi: 10.1016/j.ejps.2015.06.013

Harati, K., Slodnik, P., Chromik, A. M., Goertz, O., Hirsch, T., Kapalschinski, N., . . . Daigeler, A. (2015). Resveratrol induces apoptosis and alters gene expression in human fibrosarcoma cells. *Anticancer Res, 35*(2), 767-774.

Hata, A. N., Engelman, J. A., & Faber, A. C. (2015). The BCL2 Family: Key Mediators of the Apoptotic Response to Targeted Anticancer Therapeutics. *Cancer Discov, 5*(5), 475-487. doi: 10.1158/2159-8290.CD-15-0011

He, X., Yan, B., Liu, S., Jia, J., Lai, W., Xin, X., . . . Tao, Y. (2016). Chromatin Remodeling Factor LSH Drives Cancer Progression by Suppressing the Activity of Fumarate Hydratase. *Cancer Res, 76*(19), 5743-5755. doi: 10.1158/0008-5472.CAN-16-0268

Heberle, H., Meirelles, G. V., da Silva, F. R., Telles, G. P., & Minghim, R. (2015). InteractiVenn: a web-based tool for the analysis of sets through Venn diagrams. *BMC Bioinformatics, 16*(1), 169. doi: 10.1186/s12859-015-0611-3

Heijink, A. M., Krajewska, M., & van Vugt, M. A. (2013). The DNA damage response during mitosis. *Mutat Res, 750*(1-2), 45-55. doi: 10.1016/j.mrfmmm.2013.07.003

Heise, R., Skazik, C., Marquardt, Y., Czaja, K., Sebastian, K., Kurschat, P., . . . Baron, J. M. (2012). Dexpanthenol modulates gene expression in skin wound healing in vivo. *Skin Pharmacol Physiol, 25*(5), 241-248. doi: 10.1159/000341144

Henley, S. A., & Dick, F. A. (2012). The retinoblastoma family of proteins and their regulatory functions in the mammalian cell division cycle. *Cell Div, 7*(1). doi: 10.1186/1747-1028-7-10

Hikisz, P., & Kilianska, Z. M. (2012). PUMA, a critical mediator of cell death--one decade on from its discovery. *Cell Mol Biol Lett, 17*(4), 646-669. doi: 10.2478/s11658-012-0032-5

Hochegger, H., Takeda, S., & Hunt, T. (2008). Cyclin-dependent kinases and cell-cycle transitions: does one fit all? *Nat Rev Mol Cell Biol, 9*(11), 910-916. doi: 10.1038/nrm2510

Hodgson, E., & Levi, P. E. (2004). Nephrotoxicity. In E. Hodgson (Ed.), *A Textbook of Modern Toxicology* (3rd ed., pp. 273-278). New Jersey, USA: John Wiley & Sons, Inc.

Holland, P. M. (2014). Death receptor agonist therapies for cancer, which is the right TRAIL? *Cytokine Growth Factor Rev, 25*(2), 185-193. doi: 10.1016/j.cytogfr.2013.12.009

Holzapfel, N. P., Holzapfel, B. M., Champ, S., Feldthusen, J., Clements, J., & Hutmacher, D. W. (2013). The potential role of lycopene for the prevention and therapy of prostate cancer: from molecular mechanisms to clinical evidence. *Int J Mol Sci, 14*(7), 14620-14646. doi: 10.3390/ijms140714620

Hosoya, N., & Miyagawa, K. (2014). Targeting DNA damage response in cancer therapy. *Cancer Sci, 105*(4), 370-388. doi: 10.1111/cas.12366

Housman, G., Byler, S., Heerboth, S., Lapinska, K., Longacre, M., Snyder, N., & Sarkar, S. (2014). Drug resistance in cancer: an overview. *Cancers (Basel), 6*(3), 1769-1792. doi: 10.3390/cancers6031769

Hua, C., Zhao, G., Li, Y., & Bie, L. (2014). Minichromosome Maintenance (MCM) Family as potential diagnostic and prognostic tumor markers for human gliomas. *BMC Cancer, 14*, 526. doi: 10.1186/1471-2407-14-526

Huang, P., Han, J., & Hui, L. (2010). MAPK signaling in inflammation-associated cancer development. *Protein Cell, 1*(3), 218-226. doi: 10.1007/s13238-010-0019-9

Hussin, F., Eshkoor, S. A., Rahmat, A., Othman, F., & Akim, A. (2014). The centella asiatica juice effects on DNA damage, apoptosis and gene expression in hepatocellular carcinoma (HCC). *BMC Complement Altern Med, 14*, 32-32. doi: 10.1186/1472-6882-14-32

Hyun, S. Y., Hwang, H. I., & Jang, Y. J. (2014). Polo-like kinase-1 in DNA damage response. *BMB Rep, 47*(5), 249-255.

Iqbal, N., & Iqbal, N. (2014). Human Epidermal Growth Factor Receptor 2 (HER2) in Cancers: Overexpression and Therapeutic Implications. *Mol Biol Int, 2014*, 852748. doi: 10.1155/2014/852748

Ishiguro, A., Takahata, T., Saito, M., Yoshiya, G., Tamura, Y., Sasaki, M., & Munakata, A. (2006). Influence of methylated p15 and p16 genes on clinicopathological features in colorectal cancer. *J Gastroenterol Hepatol, 21*(8), 1334-1339. doi: 10.1111/j.1440-1746.2006.04137.x

Ismail, N., Jambari, N. N., Zareen, S., Akhtar, M. N., Shaari, K., Zamri-Saad, M., . . . Israf, D. A. (2012). A geranyl acetophenone targeting cysteinyl leukotriene synthesis prevents allergic airway inflammation in ovalbumin-sensitized mice. *Toxicol Appl Pharmacol, 259*(2), 257-262. doi: 10.1016/j.taap.2012.01.003

Iwakura, Y., Ishigame, H., Saijo, S., & Nakae, S. (2011). Functional specialization of interleukin-17 family members. *Immunity, 34*(2), 149-162. doi: 10.1016/j.immuni.2011.02.012

Jaishankar, M., Tseten, T., Anbalagan, N., Mathew, B. B., & Beeregowda, K. N. (2014). Toxicity, mechanism and health effects of some heavy metals. *Interdisciplinary Toxicology, 7*(2), 60-72. doi: 10.2478/intox-2014-0009

Jaiswal, Y., Liang, Z., & Zhao, Z. (2016). Botanical drugs in Ayurveda and Traditional Chinese Medicine. *J Ethnopharmacol, 194*, 245-259. doi: 10.1016/j.jep.2016.06.052

Jaluria, P., Konstantopoulos, K., Betenbaugh, M., & Shiloach, J. (2007). A perspective on microarrays: current applications, pitfalls, and potential uses. *Microbial Cell Factories, 6*, 4-4. doi: 10.1186/1475-2859-6-4

Jan, A. T., Azam, M., Siddiqui, K., Ali, A., Choi, I., & Haq, Q. M. R. (2015). Heavy Metals and Human Health: Mechanistic Insight into Toxicity and Counter Defense System of Antioxidants. *Int J Mol Sci, 16*(12), 29592-29630. doi: 10.3390/ijms161226183

Janus, J. R., Laborde, R. R., Greenberg, A. J., Wang, V. W., Wei, W., Trier, A., . . . Smith, D. I. (2011). Linking expression of FOXM1, CEP55 and HELLS to tumorigenesis in oropharyngeal squamous cell carcinoma. *Laryngoscope, 121*(12), 2598-2603. doi: 10.1002/lary.22379

Jarup, L., & Akesson, A. (2009). Current status of cadmium as an environmental health problem. *Toxicol Appl Pharmacol, 238*(3), 201-208. doi: 10.1016/j.taap.2009.04.020

Jazirehi, A. R., Lim, A., & Dinh, T. (2016). PD-1 inhibition and treatment of advanced melanoma-role of pembrolizumab. *Am J Cancer Res, 6*(10), 2117-2128.

Jendrossek, V. (2012). The intrinsic apoptosis pathways as a target in anticancer therapy. *Curr Pharm Biotechnol, 13*(8), 1426-1438.

Jia, H. L., Ye, Q. H., Qin, L. X., Budhu, A., Forgues, M., Chen, Y., . . . Wang, X. W. (2007). Gene expression profiling reveals potential biomarkers of human hepatocellular carcinoma. *Clin Cancer Res, 13*(4), 1133-1139. doi: 10.1158/1078-0432.ccr-06-1025

Jia, L. T., Zhang, R., Shen, L., & Yang, A. G. (2015). Regulators of carcinogenesis: emerging roles beyond their primary functions. *Cancer Lett, 357*(1), 75-82. doi: 10.1016/j.canlet.2014.11.048

Jia, Q., Zhou, W., Yao, W., Yang, F., Zhang, S., Singh, R., . . . Wang, N. (2016). Downregulation of YAP-dependent Nupr1 promotes tumor-repopulating cell growth in soft matrices. *Oncogenesis, 5*, e220. doi: 10.1038/oncsis.2016.29

Kalinina, E. V., Chernov, N. N., & Novichkova, M. D. (2014). Role of glutathione, glutathione transferase, and glutaredoxin in regulation of redox-dependent processes. *Biochemistry (Mosc), 79*(13), 1562-1583. doi: 10.1134/s0006297914130082

Kaltalioglu, K., & Coskun-Cevher, S. (2015). A bioactive molecule in a complex wound healing process: platelet-derived growth factor. *Int J Dermatol, 54*(8), 972-977. doi: 10.1111/ijd.12731

Kaltenboeck, B., & Wang, C. (2005). Advances in real-time PCR: application to clinical laboratory diagnostics. *Adv Clin Chem, 40*, 219-259. doi: 10.1016/S0065-2423(05)40006-2

Kamperdick, C., Van, N. H., Sung, C., & Adam, G. (1999). Bisquinolinone alkaloids from *Melicope ptelefolia*. *Phytochemistry, 50*, 177-181.

Kamperdick, C., Van, N. H., Van Sung, T., & Adam, G. (1997). Benzopyrans from Melicope ptelefolia leaves. *Phytochemistry, 45*(5), 1049-1056.

Karapanagioti, E. G., & Assimopoulou, A. N. (2016). Naturally Occurring Wound Healing Agents: An Evidence-Based Review. *Curr Med Chem, 23*(29), 3285-3321.

Karthikeyan, S., & Hoti, S. L. (2015). Development of Fourth Generation ABC Inhibitors from Natural Products: A Novel Approach to Overcome Cancer Multidrug Resistance. *Anticancer Agents Med Chem, 15*(5), 605-615.

Kastenhuber, E. R., & Lowe, S. W. (2017). Putting p53 in Context. *Cell, 170*(6), 1062-1078. doi: https://doi.org/10.1016/j.cell.2017.08.028

Kasuya, A., & Tokura, Y. (2014). Attempts to accelerate wound healing. *J Dermatol Sci, 76*(3), 169-172. doi: 10.1016/j.jdermsci.2014.11.001

Katoh, M. (2016). Therapeutics Targeting FGF Signaling Network in Human Diseases. *Trends Pharmacol Sci, 37*(12), 1081-1096. doi: 10.1016/j.tips.2016.10.003

Katz, L., & Baltz, R. H. (2016). Natural product discovery: past, present, and future. *J Ind Microbiol Biotechnol, 43*(2-3), 155-176. doi: 10.1007/s10295-015-1723-5

Katz, L. H., Li, Y., Chen, J. S., Munoz, N. M., Majumdar, A., Chen, J., & Mishra, L. (2013). Targeting TGF-beta signaling in cancer. *Expert Opin Ther Targets, 17*(7), 743-760. doi: 10.1517/14728222.2013.782287

Kavanagh, E., & Joseph, B. (2011). The hallmarks of CDKN1C (p57, KIP2) in cancer. *Biochim Biophys Acta, 1816*(1), 50-56. doi: 10.1016/j.bbcan.2011.03.002

Kelly, G. S. (2011). Quercetin. Monograph. *Altern Med Rev, 16*(2), 172-194.

Kelly, R. J., Lopez-Chavez, A., Citrin, D., Janik, J. E., & Morris, J. C. (2011). Impacting tumor cell-fate by targeting the inhibitor of apoptosis protein survivin. *Mol Cancer, 10*. doi: 10.1186/1476-4598-10-35

Khan, M. M., Ahmad, A., Ishrat, T., Khan, M. B., Hoda, M. N., Khuwaja, G., . . . Islam, F. (2010). Resveratrol attenuates 6-hydroxydopamine-induced oxidative damage and dopamine depletion in rat model of Parkinson's disease. *Brain Res, 1328*, 139-151. doi: 10.1016/j.brainres.2010.02.031

Kim, H. S., Kim, Y. J., & Seo, Y. R. (2015). An Overview of Carcinogenic Heavy Metal: Molecular Toxicity Mechanism and Prevention. *Journal of Cancer Prevention, 20*(4), 232-240. doi: 10.15430/JCP.2015.20.4.232

Kim, J., Song, H., Heo, H. R., Kim, J. W., Kim, H. R., Hong, Y., . . . Hong, S. H. (2017). Cadmium-induced ER stress and inflammation are mediated through C/EBP-DDIT3 signaling in human bronchial epithelial cells. *Exp Mol Med, 49*(9), e372. doi: 10.1038/emm.2017.125

Kim, J. J., Lee, S. B., Park, J. K., & Yoo, Y. D. (2010). TNF-alpha-induced ROS production triggering apoptosis is directly linked to Romo1 and Bcl-X(L). *Cell Death Differ, 17*(9), 1420-1434. doi: 10.1038/cdd.2010.19

Kim, S. J., Shin, B. G., Choi, I. Y., Kim, D. H., Kim, M. C., Myung, N. Y., . . . Hong, S. H. (2009). Hwanggunchungyitang prevents cadmium-induced ototoxicity through suppression of the activation of caspase-9 and extracellular signal-related kinase in auditory HEI-OC1 cells. *Biol Pharm Bull, 32*(2), 213-219.

Kim, W. Y., & Sharpless, N. E. (2006). The regulation of INK4/ARF in cancer and aging. *Cell, 127*(2), 265-275. doi: 10.1016/j.cell.2006.10.003

Kinch, M. S., Haynesworth, A., Kinch, S. L., & Hoyer, D. (2014). An overview of FDA-approved new molecular entities: 1827-2013. *Drug Discov Today, 19*(8), 1033-1039. doi: 10.1016/j.drudis.2014.03.018

Klaassen, C. D., Liu, J., & Diwan, B. A. (2009). Metallothionein Protection of Cadmium Toxicity. *Toxicol Appl Pharmacol, 238*(3), 215-220. doi: 10.1016/j.taap.2009.03.026

Kolovou, G. D., Kolovou, V., & Mavrogeni, S. (2014). We are ageing. *Biomed Res Int, 2014*, 808307. doi: 10.1155/2014/808307

Kong, X., Shen, Y., Jiang, N., Fei, X., & Mi, J. (2011). Emerging roles of DNA-PK besides DNA repair. *Cell Signal, 23*(8), 1273-1280. doi: 10.1016/j.cellsig.2011.04.005

Kregel, K. C., & Zhang, H. J. (2007). An integrated view of oxidative stress in aging: basic mechanisms, functional effects, and pathological considerations. *Am J Physiol Regul Integr Comp Physiol, 292*(1), R18-36. doi: 10.1152/ajpregu.00327.2006

Kris, M. G., Hellmann, M. D., & Chaft, J. E. (2014). Chemotherapy for lung cancers: here to stay. *Am Soc Clin Oncol Educ Book*, e375-380. doi: 10.14694/EdBook_AM.2014.34.e375

Krishnappa, P., Venkatarangaiah, K., Venkatesh, Shimoga Rajanna, S. K., & Kayattukandy Balan, R. (2016). Wound healing activity of Delonix elata stem bark extract and its isolated constituent quercetin-3-rhamnopyranosyl-(1-6) glucopyranoside in rats. *Journal of Pharmaceutical Analysis, 6*(6), 389-395. doi: https://doi.org/10.1016/j.jpha.2016.05.001

Kubista, M., Andrade, J. M., Bengtsson, M., Forootan, A., Jonak, J., Lind, K., . . . Zoric, N. (2006). The real-time polymerase chain reaction. *Mol Aspects Med, 27*(2-3), 95-125. doi: 10.1016/j.mam.2005.12.007

Kwok, G., Yau, T. C. C., Chiu, J. W., Tse, E., & Kwong, Y.-L. (2016). Pembrolizumab (Keytruda). *Human Vaccines & Immunotherapeutics, 12*(11), 2777-2789. doi: 10.1080/21645515.2016.1199310

Kyrylenko, S., & Baniahmad, A. (2010). Sirtuin family: a link to metabolic signaling and senescence. *Curr Med Chem, 17*(26), 2921-2932.

Lawal, A. O., & Ellis, E. M. (2011). The chemopreventive effects of aged garlic extract against cadmium-induced toxicity. *Environ Toxicol Pharmacol, 32*(2), 266-274. doi: 10.1016/j.etap.2011.05.012

Le Grand, J. N., Chakrama, F. Z., Seguin-Py, S., Fraichard, A., Delage-Mourroux, R., Jouvenot, M., & Boyer-Guittaut, M. (2011). GABARAPL1 (GEC1): original or copycat? *Autophagy, 7*(10), 1098-1107. doi: 10.4161/auto.7.10.15904

Lee, Y. Z., Shaari, K., Cheema, M. S., Tham, C. L., Sulaiman, M. R., & Israf, D. A. (2017). An orally active geranyl acetophenone attenuates airway remodeling in a murine model of chronic asthma. *European Journal of Pharmacology, 797*, 53-64. doi: https://doi.org/10.1016/j.ejphar.2017.01.011

Lerit, D. A., & Poulton, J. S. (2016). Centrosomes are multifunctional regulators of genome stability. *Chromosome Res, 24*(1), 5-17. doi: 10.1007/s10577-015-9506-4

Leroy, B., Girard, L., Hollestelle, A., Minna, J. D., Gazdar, A. F., & Soussi, T. (2014). Analysis of TP53 mutation status in human cancer cell lines: a reassessment. *Hum Mutat, 35*(6), 756-765. doi: 10.1002/humu.22556

Lewerenz, J., & Maher, P. (2009). Basal levels of eIF2alpha phosphorylation determine cellular antioxidant status by regulating ATF4 and xCT expression. *J Biol Chem, 284*(2), 1106-1115. doi: 10.1074/jbc.M807325200

Li, J., & Yuan, J. (2008). Caspases in apoptosis and beyond. *Oncogene, 27*(48), 6194-6206. doi: 10.1038/onc.2008.297

Li, W.-M., Huang, C.-N., Ke, H.-L., Li, C.-C., Wei, Y.-C., Yeh, H.-C., . . . Wu, W.-J. (2016). MCM10 overexpression implicates adverse prognosis in urothelial carcinoma. *Oncotarget, 7*(47), 77777-77792. doi: 10.18632/oncotarget.12795

Li, X., Song, Y., Zhang, P., Zhu, H., Chen, L., Xiao, Y., & Xing, Y. (2016). Oleanolic acid inhibits cell survival and proliferation of prostate cancer cells in vitro and in vivo through the PI3K/Akt pathway. (1423-0380 (Electronic)).

Liebermann, D. A., & Hoffman, B. (2007). Gadd45 in the response of hematopoietic cells to genotoxic stress. *Blood Cells Mol Dis, 39*(3), 329-335. doi: 10.1016/j.bcmd.2007.06.006

Lim, H. W., Collins, S. A. B., Resneck, J. S., Jr., Bolognia, J. L., Hodge, J. A., Rohrer, T. A., . . . Moyano, J. V. (2017). The burden of skin disease in the United States. *J Am Acad Dermatol, 76*(5), 958-972.e952. doi: 10.1016/j.jaad.2016.12.043

Lim, S., & Kaldis, P. (2013). Cdks, cyclins and CKIs: roles beyond cell cycle regulation. *Development, 140*(15), 3079-3093. doi: 10.1242/dev.091744

Lin, E., & Tsai, S. J. (2016). Genome-wide microarray analysis of gene expression profiling in major depression and antidepressant therapy. *Prog Neuropsychopharmacol Biol Psychiatry, 64*, 334-340. doi: 10.1016/j.pnpbp.2015.02.008

Liu, F. S. (2009). Mechanisms of chemotherapeutic drug resistance in cancer therapy--a quick review. *Taiwan J Obstet Gynecol, 48*(3), 239-244. doi: 10.1016/s1028-4559(09)60296-5

Liu, J., Qu, W., & Kadiiska, M. B. (2009). Role of oxidative stress in cadmium toxicity and carcinogenesis. *Toxicol Appl Pharmacol, 238*(3), 209-214. doi: 10.1016/j.taap.2009.01.029

Liu, R. H., & Finley, J. (2005). Potential cell culture models for antioxidant research. *J Agric Food Chem, 53*(10), 4311-4314.

Liu, X., Xue, L., & Yen, Y. (2008). Redox property of ribonucleotide reductase small subunit M2 and p53R2. *Methods Mol Biol, 477*, 195-206. doi: 10.1007/978-1-60327-517-0_15

Livak, K. J., & Schmittgen, T. D. (2001). Analysis of relative gene expression data using real-time quantitative PCR and the 2(-Delta Delta C(T)) Method. *Methods, 25*(4), 402-408. doi: 10.1006/meth.2001.1262

Longo, V. D., Antebi, A., Bartke, A., Barzilai, N., Brown-Borg, H. M., Caruso, C., . . . Fontana, L. (2015). Interventions to Slow Aging in Humans: Are We Ready? *Aging Cell, 14*(4), 497-510. doi: 10.1111/acel.12338

Lopez-Mejia, I. C., & Fajas, L. (2015). Cell cycle regulation of mitochondrial function. *Curr Opin Cell Biol, 33*, 19-25. doi: 10.1016/j.ceb.2014.10.006

Lopez-Otin, C., Blasco, M. A., Partridge, L., Serrano, M., & Kroemer, G. (2013). The hallmarks of aging. *Cell, 153*(6), 1194-1217. doi: 10.1016/j.cell.2013.05.039

Ls, R., & Nja, S. (2016). Anticancer Properties of Phenolic Acids in Colon Cancer – A Review. *Journal of Nutrition & Food Sciences, 06*(02). doi: 10.4172/2155-9600.1000468

Lui, K., An, J., Montalbano, J., Shi, J., Corcoran, C., He, Q., . . . Huang, Y. (2013). Negative regulation of p53 by Ras superfamily protein RBEL1A. *J Cell Sci, 126*(Pt 11), 2436-2445. doi: 10.1242/jcs.118117

Lundstrom, K. (2013). Past, present and future of nutrigenomics and its influence on drug development. *Curr Drug Discov Technol, 10*(1), 35-46.

Luparello, C., Sirchia, R., & Longo, A. (2011). Cadmium as a transcriptional modulator in human cells. *Crit Rev Toxicol, 41*(1), 75-82. doi: 10.3109/10408444.2010.529104

Lynes, M. A., & Yin, X. (2006). Metallothionein and anti-metallothionein, complementary elements of cadmium-induced renal disease. *Toxicol Sci, 91*(1), 1-3. doi: doi:10.1093/toxsci/kfj149

Macheret, M., & Halazonetis, T. D. (2015). DNA replication stress as a hallmark of cancer. *Annu Rev Pathol, 10*, 425-448. doi: 10.1146/annurev-pathol-012414-040424

Maenthaisong, R., Chaiyakunapruk, N., Niruntraporn, S., & Kongkaew, C. (2007). The efficacy of aloe vera used for burn wound healing: a systematic review. *Burns, 33*(6), 713-718. doi: 10.1016/j.burns.2006.10.384

Mahadi, M., Abdul Rahman, N., Viswanathan, D., Taib, I. S., Sulong, A., Hakeem, W. A., . . . Yusuf, Z. (2016). The potential effects of Melicope ptelefolia root extract as an anti-nociceptive and anti-inflammatory on animal models. *Bulletin of Faculty of Pharmacy, Cairo University, 54*(2), 237-241. doi: https://doi.org/10.1016/j.bfopcu.2016.06.005

Malumbres, M. (2011). Physiological relevance of cell cycle kinases. *Physiol Rev, 91*(3), 973-1007. doi: 10.1152/physrev.00025.2010

Mamedov, N. (2012). Medicinal Plants Studies: History, Challenges and Prospective. *Med Aromat Plants, 1*(8). doi: 10.4172/2167-0412.1000e133

Mandinova, A., & Lee, S. W. (2011). The p53 pathway as a target in cancer therapeutics: obstacles and promise. *Sci Transl Med, 3*(64), 64rv61. doi: 10.1126/scitranslmed.3001366

Markopoulou, S., Kontargiris, E., Batsi, C., Tzavaras, T., Trougakos, I., Boothman, D. A., . . . Kolettas, E. (2009). Vanadium-induced apoptosis of HaCaT cells is mediated by c-fos and involves nuclear accumulation of clusterin. *FEBS J, 276*(14), 3784-3799. doi: 10.1111/j.1742-4658.2009.07093.x

Maru, G. B., Hudlikar, R. R., Kumar, G., Gandhi, K., & Mahimkar, M. B. (2016). Understanding the molecular mechanisms of cancer prevention by dietary phytochemicals: From experimental models to clinical trials. *World J Biol Chem, 7*(1), 88-99. doi: 10.4331/wjbc.v7.i1.88

Maver, T., Maver, U., Stana Kleinschek, K., Smrke, D. M., & Kreft, S. (2015). A review of herbal medicines in wound healing. *Int J Dermatol, 54*(7), 740-751. doi: 10.1111/ijd.12766

Mazucanti, C. H., Cabral-Costa, J. V., Vasconcelos, A. R., Andreotti, D. Z., Scavone, C., & Kawamoto, E. M. (2015). Longevity Pathways (mTOR, SIRT, Insulin/IGF-1) as Key Modulatory Targets on Aging and Neurodegeneration. *Curr Top Med Chem, 15*(21), 2116-2138.

McDonell, L. M., Kernohan, K. D., Boycott, K. M., & Sawyer, S. L. (2015). Receptor tyrosine kinase mutations in developmental syndromes and cancer: two sides of the same coin. *Hum Mol Genet, 24*(R1), R60-66. doi: 10.1093/hmg/ddv254

Merched, A. J., & Chan, L. (2013). Nutrigenetics and nutrigenomics of atherosclerosis. *Curr Atheroscler Rep, 15*(6), 328. doi: 10.1007/s11883-013-0328-6

Meulmeester, E., & Ten Dijke, P. (2011). The dynamic roles of TGF-beta in cancer. *J Pathol, 223*(2), 205-218. doi: 10.1002/path.2785

Mi, H., Huang, X., Muruganujan, A., Tang, H., Mills, C., Kang, D., & Thomas, P. D. (2017). PANTHER version 11: expanded annotation data from Gene Ontology and Reactome pathways, and data analysis tool enhancements. *Nucleic Acids Res, 45*(D1), D183-d189. doi: 10.1093/nar/gkw1138

Mi, H., Muruganujan, A., Casagrande, J. T., & Thomas, P. D. (2013). Large-scale gene function analysis with the PANTHER classification system. *Nat Protoc, 8*(8), 1551-1566. doi: 10.1038/nprot.2013.092

Mi, H., & Thomas, P. (2009). PANTHER pathway: an ontology-based pathway database coupled with data analysis tools. *Methods Mol Biol, 563*, 123-140. doi: 10.1007/978-1-60761-175-2_7

Mirończuk-Chodakowska, I., Witkowska, A. M., & Zujko, M. E. (2018). Endogenous non-enzymatic antioxidants in the human body. *Advances in Medical Sciences, 63*(1), 68-78. doi: https://doi.org/10.1016/j.advms.2017.05.005

Mjelle, R., Hegre, S. A., Aas, P. A., Slupphaug, G., Drablos, F., Saetrom, P., & Krokan, H. E. (2015). Cell cycle regulation of human DNA repair and chromatin remodeling genes. *DNA Repair (Amst), 30*, 53-67. doi: 10.1016/j.dnarep.2015.03.007

Molnar, J., Ocsovszki, I., Puskas, L., Ghane, T., Hohmann, J., & Zupko, I. (2013). Investigation of the Antiproliferative Action of the Quinoline Alkaloids Kokusaginine and Skimmianine on Human Cell Lines. *Current Signal Transduction Therapy, 8*(2), 148-155.

Mulders, P. F., De Santis, M., Powles, T., & Fizazi, K. (2015). Targeted treatment of metastatic castration-resistant prostate cancer with sipuleucel-T immunotherapy. *Cancer Immunol Immunother, 64*(6), 655-663. doi: 10.1007/s00262-015-1707-3

Muller, Patricia A., & Vousden, Karen H. (2014). Mutant p53 in Cancer: New Functions and Therapeutic Opportunities. *Cancer Cell, 25*(3), 304-317. doi: 10.1016/j.ccr.2014.01.021

Nag, S., Zhang, X., Srivenugopal, K. S., Wang, M. H., Wang, W., & Zhang, R. (2014). Targeting MDM2-p53 interaction for cancer therapy: are we there yet? *Curr Med Chem, 21*(5), 553-574.

Naidu, C., & Suneetha, Y. (2012). Current knowledge on microarray technology-an overview. *Tropical Journal of Pharmaceutical Research, 11*(1), 153-164. doi: http://dx.doi.org/10.4314/tjpr.v11i1.20

Nair, A. R., Lee, W. K., Smeets, K., Swennen, Q., Sanchez, A., Thevenod, F., & Cuypers, A. (2015). Glutathione and mitochondria determine acute defense responses and adaptive processes in cadmium-induced oxidative stress and toxicity of the kidney. *Arch Toxicol, 89*(12), 2273-2289. doi: 10.1007/s00204-014-1401-9

Nasri, H., Bahmani, M., Shahinfard, N., Moradi Nafchi, A., Saberianpour, S., & Rafieian Kopaei, M. (2015). Medicinal Plants for the Treatment of Acne Vulgaris: A Review of Recent Evidences. *Jundishapur Journal of Microbiology, 8*(11), e25580. doi: 10.5812/jjm.25580

Navarro, E., Serrano-Heras, G., Castano, M. J., & Solera, J. (2015). Real-time PCR detection chemistry. *Clin Chim Acta, 439*, 231-250. doi: 10.1016/j.cca.2014.10.017

Nawrot, T. S., Staessen, J. A., Roels, H. A., Munters, E., Cuypers, A., Richart, T., . . . Vangronsveld, J. (2010). Cadmium exposure in the population: from health risks to strategies of prevention. *Biometals, 23*(5), 769-782. doi: 10.1007/s10534-010-9343-z

Neeha, V. S., & Kinth, P. (2013). Nutrigenomics research: a review. *Journal of Food Science and Technology, 50*(3), 415-428. doi: 10.1007/s13197-012-0775-z

Ness, S. A. (2007). Microarray analysis: basic strategies for successful experiments. *Molecular Biotechnology, 36*(3), 205-219. doi: 10.1007/s12033-007-0012-6

Nimse, S. B., & Pal, D. (2015). Free radicals, natural antioxidants, and their reaction mechanisms. *RSC Advances, 5*(35), 27986-28006. doi: 10.1039/C4RA13315C

O'Connor, M. J. (2015). Targeting the DNA Damage Response in Cancer. *Mol Cell, 60*(4), 547-560. doi: 10.1016/j.molcel.2015.10.040

Odewumi, C. O., Badisa, V. L., Le, U. T., Latinwo, L. M., Ikediobi, C. O., Badisa, R. B., & Darling-Reed, S. F. (2011). Protective effects of N-acetylcysteine against cadmium-induced damage in cultured rat normal liver cells. *Int J Mol Med, 27*(2), 243-248. doi: 10.3892/ijmm.2010.564

Ornitz, D. M., & Itoh, N. (2015). The Fibroblast Growth Factor signaling pathway. *Wiley Interdiscip Rev Dev Biol, 4*(3), 215-266. doi: 10.1002/wdev.176

Ouyang, F., Liu, J., Xia, M., Lin, C., Wu, X., Ye, L., . . . He, M. (2017). GINS2 is a novel prognostic biomarker and promotes tumor progression in early-stage cervical cancer. *Oncol Rep, 37*(5), 2652-2662. doi: 10.3892/or.2017.5573

Ouyang, L., Luo, Y., Tian, M., Zhang, S. Y., Lu, R., Wang, J. H., . . . Li, X. (2014). Plant natural products: from traditional compounds to new emerging drugs in cancer therapy. *Cell Prolif, 47*(6), 506-515. doi: 10.1111/cpr.12143

Pakos-Zebrucka, K., Koryga, I., Mnich, K., Ljujic, M., Samali, A., & Gorman, A. M. (2016). The integrated stress response. *EMBO Rep, 17*(10), 1374-1395. doi: 10.15252/embr.201642195

Pan, S. T., Li, Z. L., He, Z. X., Qiu, J. X., & Zhou, S. F. (2016). Molecular mechanisms for tumour resistance to chemotherapy. *Clin Exp Pharmacol Physiol, 43*(8), 723-737. doi: 10.1111/1440-1681.12581

Panahi, Y., Poursaleh, Z., & Goldust, M. (2015). The efficacy of topical and oral ivermectin in the treatment of human scabies. *Ann Parasitol, 61*(1), 11-16.

Paul, M. K., & Mukhopadhyay, A. K. (2004). Tyrosine kinase – Role and significance in Cancer. *International Journal of Medical Sciences, 1*(2), 101-115.

Pazyar, N., Yaghoobi, R., Bagherani, N., & Kazerouni, A. (2013). A review of applications of tea tree oil in dermatology. *Int J Dermatol, 52*(7), 784-790. doi: 10.1111/j.1365-4632.2012.05654.x

Peng, C., Wang, X., Chen, J., Jiao, R., Wang, L., Li, Y. M., . . . Chen, Z. Y. (2014). Biology of ageing and role of dietary antioxidants. *Biomed Res Int, 2014*, 831841. doi: 10.1155/2014/831841

Pereira, D. M., Valentão, P., Pereira, J. A., & Andrade, P. B. (2009). Phenolics: From Chemistry to Biology. *Molecules, 14*(6), 2202-2211. doi: 10.3390/molecules14062202

Pérez-Herrero, E., & Fernández-Medarde, A. (2015). Advanced targeted therapies in cancer: Drug nanocarriers, the future of chemotherapy. *European Journal of Pharmaceutics and Biopharmaceutics, 93*, 52-79. doi: https://doi.org/10.1016/j.ejpb.2015.03.018

Perrimon, N., Pitsouli, C., & Shilo, B. Z. (2012). Signaling mechanisms controlling cell fate and embryonic patterning. *Cold Spring Harb Perspect Biol, 4*(8), a005975. doi: 10.1101/cshperspect.a005975

Perry, L. M., & Metzger, J. (1980). *Medicinal plants of East and Southeast Asia : attributed properties and uses*. Cambridge: MIT Press.

Pham-Huy, L. A., He, H., & Pham-Huy, C. (2008). Free Radicals, Antioxidants in Disease and Health. *International Journal of Biomedical Science : IJBS, 4*(2), 89-96.

Pillai, V. B., Sundaresan, N. R., & Gupta, M. P. (2014). Regulation of Akt signaling by sirtuins: its implication in cardiac hypertrophy and aging. *Circ Res, 114*(2), 368-378. doi: 10.1161/CIRCRESAHA.113.300536

Pistritto, G., Trisciuoglio, D., Ceci, C., Garufi, A., & D'Orazi, G. (2016). Apoptosis as anticancer mechanism: function and dysfunction of its modulators and targeted therapeutic strategies. *Aging (Albany NY), 8*(4), 603-619. doi: 10.18632/aging.100934

Poniatowski, #x141, A., u., Wojdasiewicz, P., Gasik, R., & Szukiewicz, D. (2015). Transforming Growth Factor Beta Family: Insight into the Role of Growth Factors in Regulation of Fracture Healing Biology and Potential Clinical Applications. *Mediators of Inflammation, 2015*, 17. doi: 10.1155/2015/137823

Pontarin, G., Ferraro, P., Bee, L., Reichard, P., & Bianchi, V. (2012). Mammalian ribonucleotide reductase subunit p53R2 is required for mitochondrial DNA replication and DNA repair in quiescent cells. *Proc Natl Acad Sci U S A, 109*(33), 13302-13307. doi: 10.1073/pnas.1211289109

Proksch, E., de Bony, R., Trapp, S., & Boudon, S. (2017). Topical use of dexpanthenol: a 70th anniversary article. *J Dermatolog Treat, 28*(8), 766-773. doi: 10.1080/09546634.2017.1325310

Rahimzadeh, M. R., Rahimzadeh, M. R., Kazemi, S., & Moghadamnia, A. A. (2017). Cadmium toxicity and treatment: An update. *Caspian Journal of Internal Medicine, 8*(3), 135-145. doi: 10.22088/cjim.8.3.135

Rates, S. M. K. (2001). Plants as a source of drugs. *Toxicon, 39*, 603-613.

Rauth, S., Ray, S., Bhattacharyya, S., Mehrotra, D. G., Alam, N., Mondal, G., . . . Murmu, N. (2016). Lupeol evokes anticancer effects in oral squamous cell carcinoma by inhibiting oncogenic EGFR pathway. *Molecular and Cellular Biochemistry, 417*(1-2), 97-110. doi: 10.1007/s11010-016-2717-y

Razavi, S. M., Jafari, M., Heidarpoor, M., & Khalesi, S. (2015). Minichromosome maintenance-2 (MCM2) expression differentiates oral squamous cell carcinoma from pre-cancerous lesions. *Malays J Pathol, 37*(3), 253-258.

Re, R., Pellegrini, N., Proteggente, A., Yang, M., & Rice-Evans, C. (1999). Antioxidant activity applying an improved ABTS radical cation decolorization assay. *Free Radical Biology & Medicine, 26*, 1231-1237.

Reinke, J. M., & Sorg, H. (2012). Wound repair and regeneration. *Eur Surg Res, 49*(1), 35-43. doi: 10.1159/000339613

Ren, W.-H., Li, Y.-W., Li, R., Feng, H.-B., Wu, J.-L., & Wang, H.-R. (2015). P15 gene methylation in hepatocellular carcinomas: a systematic review and meta-analysis. *International Journal of Clinical and Experimental Medicine, 8*(4), 4762-4768.

Richardson, J. S., Sethi, G., Lee, G. S., & Malek, S. N. (2016). Chalepin: isolated from Ruta angustifolia L. Pers induces mitochondrial mediated apoptosis in lung carcinoma cells. *BMC Complement Altern Med, 16*(1), 389. doi: 10.1186/s12906-016-1368-6

Riedl, S. J., & Shi, Y. (2004). Molecular mechanisms of caspase regulation during apoptosis. *Nat Rev Mol Cell Biol, 5*(11), 897-907. doi: 10.1038/nrm1496

Riscuta, G. (2016). Nutrigenomics at the Interface of Aging, Lifespan, and Cancer Prevention. *J Nutr, 146*(10), 1931-1939. doi: 10.3945/jn.116.235119

Rolfe, H. M. (2014). A review of nicotinamide: treatment of skin diseases and potential side effects. *J Cosmet Dermatol, 13*(4), 324-328. doi: 10.1111/jocd.12119

Rosemary Siafakas, A., & Richardson, D. R. (2009). Growth arrest and DNA damage-45 alpha (GADD45alpha). *Int J Biochem Cell Biol, 41*(5), 986-989. doi: 10.1016/j.biocel.2008.06.018

Roth, M., Wang, Z., & Chen, W. Y. (2013). Sirtuins in hematological aging and malignancy. *Crit Rev Oncog, 18*(6), 531-547.

Rovida, E., & Stecca, B. (2015). Mitogen-activated protein kinases and Hedgehog-GLI signaling in cancer: A crosstalk providing therapeutic opportunities? *Semin Cancer Biol, 35*, 154-167. doi: 10.1016/j.semcancer.2015.08.003

Rubino, F. M. (2015). Toxicity of Glutathione-Binding Metals: A Review of Targets and Mechanisms. *Toxics, 3*(1), 20-62. doi: 10.3390/toxics3010020

Ruiz-Laguna, J., Velez, J. M., Pueyo, C., & Abril, N. (2016). Global gene expression profiling using heterologous DNA microarrays to analyze alterations in the transcriptome of Mus spretus mice living in a heavily polluted environment. *Environ Sci Pollut Res Int, 23*(6), 5853-5867. doi: 10.1007/s11356-015-5824-5

Russo, M., Spagnuolo, C., Tedesco, I., & Russo, G. L. (2010). Phytochemicals in cancer prevention and therapy: truth or dare? *Toxins (Basel), 2*(4), 517-551. doi: 10.3390/toxins2040517

Ruttkay-Nedecky, B., Nejdl, L., Gumulec, J., Zitka, O., Masarik, M., Eckschlager, T., . . . Kizek, R. (2013). The role of metallothionein in oxidative stress. *Int J Mol Sci, 14*(3), 6044-6066. doi: 10.3390/ijms14036044

Sadowska-Bartosz, I., & Bartosz, G. (2014). Effect of antioxidants supplementation on aging and longevity. *Biomed Res Int, 2014*, 404680. doi: 10.1155/2014/404680

Salminen, A., Kaarniranta, K., & Kauppinen, A. (2018). Phytochemicals inhibit the immunosuppressive functions of myeloid-derived suppressor cells (MDSC): Impact on cancer and age-related chronic inflammatory disorders. *Int Immunopharmacol, 61*, 231-240. doi: 10.1016/j.intimp.2018.06.005

Salvador, J. M., Brown-Clay, J. D., & Fornace, A. J., Jr. (2013). Gadd45 in stress signaling, cell cycle control, and apoptosis. *Adv Exp Med Biol, 793*, 1-19. doi: 10.1007/978-1-4614-8289-5_1

Sampson, J. H., Raman, A., Karlsen, G., Navsaria, H., & Leigh, I. M. (2001). In vitro keratinocyte antiproliferant effect of Centella asiatica extract and triterpenoid saponins. *Phytomedicine, 8*(3), 230-235. doi: 10.1078/0944-7113-00032

Samuel, A. J. S. J., Kalusalingam, A., Chellappan, D. K., Gopinath, R., Radhamani, S., Husain, H. A., . . . Promwichit, P. (2010). Ethnomedical survey of plants used by the Orang Asli in Kampung Bawong, Perak, West Malaysia. *Journal of Ethnobiology and Ethnomedicine, 6*(1), 5. doi: 10.1186/1746-4269-6-5

Sandbichler, A. M., & Hockner, M. (2016). Cadmium Protection Strategies--A Hidden Trade-Off? *Int J Mol Sci, 17*(1). doi: 10.3390/ijms17010139

Santo, L., Siu, K. T., & Raje, N. (2015). Targeting Cyclin-Dependent Kinases and Cell Cycle Progression in Human Cancers. *Semin Oncol, 42*(6), 788-800. doi: 10.1053/j.seminoncol.2015.09.024

Saraswathy, M., & Gong, S. (2013). Different strategies to overcome multidrug resistance in cancer. *Biotechnol Adv, 31*(8), 1397-1407. doi: 10.1016/j.biotechadv.2013.06.004

Satyanarayana, A., & Kaldis, P. (2009). Mammalian cell-cycle regulation: several Cdks, numerous cyclins and diverse compensatory mechanisms. *Oncogene, 28*(33), 2925-2939. doi: 10.1038/onc.2009.170

Schmucker, S., & Sumara, I. (2014). Molecular dynamics of PLK1 during mitosis. *Mol Cell Oncol, 1*(2), e954507. doi: 10.1080/23723548.2014.954507

Schnekenburger, M., Karius, T., & Diederich, M. (2014). Regulation of epigenetic traits of the glutathione S-transferase P1 gene: from detoxification toward cancer prevention and diagnosis. *Frontiers in Pharmacology, 5*, 170. doi: 10.3389/fphar.2014.00170

Schwermer, M., Dreesmann, S., Eggert, A., Althoff, K., Steenpass, L., Schramm, A., . . . Temming, P. (2017). Pharmaceutically inhibiting polo-like kinase 1 exerts a broad anti-tumour activity in retinoblastoma cell lines. *Clin Exp Ophthalmol, 45*(3), 288-296. doi: 10.1111/ceo.12838

Segaliny, A. I., Tellez-Gabriel, M., Heymann, M. F., & Heymann, D. (2015). Receptor tyrosine kinases: Characterisation, mechanism of action and therapeutic interests for bone cancers. *J Bone Oncol, 4*(1), 1-12. doi: 10.1016/j.jbo.2015.01.001

Sever, R., & Brugge, J. S. (2015). Signal Transduction in Cancer. *Cold Spring Harbor Perspectives in Medicine, 5*(4), a006098. doi: 10.1101/cshperspect.a006098

Shaari, K., Suppaiah, V., Wai, L. K., Stanslas, J., Tejo, B. A., Israf, D. A., . . . Lajis, N. H. (2011). Bioassay-guided identification of an anti-inflammatory prenylated acylphloroglucinol from Melicope ptelefolia and molecular insights into its interaction with 5-lipoxygenase. *Bioorg Med Chem, 19*(21), 6340-6347. doi: 10.1016/j.bmc.2011.09.001

Shaari, K., Zareen, S., Akhtar, M. N., & Lajis, N. H. (2011). Chemical constituents of Melicope ptelefolia. *Nat Prod Commun, 6*(3), 343-348.

Shapiro, G. I., & Harper, J. W. (1999). Anticancer drug targets: cell cycle and checkpoint control. *The Journal of Clinical Investigation, 104*, 1645-1653.

Shapiro, M. D., & Fazio, S. (2016). From Lipids to Inflammation: New Approaches to Reducing Atherosclerotic Risk. *Circ Res, 118*(4), 732-749. doi: 10.1161/circresaha.115.306471

Sharma, O. P., & Bhat, T. K. (2009). DPPH antioxidant assay revisited. *Food chemistry, 113*(4), 1202-1205. doi: 10.1016/j.foodchem.2008.08.008

Shori, A. B. (2015). Screening of antidiabetic and antioxidant activities of medicinal plants. *J Integr Med, 13*(5), 297-305. doi: 10.1016/s2095-4964(15)60193-5

Shuib, N. H., Shaari, K., Khatib, A., Kneer, R., Zareen, S., Raof, S. M., . . . Neto, V. (2011). Discrimination of young and mature leaves of Melicope ptelefolia using 1H NMR and multivariate data analysis. *Food chemistry, 126*(2), 640-645.

Sia, D., Alsinet, C., Newell, P., & Villanueva, A. (2014). VEGF signaling in cancer treatment. *Curr Pharm Des, 20*(17), 2834-2842.

Siafakas, A. R., & Richardson, D. R. (2009). Growth arrest and DNA damage-45 alpha (GADD45 alpha). *International Journal of Biochemistry & Cell Biology, 41*(5), 986-989. doi: 10.1016/j.biocel.2008.06.018

Siew, Y. Y., Zareisedehizadeh, S., Seetoh, W. G., Neo, S. Y., Tan, C. H., & Koh, H. L. (2014). Ethnobotanical survey of usage of fresh medicinal plants in Singapore. *J Ethnopharmacol, 155*(3), 1450-1466. doi: 10.1016/j.jep.2014.07.024

Simon, N. E., & Schwacha, A. (2014). The Mcm2-7 replicative helicase: a promising chemotherapeutic target. *Biomed Res Int, 2014*, wo. doi: 10.1155/2014/549719

Sindhi, V., Gupta, V., Sharma, K., Bhatnagar, S., Kumari, R., & Dhaka, N. (2013). Potential applications of antioxidants – A review. *Journal of Pharmacy Research, 7*(9), 828-835. doi: https://doi.org/10.1016/j.jopr.2013.10.001

Singh, H., Longo, D. L., & Chabner, B. A. (2015). Improving Prospects for Targeting RAS. *J Clin Oncol, 33*(31), 3650-3659. doi: 10.1200/jco.2015.62.1052

Singh, S., Sharma, B., Kanwar, S. S., & Kumar, A. (2016). Lead Phytochemicals for Anticancer Drug Development. *Frontiers in Plant Science, 7*. doi: 10.3389/fpls.2016.01667

Singleton, V. L., & Rossi, J. A. (1965). Colorimetry of Total Phenolics with Phosphomolybdic-Phosphotungstic Acid Reagents. *American Journal of Enology and Viticulture, 16*, 144-158.

Siti, Z. M., Tahir, A., Farah, A. I., Fazlin, S. M. A., Sondi, S., Azman, A. H., . . . Zaleha, W. C. W. (2009). Use of traditional and complementary medicine in Malaysia: a baseline study. *Complementary Therapies in Medicine, 17*(5), 292-299. doi: https://doi.org/10.1016/j.ctim.2009.04.002

Snook, A. E., & Waldman, S. A. (2013). Advances in Cancer Immunotherapy. *Discovery medicine, 15*(81), 120-125.

Sodani, K., Patel, A., Kathawala, R. J., & Chen, Z.-S. (2012). Multidrug resistance associated proteins in multidrug resistance. *Chinese Journal of Cancer, 31*(2), 58-72. doi: 10.5732/cjc.011.10329

Sofowora, A., Ogunbodede, E., & Onayade, A. (2013). The role and place of medicinal plants in the strategies for disease prevention. *Afr J Tradit Complement Altern Med, 10*(5), 210-229.

Song, W., Derito, C. M., Liu, M. K., He, X., Dong, M., & Liu, R. H. (2010). Cellular antioxidant activity of common vegetables. *J Agric Food Chem, 58*(11), 6621-6629. doi: 10.1021/jf9035832

Song, X., & Qian, Y. (2013a). The activation and regulation of IL-17 receptor mediated signaling. *Cytokine, 62*(2), 175-182. doi: 10.1016/j.cyto.2013.03.014

Song, X., & Qian, Y. (2013b). IL-17 family cytokines mediated signaling in the pathogenesis of inflammatory diseases. *Cell Signal, 25*(12), 2335-2347. doi: 10.1016/j.cellsig.2013.07.021

Stepanic, V., Gasparovic, A. C., Troselj, K. G., Amic, D., & Zarkovic, N. (2015). Selected attributes of polyphenols in targeting oxidative stress in cancer. *Curr Top Med Chem, 15*(5), 496-509.

Stites, E. C., & Ravichandran, K. S. (2009). A systems perspective of ras signaling in cancer. *Clin Cancer Res, 15*(5), 1510-1513. doi: 10.1158/1078-0432.ccr-08-2753

Strebhardt, K. (2010). Multifaceted polo-like kinases: drug targets and antitargets for cancer therapy. *Nat Rev Drug Discov, 9*(8), 643-660. doi: 10.1038/nrd3184

Sulaiman, M. R., Mohd Padzil, A., Shaari, K., Khalid, S., Shaik Mossadeq, W. M., Mohamad, A. S., . . . Lajis, N. (2010). Antinociceptive Activity of Melicope ptelefolia Ethanolic Extract in Experimental Animals. *Journal of Biomedicine and Biotechnology, 2010*, 937642. doi: 10.1155/2010/937642

Sultana, S., Asif, H. M., Nazar, H. M., Akhtar, N., Rehman, J. U., & Rehman, R. U. (2014). Medicinal plants combating against cancer--a green anticancer approach. *Asian Pac J Cancer Prev, 15*(11), 4385-4394.

Sun, W., & Yang, J. (2010). Functional Mechanisms for Human Tumor Suppressors. *Journal of Cancer, 1*, 136-140.

Suragani, R. N. V. S., Zachariah, R. S., Velazquez, J. G., Liu, S. J., Sun, C. W., Townes, T. M., & Chen, J. J. (2012). Heme-regulated eIF2 alpha kinase activated Atf4 signaling pathway in oxidative stress and erythropoiesis. *Blood, 119*(22), 5276-5284. doi: 10.1182/blood-2011-10-388132

Surova, O., & Zhivotovsky, B. (2013). Various modes of cell death induced by DNA damage. *Oncogene, 32*(33), 3789-3797. doi: 10.1038/onc.2012.556

Synge, H., Akerele, O., & Heywood, V. H. (1991). *The Conservation of Medicinal Plants: Proceedings of an International Consultation, 21-27 March 1988 Held at Chiang Mai, Thailand* (H. Synge, O. Akerele & V. H. Heywood Eds.): Cambridge University Press, Cambridge, UK.

Szklarczyk, D., Franceschini, A., Wyder, S., Forslund, K., Heller, D., Huerta-Cepas, J., . . . von Mering, C. (2015). STRING v10: protein-protein interaction networks, integrated over the tree of life. *Nucleic Acids Res, 43*(Database issue), D447-452. doi: 10.1093/nar/gku1003

Szychot, E., Brodkiewicz, A., & Peregud-Pogorzelski, J. (2013). Will therapies that target tumour suppressor genes be useful in cancer treatment? *Adv Clin Exp Med, 22*(6), 861-864.

Tabassum, N., & Hamdani, M. (2014). Plants used to treat skin diseases. *Pharmacognosy Reviews, 8*(15), 52-60. doi: 10.4103/0973-7847.125531

Tan, J. W., Israf, D. A., Harith, H. H., Md Hashim, N. F., Ng, C. H., Shaari, K., & Tham, C. L. (2017). Anti-allergic activity of 2,4,6-trihydroxy-3-geranylacetophenone (tHGA) via attenuation of IgE-mediated mast cell activation and inhibition of passive systemic anaphylaxis. *Toxicol Appl Pharmacol, 319*, 47-58. doi: https://doi.org/10.1016/j.taap.2017.02.002

Tan, J. W., Israf, D. A., Md Hashim, N. F., Cheah, Y. K., Harith, H. H., Shaari, K., & Tham, C. L. (2017). LAT is essential for the mast cell stabilising effect of tHGA in IgE-mediated mast cell activation. *Biochem Pharmacol, 144*, 132-148. doi: 10.1016/j.bcp.2017.08.010

Tang, H., Ji, F., Sun, J., Xie, Y., Xu, Y., & Yue, H. (2016). RBEL1 is required for osteosarcoma cell proliferation via inhibiting retinoblastoma 1. *Mol Med Rep, 13*(2), 1275-1280. doi: 10.3892/mmr.2015.4670

Tapas, A., Sakarkar, D., & Kakde, R. (2008). Flavonoids as nutraceuticals: A review. *Trop J Pharm Res, 7*(3), 1089-1099.

Tariq, A., Mussarat, S., & Adnan, M. (2015). Review on ethnomedicinal, phytochemical and pharmacological evidence of Himalayan anticancer plants. *J Ethnopharmacol, 164*, 96-119. doi: 10.1016/j.jep.2015.02.003

Tchounwou, P. B., Yedjou, C. G., Patlolla, A. K., & Sutton, D. J. (2012). Heavy Metals Toxicity and the Environment. *EXS, 101*, 133-164. doi: 10.1007/978-3-7643-8340-4_6

Teiten, M. H., Gaascht, F., Dicato, M., & Diederich, M. (2013). Anticancer bioactivity of compounds from medicinal plants used in European medieval traditions. *Biochem Pharmacol, 86*(9), 1239-1247. doi: 10.1016/j.bcp.2013.08.007

Thirumaran, R., Prendergast, G. C., & Gilman, P. B. (2007). Cytotoxic chemotherapy in clinical treatment of cancer. In G. C. Prendergast & E. M. Jaffee (Eds.), *Cancer immunotherapy: Immune suppression and tumor growth* (pp. 101-116). California, USA: Elsevier Inc.

Thirumoorthy, N., Manisenthil Kumar, K. T., Shyam Sundar, A., Panayappan, L., & Chatterjee, M. (2007). Metallothionein: an overview. *World J Gastroenterol, 13*(7), 993-996.

Thorpe, L. M., Yuzugullu, H., & Zhao, J. J. (2015). PI3K in cancer: divergent roles of isoforms, modes of activation and therapeutic targeting. *Nat Rev Cancer, 15*(1), 7-24. doi: 10.1038/nrc3860

Tiwari BK, Brunton N, & CS, B. (2013). *Handbook of plant food phytochemicals: sources, stability and extraction.* . Hoboken N.J: Wiley-Blackwell.

Toffalorio, F., Belloni, E., Barberis, M., Bucci, G., Tizzoni, L., Pruneri, G., . . . De Pas, T. (2014). Gene expression profiling reveals GC and CEACAM1 as new tools in the diagnosis of lung carcinoids. *British Journal of Cancer, 110*(5), 1244-1249. doi: 10.1038/bjc.2014.41

Tomicic, M. T., Meise, R., Aasland, D., Berte, N., Kitzinger, R., Kramer, O. H., . . . Christmann, M. (2015). Apoptosis induced by temozolomide and nimustine in glioblastoma cells is supported by JNK/c-Jun-mediated induction of the BH3-only protein BIM. *Oncotarget, 6*(32), 33755-33768. doi: 10.18632/oncotarget.5274

Torre, L. A., Bray, F., Siegel, R. L., Ferlay, J., Lortet-Tieulent, J., & Jemal, A. (2015). Global cancer statistics, 2012. *CA Cancer J Clin, 65*(2), 87-108. doi: 10.3322/caac.21262

Twentyman, P. R., & Luscombe, M. (1987). A study of some variables in a tetrazolium dye (MTT) based assay for cell growth and chemosensitivity. *Br J Cancer, 56*(3), 279-285.

Uhlen, M., Oksvold, P., Fagerberg, L., Lundberg, E., Jonasson, K., Forsberg, M., . . . Ponten, F. (2010). Towards a knowledge-based Human Protein Atlas. *Nat Biotechnol, 28*(12), 1248-1250. doi: 10.1038/nbt1210-1248

Valdespino-Gómez, V. M., Valdespino-Castillo, P. M., & Valdespino-Castillo, V. E. (2015). Cell signalling pathways interaction in cellular proliferation: Potential target for therapeutic interventionism. *Cirugía y Cirujanos (English Edition), 83*(2), 165-174. doi: https://doi.org/10.1016/j.circen.2015.08.015

Valko, M., Leibfritz, D., Moncol, J., Cronin, M. T., Mazur, M., & Telser, J. (2007). Free radicals and antioxidants in normal physiological functions and human disease. *Int J Biochem Cell Biol, 39*(1), 44-84. doi: 10.1016/j.biocel.2006.07.001

van Diepen, J. A., Berbée, J. F. P., Havekes, L. M., & Rensen, P. C. N. (2013). Interactions between inflammation and lipid metabolism: Relevance for efficacy of anti-inflammatory drugs in the treatment of atherosclerosis. *Atherosclerosis, 228*(2), 306-315. doi: https://doi.org/10.1016/j.atherosclerosis.2013.02.028

Van Engeland, M., Nieland, L. J. W., Ramaekers, F. C. S., Schutte, B., & Reutelingsperger, C. P. M. (1998). Annexin V-affinity assay: A review on an apoptosis detection system based on phosphatidylserine exposure. *Cytometry, 31*, 1-9.

Van, N. H., Kamperdick, C., Sung, C., & Adam, G. (1998). Benzopyran dimers from *Melicope ptelefolia*. *Phytochemistry, 48*, 1055-1057.

Vasisht, K., Sharma, N., & Karan, M. (2016). Current Perspective in the International Trade of Medicinal Plants Material: An Update. *Curr Pharm Des, 22*(27), 4288-4336.

Vermeulen, K., Van Bockstaele, D. R., & Berneman, Z. N. (2003). The cell cycle: A review of regulation, deregulation and therapeutic targets in cancer. *Cell Prolif., 36*, 131-149.

von Eyss, B., Maaskola, J., Memczak, S., Mollmann, K., Schuetz, A., Loddenkemper, C., . . . Ziebold, U. (2012). The SNF2-like helicase HELLS mediates E2F3-dependent transcription and cellular transformation. *EMBO J, 31*(4), 972-985. doi: 10.1038/emboj.2011.451

Waisberg, M., Joseph, P., Hale, B., & Beyersmann, D. (2003). Molecular and cellular mechanisms of cadmium carcinogenesis. *Toxicology, 192*(2-3), 95-117.

Wan, P. T., Garnett, M. J., Roe, S. M., Lee, S., Niculescu-Duvaz, D., Good, V. M., . . . Marais, R. (2004). Mechanism of activation of the RAF-ERK signaling pathway by oncogenic mutations of B-RAF. *Cell, 116*(6), 855-867.

Wang, C., & Lin, A. (2014). Efficacy of topical calcineurin inhibitors in psoriasis. *J Cutan Med Surg, 18*(1), 8-14. doi: 10.2310/7750.2013.13059

Wang, G., Jiang, Q., & Zhang, C. (2014). The role of mitotic kinases in coupling the centrosome cycle with the assembly of the mitotic spindle. *J Cell Sci, 127*(Pt 19), 4111-4122. doi: 10.1242/jcs.151753

Wang, L., Du, F., & Wang, X. (2008). TNF-alpha induces two distinct caspase-8 activation pathways. *Cell, 133*(4), 693-703. doi: 10.1016/j.cell.2008.03.036

Wang, S. C. (2014). PCNA: a silent housekeeper or a potential therapeutic target? *Trends Pharmacol Sci, 35*(4), 178-186. doi: 10.1016/j.tips.2014.02.004

Wang, Z., Fukushima, H., Inuzuka, H., Wan, L., Liu, P., Gao, D., . . . Wei, W. (2012). Skp2 is a promising therapeutic target in breast cancer. *Front Oncol, 1*(57). doi: 10.3389/fonc.2011.00057

Wang, Z., Gerstein, M., & Snyder, M. (2009). RNA-Seq: a revolutionary tool for transcriptomics. *Nat Rev Genet, 10*(1), 57-63. doi: 10.1038/nrg2484

Weber, J. S., Yang, J. C., Atkins, M. B., & Disis, M. L. (2015). Toxicities of Immunotherapy for the Practitioner. *Journal of Clinical Oncology, 33*(18), 2092-2099. doi: 10.1200/JCO.2014.60.0379

Wee, P., & Wang, Z. (2017). Epidermal Growth Factor Receptor Cell Proliferation Signaling Pathways. *Cancers (Basel), 9*(5). doi: 10.3390/cancers9050052

Weng, Z., Zhang, B., Asadi, S., Sismanopoulos, N., Butcher, A., Fu, X., . . . Theoharides, T. C. (2012). Quercetin is more effective than cromolyn in blocking human mast cell cytokine release and inhibits contact dermatitis and photosensitivity in humans. *PLoS One, 7*(3), e33805. doi: 10.1371/journal.pone.0033805

Whitley, S. K., Horne, W. T., & Kolls, J. K. (2016). Research Techniques Made Simple: Methodology and Clinical Applications of RNA Sequencing. *J Invest Dermatol, 136*(8), e77-82. doi: 10.1016/j.jid.2016.06.003

Wicks, K., Torbica, T., Umehara, T., Amin, S., Bobola, N., & Mace, K. A. (2015). Diabetes Inhibits Gr-1+ Myeloid Cell Maturation via Cebpa Deregulation. *Diabetes, 64*(12), 4184-4197. doi: 10.2337/db14-1895

Wiederholt, T., Heise, R., Skazik, C., Marquardt, Y., Joussen, S., Erdmann, K., . . . Baron, J. M. (2009). Calcium pantothenate modulates gene expression in proliferating human dermal fibroblasts. *Exp Dermatol, 18*(11), 969-978. doi: 10.1111/j.1600-0625.2009.00884.x

Wild, T., Rahbarnia, A., Kellner, M., Sobotka, L., & Eberlein, T. (2010). Basics in nutrition and wound healing. *Nutrition, 26*(9), 862-866. doi: 10.1016/j.nut.2010.05.008

Wolf, J. B. (2013). Principles of transcriptome analysis and gene expression quantification: an RNA-seq tutorial. *Mol Ecol Resour, 13*(4), 559-572. doi: 10.1111/1755-0998.12109

Wolfe, K. L., & Liu, R. H. (2007). Cellular antioxidant assay for assessing antioxidants, foods, and dietary supplements. *J Agric Food Chem, 55*(22), 8896-8907.

Wolgemuth, D. J. (2008). Function of cyclins in regulating the mitotic and meiotic cell cycles in male germ cells. *Cell Cycle, 7*(22), 3509-3513. doi: 10.4161/cc.7.22.6978

Wong, R. S. (2011). Apoptosis in cancer: from pathogenesis to treatment. *J Exp Clin Cancer Res, 30*. doi: 10.1186/1756-9966-30-87

Wu, C., Zhu, J., & Zhang, X. (2012). Integrating gene expression and protein-protein interaction network to prioritize cancer-associated genes. *BMC Bioinformatics, 13*, 182. doi: 10.1186/1471-2105-13-182

Wu, J. Q., Kosten, T. R., & Zhang, X. Y. (2013). Free radicals, antioxidant defense systems, and schizophrenia. *Prog Neuropsychopharmacol Biol Psychiatry, 46*, 200-206. doi: 10.1016/j.pnpbp.2013.02.015

Wu, L., Liu, Y., & Kong, D. (2014). Mechanism of chromosomal DNA replication initiation and replication fork stabilization in eukaryotes. *Sci China Life Sci, 57*(5), 482-487. doi: 10.1007/s11427-014-4631-4

Xia, H., & Hui, K. M. (2014). Mechanism of cancer drug resistance and the involvement of noncoding RNAs. *Curr Med Chem, 21*(26), 3029-3041.

Xu, J.-F., Zhao, H.-J., Wang, X.-B., Li, Z.-R., Luo, J., Yang, M.-H., . . . Kong, L.-Y. (2015). (±)-Melicolones A and B, Rearranged Prenylated Acetophenone Stereoisomers with an Unusual 9-Oxatricyclo[3.2.1.13,8]nonane Core from the Leaves of Melicope ptelefolia. *Org Lett, 17*(1), 146-149. doi: 10.1021/ol5033738

Xu, J., Sun, X., Liu, X., Peng, M., Li, S., Jin, D.-Q., . . . Guo, Y. (2016). Phytochemical constituents from Melicope pteleifolia that promote neurite outgrowth in PC12 cells. *Journal of Functional Foods, 23*, 565-572. doi: https://doi.org/10.1016/j.jff.2016.03.011

Xu, L., Zhu, Y., Shao, J., Chen, M., Yan, H., Li, G., . . . He, Q. (2017). Dasatinib synergises with irinotecan to suppress hepatocellular carcinoma via inhibiting the protein synthesis of PLK1. *Br J Cancer, 116*(8), 1027-1036. doi: 10.1038/bjc.2017.55

Xu, Q., Fu, R., Yin, G., Liu, X., Liu, Y., & Xiang, M. (2016). Microarray-based gene expression profiling reveals genes and pathways involved in the oncogenic function of REG3A on pancreatic cancer cells. *Gene, 578*(2), 263-273. doi: 10.1016/j.gene.2015.12.039

Xu, Q., Zong, L., Chen, X., Jiang, Z., Nan, L., Li, J., . . . Ma, Z. (2015). Resveratrol in the treatment of pancreatic cancer. *Ann N Y Acad Sci, 1348*(1), 10-19. doi: 10.1111/nyas.12837

Yang, C. W., Lee, Y. Z., Hsu, H. Y., Wu, C. M., Chang, H. Y., Chao, Y. S., & Lee, S. J. (2013). c-Jun-mediated anticancer mechanisms of tylophorine. *Carcinogenesis, 34*(6), 1304-1314. doi: 10.1093/carcin/bgt039

Yang, J., O'Donnell, L., Durocher, D., & Brown, G. W. (2012). RMI1 promotes DNA replication fork progression and recovery from replication fork stress. *Mol Cell Biol, 32*(15), 3054-3064. doi: 10.1128/mcb.00255-12

Yarbrough, K. B., Neuhaus, K. J., & Simpson, E. L. (2013). The effects of treatment on itch in atopic dermatitis. *Dermatol Ther, 26*(2), 110-119. doi: 10.1111/dth.12032

Yoou, M. S., Kim, H. M., & Jeong, H. J. (2015). Acteoside attenuates TSLP-induced mast cell proliferation via down-regulating MDM2. *Int Immunopharmacol, 26*(1), 23-29. doi: 10.1016/j.intimp.2015.03.003

Yu, J., & Zhang, L. (2008). PUMA, a potent killer with or without p53. *Oncogene, 27 Suppl 1*, S71-83. doi: 10.1038/onc.2009.45

Zhai, Q., Narbad, A., & Chen, W. (2015). Dietary Strategies for the Treatment of Cadmium and Lead Toxicity. *Nutrients, 7*(1), 552-571. doi: 10.3390/nu7010552

Zhan, Q. (2005). Gadd45a, a p53- and BRCA1-regulated stress protein, in cellular response to DNA damage. *Mutat Res, 569*(1-2), 133-143. doi: 10.1016/j.mrfmmm.2004.06.055

Zhang, Y., Wang, F., Han, L., Wu, Y., Li, S., Yang, X., . . . Chang, Z. (2011). GABARAPL1 negatively regulates Wnt/beta-catenin signaling by mediating Dvl2 degradation through the autophagy pathway. *Cell Physiol Biochem, 27*(5), 503-512. doi: 10.1159/000329952

Zhang, Z., Wang, C.-Z., Du, G.-J., Qi, L.-W., Calway, T., He, T.-C., . . . Yuan, C.-S. (2013). Genistein induces G2/M cell cycle arrest and apoptosis via ATM/p53-dependent pathway in human colon cancer cells. *International Journal of Oncology, 43*(1), 289-296. doi: 10.3892/ijo.2013.1946

Zheng, M., Zhou, Y., Yang, X., Tang, J., Wei, D., Zhang, Y., . . . Zhu, P. (2014). High GINS2 transcript level predicts poor prognosis and correlates with high histological grade and endocrine therapy resistance through mammary cancer stem cells in breast cancer patients. *Breast Cancer Res Treat, 148*(2), 423-436. doi: 10.1007/s10549-014-3172-7

Zhu, Z., Du, S., Du, Y., Ren, J., Ying, G., & Yan, Z. (2018). Glutathione reductase mediates drug resistance in glioblastoma cells by regulating redox homeostasis. *J Neurochem, 144*(1), 93-104. doi: 10.1111/jnc.14250

Zink, A., & Traidl-Hoffmann, C. (2015). Green tea in dermatology--myths and facts. *J Dtsch Dermatol Ges, 13*(8), 768-775. doi: 10.1111/ddg.12737

Zong, A., Cao, H., & Wang, F. (2012). Anticancer polysaccharides from natural resources: a review of recent research. *Carbohydr Polym, 90*(4), 1395-1410. doi: 10.1016/j.carbpol.2012.07.026

Zulueta, A., Caretti, A., Signorelli, P., & Ghidoni, R. (2015). Resveratrol: A potential challenger against gastric cancer. *World J Gastroenterol, 21*(37), 10636-10643. doi: 10.3748/wjg.v21.i37.10636

*http://karyaku-paridahishak.blogspot.com/2016/01/tenggek-burung-dan-serai-kayu.html

.

LIST OF PUBLICATIONS

Part of the data presented in this thesis has been used to publish the following articles:

I) Kabir, M. F., Mohd Ali, J., Abolmaesoomi, M., & Hashim, O. H. (2017). *Melicope ptelefolia* leaf extracts exhibit antioxidant activity and exert anti-proliferative effect with apoptosis induction on four different cancer cell lines. *BMC Complement Altern Med*, 17(1), 252. doi: 10.1186/s12906-017-1761-9.

II) Kabir, M. F., Mohd Ali, J., & Haji Hashim, O. (2018). Microarray gene expression profiling in colorectal (HCT116) and hepatocellular (HepG2) carcinoma cell lines treated with *Melicope ptelefolia* leaf extract reveals transcriptome profiles exhibiting anticancer activity. *PeerJ*, 6, e5203. doi: 10.7717/peerj.5203.

Kabir et al. BMC Complementary and Alternative Medicine (2017) 17:252
DOI 10.1186/s12906-017-1761-9

BMC Complementary and Alternative Medicine

RESEARCH ARTICLE Open Access

Melicope ptelefolia leaf extracts exhibit antioxidant activity and exert anti-proliferative effect with apoptosis induction on four different cancer cell lines

Mohammad Faujul Kabir, Johari Mohd Ali*, Mitra Abolmaesoomi and Onn Haji Hashim

Abstract

Background: *Melicope ptelefolia* is a well-known herb in a number of Asian countries. It is often used as vegetable salad and traditional medicine to address various ailments. However, not many studies have been currently done to evaluate the medicinal benefits of *M. ptelefolia* (MP). The present study reports antioxidant, anti-proliferative, and apoptosis induction activities of MP leaf extracts.

Method: Young MP leaves were dried, powdered and extracted sequentially using hexane (HX), ethyl acetate (EA), methanol (MeOH) and water (W). Antioxidant activity was evaluated using ferric reducing antioxidant power (FRAP), 2,2′-azinobis-(3-ethylbenzothiazoline-6-sulfonic acid) (ABTS) and 1,1-Diphenyl-2-picryl-hydrazyl (DPPH) radicals scavenging and cellular antioxidant activity (CAA) assays. Anti-proliferative activity was evaluated through cell viability assay, using the following four human cancer cell lines: breast (HCC1937, MDA-MB-231), colorectal (HCT116) and liver (HepG2). The anti-proliferative activity was further confirmed through cell cycle and apoptosis assays, including annexin-V/7-aminoactinomycin D staining and measurements of caspase enzymes activation and inhibition.

Result: Overall, MP-HX extract exhibited the highest antioxidant potential, with IC_{50} values of 267.73 ± 5.58 and 327.40 ± 3.80 μg/mL for ABTS and DPPH radical-scavenging assays, respectively. MP-HX demonstrated the highest CAA activity in Hs27 cells, with EC_{50} of 11.30 ± 0.68 μg/mL, while MP-EA showed EC_{50} value of 37.32 ± 0.68 μg/mL. MP-HX and MP-EA showed promising anti-proliferative activity towards the four cancer cell lines, with IC_{50} values that were mostly below 100 μg/mL. MP-HX showed the most notable anti-proliferative activity against MDA-MB-231 (IC_{50} = 57.81 ± 3.49 μg/mL) and HCT116 (IC_{50} = 58.04 ± 0.96 μg/mL) while MP-EA showed strongest anti-proliferative activity in HCT116 (IC_{50} = 64.69 ± 0.72 μg/mL). The anticancer potential of MP-HX and MP-EA were also demonstrated by their ability to induce caspase-dependent apoptotic cell death in all of the cancer cell lines tested. Cell cycle analysis suggested that both the MP-HX and MP-EA extracts were able to disrupt the cell cycle in most of the cancer cell lines.

Conclusions: MP-HX and MP-EA extracts demonstrated notable antioxidant, anti-proliferative, apoptosis induction and cancer cell cycle inhibition activities. These findings reflect the promising potentials of MP to be a source of novel phytochemical(s) with health promoting benefits that are also valuable for nutraceutical industry and cancer therapy.

Keywords: *Melicope ptelefolia*, Antioxidant activity, Cellular antioxidant assay, Anticancer, Apoptosis, Cell cycle, HCT116, HCC1937, HepG2, MDA-MB-231

* Correspondence: johari@um.edu.my
Department of Molecular Medicine, Faculty of Medicine, University of Malaya, 50603 Kuala Lumpur, WP, Malaysia

Microarray gene expression profiling in colorectal (HCT116) and hepatocellular (HepG2) carcinoma cell lines treated with *Melicope ptelefolia* leaf extract reveals transcriptome profiles exhibiting anticancer activity

Mohammad Faujul Kabir, Johari Mohd Ali and Onn Haji Hashim

Department of Molecular Medicine, Faculty of Medicine, University of Malaya, Kuala Lumpur, Malaysia

ABSTRACT

Background. We have previously reported anticancer activities of *Melicope ptelefolia* (MP) leaf extracts on four different cancer cell lines. However, the underlying mechanisms of actions have yet to be deciphered. In the present study, the anticancer activity of MP hexane extract (MP-HX) on colorectal (HCT116) and hepatocellular carcinoma (HepG2) cell lines was characterized through microarray gene expression profiling.

Methods. HCT116 and HepG2 cells were treated with MP-HX for 24 hr. Total RNA was extracted from the cells and used for transcriptome profiling using Applied Biosystem GeneChip^{TM} Human Gene 2.0 ST Array. Gene expression data was analysed using an Applied Biosystems Expression Console and Transcriptome Analysis Console software. Pathway enrichment analyses was performed using Ingenuity Pathway Analysis (IPA) software. The microarray data was validated by profiling the expression of 17 genes through quantitative reverse transcription PCR (RT-qPCR).

Results. MP-HX induced differential expression of 1,290 and 1,325 genes in HCT116 and HepG2 cells, respectively (microarray data fold change, MA_FC $\geq \pm 2.0$). The direction of gene expression change for the 17 genes assayed through RT-qPCR agree with the microarray data. In both cell lines, MP-HX modulated the expression of many genes in directions that support antiproliferative activity. IPA software analyses revealed MP-HX modulated canonical pathways, networks and biological processes that are associated with cell cycle, DNA replication, cellular growth and cell proliferation. In both cell lines, upregulation of genes which promote apoptosis, cell cycle arrest and growth inhibition were observed, while genes that are typically overexpressed in diverse human cancers or those that promoted cell cycle progression, DNA replication and cellular proliferation were downregulated. Some of the genes upregulated by MP-HX include pro-apoptotic genes (DDIT3, BBC3, JUN), cell cycle arresting (CDKN1A, CDKN2B), growth arrest/repair (TP53, GADD45A) and metastasis suppression (NDRG1). MP-HX downregulated the expression of genes that could promote anti-apoptotic effect, cell cycle progression, tumor development and progression, which include BIRC5, CCNA2, CCNB1, CCNB2, CCNE2, CDK1/2/6, GINS2, HELLS, MCM2/10 PLK1, RRM2 and

Submitted 12 March 2018
Accepted 19 June 2018
Published 18 July 2018

Corresponding author
Johari Mohd Ali, johari@um.edu.my

Academic editor
Leticia Costa-Lotufo

Additional Information and Declarations can be found on page 25

DOI **10.7717/peerj.5203**

How to cite this article Kabir et al. (2018), Microarray gene expression profiling in colorectal (HCT116) and hepatocellular (HepG2) carcinoma cell lines treated with *Melicope ptelefolia* leaf extract reveals transcriptome profiles exhibiting anticancer activity. **PeerJ 6:e5203; DOI 10.7717/peerj.5203**